NTNU
Norwegian University of
Science and Technology

The evolution of the Triassic bivalve Daonella into Halobia in the Botneheia Formation on Svalbard

a sedimentological and palaeoenvironmental
interpretation

Nina Bakke

Geology
Submission date: June 2017
Supervisor: Atle Mørk, IGP
Co-supervisor: Mai Britt Mørk, IGB

Norwegian University of Science and Technology
Department of Geoscience and Petroleum

Abstract

The Svalbard Triassic succession represents an uplifted section of a broad epicontinental shelf at the north-eastern margin of Pangea. The Botneheia Fm. of the Middle Triassic is an organic carbon-rich bituminous shale, which records a second order transgressive−regressive cycle. The deterioration of oxygen levels in the bottom waters of the open shelf environment and widespread preservation of organic material, makes the Botneheia Fm. an important source rock in the region, containing up to 12 % organic carbon.

The anoxic/oxic bottom environment switching events that occurred during the deposition of the uppermost part of the Botneheia Fm., the Blanknuten Mb., are reflected in the marine fauna; abrupt mass mortality events are represented by marine reptilian bone fragments hosted in coquina shell beds, dominated by the bivalve *Daonella.* These events are closely followed by periods of oxygenated waters, a flourishing *Thalassinoides* tracefossil assemblage interbedded with thin fossil-free laminations.

Detailed field observations and measurements of the Botneheia Fm. were collected by the author in 2015 and 2016 as a part of the Svalbard Triassic Research Group, a cooperation between NTNU and UNIS. A total of 18 sections in central and eastern Svalbard were logged and sampled for fossil content. Numerous samples of different species of the bivalve *Daonella* where taken throughout each section, as well as other fossils, including ammonoids.

Daonella were remarkably widely distributed across the Tethys, Panthalassa and Boreal regions and therefore serve as an excellent index fossils. The evolution of *Daonella* into *Halobia,* marking the Ladinian-Carnian boundary is well documented however the systematics are incoherent. In addition to this, the mode of life for the *Daonella* is still disputed. They have been interpreted as pseudoplanktonic, nektonic and epibenthic chemosymbionts, amongst several other theories. Fossil material from the 2015/2016 field season has helped to refine the halobiid biostratigraphical scheme on Svalbard and suggests a reclining epibenthic mode of life on soft, soupy sediments, in oxic to dysoxic milieus.

Samples of *Daonella* collected for this study are compared to images of holotypes and identified specimens from various museum collections. Species identification and age estimates have contributed to a better understanding of facies dependence and shed light on the causes for change in paleoenvironment within the Botneheia Fm. Unidirectional orientation in *Daonella* indicates the presence of currents on the sea floor which is in support of the theory of a Triassic upwelling zone along the north-eastern shelf edge of Pangea during the Middle Triassic.

Sammendrag

Trias-lagrekka på Svalbard representerer en opphevet del av en bred epikontinentalsk sokkel på den nordøstlige siden av Pangea. Botneheiaformasjonen av midtre trias alder er en organisk rik skifer, som representerer en andre ordens transgressiv-regressiv syklus. Senkning av oksygeninnholdet på havbunn i et åpent sokkelmiljø førte til preservasjon av organisk materiale. Dette gjør formasjonen, med et innhold på opptil 12 % organisk karbon, til en viktig kildebergart i Barentshavregionen.

Vekslende oksidasjonsforhold mellom oksygenfattig og oksygenrik havbunn under avsetning av den øverste delen av Botneheiaformasjonen, definert som Blanknutenleddet, gjenspeiles i den marine faunaen; episodiske masseutslettelser vises gjennom bevaringen av beinfragmenter fra reptiler i skjell-lag som hovedsakelig består av muslingen *Daonella*. Disse hendelsene henger sammen med perioder med oksygenrikt vann på havbunnen hvor større ansamlinger av *Thalassinoides* sporfossiler opptrer i veksling med tynne lag uten tegn til liv.

Detaljerte feltbeskrivelser og målinger av Botneheiaformasjonen ble utført i 2015 og 2016, som en del av forskningsprosjektet Østre Svalbard Trias Forskningsgruppe, som ble opprettet som et samarbeid mellom NTNU og UNIS. Totalt 18 lokaliteter på sentrale og østlige deler av Svalbard ble logget og prøvetatt for muslingen *Daonella* og ammonoider

Daonella var spesielt utbredt i havområdene kjent som Tethys, Panthalassa og Boreal regnes derfor som et godt egnet indeksfossil. Overgangen fra *Daonella* til *Halobia* som markerer grensen mellom Ladin og Karn er godt dokumentert i litteraturen, men nomenklaturen er kompleks og uoversiktelig. I tillegg til dette er levemåten til *Daonella* fortsatt omstridt. *Daonella* er har tidligere blitt tolket som pseudoplanktoniske, nektoniske og epibentiske kjemosymbioner, Fossilmateriale fra feltarbeidet i 2015 og 2016 har bidratt til å oppklare den biostratigrafiske oversiken for halobiider på Svalbard. Observasjonen av prøvematerialet indikerer at muslingen hadde en epibentisk livsstil på myke, bløte sedimenter i et miljø med vekslende oksygeninnhold.

Prøver av *Daonella* samlet i forbindelse med denne oppgaven har blitt sammenlignet med bilder av typearter og prøver fra ulike museumssamlinger. Artsidentifikasjon og aldersdateringer har ført til en forbedret forståelse av sammenhengen mellom avsetningsmiljø og levemåten til halobiidene og regionale endringer i paleomiljø i Botneheiaformasjonen. Skjellorienteringer i prøver av *Daonella* indikerer ensrettede havbunnstrømmer og støtter oppfatningen om en oppvellingsone langs den nordøstlige kanten av sokkelen av Pangea i midtre Trias.

iv

Acknowledgements

List of Abbreviations

NTNU- Norwegian University of Science and Technology

NHM – Natural History Museum

CSE – Cambridge Spitsbergen Expeditions

CASP – Cambridge Arctic Shelf Programme

UNIS – University Centre in Svalbard

NB – Nina Bakke

AM – Atle Mørk

GSL – Gareth Steven Lord

TH – Turid Haugen

VEN – Victoria Engelschiøn Nash

MV – Martijn Vermeer

JR – Jostein Røstad

SB – Sofie Bernhardsen

BAL – Bjørn Anders Lundschien

Table of Contents

1. Introduction

The fossiliferous shales of Botneheia Fm. have had many names that characterize the sequence well; the "*Daonellen* kalk" (Mojsisovics, 1874), "*Daonella* layers" (Wimann 1910), "Escarpment Shales" (Gregory 1921), or "Oil shale series" (Falcon 1928). The Middle Triassic black shales form the most important hydrocarbon source rock in the Barents Sea region. A contributing factor to the immense organic enrichment of these shales is the presence of countless millions of *Daonella*, thin-shelled bivalves that inhabited the variably anoxic to oxic waters near the sea bottom. An unusually high species turnover rate and a global distribution make these bivalves excellent index fossils which can be used to date and correlate sediments of late Anisian to Carnian age on Svalbard and around the world.

The prime motivation of this study is the prospect of refining the halobiid biostratigraphical scheme of Svalbard and to improve our understanding of the shifting paleoenvironmental conditions within the Botneheia Fm.

Daonella are highly abundant macrofossils which are easy to find in the field and have the potential to be used as a cost-effective way of pin-pointing one's position within the Triassic stratigraphy without the need for sample preparation and lab work associated with palynological studies, or in areas where a thermal imprint has removed the possibility completely. This project is a part of the ongoing research by the Svalbard Triassic Research Group led by Atle Mørk at the University of Science and Technology (NTNU) in Trondheim.

1.1 Study area

The Svalbard Archipelago covers the north-western part of the Norwegian Arctic, situated approximately halfway between mainland Norway and the North Pole. The islands, the largest of which is Spitsbergen, followed by Nordaustlandet and Edgeøya, are situated between 74° to 81° north and 10° to 35° east (Dallmann, 2015b). Svalbard is sparsely vegetated and comprise an exhumed part of the Barents Sea, making it a unique place to study the geological evolution of the entire region, including the subsurface of the Barents Sea (Worsley, 2008). Fieldwork, in form of fossil collecting and sedimentological logging of measured section was carried out during two field seasons, one in 2015 and one in 2016. The Triassic succession was visited at localities on the eastern islands of Wilhelmøya, Barentsøya, Edgeøya and central to eastern Spitsbergen, covering a wide lateral extent for the study of the Botneheia Fm. (Figure 1.1).

Figure 1.1: A topographic overview map of Svalbard and the study area visiting during the 2015/2016 field seasons. Map from Lord et al. (2016).

1.2   Fossil collections

Identifications of halobiid species and the resulting biostratigraphical scheme presented in this work has been based on a comparison of literature and images of reported species of *Daonella* and *Halobia* from Svalbard, and visits to fossil collections at various museums to compare the fossil material collected in 2015/2016 to the identified specimens.

Two visits were made to Simon Kelly at the Cambridge Arctic Shelf Programme (CASP) in Cambridge in October and December of 2016. The fossil collections housed at the Sedgwick Museum nearby are the largest collections of *Daonella* and *Halobia* in Great Britain and are the result of the detailed stratigraphical worked carried out during Cambridge Spitsbergen Expeditions from 1949 to 1975, which then became CASP. Hamish J. Campbell wrote his PhD thesis on *Daonella* and *Halobia* on Svalbard in comparison to New Zealand and New Caledonia

2

at the University of Cambridge (Campbell, 1994), using the findings of *Daonella* on Svalbard to supplement the incomplete Triassic succession of New Zealand.

The fossil collection housed at CASP has proven to be very useful as the samples were collected by geologists and occasionally contained both *Daonella* and ammonoids. Photos of these ammonoids have since been tentatively identified using the summary of Svalbard Middle-Triassic ammonoid zones by Wolfgang Weitschat (Weitschat & Lehmann, 1983). In addition to this, large siltstone slabs allowed for the measurement of shell orientations. Unfortunately, some of the *Daonella* material has been misidentified so direct comparisons of the identified specimens to material collected on Svalbard during 2015/2016 field seasons, proved to unreliable on the rare occasion.

A small collection of *Daonella* and *Halobia* is housed that the Natural History Museum in London. Photos were taken of some of these specimens during a visit in October 2016, with the permission of Richard Twitchett. The *Daonella* specimens housed there are from all over the world, so though these did not prove to be useful for identifying Svalbard specimens, the photos have been kept for later work.

In December 2016, bivalve palaeontologist Simon Schneider at CASP kindly provided me with photos of whitened holotypes of specimens reported from Svalbard which he had taken whilst visiting various museums across Europe. These images have played an important role in the identification process of the 2015/2016 Svalbard material.

In the spring semester of 2016 I went on exchange to the University of Otago (OU) in Dunedin on the South Island of New Zealand. Part of the New Zealand *Daonella* fossil collection of H.J. Campbell is housed at the OU Geology Department, and several specimens and type specimens of *Daonella* were whitened and photographed with the help of palaeontologist Ewan Fordyce. The Triassic succession of the South Island was visit at two localities: Kaka Point, South of Dunedin and Wairaki hills in central Otago. Images and fossil samples from New Zealand have been kept for later work.

In October 2016 I visited the Natural History Museum in Oslo where I was kindly helped by Franz-Josef Lindemann in accessing the published *Daonella* collections of Kittl (1907) and Vigran *et al.* (1998). Unpublished *Daonella* material is housed at the museum, and awaits discovery.

2. Regional Geologic Setting

2.1 Svalbard and the Barents Sea Shelf

Figure 2.1: Geographical location of Svalbard in the north-western corner of the Barents Sea shelf. Modified from Dallmann (2015b)

The Barents Sea Shelf, forming the north-western corner of the Eurasian plate, covers a vast shelf area of 1.3 million km^2 (Worsley, 2008) (Figure 2.1). It stretches from Nova Zemlya in the east to the continental slope of the Norwegian-Greenland Sea in the west, and from Svalbard and Frans-Josef Land in the north to the Norwegian and Russian coasts in the south (Stemmerik & Worsley, 2005).

The Barents Sea shelf comprises of two major provinces, separated by a north-south trending monoclinal structure. The shelf has widely varying geology and a prognosed large but little explored and developed petroleum potential. The late Palaeozoic to present-day development of the Barents Shelf, reflects the continuous northwards movement of the region through equatorial to high arctic latitudes, resulting in significant climatic changes through time (Worsley, 2008).

Immediately south of Polar Eurasian basin and east of the Norwegian-Greenland Sea lies the Svalbard Archipelago. It forms the emergent north-western corner of the Barents Sea Shelf (Dallmann, 1999; Worsley, 2008), representing approximately 5 % of the total shelf area (Worsley, 2008).

Uplifted by late-Mesozoic and Cainozoic crustal movements (Dallmann, 1999), the islands display a comprehensive overview of the geology of the entire region since the Paleoproterozoic and are therefore highly relevant for understanding the entire subsurface of the south-western shelf (Dallmann, 1999; Mørk & Bjorøy, 1984; Worsley, 2008).

Important controls on sedimentation on Svalbard have been imposed by the ongoing interplay of varying processes along the Barents Sea Shelf margins - first between the compressive Uralide development to the east, and proto-Atlantic rifting in the west, and then by the opening of the polar Euramerican Basin to the north. Finally by transpression, transtension and the final opening of the Norwegian-Greenland Sea along the western margins of the shelf (Worsley, 2008).

2.2   The geological history of Svalbard

2.2.1   Precambrian-Palaeozoic

The oldest and most altered rocks in Svalbard, are those of the pre-Caledonian basement rocks informally called the "Hecla Hoek complex" exposed in the western and northern regions of the archipelago (Dallmann, 1999). They are grouped into three terranes, thought to have been brought together by large-scale lateral movements during the Caledonian movements in the Silurian (Worsley, 2008). These three provinces include: the north-eastern Precambrian terrane consisting of igneous and sedimentary rocks including Neoproterozoic tillites, a north-western province characterized by deep crustal metamorphics, and a south-western terrane with subduction zone metasediments (Worsley, 2008). Within these rocks, Neoproterozoic stromatolites, Cambrian and Ordovician trilobites, gastropods, brachiopods, cephalopods and graptolites have been found (Dallmann, 2015b).

The post-Caledonian Devonian Old Red Sandstones, are molasse sediments preserved in a down faulted crustal block in northern Svalbard (Dallmann, 1999). These strata are arranged into the Siktefjellet, Red Bay and Andrée Land groups (Dallmann, 2015b).

Figure 2.2: Geological map of Svalbard. Map from Dallmann (2015b).

During this period, the continent drifted from 5° to 20°N (Dallmann, 2015b) leading to a gradual shift in climate from hot and arid to equatorial tropics, reflected by the mid-Devonian grey sediments.

The late Devonian Svalbardian movements, were the final phase of the Caledonian deformation bringing together the elements of archipelago into their present position (Worsley, 2008). Devonian fossils found on Svalbard are small, sparse and primitive land plants reflecting dry, desert-like depositional environments. Fauna was characterized by arthropods, wingless insects

7

and high diversity of fish. At the end of the Devonian, there was a collapse of the marine shelf ecosystems, marking one of the five major marine extinction events in Earth's history (Dallmann, 2015b).

Svalbard's Late-Devonian – Early Carboniferous rocks are represented by the Billefjorden Group. During this time there was widespread intra-cratonic rifting and deposition of terrestrial tropical humid clastic sediments (Worsley, 2008). Swamp forests composed of scale trees (including *Lepidodendron* and *Sigillaria*), mosses and ferns, leading to the deposition of coal deposits both on Svalbard, and worldwide. Extremely high oxygen levels (35%) led to gigantism in some of the arthropod insects, and amphibians which evolved into the first reptilians (Blomeier, 2015).

The Gipsdalen Group of the Late-Carboniferous – Lower-Permian was deposited during a major sea-level rise which lead to the development of an immense post-rift warm-water carbonate platform around Pangea (Dallmann, 2015b; Stemmerik & Worsley, 2005; Worsley, 2008). Frequent sea-level changes due to Gondwanan glaciations and a warm and arid climate at 35°N, lead to evaporite formation (Dallmann, 2015b), and widespread karstification on land. There were significant build-ups of reefs of rugose and tabulate corals and *palaeoaplysina,* forming the most prospective reservoir rocks in the region (Stemmerik & Worsley, 2005; Worsley, 2008). Reptiles thrived on land and sharks, bryozoans, ostracods, echinoderms, and fusulinid foraminifera flourished amongst the coral reefs (Dallmann, 2015b).

The Permian saw Svalbard drift from 30°N to 45°N. The base of the Lower-Permian Bjarmeland Group coincides with a climatic shift from warm tropical carbonates to temperate cool-water carbonates (Stemmerik & Worsley, 2005). This was due to the development of the Urals, leading to the closing of the warm-water Tethys seaway (Worsley, 2008). These carbonates are characterized by bryozoans who had become the most important reef builders, sponges, crinoids and brachiopods in nearshore areas (Dallmann, 2015b). A major flooding event by the mid-Permian lead to the deposition of the highly siliceous, deep water spiculites of the Tempelfjorden Group (Stemmerik & Worsley, 2005; Worsley, 2008). The biotic cherts were then replaced by dark shales and siltstones by the late-Permian, marking the global end-Permian (PT) extinction event on Svalbard (Dallmann, 2015b).

2.2.2 Mesozoic

Svalbard saw a dramatic shift from siliceous to clastic deposition which lasted throughout the Mesozoic in a time of decreased in tectonic activity along western margins in response to the culmination of the formation of Pangea (Mørk *et al.*, 1999b; Riis *et al.*, 2008; Worsley, 2008). The Mesozoic succession of Svalbard has a composite thickness of 3000 m and occurs in two different settings: the rocks of the western Tertiary fold belt of Spitsbergen and the rocks bordering and underlying the Tertiary basin of Spitsbergen. These sediments were deposited on a stable platform in a large embayment on the northern margin of the continent (Figure 2.3), and include several possible source rocks of high petroleum potential, most notably the Middle Triassic Botneheia Fm. and the late Jurassic Agardhfjellet Fm. (Abay *et al.*, 2017; Mørk & Bjorøy, 1984).
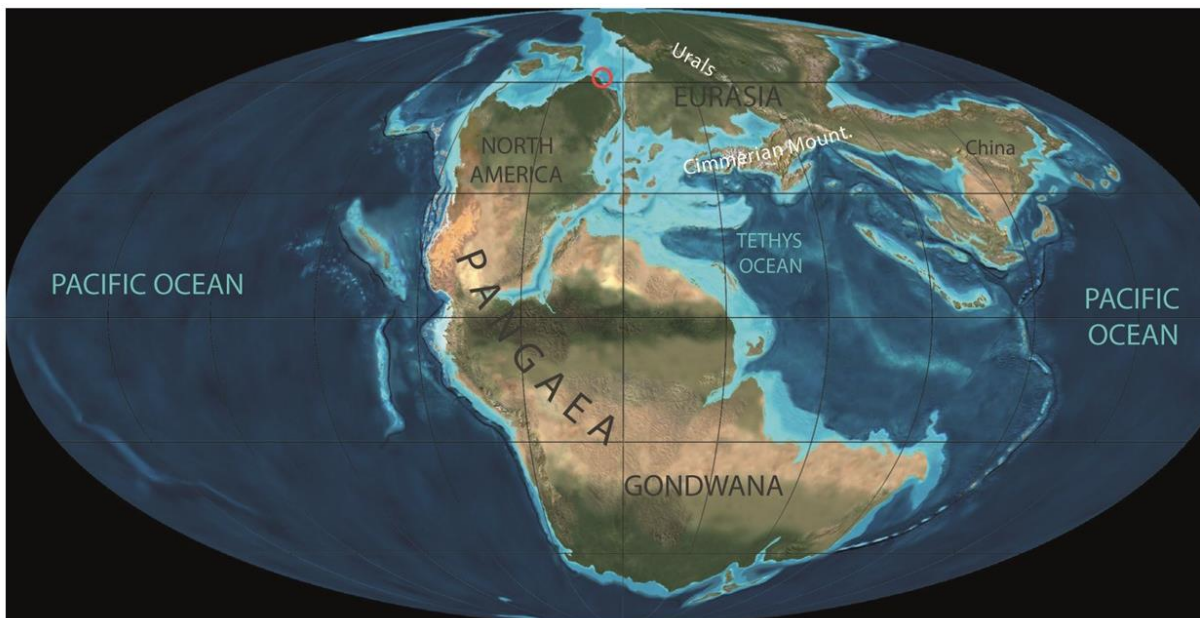
Figure 2.3: Location of the Mesozoic Svalbard embayment north-western edge of Pangea. From Mørk (2015).

A new tectonic constraint on deposition which became increasingly important through the later part of the Mesozoic was the broad northerly uplift of the entire platform, finally resulting in a significant hiatus towards the end of the era (Worsley, 1986).

The climate became dry and temperate as the continent drifted from 50°N to 70°N (Worsley, 1986). Numerous ecological niches were open following the P-T extinction and these were slowly filled and the fauna was fully developed by the Middle Triassic (Mørk, 2015).

The Sassendalen Group

The Sassendalen Group, introduced by Buchan *et al.* (1965), is exposed around the Central Tertiary Basin (CTB) on Spitsbergen, on Edgeøya, Barentsøya, the southern part of Nordaustlandet and Bjørnøya (Mørk *et al.*, 1989). It consists of three major coarsening upward sequences of shales, siltstones and sandstones that rest conformably on the Upper Permian Templefjorden Group (Mørk *et al.*, 1989). The sediments were deposited during a period of high subsidence and sedimentation rates across the entire Barents Sea shelf (Mørk & Bjorøy, 1984; Mørk *et al.*, 1982; Worsley, 2008). The main sediment sources during this period were in the west, forming a paleo-shoreline west of Spitsbergen (Mørk *et al.*, 1999b; Worsley, 2008).

The thickness of the Sassendalen Group varies greatly between major structural fault zones; from approximately 700 m in north-western exposures to 60 m on Bjørnøya (Mørk *et al.*, 1982). In the Barents Sea, thicknesses exceed 1500 m. The thicker and significantly coarser coastal to deltaic sediments exposed on western Spitsbergen generally grade into thinner fine-grained organic-rich shelf mudstones northeast and eastwards in Svalbard (Mørk *et al.*, 1982; Mørk *et al.*, 1999b). The distribution of organic carbon reflects the depositional environments, with increasing contents of type II kerogen and petroleum potential corresponding to increasing depositional depth in the basin (Mørk & Bjorøy, 1984).
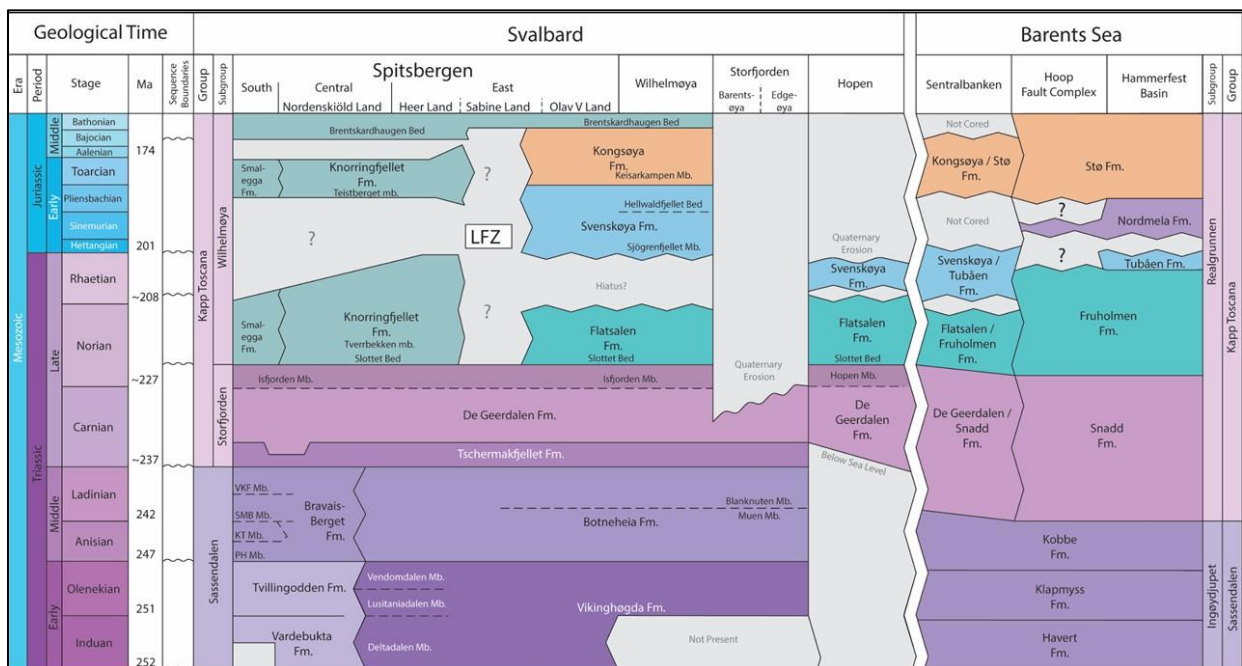
Figure 2.4: Stratigraphic chart of the Triassic to Middle-Jurassic strata of Svalbard. From Lord (2017).

10

The Early Triassic of the Sassendalen Group is represented by the Urd Fm. on Bjørnøya, the Vardebukta and Tvillingodden formations in the western Spitsbergen and the Vikinghøgda Fm. in central and eastern Svalbard (Mørk *et al.*, 1999b) (Figure 2.4). The latter formation was defined by Mørk *et al.* (1999a) from formerly Sticky Keep and Vardebukta formations of Buchan *et al.* (1965). These sediments were deposited in near-shore environments in western regions, and in open shelf sediments in the east. Typical organic content of the early Triassic sediments in the western areas is 0.5 – 6 %, increasing to 1.5 – 3 % (kerogen type III) in the east, reflecting a deepening of the basin towards the east (Mørk & Bjorøy, 1984).

A major transgression in the early Anisian led to the deposition of the Middle Triassic of the Sassendalen Group, represented by the Bravaisberget Fm. in western regions of Spitsbergen and by the Botneheia Fm. in central and eastern Spitsbergen (Figure 2.4)(Mørk *et al.*, 1982; Mørk *et al.*, 1999b). The Bravaisberget Fm. represents a coarsening upwards succession from marine shale to a shallow water, locally lagoonal, silt and very fine-grained sandstone. In southern Spitsbergen, this formation consists of deltaic sandstones with fluvial channels (Mørk *et al.*, 1982). The Bravaisberget Fm. is the proximal time-equivalent to the black shale and source rock, the Botneheia Fm. in central and eastern islands (Abay *et al.*, 2017; Brekke *et al.*, 2014; Krajewski, 2008; Mørk & Bjorøy, 1984; Mørk *et al.*, 1982; Mørk *et al.*, 1999b) (see chapter 2.4 the Botneheia Fm.).

The Kapp Toscana Group

Subsidence rates diminished throughout the Triassic, stabilized during the late Triassic to middle Jurassic. This lead to the gradual infill of the embayment and dramatic decrease in sedimentation rates (Riis *et al.*, 2008; Worsley, 2008). The thick sandstones and mudstones of the Kapp Toscana Group represent a significant change in sedimentary regime, with sediments sourced from the newly formed Ural mountains in the south-east (Mørk, 2015; Mørk *et al.*, 1999b). Mature sandstones with significant hydrocarbon reservoir potential were formed by reworking during globally rising sea levels and form the upper part of the Kapp Toscana Group (Mørk, 2015; Worsley, 2008). The group consists of the late Triassic Storfjorden Subgroup and the late Triassic to middle Jurassic Wilhelmøya Subgroup (Figure 2.4) (Mørk *et al.*, 1999b).

Storfjorden Subgroup

The Storfjorden Subgroup is made up of the Tschermakfjellet Fm. (early Carnian), the De Geerdalen Fm., (Carnian – early Norian), and the correlative Hopen and Isfjorden members (Norian) in the upper part of the formation. During the deposition of this group, a complex

paleo-geographic pattern of deltaic and floodplain environments developed over much of the province, with high but decreasing subsidence and sedimentation rates (Worsley, 2008). Deltas still prograded from the west, affecting Spitsbergen and Bjørnøya, but these diminished markedly throughout the Carnian (Worsley, 2008) and were replaced by major sediment input from the Urals in the southeast leading to the establishment of delta-plain environments over much of the northern shelf, extending to the Svalbard Archipelago (Lundschien *et al.*, 2014; Mørk, 2015; Riis *et al.*, 2008; Worsley, 2008).

The Tschermakfjellet Fm. consists of dark grey shales and siltstones, with upward increasing intercalated siltstone laminae and corresponding decrease in siderite nodules. The formation represents a shale-dominated, coarsening upward pro-delta depositional environment (Mørk *et al.*, 1999b). The unit contains abundant ammonoids, bivalves and gastropods where restricted conditions have occurred (Mørk, 2015).

The Tschermakfjellet Fm. grades upwards into the immature sandstone-prone De Geerdalen Fm., whose base is defined as the lowermost prominent sandstone bed (Mørk *et al.*, 1999b). This series of sandstone and shale alternations are organised in coarsening-upward successions. Shallow marine structures dominate in the west while thicker delta sandstones become more abundant eastwards, where paleosols and coal seams are more common in eastern Spitsbergen, Wilhelmøya, Edgeøya and Hopen (Enga, 2015; Haugen, 2016; Lord *et al.*, 2017; Mørk, 2015). These sandstones are usually texturally and mineralogically immature, making them susceptible to extensive diagenetic quartz alteration, often leading to low permeability. (Mørk *et al.*, 1982; Mørk, 2013; Støen, 2016; Worsley, 2008).

Red to greenish purple shales of the Isfjorden Member of the upper De Geerdalen Fm., are located in central and eastern Spitsbergen and Wilhelmøya (Haugen, 2016), and are indicative of restricted, perhaps lagoonal depositional environments (Mørk, 2015). On Hopen, the time-equivalent dark grey shales of the Hopen Mb. lie above the continental fluvial deposits of the De Geerdalen Fm. (Lord *et al.*, 2014; Mørk *et al.*, 1999b). The boundary to the overlying Wilhelmøya Subgroup is marked by a sudden change to a phosphate conglomerate and intensively bioturbated sandstone marker bed – the Slottet Bed (Mørk *et al.*, 1999b).

Wilhelmøya Subgroup

Following a major sea-level rise in the early Norian, a marine connection was re-established between the Tethyan and Boreal oceans along the proto-Atlantic seaway. The Barents Shelf saw greatly decreased subsidence and sedimentational rates as the Uralian-progradational

systems were no longer dominant and shallow marine, coastal environments were established throughout the province (Worsley, 2008). This led to the deposition of the condensed mineralogically and texturally mature sandstones units with excellent reservoir qualities (Mørk *et al.*, 1982). The Wilhelmøya Subgroup is the condensed time equivalent of the Realgrunnen Subgroup of the Hammerfest basin (Mørk *et al.*, 1999b).

On central Spitsbergen, the group is represented by the Knorringfjellet Fm., a thin shallow marine mixed sandstone-shale unit (Mørk *et al.*, 1982). Coeval sediments belong to the Smalegga Fm. in Sørkapp Land, which feature shallow-marine, quartzitic sandstones. On Hopen and Wilhelmøya, the correlative units are the Flatsalen, Svenskøya and Kongsøya formations (Mørk *et al.*, 1999b). The marine shales and thin siltstone beds of the Flatsalen Fm. are sharply overlain by the tidal to shallow-marine sandstones of the Svenskøya Fm. which pass up into the Jurassic (Mørk, 2015). The uppermost Kongsøya Fm. of alternating fine-grained muddy sandstone, greyish blue mudstone with siderite beds and belemnite coquina beds (Mørk *et al.*, 1999b) is well developed in the eastern areas. At top the phosphatic conglomerates are common at several horizons, such as the uppermost part of the subgroup, the Brentskardhaugen Bed (Worsley, 2008).

Adventdalen Group

The Middle-Jurassic to mid-Cretaceous Adventdalen Group is made up of shales and minor sandstones deposited as a result of the opening of the polar Euramerican Basin during the break-up of Pangea (Mørk *et al.*, 1999b; Olaussen, 2015). Widespread magmatism led to uplift of the northern margin of the Barents Sea shelf, confining sandstone depositions to these shelf areas. A subsequent global transgression cut off the supply of coarse clastics, leading to the deposition of anoxic black shales of Late Jurassic source rocks Hekkingen and Agardhfjellet formations (Mørk *et al.*, 1999b; Worsley, 2008). These are excellent source rocks and in western parts of the Barents Shelf with type II/III kerogens and organic contents of up to 20% (Abay *et al.*, 2017; Olaussen, 2015; Worsley, 2008). Silt content and bioturbation increase in western and north-western exposures, suggesting shallowing of the basin in these directions (Worsley, 1986).

The Jurassic-Cretaceous transition saw the development of open marine environments with improved bottom circulation represented by the Rurikfjellet Fm. A cataclysmic meteoric impact formed the Mjølnir crater on the north-eastern Bjarmeland Platform at this time, forming the Ragnarok Fm. (Dypvik *et al.*, 2004; Worsley, 2008).

There was an increase in diversity of both microfauna and macrofauna during the Jurassic, which culminated in an extinction event at the end of the Jurassic. Ammonites, belemnites, bivalves (*Buchia* are particularly abundant), gastropods and echinoderms together with plant, ichthyosaur and plesiosaur remains are locally abundant in the Jurassic of Svalbard (Olaussen, 2015; Worsley, 1986).

The upper part of the Adventdalen Group is represented by the sediments of the Early Cretaceous Helvetiafjellet and Carolinefjellet formations (Mørk *et al.*, 1999b). Deposition occurred on the onset of northern margin uplift in response to the opening of the Euramerica Basin. This led to southerly directed deltaic progradation and clinoforms accompanied by extensive extrusive magnetism (Worsley, 1986; 2008). Today, the nearly flat-lying Late Palaeozoic and Triassic strata of the Eastern Svalbard Platform, are locally disturbed by extensive early Cretaceous basic igneous activity, mainly in the form of sills (Harland, 1997), forming part of the High Arctic Large Igneous Province (HALIP)(Worsley, 2008). The emplacement of these sills and dykes may have locally influenced the maturation of Triassic source rocks, as seen on Edgeøya (Brekke *et al.*, 2014).

Dinosaur footprints of the herbivore *Iguanodon* and herbivore orthnipod (Hurum *et al.*, 2016) were found in early Cretaceous sediments at Festningen and around Kvalvågen, south-eastern Spitsbergen, indicating large areas of richly vegetated land in the area which was at 60°N at the time (Worsley, 1986).

By the Late Cretaceous, the ongoing uplift resulted in the largest continuous break in deposition in the entire Devonian to Tertiary sequence on Svalbard (Worsley, 1986). The highest uplift rates occurred in the northwest of the archipelago and the resultant hiatus is overlain by sediments deposited during the basal Paleogene (Dallmann *et al.*, 1999; Worsley, 2008).

2.2.3 Cainozoic

The Latest-Cretaceous to Paleogene was dominated by changing transpressive and transtensional regimes along the western plate suture in relation to the Eocene-Oligocene break-up and opening of the Norwegian-Greenland Sea (Steel *et al.*, 1985; Worsley, 2008). This resulted in the uplift of the West Spitsbergen Fold Belt whose sediments are preserved in the strike-slip Central Tertiary Basin of Spitsbergen, assigned to the Van Mijenfjorden Group (Dallmann *et al.*, 1999; Steel *et al.*, 1985; Worsley, 2008). Svalbard's Paleogene fossil fauna reflects a cooling climate and is mainly restricted to invertebrates such as pelecypods, gastropods and arthropods with occasional finds of fish and large mammals. Plant remains of

large deciduous forests, growing at an impressive 80 °N, often form coal seams and are by far the most commonly found fossils (Dallmann, 2015b).

Continuous cycles of glaciations and interglacials in the Neogene has resulted in repeated glacially induced subsidence and uplift of the Barents Sea Shelf sediments (Worsley, 2008). The shelf has experienced net erosion since the Paleogene (Riis *et al.*, 2008), with deposition restricted to the shelf margins, forming thick clastic wedges assigned to the Nordland Group. Hammerfest and Nordkapp basins were least affected by glacial erosion, with 2 km of uplift, whilst the platform areas to the north experienced 3 km of uplift. This has had significant effects on the pre-existing hydrocarbon accumulations (Worsley, 2008), exposing Triassic succession over large areas of the Barents Sea Shelf, limiting hydrocarbon plays to areas with special tectonic development (Lundschien *et al.*, 2014). Large Quaternary fossils are rare in the glacial deposits of Svalbard and are mostly limited to marine shells and foraminifera (Dallmann, 2015b).

2.3   Structural geology

The Svalbard Archipelago, which forms the uplifted north-western corner of the Barents Shelf (Worsley, 2008), is dissected by a series of N-S to NNW-SSE striking fault zones which have been reactivated at several points in time (Dallmann, 2015a). Major faults believed to start at the shelf edge north of Svalbard include the Billefjorden Fault zone (BFZ) which was first active during the Devonian (Haremo *et al.*, 1990; Mørk *et al.*, 1982; Steel *et al.*, 1985), the major strike-slip Lomfjorden Fault Zone (LFZ) (Andresen *et al.*, 1992b), active during several periods since the Neoproterozoic and the lesser understood Storfjorden Fault zone (SFZ) which has been uncovered by submarine seismic surveys (Eiken, 1985) (Figure 2.5).

The West Spitsbergen Fold-and-Thrust Belt formed in early Eocene due to a transpressional structural regime as the Barents Shelf glided past the north-eastern edge of Greenland to its present position during the opening of the Atlantic Ocean (Andresen *et al.*, 1992a; Dallmann, 2015a; Haremo *et al.*, 1990). During this time, the western part of Spitsbergen was affected by east-northeast verging folding and thrusting (Haremo *et al.*, 1990). The fold belt consists of a western 'thick-skinned' thrust zone, where Caledonian metamorphic basement rocks are involved in thrusting, and an eastern 'thin-skinned' zone, with a flat-ramp geometry affecting only the post-Caledonian sedimentary succession (Andresen *et al.*, 1992b; Dallmann, 2015a; Haremo *et al.*, 1990).
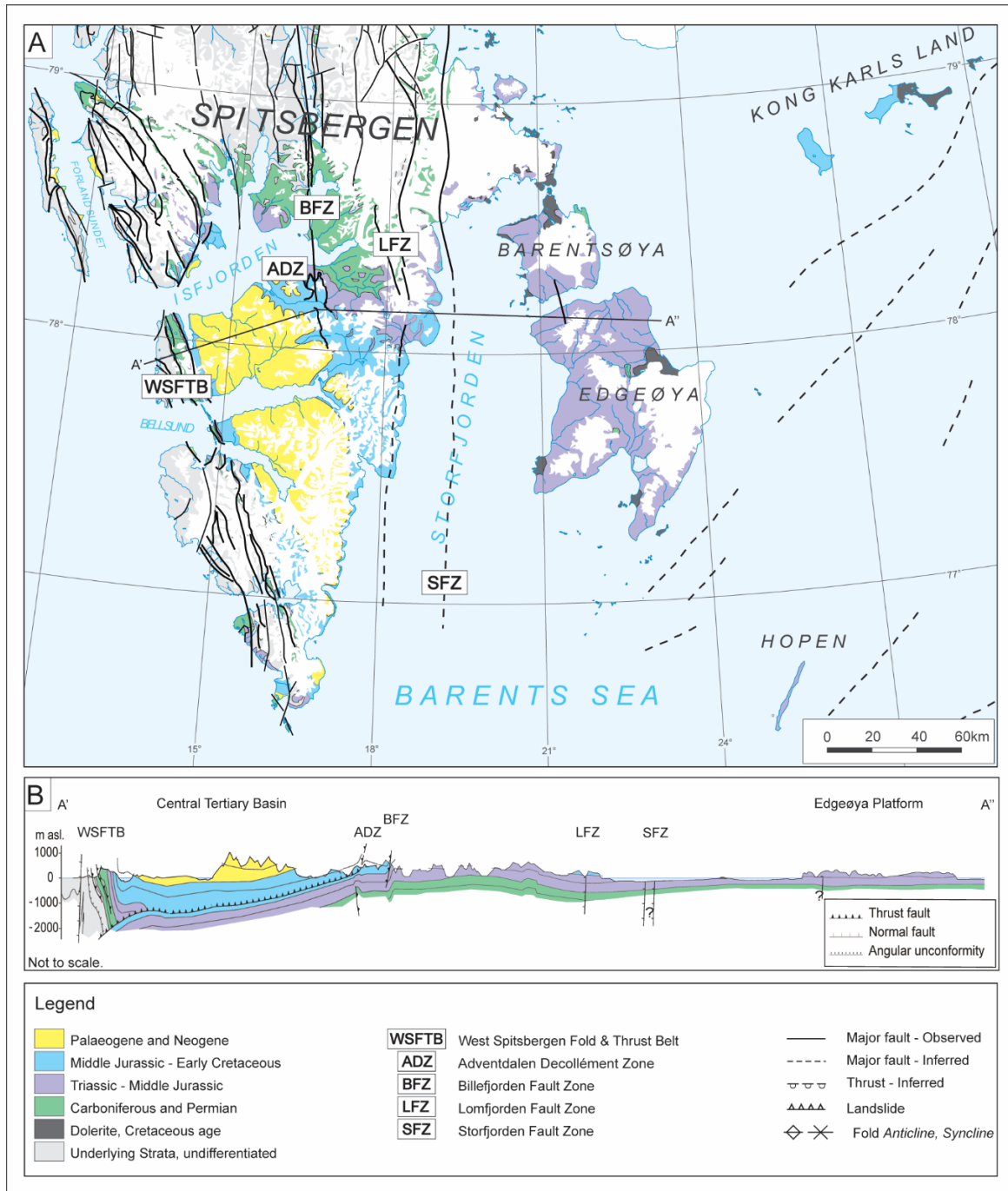
Figure 2.5: Structural geological map of Svalbard with major structural lineations denoted. B) Cross section of central Spitsbergen and Edgeøya (A' – A"). From Lord (2017), modified from Elvevold et al. (2007).

According to Andresen *et al.* (1992b), thin skinned deformation, characterized by thickening units due to extensive reverse faulting, is related to at least one and possibly two decollement zones positioned in the Triassic Sassendalen Group (Lower Decollement Zone) and the Upper Jurassic/Lower Cretaceous Janusfjellet Formation (Upper Decollement zones), referred to as the Adventdalen Decollement Zone. The reverse faulting, often resulting in duplex structures,

16

is particularly well developed in the Triassic Botneheia Fm., and can be traced from outer Isfjorden region, across Spitsbergen to Storfjorden in the west (Andresen *et al.*, 1992b). Stratigraphic thickness variations within the Mesozoic strata of central and eastern Spitsbergen are believed by some workers to be solely due to the Tertiary compressional tectonic event (Andresen *et al.*, 1992b; Haremo *et al.*, 1990), whilst other explanations include periodic subsidence along the major lineaments, through the early and middle Triassic (Mørk & Bjorøy, 1984; Mørk *et al.*, 1982).

2.4 The Middle-Triassic Botneheia Fm

The Middle Triassic sedimentary succession of Svalbard records a second-order transgressive-regressive cycle developed in an open shelf environment (Mørk & Smelror, 2001; Mørk *et al.*, 1982; Mørk *et al.*, 1989). The formations which make up this succession provides a section of the north-western Barents Shelf, from deltaic to shallow marine settings in southern Spitsbergen through inner shelf settings in western Spitsbergen ((Bravaisberget Fm.) to outer shelf settings in central and eastern Spitsbergen and eastern Svalbard (Botneheia Fm.) (Mørk & Bjorøy, 1984; Mørk *et al.*, 1982; Mørk *et al.*, 1999b). The rises in sea level led to deterioration of the bottom environment, producing the best petroleum source unit in the region (Krajewski, 2008; 2013; Mørk & Bjorøy, 1984).

2.4.1 Paleogeography

During the Triassic Period, Northern Alaska, the Beaufort-Mackenzie and Sverdrup Basins of Arctic Canada, and the Barents Shelf were located around the margin of a large enclosed "super basin" which opened up to the proto-Pacific (Leith *et al.*, 1993; Mørk *et al.*, 1989) (Figure 2.6).

Black paper shales, usually rich in phosphatic nodules and thin coquina beds were deposited in an extensive region from the Barents Sea (the Botneheia Fm.) to northern Alaska (the Shublik Fm.) to the Sverdrup basin (Murray Harbour Fm.) in Arctic Canada (Leith *et al.*, 1993; Mørk & Bjorøy, 1984; Parrish *et al.*, 2001). Deposition of organic rich mudstone reached its greatest areal extent during the Anisian-Ladinian, but ceased towards the end of the Ladinian in the Barents Sea with the progradation of siliciclastic wedges from the Uralian Orogeny (Lundschien *et al.*, 2014; Riis *et al.*, 2008). In the Sverdrup Basin and Alaska, the deposition of organic rich mudstones continued into the Carnian and Norian (Leith *et al.*, 1993).
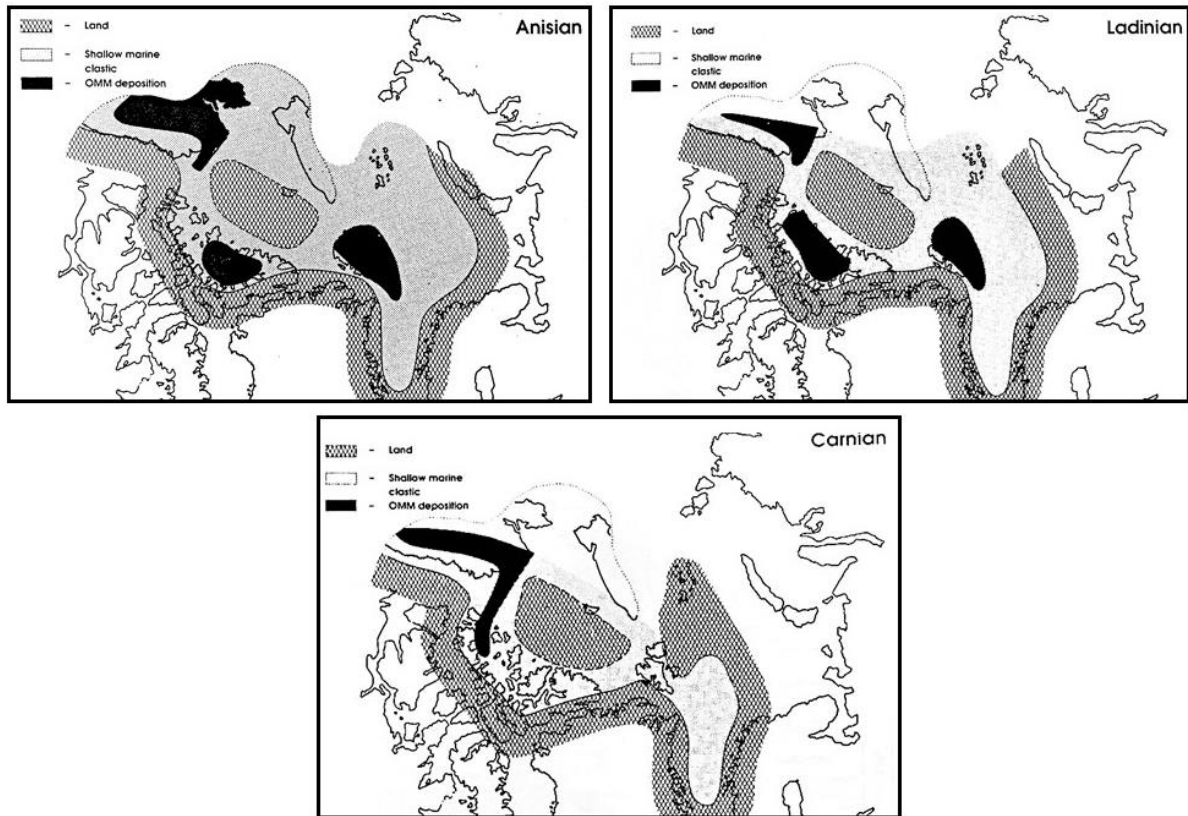
Figure 2.6: Paleogeographic map of the Anisian, Ladinian and Carnian stages of the Triassic for the circum-Arctic region. From Leith et al. (1993).

Despite similar deposits, the three basins are thought to have been formed in different settings. The organic-rich Lower to Middle Triassic shales on the Barents shelf are thought to have occurred in a shallow epicontinental sea (Mørk *et al.*, 1982). The Sverdrup Basin is a silled basin, rather than shallow sea (Embry, 1991) whilst the Shublik Formation of Alaska is thought to have been deposited with a coastal upwelling system (Leith *et al.*, 1993; Parrish *et al.*, 2001)

.

The transgressive/regressive sequences of Svalbard and the Barents Shelf can be compared with those of the Sverdrup Basin and East Siberia, all located on the northern margin of Pangea, facing the Panthalassa Ocean (Mørk & Smelror, 2001). Simultaneous transgressions, most likely controlled by common tectonism, have been recognized throughout the Arctic during the Triassic. A 2nd order transgression occurred in the earliest Anisian, and one in the earliest Carnian (Mørk, 1994; Mørk & Smelror, 2001). The early Anisian saw deposition of organic rich mudstones in the basins, recognizable all over the Arctic, from Svalbard to northern Alaska and Eastern Siberia (Leith *et al.*, 1993; Mørk, 1994). A 3rd order transgression, occurred in the

Early Ladinian, recognized in Svalbard and the Sverdrup Basin and along basin margins in the eastern Siberia (Mørk & Smelror, 2001). This independent transgression was most likely a response to local tectonic processes (Mørk, 1994).

2.4.2 The Barents Shelf

The Barents Shelf during the Anisian comprised a central marine shelf bordered by land areas to the north-west, east and south (Figure 2.7).This embayment had north connection with deep basins of the Panthalassa Ocean (Mørk *et al.*, 1989; Riis *et al.*, 2008), with an open marine connection to the southwest into the North Atlantic rift system (Smelror *et al.*, 2009).

A NE-directed system of clinoforms extended, over the Finnmark Platform, the Hammerfest Basin and onto the Bjarmeland Platform. Sands were derived from both the Fennoscandian Shield and the Urals, and deposited along a NE-SW trending coastline. Here, the Kobbe Fm. was deposited in the form of sands, siltstones and shales (Smelror *et al.*, 2009). In western Spitsbergen, the deltaic sediments of the Bravaisberget Fm. were deposited with sediment input from the west (Mørk *et al.*, 1982; Riis *et al.*, 2008), and in the east and south of the Barents Shelf, the Botneheia Fm. and Kobbe Fm. were deposited in a restricted shelf. The Kobbe Fm. mostly has similarities with the Bravaisberget Fm. of Spitsbergen (Mørk *et al.*, 1999b). Southwards on the western Barents shelf the Steinkobbe Fm. was deposited, a restricted shelf shale that is correlative and time-equivalent (Spathian to Anisian age) to the Botneheia Fm. (Lundschien *et al.*, 2014; Mørk *et al.*, 1999b). Deposition of the Steinkobbe Fm at the Svalis dome heralded the onset of widespread organic sedimentation in the entire arctic (Vigran *et al.*, 1998). Erosion of the Early to early Middle Triassic organic rich marine mudrocks from the area now occupied by Bjørnøya is suggested by the occurrence of the phosphatic nodule conglomerate which comprises the Verdande Bed (Mørk *et al.*, 1990). In the eastern Barents Sea, the Middle Triassic is represented by non-marine siltstones and sandstones with plant bearing mudstones, deposited in flood plain and alluvial-plain settings (Smelror *et al.*, 2009).

Sediments sourced from the ESE approached the Svalbard region in the late Ladinian. At this time there was deeper environment in Kong Karls Land, and at Sentralbanken there were tidal deposits (Riis *et al.*, 2008). By the Carnian there was an overall regional regression in the Barents Shelf, and the open marine shelf was replaced by a widespread coastal plain stretching from Novya Zemlya to the Hammerfest Basin (Figure 2.7) (Riis *et al.*, 2008; Smelror *et al.*, 2009). As a result of this progradation, Middle and Upper Triassic formational boundaries are diachronous, being older in the south-east than in the north-west (Riis *et al.*, 2008).
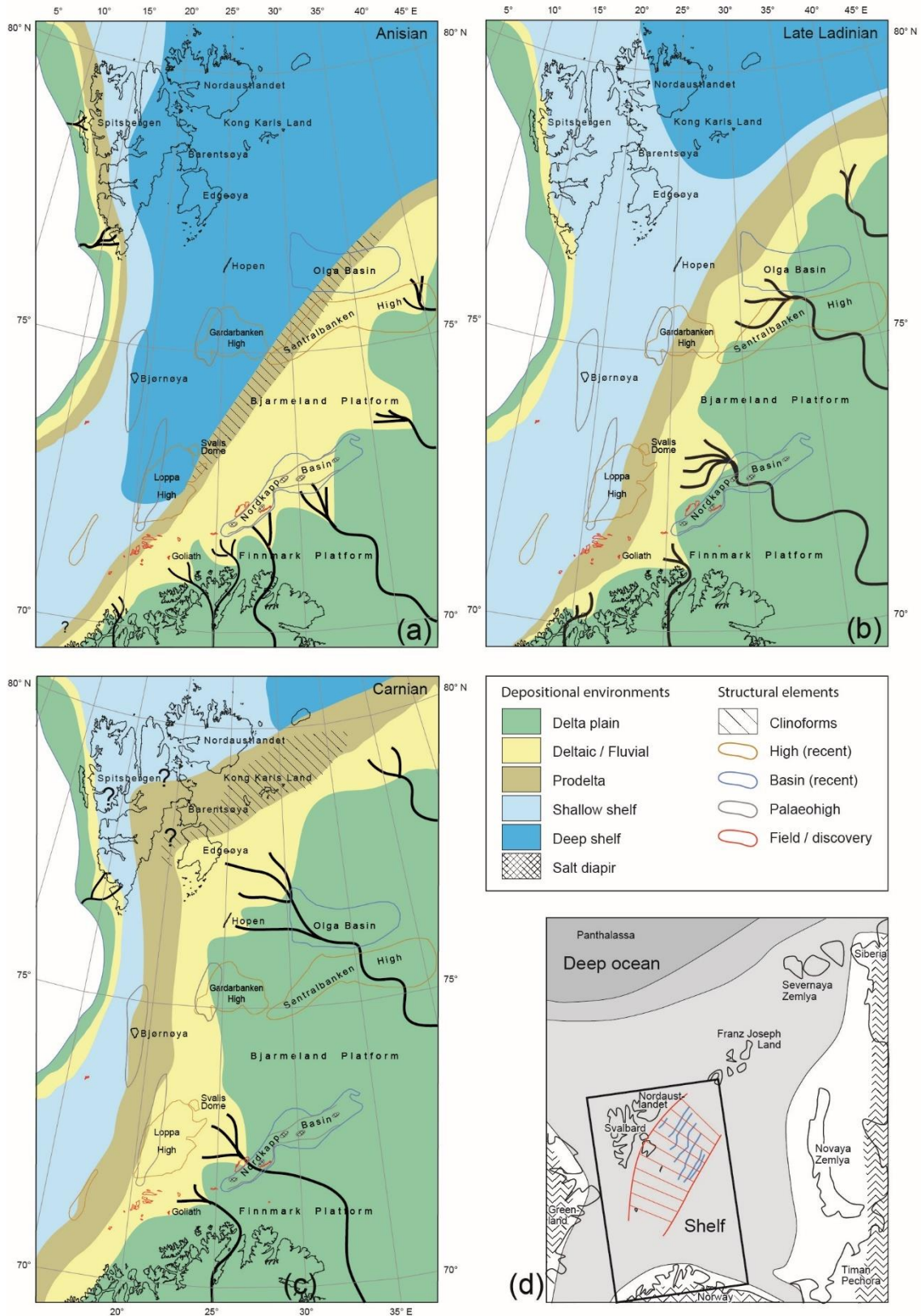
Figure 2.7: Interpretation of the regional paleogeography during the Anisian, Ladinian and Carnian. The Early Triassic basin was gradually filled by large volumes of sediment from source areas in the east and in the south, and by small volumes in the west and north-west. From Riis et al. (2008).

2.4.3 Hydrocarbon potential

Of the abundant organic carbon-rich shale and siltstones of the Mesozoic of Svalbard, The Botneheia Fm. is a particularly high quality source rock (TOC > 12%) due to the hydrogen-rich nature of its kerogens (type II) ((Mørk & Bjorøy, 1984). The kerogen (type II) content steadily increases in quality toward north and northeast of Svalbard, peaking in Edgeøya and Barentsøya.

Algal-rich kerogen gives the highest transformation ratio of kerogen to hydrocarbons than any other type of kerogen, producing paraffinic oil. Samples with the highest TOC contents contain abundant *Tasmanites* (Mørk & Bjorøy, 1984).
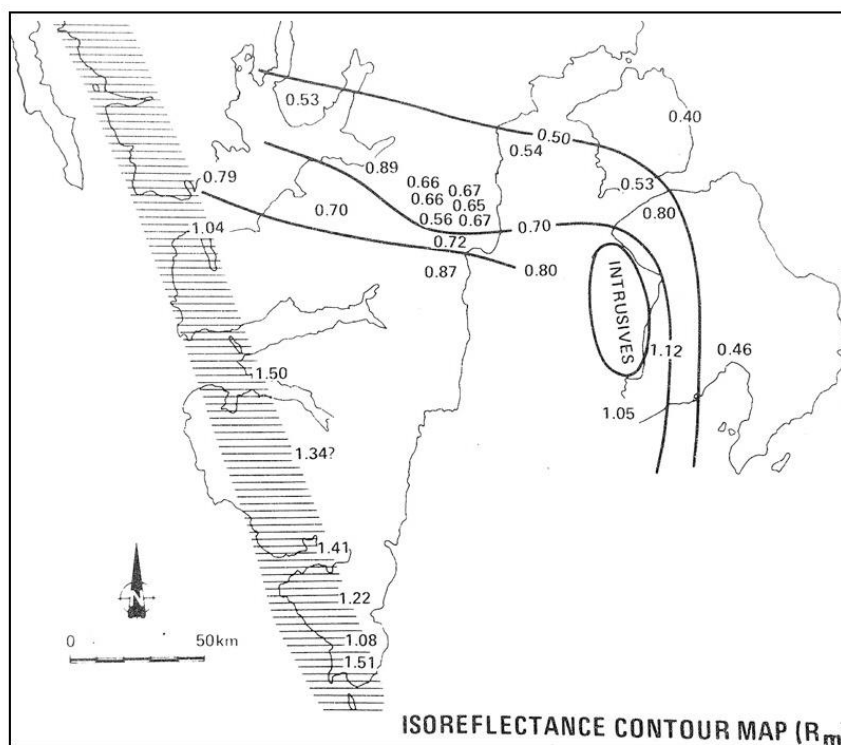
Figure 2.8: Regional variation in isoreflectance values indicating maturity for Middle Triassic samples. Modified from Mørk and Bjorøy (1984)

The maturity of the Botneheia Fm. varies from early mature to very high (Abay *et al.*, 2017). Maturity indicators such as iso-vitrinite reflectance contours (Figure 2.8), indicate a systematic and rapid decrease in maturity in the northeast and north of Svalbard. The reason is thinning and wedging out of overburden of mainly Tertiary-age sediments at the edge of the Central Tertiary Basin. The highest maturity levels (mature – over-mature) were recorded above dolerite intrusions on Edgeøya (Brekke *et al.*, 2014) and within the Tertiary deformation zone, and immature sediments found in the northeast and on eastern islands (Mørk & Bjorøy, 1984).

Other potential Mesozoic source rocks have lower petroleum potential due to type III and IV kerogens (Mørk & Bjorøy, 1984). However, the Upper Jurassic Agardhfjellet Fm., equivalent to the Hekkingen/ Spekk/ Draupne/ Kimmeridge formations, is also considered to have good source rock potential, having a high organic content of on average 3%, containing kerogen type II/III. The Agardhfjellet Fm. has reached late oil window maturity (Abay *et al.*, 2017; Mørk & Bjorøy, 1984).

2.4.4 Lithostratigraphy

According to Mørk *et al.* (1999b), the sequence consists of mudstone and calcareous siltstone, forming a coarsening upwards succession, where basal mudstones grade into siltstones. The black shale forms bluish weathering surfaces and has abundant small phosphate nodules. Thin to medium thick, yellow weathering carbonaceous siltstone beds occur throughout the unit. The upper part is highly calcitic due to abundant thin-shelled bivalves forming a pronounced cliff. The type section of the Botneheia Fm. is located at Sticky Keep, Nordenskïold Land. Early and middle Anisian sections form over half of the thickness of the Botneheia Fm. due to higher sedimentation rate, whereas the late Anisian and early Ladinian sections are condensed (Hounslow *et al.*, 2008).

Krajewski (2008), subdivided the Botneheia Fm. in eastern Svalbard into two members: the Muen Mb., with a type section at Muen on Edgeøya, and the overlying Blanknuten Mb., defined by Mørk *et al.* (1999b) has a type section at Blanknuten on Edgeøya. The Botneheia Fm. in eastern Svalbard is subdivided into nine informal lithostratigraphic units, five in Muen Mb. and four in the Blanknuten Mb. by Krajewski (2008).

The Muen Member

The lower boundary of the Botneheia Fm., synonymous with the lower boundary of the Muen Mb., is defined in Mørk *et al.* (1999b) as a soft, black mudstone with small phosphate nodules sharply overlying a yellow weathering, silty dolomite bed at the top of the underlying Vikinghøgda Fm. The Botneheia Fm. in central Spitsbergen contains a basal phosphate-bearing unit which is missing in eastern Svalbard (Hounslow *et al.*, 2008; Krajewski, 2013). In the Sassendalen area, the base of the Botneheia Fm. can be traced by a *Rhizocorallium*-bearing siltstone, some 7 m above the base of the Botneheia Fm. (Mørk *et al.*, 1999a). This marker bed is dated to the early to middle Anisian boundary, and can be traced throughout central and

eastern Spitsbergen, with the exception of Sørkapp High and the extreme northeast (Hounslow *et al.*, 2008).

In eastern areas, the lower boundary is less distinct and defined by the first appearance of the characteristic black shale (Mørk *et al.*, 1999b). This is elaborated on by Krajewski (2008), who notes that on Edgeøya, phosphate nodules only first appear in the upper part of the Muen Mb. The topmost Vikinghøgda Fm. on the eastern islands is suggested by (Krajewski, 2008) to commonly form a pile of carbonate cementstone beds, approximately 0.5 - 2 m thick.

The Muen Mb. is considered to be of early to middle Anisian age, following an extensive regional transgression in the early Anisian (Hounslow *et al.*, 2008; Korčhinskaya, 1982; Krajewski, 2008; 2013; Mørk *et al.*, 1982). According to Korčhinskaya (1982), thicknesses of the Anisian varies from 15 m in Sørkapp Land to 125 m in Van Keulenfjorden.

The Blanknuten Member

The characteristic cliff-forming Blanknuten Mb. at the top of the Sassendalen Group is distributed throughout the Botneheia Fm. of central and eastern Svalbard. First defined as the Blanknuten Bed by Mørk *et al.* (1982), the currently defined Blanknuten Mb. (Mørk *et al.*, 1999b) is approximately 30-40 m thick on Edgeøya, thinning towards the northeast. It consists of calcareous fine-grained organic carbon rich clastic deposits of mudstone and shale, deposited in open marine shelf. The high calcite content is due to numerous thin shelled bivalves (Mørk *et al.*, 1999b), attaining a maximum biogenic calcite in the coquina layers in the upper part of the member (Krajewski, 2008).

The lower boundary is defined at the base of cliff-forming mudstones and shales of the upper part of the Botneheia Fm. (Mørk *et al.*, 1982; Mørk *et al.*, 1999b). Krajewski (2008) adds that the boundary often is placed at the top of a distinct carbonate cementstone with abundant, flatted ammonoids that caps soft black shale interval with phosphate nodules of the uppermost part of the Muen Mb.

The upper boundary of the Blanknuten Mb., synonymous with the upper boundary of the Botneheia Fm. and the Sassendalen Group, is defined where a concentration horizon of reworked phosphate nodules containing reptilian bone fragments and ammonoids are overlain by dark grey to black shales with abundant purple-weathering siderite concretions of the Tschermakfjellet Fm. (Mørk *et al.*, 1999b). Krajewski (2008) suggests that the boundary occurs slightly above the top of the Blanknuten Mb. cliff in eastern areas, where an erosional surface

cuts the soft, black phosphatic shale overlying the phosphorite concentration horizon (conglomerate) discordantly.

The Blanknuten Mb. is considered to be of late Anisian – Ladinian age, with the boundary between the Anisian and Ladinian occurring in the middle of the Blanknuten Mb., based on ammonoids and Re-Os geochronology (Hounslow *et al.*, 2007a; Hounslow *et al.*, 2008; Korčhinskaya, 1982; Weitschat & Lehmann, 1983; Xu *et al.*, 2009). According to Korčhinskaya (1982), thickness of Ladinian sediments varies from 16 m on Barentsøya to 85 m in Van Keulenfjorden. She reports that the upper substage of the Anisian (and thus the bottom of the Blanknuten Mb.) is characteristically the first appearance of *Daonella* on Svalbard.

The upper boundary of the Blanknuten Mb., is the only Triassic boundary that can be traced throughout Svalbard and it is therefore an important stratigraphic datum (Buchan *et al.*, 1965). This boundary is sharp, and is interpreted as a shallowing of the basin from deep shelf to prodeltaic conditions in the overlying formation (Mørk *et al.*, 1999b).

According to Lock *et al.* (1978), Buchan *et al.* (1965) and Tozer and Parker (1968), the late Ladinian is missing due to condensation, non-deposition and erosion of the top of the Botneheia Fm., and therefore the transition between the Sassendalen and Kapp Toscana Group occurs between the early and middle Ladinian. Campbell (1994), notes that late Ladinian faunas have not been recognized and that late Ladinian time occurs between Botneheia Fm. and the overlying Tschermakfjellet Fm.

Other workers suggest that the upper boundary approximates the Ladinian-Carnian boundary (Korčhinskaya, 1982; Mørk *et al.*, 1989; Weitschat & Dagys, 1989). According to Korčhinskaya (1982), the *Poseidon* Zone (late early-Ladinian) is represented on Svalbard but that the *Nathorstites macconelli* beds as a whole would range through to the end of Ladinian time. According to Hounslow *et al.* (2008), the late Ladinian is present, but the two latest Boreal Ladinian ammonoid zones are absent as a result of erosional truncation below the Tschermakfjellet Fm. at Milne Edwardsfjellet in Sassendalen.

3. Background palaeontology

3.1 The Bivalvia

The phylum Mollusca, which include the bivalves, gastropods and cephalopods are a diverse group of organisms which evolved and diverged from a simple common ancestor to become one of the most successful animal phyla. They are soft-bodied invertebrate creatures who due to their hard, calcareous shell, have an extensive fossil record, occurring as dominant members of the Mesozoic to modern evolutionary fauna (Black, 1970; Doyle, 1996).

Today the bivalves are wholly aquatic and found in marine and fresh water. No members of the class can respire, feed or remain active except in an aqueous medium (Cox, 1969; Doyle, 1996). They are characterized by their two-halved, usually aragonitic calcareous shells which are hinged by an elastic ligament to allow for functions of burrowing, respiration and feeding. Bivalves have only limited capability for movement, and most live a sedentary life, in burrows or attached to substrate (Black, 1970; Doyle, 1996).

3.1.1 Morphology

The bivalve shell consists of two valves, one left and one right, united by an elastic ligament, which is secreted from the mantle (Figure 3.1).
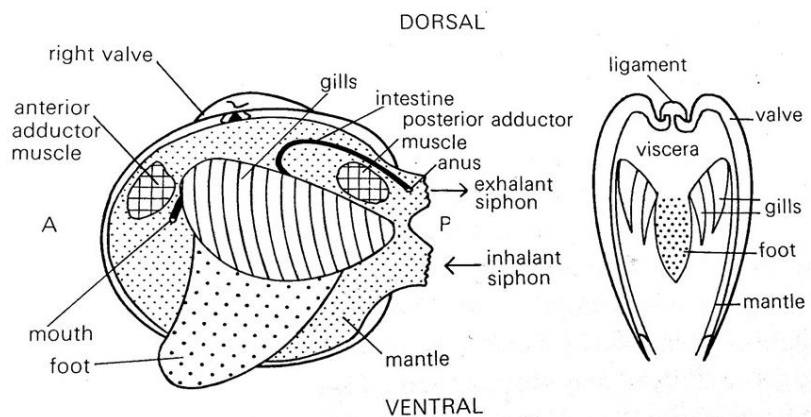
Figure 3.1 Simplified diagram of soft parts of a bivalve shell with left valve and the left flap of the mantle removed and transect. A = anterior, P = posterior. From Black (1970).

The valve margins are distinguished into the anterior (where the mouth is situated) and the posterior (where the anus opens). The main mass of the body is located in the dorsal part of the shell, including the guts and heart. Two siphons separate inhalant and exhalant water which is passed through the gills where food particles are sieved out. The foot is a muscular organ which

can be extended outside the shell and is used to pull the shell through soft sediment. At the apex of each shell is the umbo, which represents the earliest parts of the shell. Ornamentation may form, consisting of radial (ribs or costae) or concentric markings (growth lines or annulae), and occasionally spines (Black, 1970) (Figure 3.2 b).
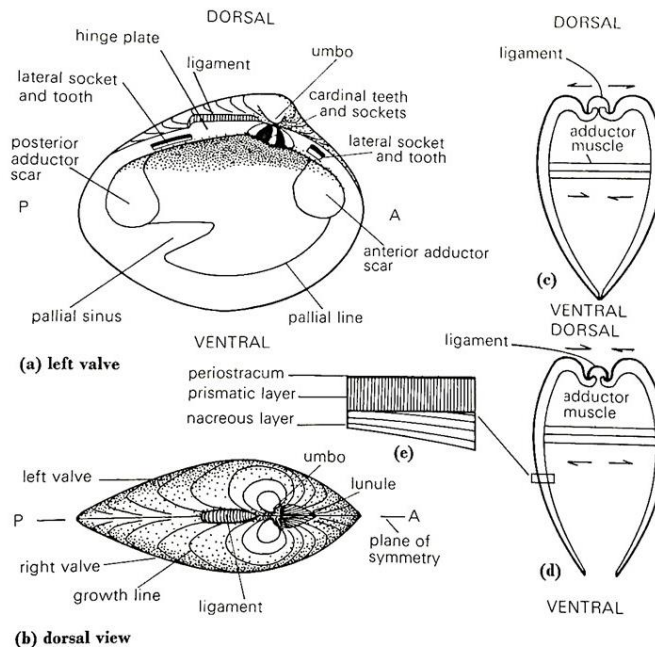
Figure 3.2: a) Interior view of left valve of an equivalve and inequilateral shell, b) exterior dorsal view, c-d) transects of closed and open shells showing a contracted and relaxed adductor muscle, and e) a type microscopic shell structure commonly found in bivalves. From Black (1970).

On the inner surface, the hinge plate may have teeth, guiding the valves into correct position (Figure 3.2 a). The ligament holding the two valves together may be external, positioned between the umbos (amphidetic), posterior to the umbo (opisthodetic) or anterior to the umbo (prosodetic) or may occasionally be internal (resilium). The adductor muscles, anterior and posterior, the position of which is marked by scars on the inner surface of the shell, hold the valves shut. Shells with two equal scars are isomyarian, those with one larger than the other are anisomyarian and those lacking an anterior scar at monomyarian. The pallial line along which the mantle is attached, gives an indication of the length of the siphons by the depth of the sinus. Bivalves can be bilaterally symmetrical along a plane passing between the two valves (equivalve) or asymmetrical (inequivalve), and are usually asymmetrical from the umbo to the ventral margin (inequilateral) (Black, 1970).

3.1.2 Distribution

Bivalves are of great value in paleoenvironmental analysis because of their association with substrates. They are almost all benthonic and are commonly limited by water depth, substrate, salinity and oxygenation (Schneider *et al.*, 2010; Stanley, 1970). Certain substrate preferences and feeding strategies are associated with certain environments. For example, epifaunal suspension feeders are commonly associated with hostile, low salinity or low oxygen environments, while a greater diversity of infaunal suspension-feeding groups may occur in more open marine conditions (Doyle, 1996).

3.1.3 Life habits

Typical feeding strategies for bivalves are as infaunal suspension feeders, relying on inhalant currents carrying phytoplankton, whilst a handful of other species are specialized of detritus feeders and predators (Cox, 1969; Doyle, 1996). Reproduction occurs without copulation and the majority of Bivalvia pass through a pelagic larval stage (planktotrophic). The mollusc emerges from the egg early in ontogeny, and continues to lead a pelagic life feeding on phytoplankton for a relatively long period before sinking to the bottom and undergoing metamorphosis. When the larva assumes a bottom life, significant changes take place in it organs and a byssus gland of some species begins to function within a few days after settlement (Cox, 1969).

Shallow infaunal bivalves

These bivalves generally have a sub-circular equivalve shell form, which is often heavily ribbed and has strong hinge teeth. This is to give the shell strength if washed out or otherwise exhumed from their burrows. They possess two sub-equal muscle scars, designed to allow the shell to have a short, protective hinge mechanism. They burrow by muscular contractions of a foot which protrudes from the front or anterior of the margin (Doyle, 1996).

Deep infaunal bivalves

Bivalves of this group live a sedentary life and generally have an elongate, equivalve shell form, usually unornamented with ribs to improve efficiency for deeper burrowing. They often possess a shell gape at the anterior and posterior for the extrusion of both a foot and a siphon. They have reduced or no hinge teeth, two unequal muscle scars and a large pallial sinus, a function of the elongate siphons needed to reach the sediment surface (Cox, 1969; Doyle, 1996).

Epifaunal bivalves

Bivalves form an important element of benthic epifauna, occurring in mostly as inequivalve (either strongly or weakly), with a rounded or irregular shape, no hinge teeth, an enlarged ligament and a single large, sub-central muscle scar. The inequivalve bivalves reflect a reclining or cemented mode of life leading to the unequal shape and size of the valves. Vagile bivalves are rare and include free-swimming family *Pecten,* the most active living Bivalvia (Cox, 1969; Doyle, 1996)*.*

Byssally attached equivalve epifaunal bivalves (such as *Mytilus*) have greatly reduced hinge teeth located at the apex of the shell and two unequal muscle scars. The byssus is extruded from a gape in the lower surface of the shell (Doyle, 1996). Structure associated with formation of the byssus consist of the byssal pit, a cavity at the posterior end of the foot, the byssal gland, situated around the byssal pit and the byssal groove. The byssal glands secrete a sticky fluid which solidifies upon contact with water to form each byssal thread (Cox, 1969).

3.1.4 Evolution of the Bivalvia

The bivalves have an evolutionary history which extends back to the early Cambrian (Black, 1970; Cox, 1969). The bivalves radiated in the Ordovician when all major bivalve groups appeared. By this time, marine communities had acquired fundamental characteristics which they would retain for more than three hundred million years during the remainder of the Palaeozoic and early Mesozoic (Vermeij, 1977). A second adaptive radiation took place during the Devonian, when bivalves displaced the brachiopods as dominant suspension feeders in the shelf environment. At this time the bivalve perfected their siphons to allow deeper burrowing and exploitation of a greater range of shallow marine environments. Faunas of this age have been described from every continent (Cox, 1969; Doyle, 1996).

Following the end-Permian mass extinction, benthic ecosystems underwent a remarkable reorganization, which resulted in the diminishment of typical Late Palaeozoic brachiopod, pelmatozoan and stenolaematid bryozoan bottom-level marine communities in favour of communities dominated by an essentially modern fauna of bivalves, gastropods, bony fish, gymnolaemate bryozoans, echinoids and certain crustaceans (McRoberts, 2010; Vermeij, 1977).

During the Mesozoic era, one of the most spectacular radiations of plant and animal taxa of the Phanerozoic took place: The Marine Mesozoic revolution (MMR) (Vermeij, 1977). Marine

28

bivalves document the long-term increase in generic richness through the early Mesozoic, which was not completed until the Ladinian. Diversity slowly increased in the Middle Triassic and peaked during the Late Triassic (McRoberts, 2001).

At the end of the Triassic, a profound extinction occurred and as little as 35% of bivalve genera survived into the Jurassic (McRoberts, 2001). In benthic communities, as a whole, many groups (echinoids, gastropods, bivalves, crustaceans, fishes) diversified dramatically beginning in the Middle Jurassic and continuing through the Cretaceous and Tertiary periods. From the Jurassic to Cretaceous there was an accelerated pace in intensity of predation and this led to epifaunal and semi-infaunal forms being largely replaced by infaunal forms by the Late Cretaceous (Vermeij, 1977).

A great diversity of bivalve forms appeared during the Mesozoic and the class reached its acme during the Tertiary and remains a very important group. During the Tertiary bivalves share with gastropods a predominant position in the shallow water faunas of the Tertiary rocks, many of which are forms that still exist today (Black, 1970).

3.2   The Middle to early Late-Triassic halobiids: *Daonella* and *Halobia*

Bivalves are traditionally not considered good index fossils due to their strong facies dependency and non-free-swimming, slow-evolving nature (Doyle, 1996). However, the Triassic 'flat clams', so named because of their very thin and flat shells, had global distributions and exceptionally high species turnover rates, making them excellent biochronological macrofossils of the Triassic (Brack & Rieber, 1993; Campbell, 1994; Hopkin & McRoberts, 2005; McRoberts, 2000; 2010; Schatz, 2004). Whereas the mean duration of bivalve species is estimated to be around 15 Ma, the Triassic flat clam species are suggested to be closer to the average durations of ammonoids species: 1 -2 Ma or less (McRoberts, 2010).

Daonella and *Halobia* form part of the flat clam group who were among the bivalves that evolved during the Triassic radiation to become the most abundant macrofauna in deep-water marine facies of the Triassic. *Daonella* occurs in the upper Anisian continuing to the uppermost Ladinian, which can be divided into 5-7 *Daonella* zones of regional and global significance. The Carnian to Norian can be subdivided into several zones by *Halobia* (McRoberts, 2010).

Despite their widespread distribution and high species turnover rates, the classification of daonellids is difficult. Most *Daonella* species lack distinct characters and have a wide range of morphologic variation (Schatz, 2001; 2004). In addition to this, a very large number of species names and a high uncertainty in taxonomy are due to poor preservation and inadequate material, a poor understanding of natural variation in morphological traits and unrecognized provincialism. In the past 50 years workers have introduced more than 75 new species of *Daonella,* in addition to the numerous species identified by workers in the 19th and early 20th century. According to McRoberts (2010), although there exist more than 300 species names for *Halobia,* no more than 30 species are likely valid with significant occurrences in Alpine-Mediterranean (Austria, Italy, Balkans) and circum-Pacific (Canada).

3.2.1 Distribution

Daonella and *Halobia* have been reported in Middle to Late Triassic deposits from all over the world, occurring in the Tethys, Panthalassa and Boreal regions (Campbell, 1994; McRoberts, 2010). At this time the assembly of Pangea had created the Panthalassa ocean, which spread from pole to pole, and an east-west tropical seaway – the Tethys. Triassic flat clams became distributed across most regions in which marine strata are preserved, commonly occurring in the Western Tethys (northern and southern alps, Sicily and the Balkans), central and eastern Tethys (Crimea, Kashmir, Nepal, Tibet, China, Timor, Thailand, Vietnam), and Boreal regions which seem to be a centre of diversity (Siberia, northern Alaska, Canadian Arctic, NE Greenland and Svalbard), (Figure 3.3) (McRoberts, 2010). This enormous range was most likely due to the dispersion of the bivalve species through passive transport of larvae via surface currents (McRoberts, 2010).
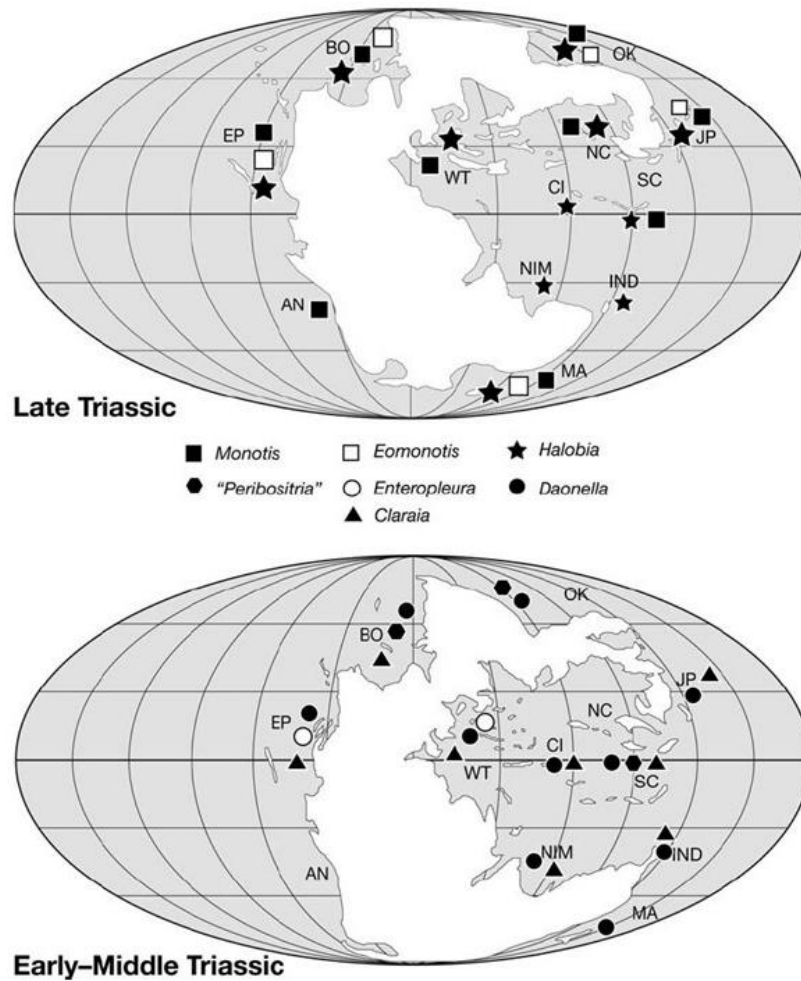
Figure 3.3: Biogeographical distributions of significant occurrences of Triassic 'flat clams'. BO = Boreal regions, a centre of diversity. From McRoberts (2010).

These bivalves occurred at a variety of marine facies and water depths, but are most notable for their thick monospecific or paucispecific shell accumulations in deeper-water oxygen deficient environments (McRoberts, 2000; 2010; Waller & Stanley, 2005). Schatz (2005) noted that these shell beds usually consist of fragmented disarticulated valves, occasionally in articulated butterflied position, interpreted to be allochthonous assemblages. Rare, autochthonous assemblages of articulated specimens with closed valves show population structures dominated by sub-adults and adults (Schatz, 2005).

The halobiids are typically described as opportunists (Campbell, 1994; Hopkin & McRoberts, 2005), forming a major component in of the exaerobic biofacies that are characterized by organic-laminated sediments and epibenthic macroinvertebrate fossil assemblages in oxygen deficient benthic conditions (Savrda & Bottjer, 1991).

3.2.2 Morphology

Daonella has been described by some workers as an equivalve bivalve (Alsen *et al.*, 2017; Campbell, 1994; McRoberts, 2000). According to a detailed morphological study of daonellids by Schatz (2001; 2004), *Daonella* are in fact inequivalve (with a slightly larger right valve), monomyarian bivalves with a dysodont, straight and long hinge line. They are generally extremely flat with inflation value (ratio thickness to height) always less than 0.2.
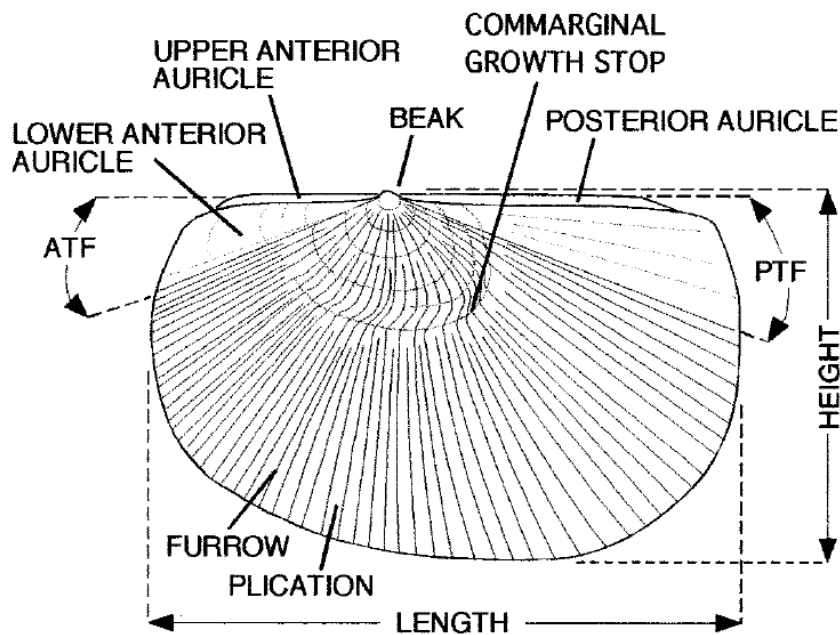

Figure 3.4: Schematic diagram of Halobiid morphology. Posterior triangular field (PTF), Anterior triangular filed (ATF), referred to as the byssal tube (Campbell, 1994), anterodorsal shell tube (Waller & Stanley, 2005). From McRoberts (2000)

Mojsisovics (1874), was the first to separate *Daonella* from *Halobia* based on the presence of an anterior tube (ATF in Figure 3.4). More than one hundred years later, Campbell (1994) suggested that *Halobia* could be differentiated from *Daonella* based on the presence of auricles and what he coined a byssal tube, assigning species one characteristic to the transitional genus *Aparimella.* According to Christopher McRoberts in Alsen *et al.* (2017) auricles occur in several species across the species groups and therefore avoided to transfer species from *Daonella* to *Halobia.* In fact, a complex evolution transition occurred between *Daonella* and *Halobia*, near the base of the Carnian. Several occurrences of *Daonella* are known from lower Carnian strata, overlapping with true Halobia (McRoberts, 2000; 2010).

In all halobiids with growth stops (Figure 3.4), normal growth proceeds after the development of the growth stop. This was by Campbell (1994) to be an indication of a change in mode of life, or the onset of reproductive capability, or some other growth related stress response, such as winter pauses, though he found little evidence to support these possibilities.

3.2.3 Mode of life

Countless life habits for the halobiids have been proposed by workers over the years: semi-infaunal mud-stickers (Wignall, 1994), epibenthic chemosymbionts (Seilacher, 1990; Waller & Stanley, 2005), nektoplankton (Hayami, 1969) or the previously most widely encountered interpretation, byssally attached pseudoplankton (Campbell, 1994). More recently advocated mode of life for the halobiids is epibenthic reclining life habit (McRoberts, 2010; Schatz, 2005) (Figure 3.5).

Wignall (1994) suggested a semi-infaunal muds-sticker mode of life for halobiids (Figure 3.5 A). According to Schatz (2005), recent mud-stickers such as the Mytilidae, are elongate, flat and thin shells with byssus threads attaching them to the substrate, and maintenance of water circulation facilitated through an occasional posterior gape. According to his observations, most daonellids have sub-circular outlines, not suitable for infaunal mode of life, and articulated closed valves of autochthonous assemblages are always preserved horizontally. In addition to this, *Daonella* did not have a gape, suggesting that opening and closing of the valve would have been necessary for respiration and feeding.

Seilacher (1990) suggested that the anterior tube of the genus *Halobia* represents a mantle gape related to feeding by means of an inhalant mantle tube, possibly to bring in hydrogen sulphide for chemosymbiotic bacteria. This mode of life was advocated by Waller in Waller and Stanley (2005), in part due to a specimen of *Halobia* with a pallial line well removed from the shell margin.

McRoberts (2010) suggested this was unlikely as the anterior tube is not present in the ancestral genus *Daonella,* which appear in similar benthic settings. Schatz (2005) reported that the *Halobia* tube is often closed at maturity and that no burrowing structures have been found.

Hayami (1969) suggest a nektoplanktonic (actively swimming) mode of the life for the halobiids. Schatz (2005) notes that some species are nearly equilateral valves with sparse costation.
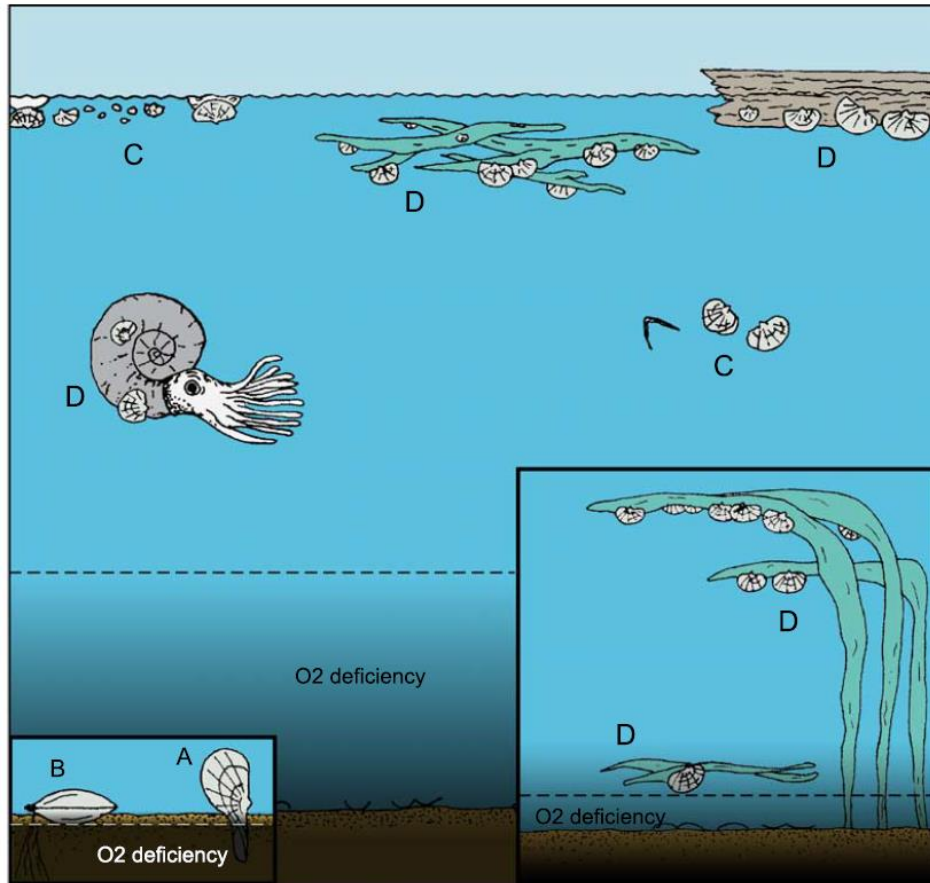
Figure 3.5: Proposed mode of life for the halobiids. A) semi-infaunal mud-stickers, B) epibenthic chemosymbionts, C) nektoplankton, D) byssally attached pseudoplankton. From Schatz (2005).

These characters are described of bivalves with swimming capability in Stanley (1970) (*See Daonella frami* in chapter on morphometrics). According to Stanley (1970), swimming bivalves typically have an inequivalve, convex-up shape so that water should emerge from their lower valve in an upwards direction. He added that no living bivalves truly belong to the nekton. Schatz (2005) noted that the single adductor muscle of the daonellids is small and lies near the beak, creating poor leverage in addition to that the extremely thin shell is not mechanically resistant.

The "byssal tube" of *Halobia,* named by Campbell (1994), was used in combination with the cosmopolitan distribution of the genera, and the rarity of finds of closed articulated shells, to come to the conclusion of pseudoplanktonic mode of life for both *Halobia* and *Daonella.* These halobiids were interpreted to have had the ability to attach themselves to floating objects in the water column via byssus threads. Candidates for such objects include driftwood, pumice, algae or cephalopod shells (Campbell, 1994). More recently, regarded the reptile, halobiid and

34

ammonoid fauna found in the black shales in Guanling, south-west China, to have been inhabiting poorly oxygenated surface waters over stagnant, oxygen-deficient and H_2S-enriched bottom water.

According to Schatz (2005), this is an unlikely scenario as *Daonella* do not show a morphological trait interpretable in terms of a byssus gland and have never been found attached to any object or in explicit spatial relation to floats. If they were limited by attachment sites, halobiids should be very rare. Waller and Stanley (2005) added that the evolutionary trajectory from *Posidonia* to *Bositra* to *Daonella* and *Aparimella* (see chapter 7. Systematics) is one of decreasing dependence on a byssus, and that a reversal of this trend in *Halobia* is unlikely. He suggested that the imprints of byssal threads found by Campbell (1994), could be bacterial filaments associated with life adjacent to bacterial mats in a sulphur rich environment (Seilacher, 1990).

According to Schatz (2005), all of the above proposed modes of life are based on the assumption that black laminated shale imply anoxic, hostile conditions. He agreed with Wignall (1994) that laminated undisturbed black shales can also be produced under exaerobic or dysaerobic conditions. Epibenthic bivalves are known from fossil exaerobic environments (Savrda & Bottjer, 1991). Schatz (2005) noted that recent examples of bivalves in exaerobic and dysoxic environments were well equipped based on their efficient respiration and facultative anaerobic metabolism. He suggests that the low convexity of the shell allowed for reduced oxygen consumption, which correlates negatively with body weight. He concluded that daonellids most likely employed a snow shoe strategy, well suited for soft soupy sediments, a view supported by Waller and Stanley (2005).

Schatz (2005) summarized that *Daonella* were most likely epibenthic, pleurothetic bivalves showing adaptive features to dysoxic milieus, like sub-circular, flat, thin shelled valves, which were specialized for soft, soupy substrates. He suggested that they are strongly facies dependant and that death assemblages of *Daonella* are typically monospecific or paucispecific, reflecting true biocoenoses of this opportunistic species. McRoberts (2010) supports this interpretation, suggesting the halobiids, in addition to the other Triassic flat clams, were likely resting or reclining benthic bivalves that were part of episodic opportunistic paleocommunities in or near oxygen deficient settings. However, he suggested lower facies dependency as *Daonella* has been found in fully oxygenated marine settings and many are known from presumable shallow-water environments from Russia, New Zealand and Japan.

According to of the general shell form and life habits of modern and fossil bivalves by Stanley (1970), few full-time reclining species exist today, but they were more common in the geological past. They are almost always inequivalve and their more inflated valve typically lies buried in the mud. Most reclining species have evolved from byssally attached species. Flattening of the shell serves to increase stability, lowering the centre of gravity and offering little cross-sectional area for resistance to currents. Extremely thin shells are typical of mud-dwellers. Stanley mentions one example of modern species, commonly known as "window pane oyster", or *Placuna placenta*, and can be seen as a modern analogue for this life habit (Figure 3.6).

Figure 3.6: Modern Placuna placenta, on display in the Osaka Museum of Natural History, Osaka, Japan. Source: Daderot (2015)

According to Yonge (1977), *Placuna placenta* is commonly found wide spread throughout the tropical Indo-West Pacific. They form thin shells that are more or less translucent, that are almost circular in outline. The valves are greatly compressed laterally, the lower (right) valve flat, the upper (left) valve with slight convexity. Lying on the right valve, they often form in dense communities, on the surfaces of soft muddy to sandy-mud bottoms, from low tide levels to a depth of about 100 m. According to Brack and Rieber (1993), the interplatform basins with daonellids from the southern Alps are interpreted to be around one hundred meter in depth.

4. Triassic biostratigraphy of Svalbard

The Triassic succession on Svalbard, with its rich fossil faunas of ammonoids, bivalves and vertebrates, has attracted the attention of many palaeontologists for more than 150 years (Vigran *et al.*, 2014; Weitschat & Lehmann, 1983). Three epochs describe the studies of Triassic rocks on Svalbard:

First were the Swedish scientists of the 1865-1925, many of whom established holotypes of the fossils they found (Böhm, Kittl, Lindström, Öberg, amongst others). Mojsisovics (1874) was the first to distinguish three units in the Triassic of Spitsbergen: The "*Posidonomyen*-Kalk", "*Daonella*-Kalk" and the "Schichten mit *Halobia zitteli*". The second epoch was dominated by the Norwegian, British and Russian geologists whom after WWII mapped the archipelago and carried out detailed stratigraphical studies (Buchan, Flood, Harland, Korčinskaya, Pčelina, Smith, Worsley, amongst others). The third epoch of industry funded petroleum exploration of the Barents Shelf in the 1970's led to extensive sedimentological research on Svalbard (Mørk, Weitschat, Worsley, amongst others) with a large staff of palynologists (Hochuli, Mangerud, Paterson, Vigran) (Vigran *et al.*, 2014).

Generally, classical biostratigraphic zonations of the Triassic succession have been based mostly on ammonoids and in part on bivalves from marine sediments, whilst core material and non-marine sediments have been dated using palynology (Vigran *et al.*, 2014).

4.1 Established biostratigraphical schemes on Svalbard

Unfortunately, the ammonoid studies of the Svalbard archipelago conducted by the early Swedish scientists were not accompanied by precise sampling records. Collections made during this time are housed at various natural history museums around Europe, in particular Vienna, housing collections of Mojsisovics (1874), Stockholm, housing collections of Lindstroem (1865), Böhm (1914) and Oeberg (1877), and Oslo, housing the collections of Kittl (1907).

From 1962, the Spitsbergen Expeditions of the University of Cambridge obtained large fossil collections, accurately located within the rock sequence. Material collected during these expeditions was the foundation for the lithostratigraphical scheme for the Triassic of Spitsbergen proposed by Buchan *et al.* (1965) and the biostratigraphical scheme presented by Tozer and Parker (1968), on which most later works have been based. Campbell (1994) based his study of the Triassic bivalves *Daonella* and *Halobia* on Svalbard on fossil material in this

large collection in addition to material collected in the field. The Cambridge Spitsbergen Expedition (CSE) collection is currently housed at the Sedgewick Museum, at the Cambridge Arctic Survey Programme (CASP), in Cambridge. The collection was visited by NB in October and December 2016.

Soviet scientists undertook detailed biostratigraphical investigations on the Triassic of Svalbard (Korčhinskaya, 1982; Pčelina, 1985) parallel to detailed ammonoid collections made by Wolfgang Weitschat (Weitschat & Lehmann, 1983; Weitschat & Dagys, 1989). A summary of the Russian Triassic ammonoid findings on Svalbard, which includes identification of halobiids, was given in Korčhinskaya (1982). Weitschat published a revised interpretation on the ammonoid zonal based on specimens collected bed by bed on the several years of Spitsbergen expeditions of the Geological-Paleontological Institute of the University of Hamburg. Single Svalbardian ammonoid horizons were correlated to the more complete and detailed zonal sequences found in the Boreal Triassic of Siberia by Algirdas Dagys, and subsequently summarized (Dagys *et al.*, 1993; Weitschat & Lehmann, 1983; Weitschat & Dagys, 1989). In Mørk *et al.* (1993) Wolfgang Weitschat presented a summarizing correlation scheme comparing the ammonoid zones of Svalbard, Sverdrup Basin, British Columbia and Siberia.

Since this publication, an integrated biomagnetostratigraphic study of the Triassic ammonoid zones at Milne Edwardsfjellet was presented, where Re-Os isotope geochronological dating provided a precise boundary between the Anisian and Ladinian at 239.3 ± 2.7 Ma (Hounslow *et al.*, 2007a; Hounslow *et al.*, 2008; Xu *et al.*, 2009). Fossil associations and the accurate age constraint of this boundary have been included in the overview in Table 1.

According to Mørk *et al.* (1989), four ammonoid zone have been established in the Middle Triassic of Svalbard (Table 1): two in the Early Anisian (*Karangatites evolutus* Zone (Dagys & Weitschat, 1993)) and (*Lenotropites caurus* zone (Korčhinskaya, 1982)), one Middle Anisian (*Anagymnotceras varium* Zone (Dagys & Weitschat, 1993)), and one Late Anisian (*Frechites laqueatus* Zone (Weitschat & Lehmann, 1983)), occurring with *Daonella lindstroemi*. The first Ladinian ammonoid fauna contains *Tsvetkovites varius,* and *Aristoptychites euglyphus* together with *Daonella lindstroemi (Weitschat & Lehmann, 1983).* The upper Ladinian contains two ammonoid levels: the lower one containing *Indigirites tozeri, Ussurites (Indigirophyllites) spetsbergensis and Daonella degeeri,* possibly correlating with *Daonella frami* beds of Arctic Canada (Weitschat & Lehmann, 1983) and an upper one with *Protrachyceras* sp., *Indigirites*
38

sp., *Daonella subarctica* (Mørk *et al.*, 1989) and *Indigirophyllites spetsbergensis* (Hounslow *et al.*, 2007b). A characteristic Carnian fauna is presented by *Stolleyites tenuis, Discophyllites taymyrensis* and *Halobia zitteli* 1 m above the group boundary (Hounslow *et al.*, 2007b; Korčhinskaya, 1982).

4.2   Reports of Triassic flat clams on Svalbard

A comprehensive study has been carried out of literature reporting findings of *Posidonia, Daonella* and early *Halobia* on the Svalbard Archipelago and their interpreted age correlations. The ammonoid zones and corresponding *Daonella* established by Wolfgang Weitschat in Mørk *et al.* (1993) have been chosen as a reference point, with the age constraint of the Anisian-Ladinian defined by Xu *et al.* (2009). This overview has been used to identify fossils in material collected during the field campaigns of 2015 and 2016. The systematics of each species is discussed in Chapter 7. Systematics. The summary of this information is presented in Table 1.

*Note in Table 1: Since the publishing of Mørk *et al.* (1993), *Daxatina canadensis* has been found to predate *Trachyceras,* and was therefore chosen to replace it as the primary maker for the early Carnian after investigations by Marco Balini in Nevada, the Dolomites and Spiti (Himalayas) (Balini *et al.*, 2010). This decision was supported by Mietto *et al.* (2008) after investigations of the Ladinian-Carnian boundary in the southern Alps. A new stratotype for the Carnian GSSP was adopted at Prati di Stuores/Stuores Wiesen, in north-eastern Italy. The species appears as described and published in ammonoid zones of Nevada, Tethys and the Southern Alps in Jenks *et al.* (2015).

Table 1: Triassic stages and corresponding Svalbardian ammonoid zones (Mørk et al., 1993) and summary of correlating reported finds of Posidonia, Daonella *and* Halobia *on Svalbard based on various workers. *see text for note concerning Daxatina canadensis zone. (+ species reported together)*

AGE (MA)	SERIES	STAGES	SUB-STAGES	SVALBARD AMMONOID STAGES AFTER MØRK ET AL. (1993)	TRIASSIC FLAT CLAMS REPORTED FROM SVALBARD				
					BASED ON WEITSCHAT & DAGYS (1989), MØRK ET AL. (1989), HOUNSLOW ET AL. (2008)	BASED ON PCELINIA (1965, 1977), and KORCINSKAYA (1982).	BASED ON CAMPBELL (1994)	BASED ON TOZER & PARKER (1968), LOCK ET AL. (1978)	SW BARENTS SEA AT SVALIS DOME IN VIGRAN ET AL. (1998)
	L.T.	CARNIAN	EARLY	*Stolleites tenuis* / *Daxatina canadensis**	*Halobia zitteli*	*Halobia zitteli*	*Halobia zitteli* + *Aparimella rugosoides*	*Halobia zitteli*	
	MIDDLE TRIASSIC	LADINIAN	LATE	*Indigirites tozeri*	*Daonella subarctica*	*Daonella subarctica* *Daonella lommeli* + *Daonella densisulcata* + *Daonella frami*		*Daonella subarctica* + *Daonella lommeli* + *Daonella densisulcata* + *Daonella frami* + *Daonella moussoni*	
			EARLY	*Tsvetkovites varius*	*Daonella degeeri* (= *Daonella frami*)	*Daonella degeeri*	*Daonella degeeri* + *Daonella frami*	*Daonella degeeri* (= *Daonella frami*)	*Aparimella*
					Daonella lindstroemi				
		ANISIAN	LATE	*Frechites laqueatus*	*Daonella lindstroemi*	*Daonella lindstroemi* + *Daonella arctica* + *Daonella americana?*	*Daonella lindstroemi* + *Daonella haraldi*	*Daonella lindstroemi*	*Daonella lindstroemi*
			MIDDLE	*Anagymnoceras varium*					
239.3 +/- 2.7			EARLY	*Lenotropites caurus* / *Karangatites evolutus*					
	E.T.	OLE-NEKIAN	SPATHIAN	*Keyserlingites subrobustus*		*Claria aranea*		*Posidonia aranea*	*Posidonia aranea*

The overview in Table 1 reveals a complex picture of the species of *Daonella* reported from the Archipelago and the Barents Sea, however general trends are apparent. The correlations are based on finds of ammonoids with associated bivalves, and relative ages of these zones are not the same from worker to worker. With this is mind, the relative position of reported halobiid species within the stratigraphy is considered most informative.

The appearance of *Posidonia aranea* (synonymous with *Claraia aranea*) together with *Keyserlingites subrobustus* is a well-known indicator of the upper parts of the Vendomdalen Mb. of the Vikinghøgda Fm., showing late Olenekian age (Hounslow *et al.*, 2008). This has been reported by several workers, as seen in Table 1.

The first reported appearances of *Daonella* all occur in the late Anisian, corresponding to the base of the Blanknuten Mb. (Korčhinskaya, 1982; Krajewski, 2008). *Daonella lindstroemi* is reported by all workers and was reported in sediments containing both *Frechites laqueatus* and *Tsvetkovites varius*, indicating late Anisian and early Ladinian age (Hounslow *et al.*, 2008). Infrequent reports of *Daonella americana* and *Daonella arctica* were made occurring together with the first appearances of *Daonella lindstroemi* by Russian workers (Korčhinskaya, 1982; Pčelina, 1965). Campbell (1994) reported finding *Daonella haraldi* together with *Daonella lindstroemi* of late Anisian age some 30 m below the *Daonella degeeri* coquina beds. These species are therefore considered to be some of the earliest forms of *Daonella* found on Svalbard and are likely to be of late Anisian age.

The species of *Daonella* that are reported from the early to late Ladinian in Svalbard vary from author to author, however *Daonella degeeri* is always reported to occur stratigraphically above *Daonella lindstroemi,* and below *Daonella subarctica.* In Hounslow *et al.* (2008), Wolfgang Weitschat assigned the beds containing *Daonella degeeri* to early late Ladinian age. This agrees with the order in which I found these species in at all localities in 2015/2016 field seasons (Chapter 6. Results). The easily recognizable *Daonella degeeri* coquina beds towards the top of the Botneheia Fm. are therefore regarded to be of early late Ladinian age.

Daonella frami is described as younger than, co-occurring, or synonymous with *Daonella degeeri.* This species was not described or dated in Hounslow *et al.* (2008). However, it was found in beds directly above *Daonella degeeri* at the four localities where both species were found during the 2015/2016 field season. This species is therefore considered most likely slightly younger in age than early Late Ladinian *Daonella degeeri*.

Daonella subarctica is reported to occur above beds containing *Daonella degeeri* and is dated as the upper Late Ladinian by Hounslow *et al.* (2008). It is reported to occur above *Daonella densisulcata, Daonella lommeli* and *Daonella frami* by Korčhinskaya (1982), so these are considered to be slightly older forms. Tozer and Parker (1968) also reported these species from the Upper Ladinian, in addition to *Daonella moussoni.* Further investigation is needed to establish the relative positions of these Upper Ladinian species.

4.3 Triassic flat clam of other regions

A global biochronological scheme of Triassic flat clams was presented by McRoberts (2010).

A summary of global reports of the late Early Triassic to early Late Triassic flat clams is presented here based on McRoberts (2010) in comparison to ammonoid zones with associated bivalves reported from Svalbard by Wolfgang Weitschat (Mørk *et al.*, 1993; Weitschat & Lehmann, 1983), with additional information from north-eastern Siberia, as presented by Konstantinov *et al.* (2013).

According to Konstantinov et al. (2013), northern Siberia and north-eastern Asia strata preserve the most complete representation of marine Triassic strata from the Boreal realm.

This summary is based on the most recent published literature by McRoberts (2010), so reports by for example Tozer (1967) in arctic Canada, and Smith (1914) has not been included here. This may be an important limitation as the bivalve zones presented for the Boreal region are quite different to that of Svalbard and Northern Siberia. The first reports of *Daonella* occur in the late Anisian.

Table 2: Triassic stages and Svalbardian ammonoid zones with corresponding bivalves by Wolfgang Weitschat in Mørk et al. (1993) and summary of a literature study of correlating reported finds of flat clams from the Boreal region, North America and West Tethys (McRoberts, 2010) and north-eastern Russia by Konstantinov et al. (2013). *see text for note on Daxatina canadensis. ** Genus name change from Daonella *to* Magnolobia *in literature, defined by Kurushin and Truschelev (2001).*

GLOBAL TRIASSIC BIVALVE ZONES

AGE (MA)	SERIES	STAGES	SUB-STAGES	SVALBARD AMMONOID STAGES AFTER MØRK ET AL. (1993)	BASED ON WEITSCHAT & DAGYS (1989), MØRK ET AL. (1989), HOUNSLOW ET AL. (2008)	BOREAL REGION BASED ON MCROBERTS (2010)	NORTHERN SIBERIA AND NORTHEASTERN RUSSIA, BASED ON KONSTANTINOV (2013)	NORTH AMERICA BASED ON MCROBERTS (2010)	WEST TETHYS BASED ON MCROBERTS (2010)
229 +/- 5	L.T.	CARNIAN	EARLY	Stolleites tenuis / Daxatina canadensis*	Halobia zitteli	Halobia zitteli + Halobia zhilnensis	Halobia zitteli	Halobia rugosa	Halobia rugosa
	MIDDLE TRIASSIC	LADINIAN	LATE	Indigirites tozeri	Daonella subarctica	Daonella subarctica	Daonella subarctica**	Daonella elegans	Daonella lommeli
					Daonella degeeri (= Daonella frami)	Daonella frami	Daonella frami / Daonella prima**	Daonella nitinae	Daonella picheri
			EARLY	Tsvetkovites varius	Daonella lindstroemi	Daonella frami / Daonella lindstroemi	Daonella vavilovi	Daonella rieberi	Daonella moussoni
233 +/- 4		ANISIAN	LATE	Frechites laqueatus	Daonella lindstroemi	Daonella dubia	Daonella dubia	Daonella dubia / Daonella sturi	Daonella elongata
						Daonella americana	Daonella americana	Daonella americana	Daonella sturi
			MIDDLE	Anagymnotceras varium					
			EARLY	Lenotropites caurus					
				Karangatites evolutus					
239 +/- 5	E.T.	OLE-NEKIAN	SPATHIAN	Keyserlingites subrobustus	Posidonia aranea	Ellesmerella aranea	Claria aranea		

43

5. Methods

This project is the result of two field seasons on eastern and central Spitsbergen followed by extensive laboratory work, visits to the CSE fossil collections at CASP in Cambridge, a rummage through the specimens of *Daonella* housed at the Natural History Museum in London and the Natural History Museum at the University of Oslo. A brief outline of methods used in the field and in the laboratory, is provided here.

5.1 Fieldwork

Detailed field observations and measurements of the Botneheia Fm. were collected at a total of eighteen locations in central and eastern Spitsbergen, Wilhelmøya, Barentsøya and Edgeøya. Logging and fossil collection took place over the course of two summer field campaigns in August 2015 and August 2016.

5.1.1 Fieldwork 2015

In 2015, field data was collected during an expedition from 03.08.15-27.08.15 aboard M/V *Sigma* throughout eastern Spitsbergen, Wilhelmøya and Barentsøya. This three-and-a-half-week long field season was in cooperation with geologists from the Norwegian Petroleum Directorate (NPD) and Capricorn Norge AS. Fieldwork was conducted by seven NTNU students, led by Atle Mørk, as a part of the Svalbard Triassic Research Group. The resulting PhD and MSc theses published in 2016 and 2017 (Haugen, 2016; Johansen, 2016; Lord, 2017; Støen, 2016).

Data was collected for this thesis by NB at a total of nine localities around Storfjorden and Wilhelmøya (Figure 5.1). Data collected included:

(i) Muen, western Edgeøya, with log (ii) Blanknuten, north-western Edgeøya, with log data and fossil samples, (iii) Wilhelmøya, log and fossil samples, (iv) Kapp Payer, north-eastern Spitsbergen, fossil photos and samples from 7 localities, (v) Hahnfjella, eastern Spitsbergen, one log with fossil samples (vi) Kvitberget, north-eastern Spitsbergen, no log data nor fossils, (vii) Vossebukta, western Barentsøya, log data and fossil samples, (viii) Krefftberget, southwestern Barentsøya, log data and samples.
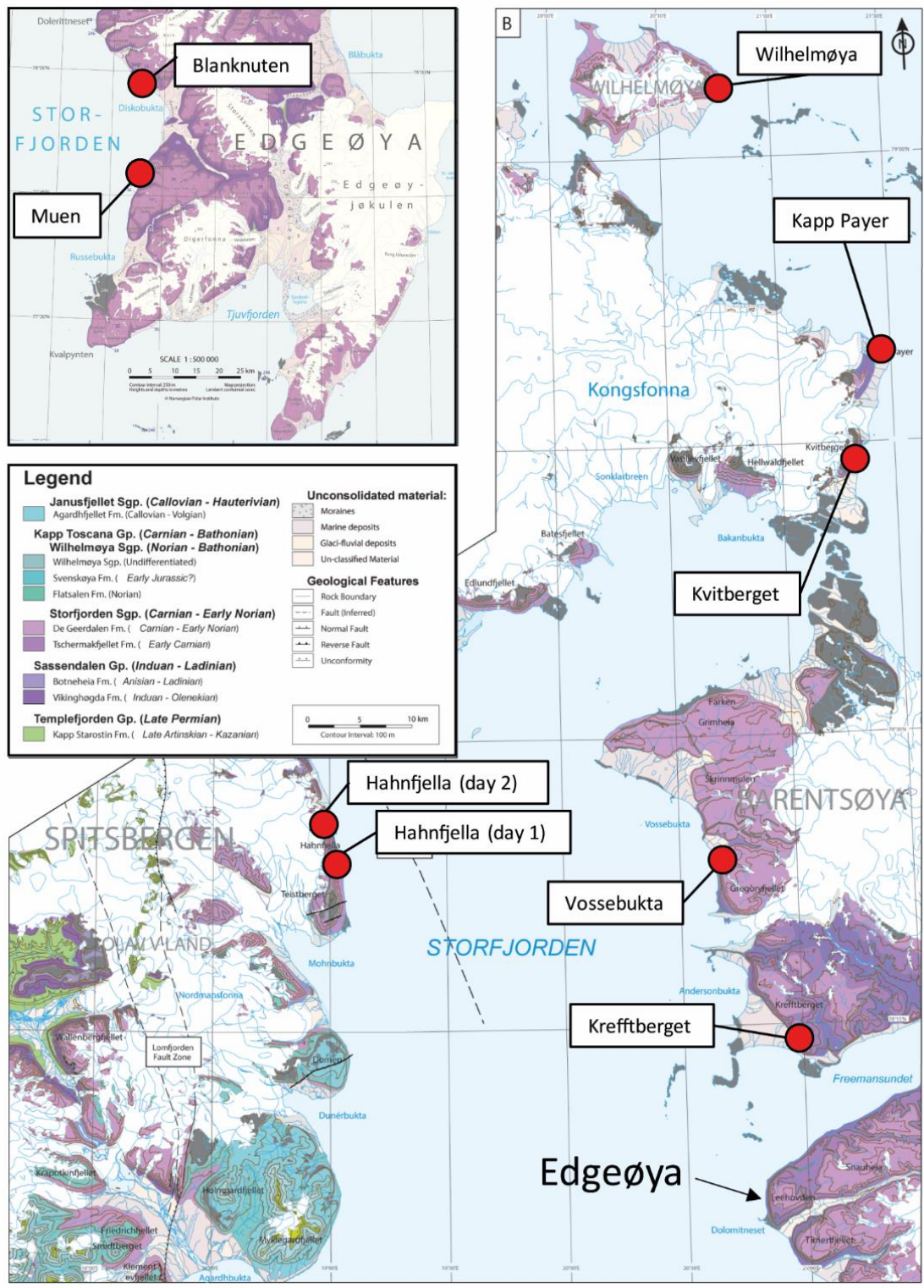
Figure 5.1: Localities visited in eastern Spitsbergen, Wilhelmøya, Edgeøya and Barentsøya during the field campaign in 2015. Localities visited on Edgeøya, located to the southeast of the main map are shown in top left corner. Modified by Lord et al. (2017) from Dallmann (2015b).

5.1.2 Fieldwork 2016

In 2016, field data was gathered during two separate expeditions. The first was a collaboration between three master students from NTNU, transported by helicopter and conducting fieldwork for from a tented camp from the 12.08.16-21.08.16 in Fulmardalen in central Spitsbergen. In addition to myself, the field party consisted of two other master students, Cathinka S. Forsberg (Forsberg, 2017) and Bård Heggem (Heggem, 2017) investigating the sedimentology of the De Geerdalen Fm. in outcrops stratigraphically above the Botneheia Fm. Three field assistants helped us in collecting data in the field and other camp activities. During the nine-day period, six localities were visited along the eastern and western slopes of the valley.

The second part of the of 2016 field season was conducted from M/V *Stålbas* from 25.08.16-30.08.16, once again in cooperation with geologists from the NPD. Two master students, Bård Heggem and myself and field assistants were deployed to various localities around Isfjorden. The Botneheia Fm. was visited at three more localities, two at Botneheia on the southern shores of Sassenfjorden and at Tschermakfjellet mountain on Dickson land (Figure 5.2).

Data collected in 2016 included:

(i) Wallenbergfjellet, Fulmardalen, log data and fossil samples collected, (ii) Milne Edwardsfjellet, Fulmardalen, log data and samples collected, (iii) Dyrhø, Fulmardalen, logs and fossil samples collected at three separate localities, (iv) Ryssen, no log data, fossil samples collected, (v) Botneheia, Sassenfjorden, logs and fossil samples collected at 2 separate localities, (vi) Tschermakfjellet, Dicksonland, log data and fossil samples collected.

The Botneheia Fm. does not appear along the entire south-western valley side in Fulmardalen on the map by the Norwegian Polar Institute printed in Dallmann (2015b)(Figure 5.2), nor on their digital map (http://svalbardkartet.npolar.no). The Botneheia Fm. was logged at four localities along south-eastern Milne Edwardsfjellet and the north-western slopes of Dyrhø, all of which are missing from the map.
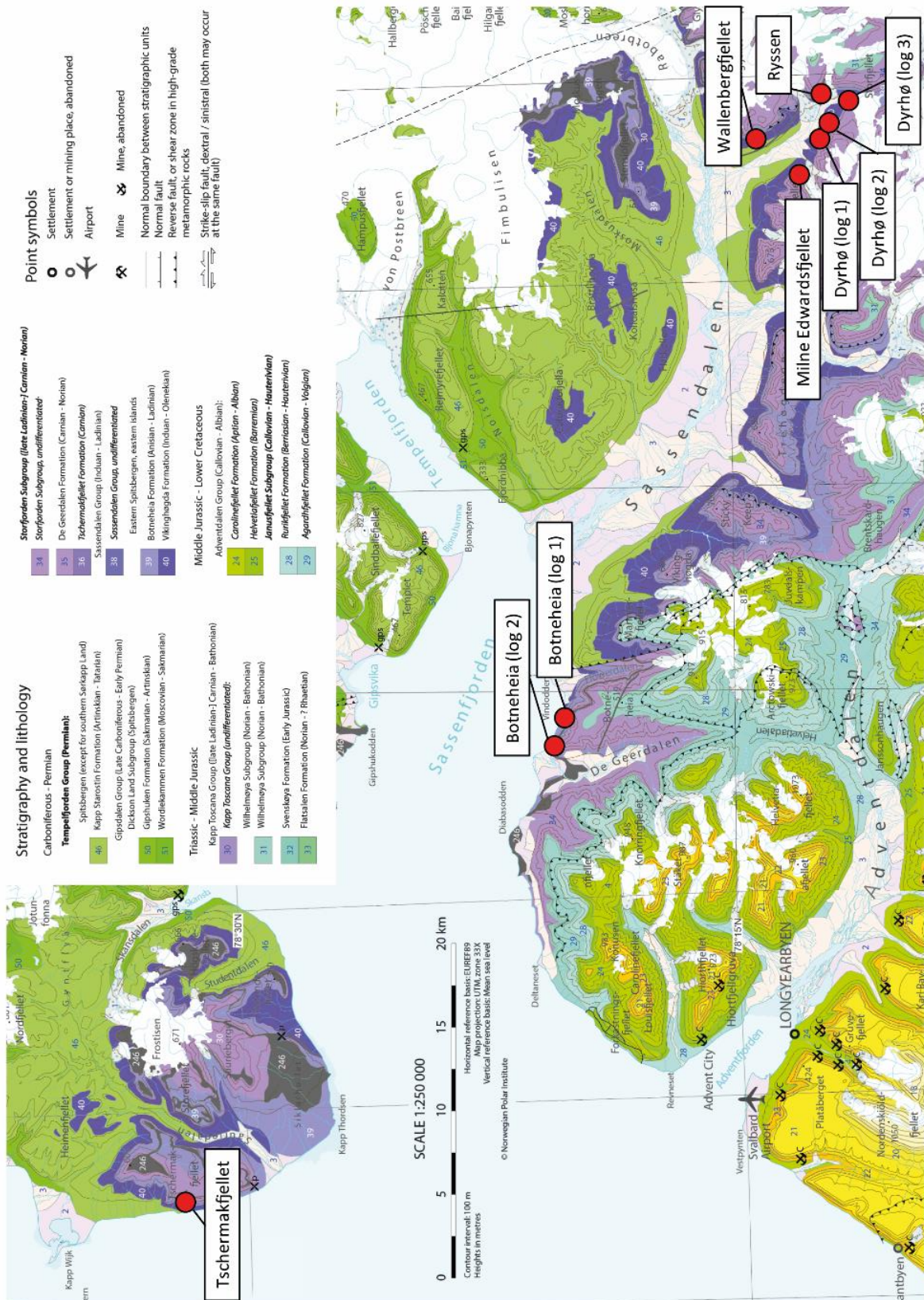
Figure 5.2: Overview of localities visited in Fulmardalen, Sassenfjorden and Dicksonland during the field campaign of 2016. Maps modified from Dallmann (2015b) and Lord et al. (2017)

5.1.3 Fieldwork procedure

On arrival at a new locality, a marker bed indicating the position in the stratigraphy was located, usually at the top of the Vikinghøgda Fm. A GPS was used to note standard UTM coordinates at the base and the top of each log, and additionally at certain marker beds (see Appendix 2 UTM Coordinates). Observations of grainsize, sedimentary structures, bed thicknesses, and lithology were recorded in a log in a field notebook, generally drawn at a scale of 1 : 50. Special attention was given to the presence of bioturbation, fossils and phosphate nodules and their relationship to one other. A 1 m measuring stick was used to measure the sections and a hand lense was used to determine grainsize and identify small fossils. Digital cameras were used to document fossil finds, the nature of the outcrop and mountain sides, and other features of interest. Samples of bivalves and other fossils such as ammonoids and bone fragments, were collected in sample bags and covered in aluminium foil for protection. When possible, samples for palynology were taken systematically, approximately every 10 m, for future projects.

5.1.4 Digitalization of log data

Logs in field books were redrawn on log paper, scanned and subsequently digitalized using Adobe Illustrator CC 2017. The style, symbols and lithology patterns (swatches) were based on those in Vigran *et al.* (2014). The corresponding legend is included in Chapter 6. Results.

5.2 Fossil preparation and lab work

The samples and fossil material collected in the field were subsequently transported back to Trondheim and were processed in a laboratory at NTNU Dora core storage facility. Fossil preparation methods are largely based on those described in Campbell (1994) and the University of Oslo Paleozoology II course guide in GEO 4740 provided by Hans Arne Nakrem. Helpful guidance on preparation methods was also received from palaeontologist Simon Kelly at CASP and Sedgewick museum conservator Sarah Finney. I was taught skills in fossil photography by Ewan Fordyce during my exchange semester at the University of Otago in New Zealand. Materials and assistance in fossil preparation was kindly provided by Atle Mørk and Torill Sørløkk at the Department of Geoscience and Petroleum at NTNU.

Fossil preparation procedure:

1) Preparation of the material involved removal of adhering clay and silt by scrubbing the specimens in warm water.

2) Rock samples were split along bedding planes using a hammer and small chisel.

3) An engraver was used in finer preparation work, to remove matrix surrounding the fossil.

4) Rubber casts were made of some of the specimens following procedures outline in Kelly (1980) using Mold Max Series silicon rubber compounds.
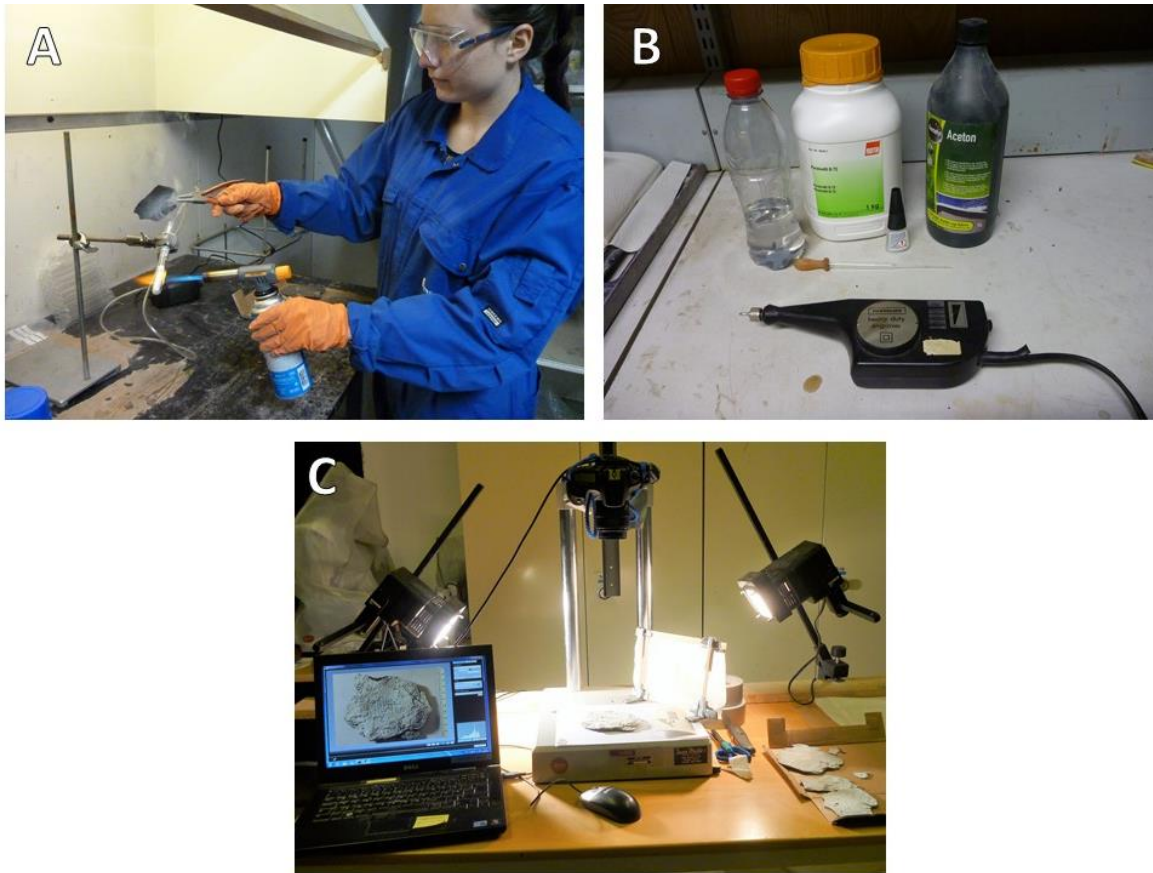

Figure 5.3: Fossil preparation procedures: A) Fossil whitening by heating a test tube of ammonium chloride connected to an air pump. The resulting white gas was directed towards the fossil specimen in a fume closet. B) Acrylic resin Paraloid B-72 dissolved with acetone was applied to shale samples using a pipette. An electric engraver tool was used in finer preparation work. C) Photographs were taken of live images of each fossil sample using a mounted camera. Spot lighting was filtered using transparent paper.

5) Particularly fragile fossil bearing shale samples, were treated using Paraloid B-72, an acrylic resin with an outstanding resistance to degradation and an ability to remain clear, soluble and removable over time, as outlined in Davidson and Brown (2012). This resin can be dissolved and re-dissolved easily using acetone (see Figure 5.3B).

6) Prepared samples containing one or more specimens were coated with ammonium chloride in order to accentuate the details of the surface of the fossil. A rubber tube was attached to an aquarium pump in order to provide a constant airflow into a test tube containing the ammonium chloride powder. The test tube was heated using a gas burner. Each fossil specimen was placed in the white gas which flowed out of the end of the test tube and the result was an evenly spread fine coating on the surface of the fossil (Figure 5.3A). The result is shown in Figure 5.4B.
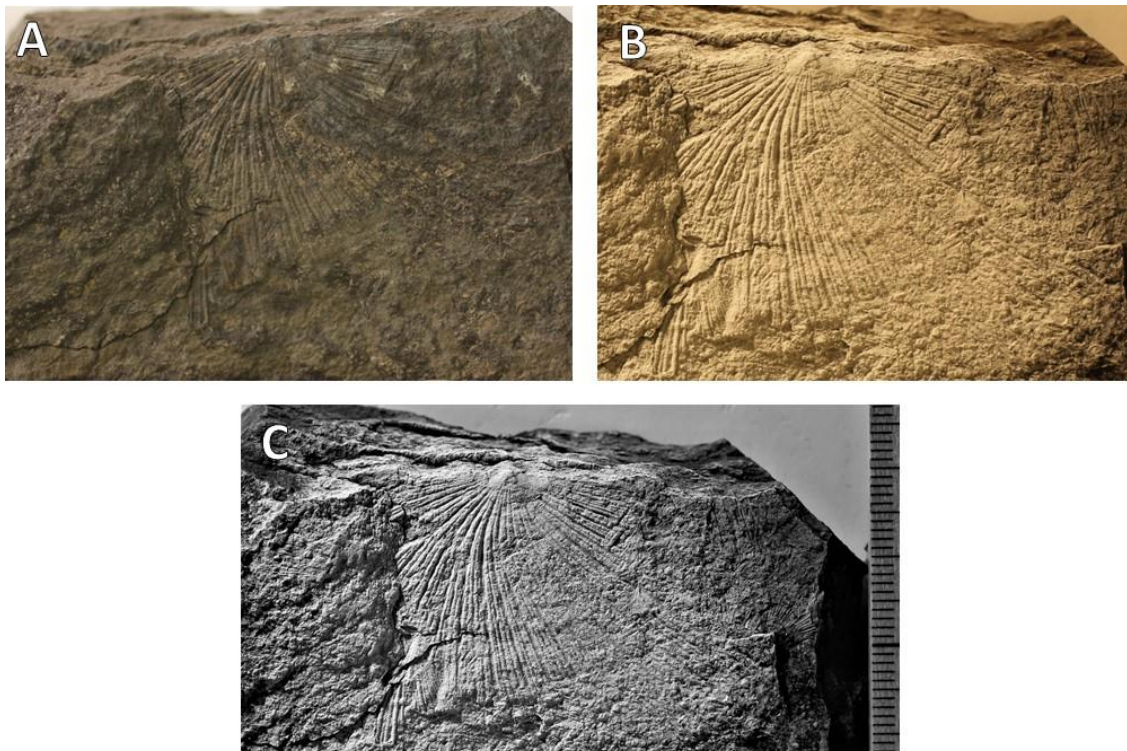
Figure 5.4: Fossil preparation procedure of Daonella subarctica *from Tschermakfjellet FOS 7 63m NB IMG 0115. A) washed specimen B) specimen after ammonium chloride coating C) Final processed image with scalebar in grayscale.*

7) After preparation and whitening, photographs were taken using a Canon EOS 60D 50mm camera. Photos were taken of entire rock samples and close-ups were taken of particularly well preserved specimens. EOS 60D Utility version 2 software for live viewing was used for making adjustments in placement and lighting before photos were taken. Care was taken to standardize lighting to the top left of the photo and spot lighting was filtered using transparent paper in order to soften lighting and best bring out surface features of the fossil specimens. A scale bar was always included in the photograph.

8) Selected photographs were digitally processed to grayscale and sharpened using Microsoft Photos 2017, the result of which is displayed in Figure 5.4 C.

Approximately 800 photos were taken of *Daonella* or other macrofossils. Though time consuming, this created a large digital dataset of photographs that were subsequently used for statistical analysis using the software programs tpsDig 232, PAST 3.14 and Adobe Illustrator CC 2017, as described in Chapter 8. Data Analysis. This large digital dataset was also used in addition to field photos of *Daonella* as a training set for machine learning and a fossil recognition application, as described in Appendix 1. Image recognition technology.

A similar method of whitening and photography was also carried out on fossil samples containing *Daonella* in the Cambridge Expedition Collection at the Sedgwick museum in Cambridge with the guidance of Simon Kelly, and of holotype specimens defined by Hamish Campbell, housed at the University of Otago in New Zealand, with the guidance of Ewan Fordyce. These photos have also been used in the current study for identification purposes and additional data in the statistical analysis.

5.3 Thin sections

Standard polished thin sections were made of selected samples at the thin section laboratory at the Department Geoscience and Petroleum, NTNU. Photographs of the thin sections were taken and are presented and discussed in later chapters.

6. Results

In this chapter, a summary of logs and field observations is provided from the eighteen localities visited during field campaigns of 2015 and 2016. Images of prepared specimens or field photos of *Daonella* and other macrofossils are shown in order of relative position in stratigraphy, with the exact vertical position in log indicated. Approximate boundaries of lithostratigraphic units are given on the left side of the log. Overview pictures indicate an approximate position of the log in the outcrop and major boundaries in the stratigraphy. A legend symbols used in the logs is given in Figure 6.1.
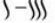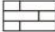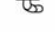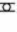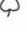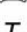
Legend

Sand- and siltstone	
Mudstone / Debris flow	
Limestone	
Siderite	
Covered / partly covered	
+	Dolerite
■	Pyrite
	Phosphate nodules
	Phosphate beds
●●●●	Phosphate conglomerate
Φ	Peloids (often phosphatic)
	Nodules
	Septarian nodules
	Siderite nodules
	Dolomite cement
	Calcite cementation
	Siderite cementation
♦	Highly organic/bitumous

⁓	Erosional surface
=	Planar lamination
	Thrust fault
ƧƧƧ	Highly deformed
✷	Echinoderms
☺	Ammonoids
	Bivalves (unidentified)
	Coquinas
	Daonella/Halobia
◦◦	Bivalve microcoquina
▽	Brachiopods
	Gastropods
◇	Plant fossils
	Vertebrate remains
T	*Tasmanites*
	Fish remains

∫ –ƧƧƧ	Increasing bioturbation
∏	*Skolithos*
	Rhizocorallium
	Zoophycos
	Diplocraterion
	Taenidium
Y	*Polykladichnus*
	Thalassinoides
	Chondrites
//	*Palaeophycus*
	(+ unidentified tunnels)
	No bioturbation

Figure 6.1: Legend corresponding to logs from field campaigns 2015 and 2016.

6.1 Fieldwork 2015

6.1.1 Muen, Edgeøya

Figure 6.2: Overview image of the Muen plateau formed by the upper Blanknuten Mb. at Muen on Edgeøya, with approximate formation boundaries (white), members (yellow), and location of the logged section (orange).
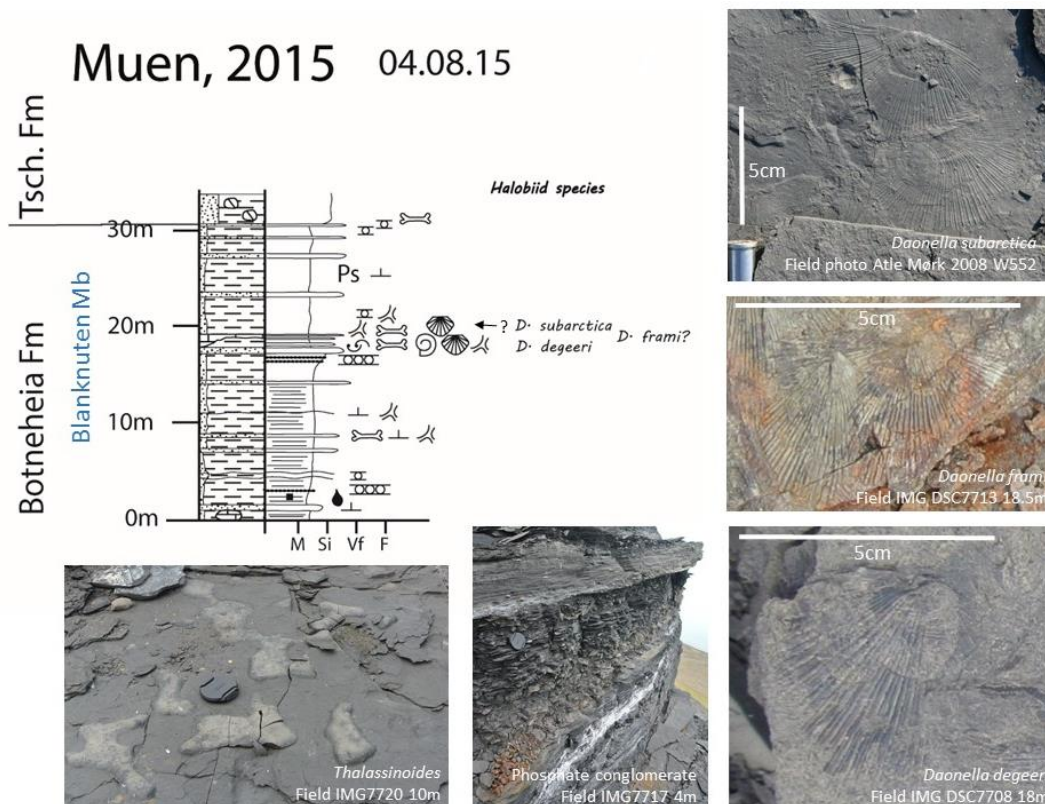
Figure 6.3: Log of fossil finds in the Blanknuten Mb. of the Botneheia Fm. at Muen, Edgeøya. Two horizons of coquina beds were found to contain Daonella degeeri *and* Daonella frami, *in close proximity to unfossiliferous beds and those containing abundant* Thalassinoide*s. Logged by: NB, field assistant: TH.*

54

The Muen plateau, rimmed by slopes and cliffs of a steep gorge, was the first locality visited in the field campaign of 2015 (See Figure 6.2). This locality was defined as the type section for the lower lying Muen Mb. of the Botneheia Fm. in eastern Svalbard by Krajewski (2008). A 31 m log was drawn of the upper part of the Botneheia Fm. (Blanknuten Mb.) up to the boundary to the overlying prodelta shale Tschermakfjellet Fm. marked by purple siderite nodules (Mørk *et al.*, 1999b).

Fossils were not collected on this day but field photos and GPS points document the recurrent anoxic episodes indicated by alternations of beds containing *Thalassinoides* and *Daonella* coquina layers with ammonoid imprints and vertebrate remains.

This plateau provides several excellent bedding planes along which population studies could be carried out in future. *Ichthyosaur* remains were found in various sizes (Hurum *et al.*, 2014) by large and small spinal discs. Two coquina horizons containing vertebrate remains and ammonoid imprints were identified 10 m below the Botneheia Fm.-Tschermakfjellet Fm. boundary. From photographic evidence, the first horizon contains *Daonella degeeri* in varying degrees of fragmentation, overlain by coquina containing the coarse ribbed and smaller *Daonella frami*. Often large, well preserved individuals were found in a matrix of crushed coquina together with rib bones and spinal discs and ammonoid imprints. Between these layers 5-10 cm thick dark grey shales contain no fossils at all. Below the first coquina layers bedding planes fully developed of *Thalassinoides* tunnels alternate with unfossiliferous layers. Vertebrate remains were also documented in siltstone beds without *Daonella* at 9 m and in large siderite concretions in the Tschermakfjellet Fm. Phosphate nodules occur regularly lower down in the section and phosphate conglomerates are found at 4 m and 16 m.

6.1.2 Blanknuten, Edgeøya

The type locality of the Blanknuten Mb. is located at the southern foot of the Blanknuten mountain on Edgeøya (Mørk *et al.*, 1982; Mørk *et al.*, 1999b; Vigran *et al.*, 2014). Here, the Botneheia Fm. forms a steep rocky gorge running N-S and filled with nesting birds on the northern side of Diskobukta, Edgeøya.

Figure 6.4: Overview of the type section of the Blanknuten Mb. at Blanknuten, Edgeøya, with approximate location of the logged section (orange).
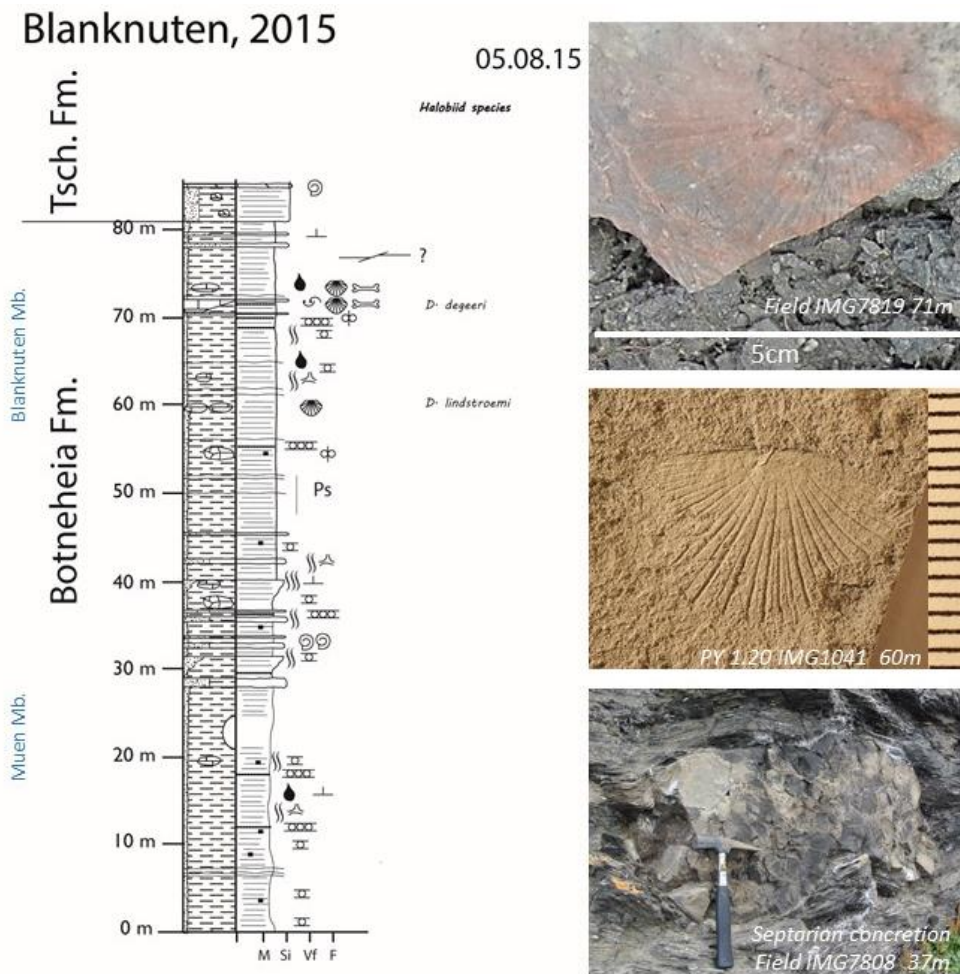
Figure 6.5: Log and fossil finds at Blanknuten, Edgeøya. Coquina beds containing Daonella degeeri *were found 12 m above a specimen of* Daonella lindstroemi. *Logged by: GSL, field assistant: NB.*

The lower most part of the cliff is covered in scree so the 82 m log was drawn from the steep slopes of the lower part of the Botneheia Fm. (Muen Mb.) to the siderite nodules of the Tschermakfjellet Fm. above. The logged section assigned to the Muen Mb. contained phosphate nodules and conglomerates and is therefore phosphogenic unlike the section of the Muen Mb. logged at Muen by Krajewski (2008) . Abundant pyrite nodules were found in the lower and middle part of the section, and sections with unfossiliferous highly organic black paper shale was found at several horizons. Bioturbation mostly in the form of *Thalassinoides* and phosphatised faecal pellets were found in the middle and upper parts. The upper cliff forming part, the type section of the Blanknuten Mb., was strongly bioturbated and contained bivalve coquina beds with ichthyosaur bone. The upper 10 m of the Blanknuten Mb. appeared to be locally deformed and uplifted to the east of the log.

Unfortunately, little fossil evidence was collected from the site but a *Daonella degeeri* coquina layer was found at the top of the Botneheia Fm., 9 m below the siderite nodules at the base of the Tschermakfjellet Fm. A bone bed containing a large ichthyosaur tooth lay 2 m above this bed. A sample containing *Daonella lindstroemi* was taken 12 m below the coquina bed.

6.1.3 Wilhelmøya

A log was made of a cliff-face on a small beach located on the south-eastern shore of the Wilhelmøya Island, at Tumlingodden (Figure 6.6).

The bottom of the succession at Wilhelmøya was defined as the Botneheia Fm. without fossil evidence in Buchan *et al.* (1965). This was later ratified by Smith (1975) and Klubov (1965) who defined the base of the exposed succession as Tschermakfjellet Fm. based on findings of *Halobia zitteli* and *Nathorstites sp.*.

The 5 m logged section consisted of dark grey shales with abundant siderite concretions, nodules and horizons containing halobiid bivalves. All fossil material collected contained juvenile and adult forms of *Halobia zitteli* (see Figure 6.7) and the base of the succession at Wilhelmøya is therefore considered to the Tschermakfjellet Fm. (Klubov, 1965; Smith, 1975) of Carnian age (Korčhinskaya, 1982; Tozer & Parker, 1968; Weitschat & Lehmann, 1983).

Figure 6.6: Overview of the measured section, located on a small beach on the eastern shore of Wilhelmøya at Tumlingodden with approximate formation boundaries (white), and location of the logged section (orange).
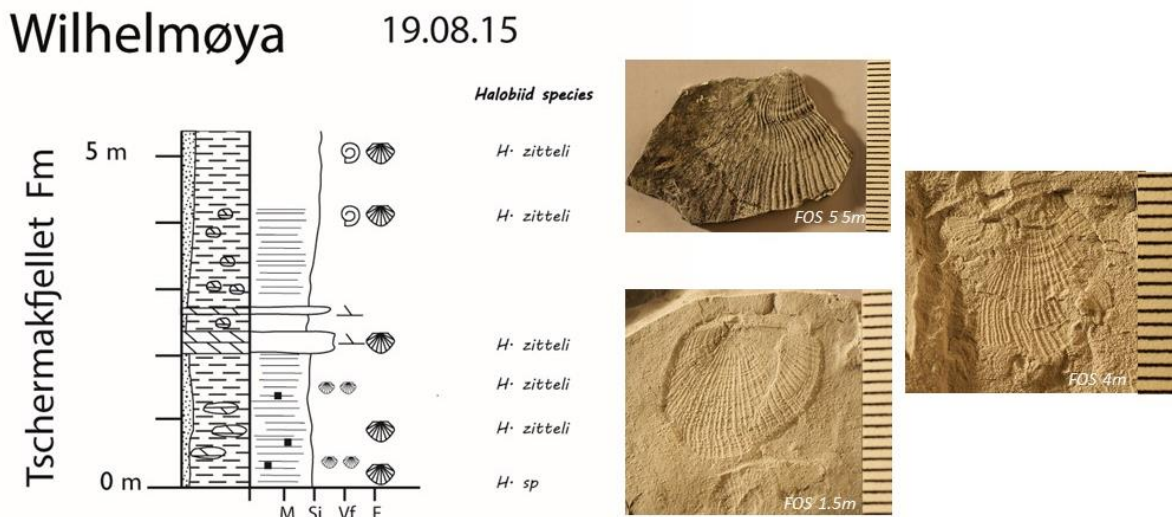
Figure 6.7: Log of section at south-eastern Wilhelmøya. All fossil samples contained specimens of Halobia zitteli. *Logged by NB, field assistant VEN, assisted by AM, BAL.*

6.1.4 Kapp Payer

Two field days were spent on a large plateau at Kapp Payer on the east coast of Olav V Land, north-eastern Spitsbergen. Although no suitable log data could be collected, GPS positioned fossil material and field photos from 5 localities provide valuable insights into the different species found within the Botneheia Fm. in this area.

Figure 6.8: Overview of a plateau formed at Kapp Payer, located along the eastern coast of Olav V Land, eastern Spitsbergen. Photo: BH.
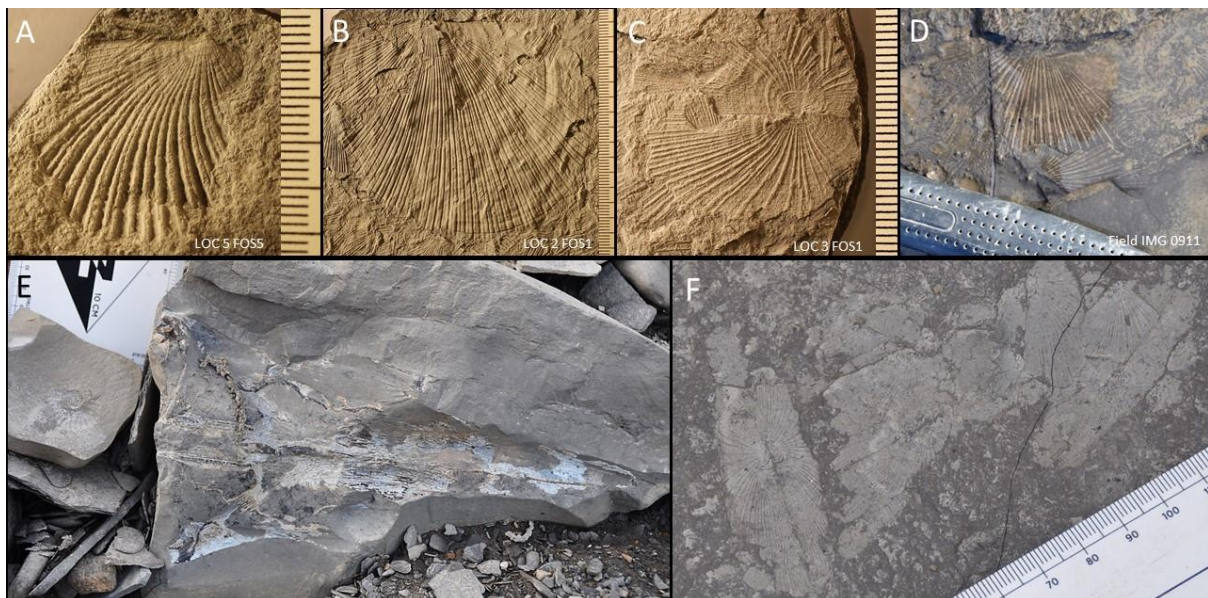
Figure 6.9: Fossils from Kapp Payer A) a specimen identified as Daonella subarctica, *but with very strong resemblance to* Daonella prima*. B) a large and well preserved flattened specimen of* Daonella degeeri *lying on top of a highly fragmented coquina layer. C) A whitened articulated specimen of* Daonella lindstroemi *with a flared ribbing pattern. D) Field photo of possible specimen of* Daonella prima*. E) A skull of an ichthyosaur (?), found in a large concretion in a riverbed. F) Many articulated specimens of* Daonella lindstroemi*. Photos and fossil samples collected by NB, BH, VEN and AM.*

Several unique finds of species were made here, for example of a specimen identified as *Daonella subarctica*, but with very strong resemblance to *Daonella prima,* not currently described from Svalbard but described from Ladinian of Frans Josef Land by Korčhinskaya (1985) and northeast Siberia by Kurushin and Truschelev (2001). Several other species of *Daonella* which have been collected from this location do not resemble species identified from elsewhere in Spitsbergen.

The large bedding planes at Kapp Payer allowed a rare glimpse into the paleoenvironment on the sea floor in the middle part of the Botneheia Fm. The following observations to be made and photographically documented whilst moving south, upward in the stratigraphy along gently upwards tilting layers along an outcrop on a cliff along a beach. Judging by the species of *Daonella* present, this was most likely the transition between the upper part of the Muen Mb. and the Lower part of the Blanknuten Mb.:

i) Zoophycos without *Daonella*, ii) *Zoophycos* with small *Daonella* sp. and large ammonoid imprints with no traces of *Thalassinoides,* iii) Above this many pyritised articulated medium sized *Daonella lindstroemi* with large ammonoid imprints and *Zoophycos*, iv) Smaller ammonoid imprints and small phosphate nodules, no *Daonella*, v) large articulated *Daonella* and *Zoophycos*, vi) a bed full of both single-valve and articulated *Daonella lindstroemi* with straighter ribs and a large ammonoid imprint, vii) Above this, a phosphate conglomerate with large ammonoid imprints and no *Daonella*, and a strong smell of hydrocarbons, viii) 10 m above this, oolitic grainstones and large concretions with no *Daonella* observed.

Although not accurately recorded in a log, one could imagine from these observations a shift from a *Zoophycos* dominated oxygenated deep offshore environment gradually colonized by benthic *Daonella lindstroemi* to a shallower higher energy environment with disarticulated *Daonella lindstroemi.* This is replaced by an oxygenated environment dominated by *Thalassinoides,* which were subsequently reworked and deposited in an anoxic environment without benthos but a healthy planktonic community. Such a development fits well with the paleoenvironmental interpretation of Krajewski (2008): prevailing oxic conditions which became dysoxic in the upper part of the Muen Mb. and lower Blanknuten Mb., to euxinic conditions in the middle part of the Blanknuten Mb. followed a regression. If *Daonella* were indeed pseudoplanktonic (Campbell, 1994), they should be found in the same associations as the ammonoids, in corresponding numbers and sizes (corresponding to age).

6.1.5 Hahnfjella

Two sections were logged at Hahnfjella, eastern Spitsbergen during the 2015 field campaign. A log of the first section visited furthest south, is presented here as the second log focused on the yellow siltstone beds at the top of the Muen Mb. where no fossil information was noted or collected.
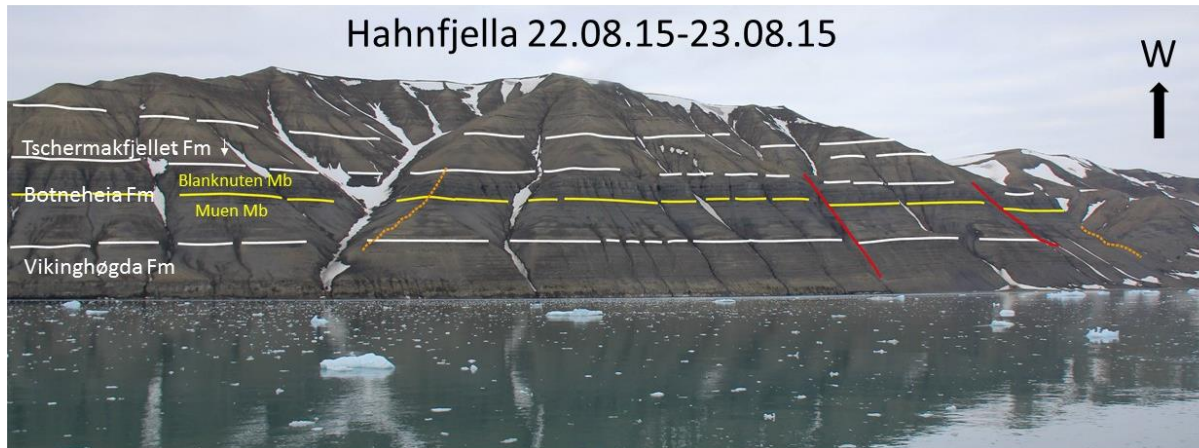
Figure 6.10: Overview of the eastern slopes of Hahnfjella, eastern Spitsbergen, with approximate formation boundaries (white) and members (yellow), and location of faults (red). Two sections were logged during two days (orange stippled lines), logged section to the right.

The Botneheia Fm. was 115 m thick which is the greatest thickness measured during the two field seasons. No obvious signs of deformation were seen except for two normal faults seen in the mountain side (Figure 6.10).

The Botneheia section of the eastward facing slopes of Hahnfjella, form a steep angle down to the sea, where the Vikinghøgda and lowermost 20 m of the Botneheia Fm. are largely covered by scree. The upper part of the Blanknuten Mb. contains bivalve coquina beds forming large bedding surfaces towards the top of the section. Phosphate nodules were found throughout the section except for the lower part of the Muen Mb. Phosphate conglomerates were found at several horizons near phosphatised faecal pellets.   Two prominent siltstones were found containing reworked phosphate nodules 65 m above the lower boundary of the Botneheia Fm.

The base of the Botneheia Fm. was identified by a yellow siltstone bench containing abundant *Rhizocorallium,* a known marker bed from the Sassendalen area (Mørk *et al.*, 1999b). *Daonella lindstroemi* was found 15 m below coquina beds containing *Daonella degeeri* at 102 m. Echinoderms and brachiopods, and other bivalve species were found in the upper parts of the Blanknuten Mb.
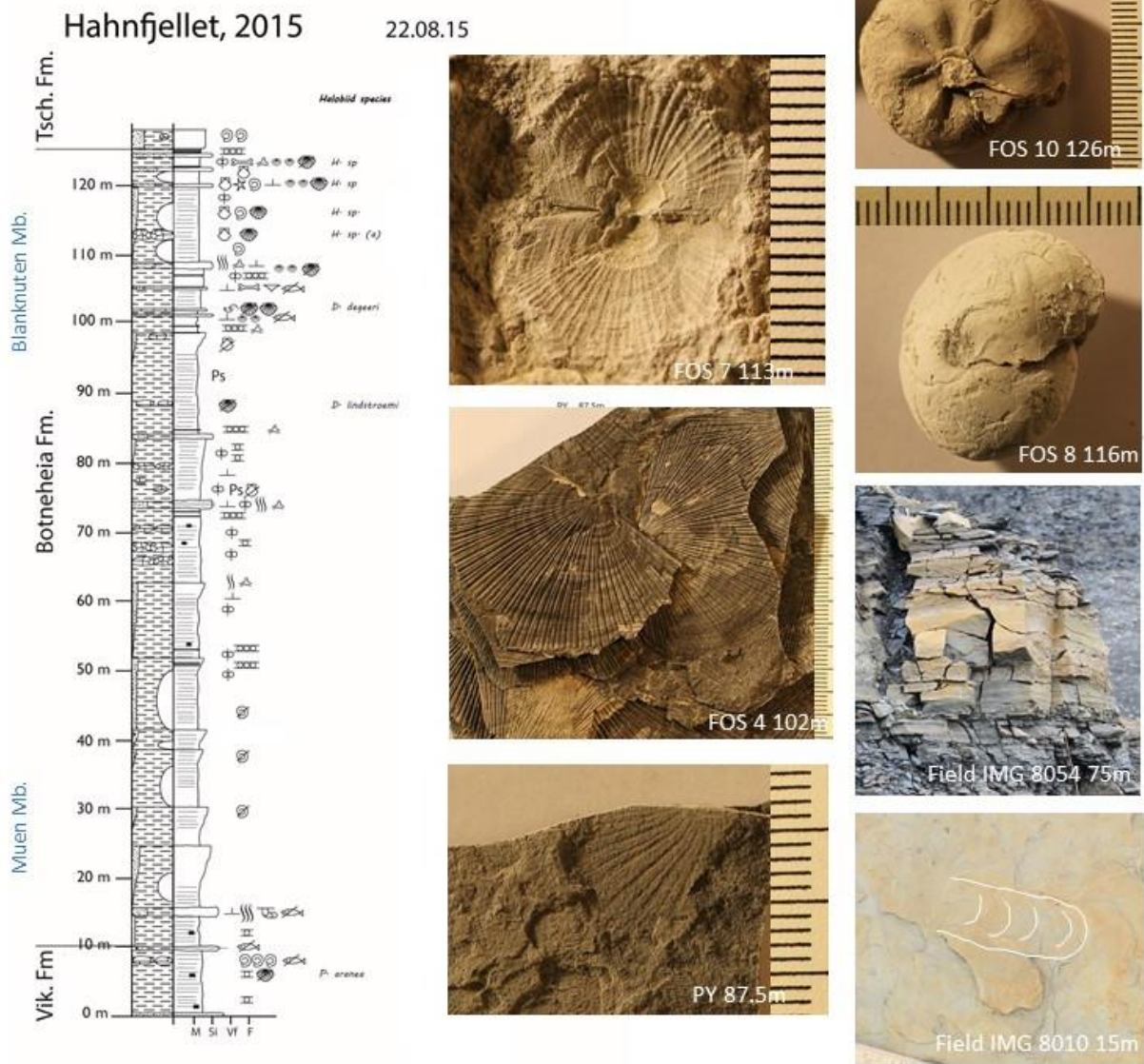
Figure 6.11: Log of the Botneheia Fm. at Hahnfjella. A yellow Rhizocorallium *bed and prominent yellow siltstone with reworked phosphate nodules are shown.* Daonella lindstroemi *was found 15 m below* Daonella degeeri *at 102 m. Specimens of a transitional form with characteristics of juvenile* Halobia zitteli *were found 10 m below Tschermakfjellet Fm. boundary, stratigraphically below Ladinian ammonoid* Indigirites tozeri *at 116 m (Weitschat & Lehmann, 1983). Ammonoid* Stolleyites planus *found above base Tschermakfjellet Fm. is known from the Lower Carnian (Dagys et al. (1993). Logged by NB, with assistance of AM.*

At Hahnfjella, the *Daonella degeeri* coquina beds occur 23 m below the siderite nodules of the overlying Tschermakfjellet Fm. (Mørk *et al.*, 1999b). This is the thickest sequence overlying the *Daonella degeeri* coquina beds measured at any location during the 2015 and 2016 field seasons. Krajewski (2008) correlated sections he made on Edgeøya and Barentsøya placing a datum at the coquina layers at the top of the Blanknuten Mb. In doing so he noticed significant thickness changes at the boundary to the Tschermakfjellet Fm. Interestingly, within the siltstone

beds of this uppermost sequence, several halobiid specimens were found with characteristics typical of juveniles of *Halobia*, including auricles which are wide, especially on the posterior side. The flattened area could be interpreted to represent the "byssal tube" of Campbell (1994). The specimens were too small to form the characteristic growth stop found in adult specimens of *Halobia zitteli*, which according to measurements outlined in Chapter 8. Data Analysis, usually occur at the growth stage corresponding to approximately 1 cm height. The specimen identified as *Halobia* sp. in

Figure 6.11, was found 3 m below an ammonoid tentatively identified as *Indigirites tozeri* of Weitschat and Lehmann (1983). This species is known from the uppermost substage of the Ladinian on Svalbard. This suggests that the halobiid in question is a Ladinian form possessing some characteristics of *Halobia*.

The siltstone beds and phosphate conglomerates usually found at the boundary between the upper Blanknuten Mb. and overlying Tschermakfjellet Fm. (Krajewski, 2008), rarely contain bivalve fossils which are well preserved. One can therefore speculate that transitional forms between *Daonella* and *Halobia* which are usually not well preserved at this boundary elsewhere, occur at Hahnfjella because a thicker sequence is preserved here. As discussed in Chapter 2.3. Structural Geology, the NNW-SSE Lomfjorden fault runs 15 km to the west of Hahnfjellet (Figure 2.5) and is suggested to have had impact on facies and thickness developments of the Sassendalen Group (Mørk *et al.*, 1982). This will be investigated further in Chapter 9.5.1 Thickness variations of the Botneheia Fm.

6.1.6 Kvitberget

No fossil data was collected from Kvitberget and the log from this locality is poor due to bad weather and a visit from a polar bear who indicated interest our rubber boats. Information from this location is therefore not included here.

6.1.7 Vossebukta

A small outcrop was logged along a beach on the eastern shore of Vossebukta on Barentsøya. The outcrop lies below a large fold and overlying dolerite sill.

The extensive deformation of the overlying strata limited the outcrop to the beach section where fossil specimens of *Daonella lindstroemi,* ammonoid imprints and phosphate nodules were documented and collected (see Figure 6.13).

Figure 6.12: Overview image of logged section at Vossebukta
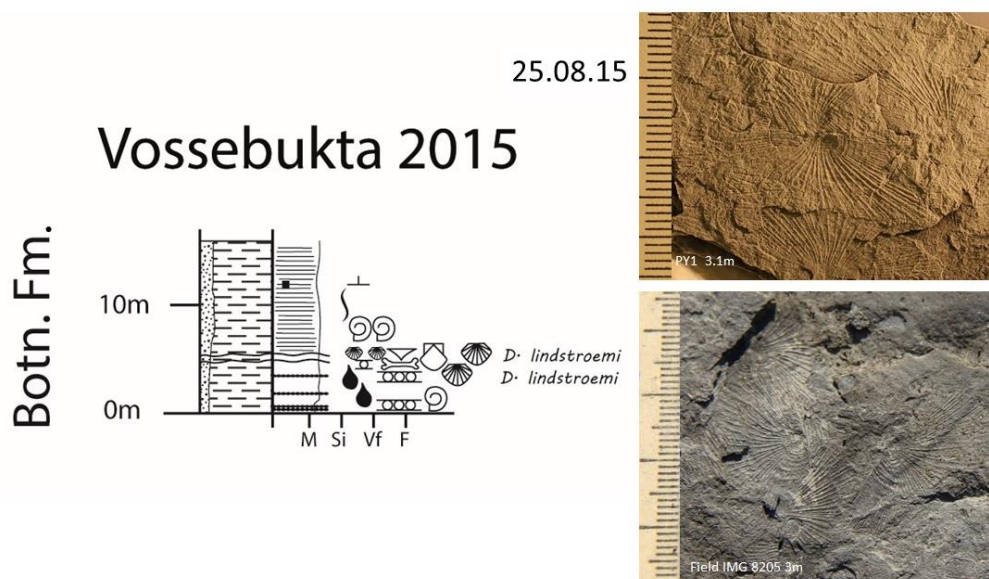
Figure 6.13: 15 m log from a beach section at Vossebukta. Both articulated and single-valves where found of Daonella lindstroemi *indicating Late Anisian to Early Ladinian age of the beds at this outcrop, likely near the base of the Blanknuten Mb. Logged by GSL, assisted by NB and VEN.*

64

6.1.8 Krefftberget

Krefftberget, a mountain at the southern edge of Barentsøya, was the last locality visited during the field campaign in 2015.
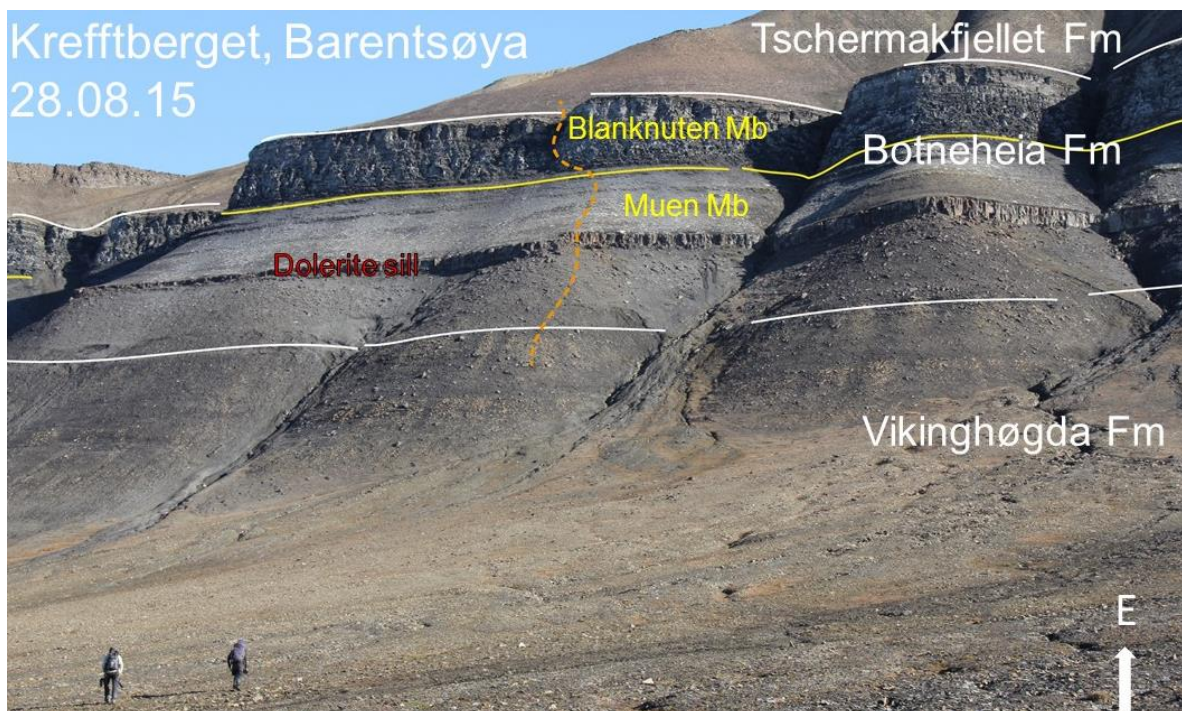
Figure 6.14: Overview of log at Krefftberget, Barentsøya, with approximate formation (white) and member (yellow) boundaries and section logged (orange stippled line).

An 86 m log was drawn from the top of the Vikinghøgda Fm. to the base of the Tschermakfjellet Fm. An approximately 5 m thick dolerite sill cuts the Muen Mb. in two, above and below which there is a considerable amount of scree.

The cliff-forming Blanknuten Mb. is well exposed here but forms very steep cliffs which are not ideal for fossil collecting activities. A handful of fossil specimens were collected including *Posidonia aranea* at the top of the Vikinghøgda Fm., *Daonella degeeri* coquina in the upper part of the Blanknuten Mb. and *Halobia zitteli* juveniles in siderite nodules. I was kindly given a large collection of ammonoids, bivalves and nautiloids collected along the base of the Tschermakfjellet by Russian researcher Marina Tugarova and assistants at Krefftberget. This includes *Halobia zitteli* juvenile and adult specimens and ammonoid *Stolleyites planus* (tentative identification) in siderite concretions in the overlying Tschermakfjellet Fm. *Daonella degeeri* coquina layers were found a mere 2 m below the purple siderite nodules of the

Tschermakfjellet Fm. This may support the observations of Krajewski (2008) of thinning of the upper Blanknuten from Muen on Edgeøya to Skarpryttaren on Barentsøya due to the discordant erosional boundary under the Tschermakfjellet Fm.
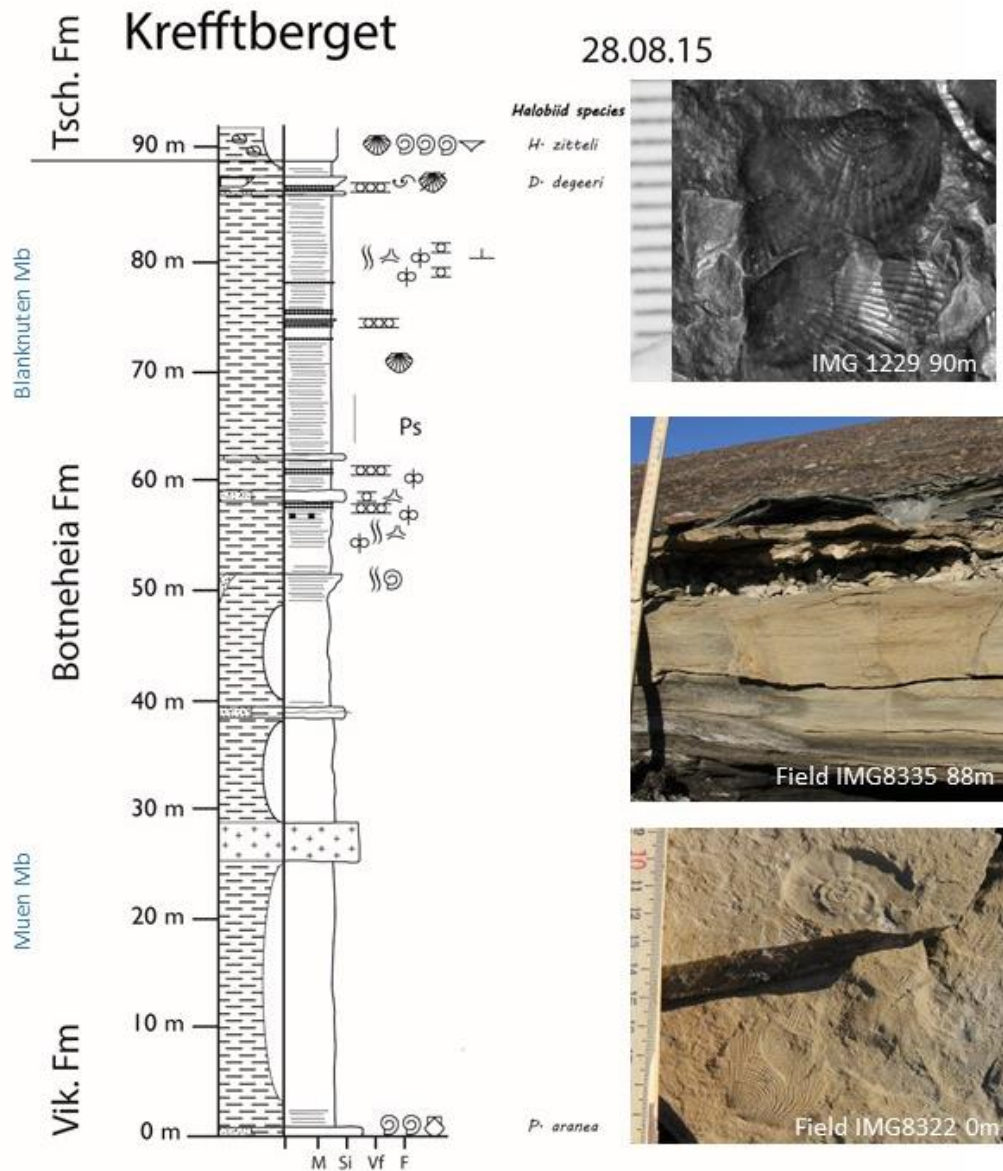
Figure 6.15: Log of the Botneheia Fm. at Krefftberget, Barentsøya. Posidonia aranea, a known marker bed indicating the top of the Vikinghøgda Fm. (Hounslow et al., 2008). Daonella degeeri coquina layers found at the top of the cliff-forming unit. Halobia zitteli juveniles were found in siderite concretions above the coquina beds. Abundant pellets and phosphate conglomerate were found near the base and top of the Blanknuten Mb. Logged by NB, assisted by VEN and AM.

6.2 Fieldwork 2016

6.2.1 Wallenbergfjellet
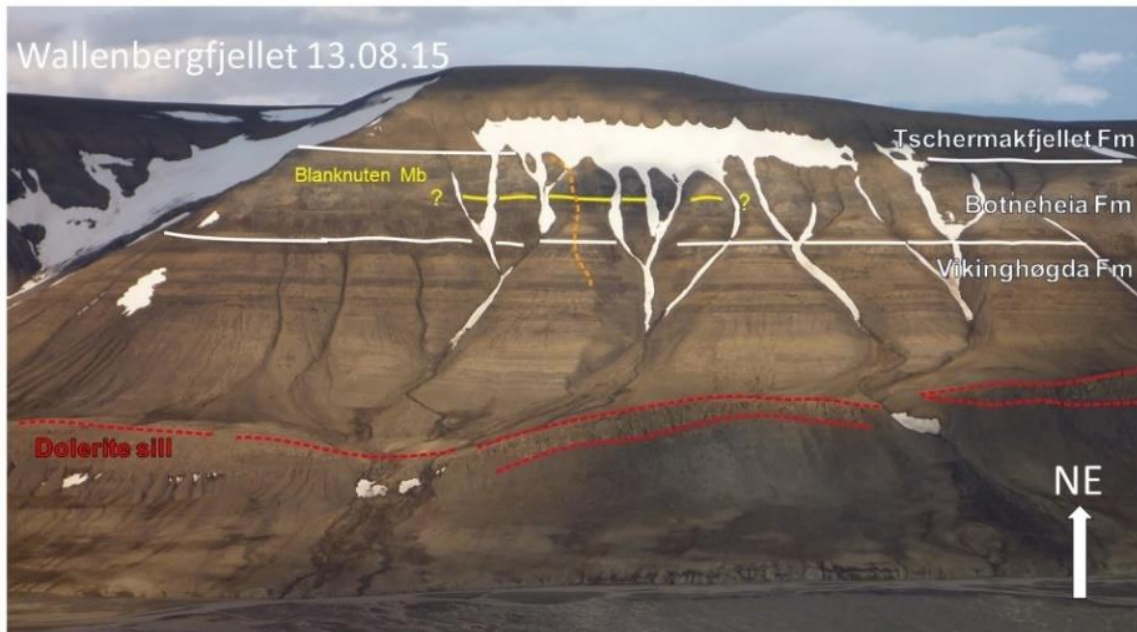
Figure 6.16: Overview of the SW slope of Wallenbergfjellet, Fulmardalen, with approximate formation (white) and member (yellow) boundaries and section logged (orange stippled line). A dolerite sill climbs through the Vikinghøgda Fm. and Botneheia Fm. towards the east. The boundary to the Tschermakfjellet Fm is strongly deformed and covered by snow.

The first log of 2016 field season was made at Wallenbergfjellet, on the north-eastern side of Fulmardalen. A total of 140 m were logged from the Upper Vikinghøgda Fm. to the lower parts of the Blanknuten Mb. Strong deformation of the uppermost beds of Botneheia and snow cover cut the top of log short.

A yellow siltstone containing abundant *Rhizocorallium, Thalassinoides,* and *Phycosiphon* (tentative identification) was found at Wallenbergfjellet and is a known marker bed appearing 7 m above the base of the Botneheia Fm. in Sassendalen (Hounslow *et al.*, 2008). This marker bed was found at all the localities visited in Fulmardalen. Two prominent yellow siltstones containing reworked phosphate nodules were found 45 m above the base of the Botneheia Fm., equivalent to those found at Hahnfjella, day 2. *Daonella lindstroemi* was found 33 m below coquina beds containing *Daonella degeeri.* In between these two fossil finds is a large deformation zone, making thickness measurements between these layers unreliable.
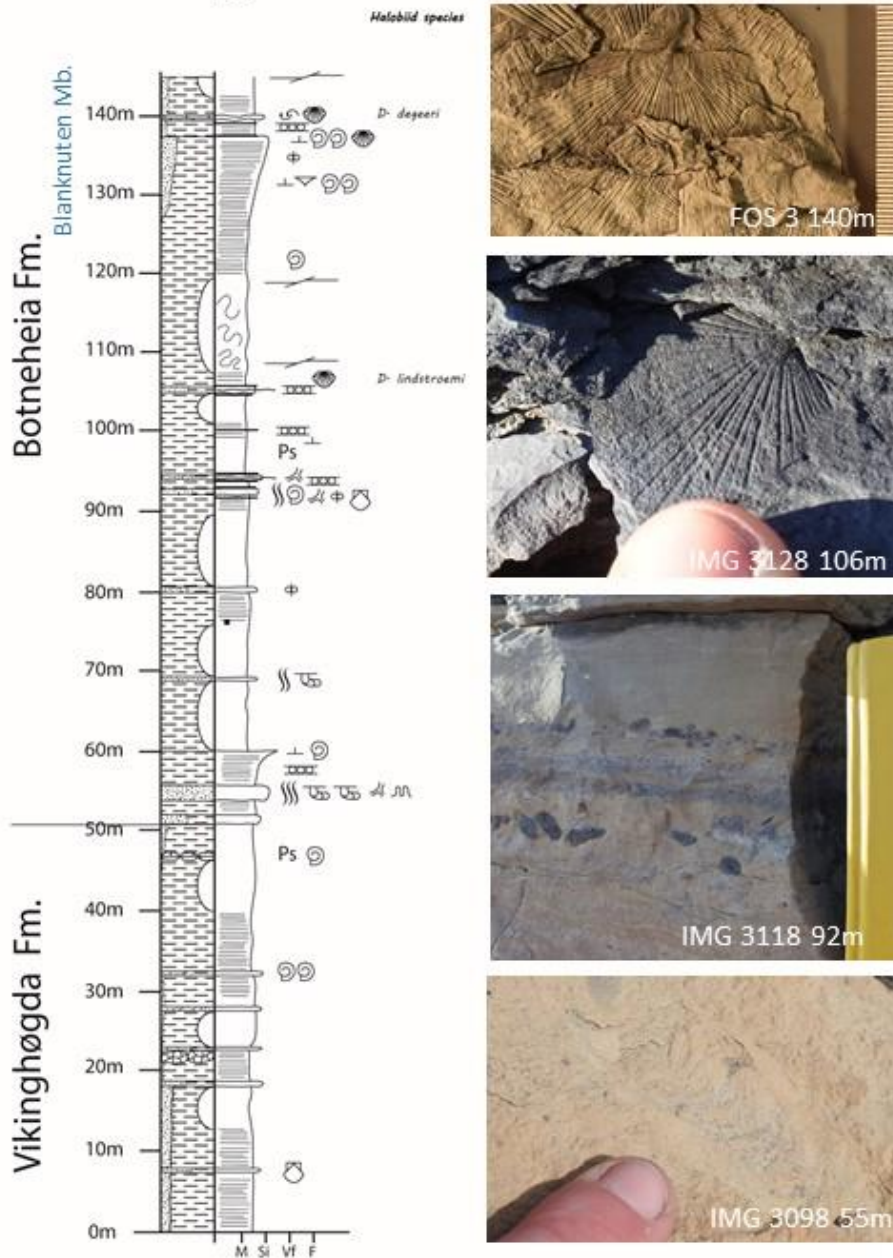
Figure 6.17: Log of SE slope of Wallenbergfjellet, Fulmardalen. The yellow siltstone containing abundant Rhizocorallium *is located 7 m above base Botneheia Fm. Two prominent yellow siltstone beds appear 40 m above this boundary.* Daonella lindstroemi *(with straight ribs) occurs 33 m below* Daonella degeeri *coquina beds. Logged by NB, assisted by MV and JR.*

6.2.2 Dyrhø

The Botneheia Fm. exposed on the north-eastern slopes of Dyrhø Mountain was logged at 3 locations. The black cliffs gently dip towards the southeast, eventually disappearing under scree of the surrounding mountain sides and Marmorbreen at the innermost part of Fulmardalen (

Figure 6.18). The boundary between Botneheia Fm. and Tschermakfjellet Fm. was often covered in scree so could not be accurately measured except for at Log 2.
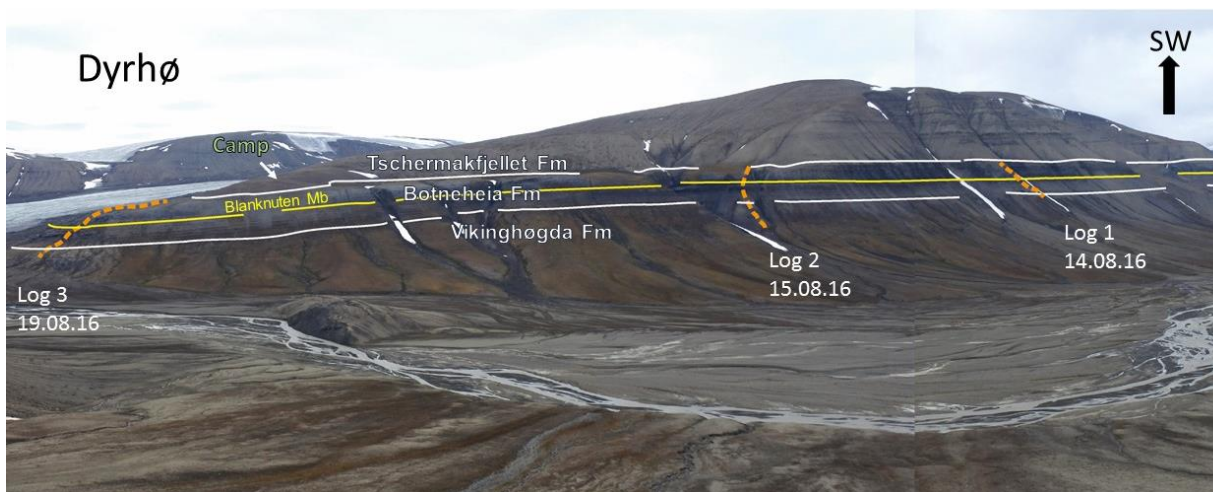
Figure 6.18: Overview of Dyrhø mountain, southwestern Fulmardalen, with locations of 3 logs (orange stippled lines) and approximate formation (white) and member (yellow), and location of the field camp (light green). The Triassic succession dips towards the southeast in Fulmardalen.

The first log started at a prominent yellow siltstone with oolitic grainstone layers. A vivianite enriched vertebrate bone fragment was found in highly organic, calcite cemented black paper shales at 40 m, with small brachiopods. Phosphatised faecal pellets and phosphate conglomerates were found near the base and top of the log. *Daonella degeeri* coquina layers were found at the top of the log. Scree containing articulated *Halobia zitteli, Daonella degeeri*, and fragments of omission surfaces containing reptile and fish remains, covered the boundary to the overlying Tschermakfjellet Fm. (Figure 6.19).
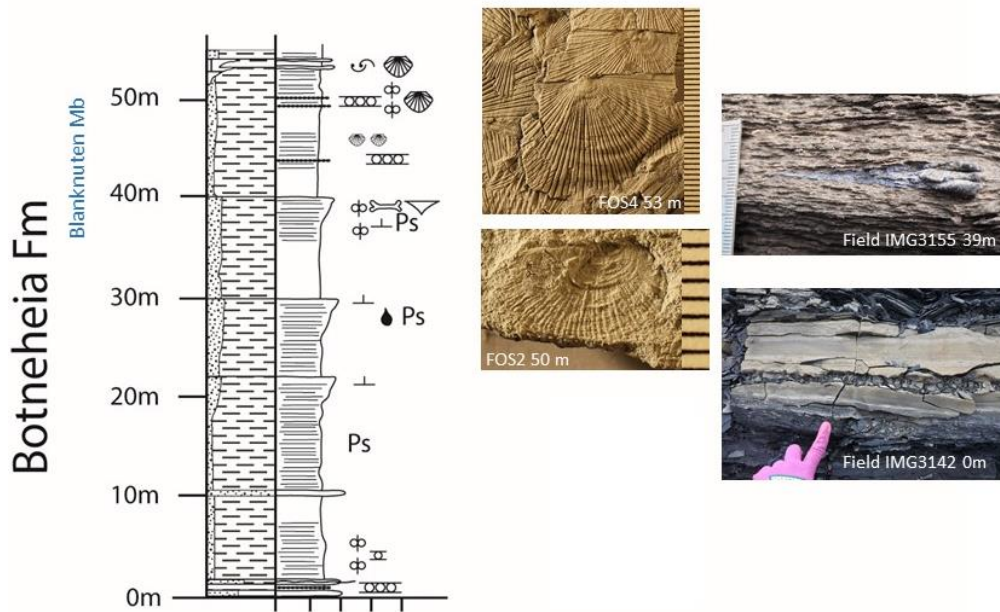
Figure 6.19: Log 1 at Dyrhø. Samples of Daonella lindstroemi *coquina beds were collected from the top of the section. Logged by NB, assisted by MV and SB.*
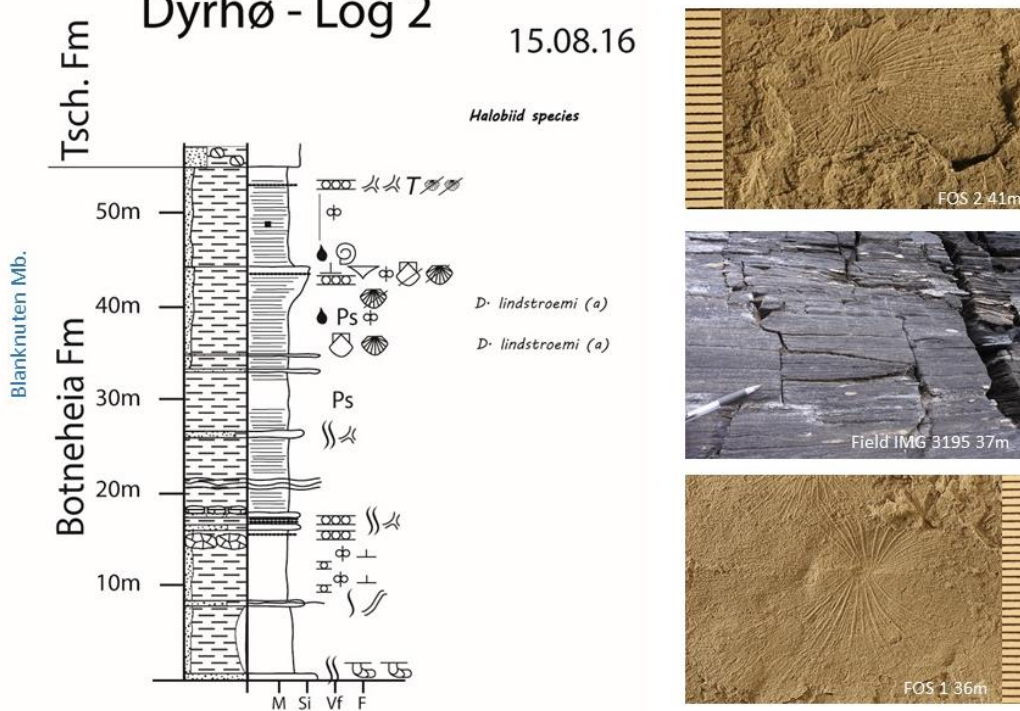
Figure 6.20: Log 2 of Dyrhø. Articulated Late Anisian to Ladinian age Daonella lindstroemi *was identified from two beds half-way up the log. Logged by NB, assisted by SB and JR.*

The second log was started at a prominent yellow siltstone containing abundant *Rhizocorallium*. Approximately 16 m above this bed two prominent yellow siltstones containing reworked phosphate nodules and thin oolitic grainstone horizons. Beds containing *Daonella lindstroemi* were found 15-20 m below the siderite nodules of Tschermakfjellet Fm. The two beds containing *Daonella lindstroemi* were separated by a black, highly organic paper shale. The *Daonella degeeri* coquina beds recognised from all other localities where this formation boundary was logged, was not present here, possibly due to discordant erosion of the upper boundary (Krajewski, 2008) or Tertiary age deformation, however no repeating fossil finds or obvious signs of distortion were recorded from this locality. If one were to consider the *Rhizocorallium* bed to be a true indicator of the base of the Botneheia Fm. in this area, then the entire formation is not more than 56 m thick at this location (Figure 6.20).
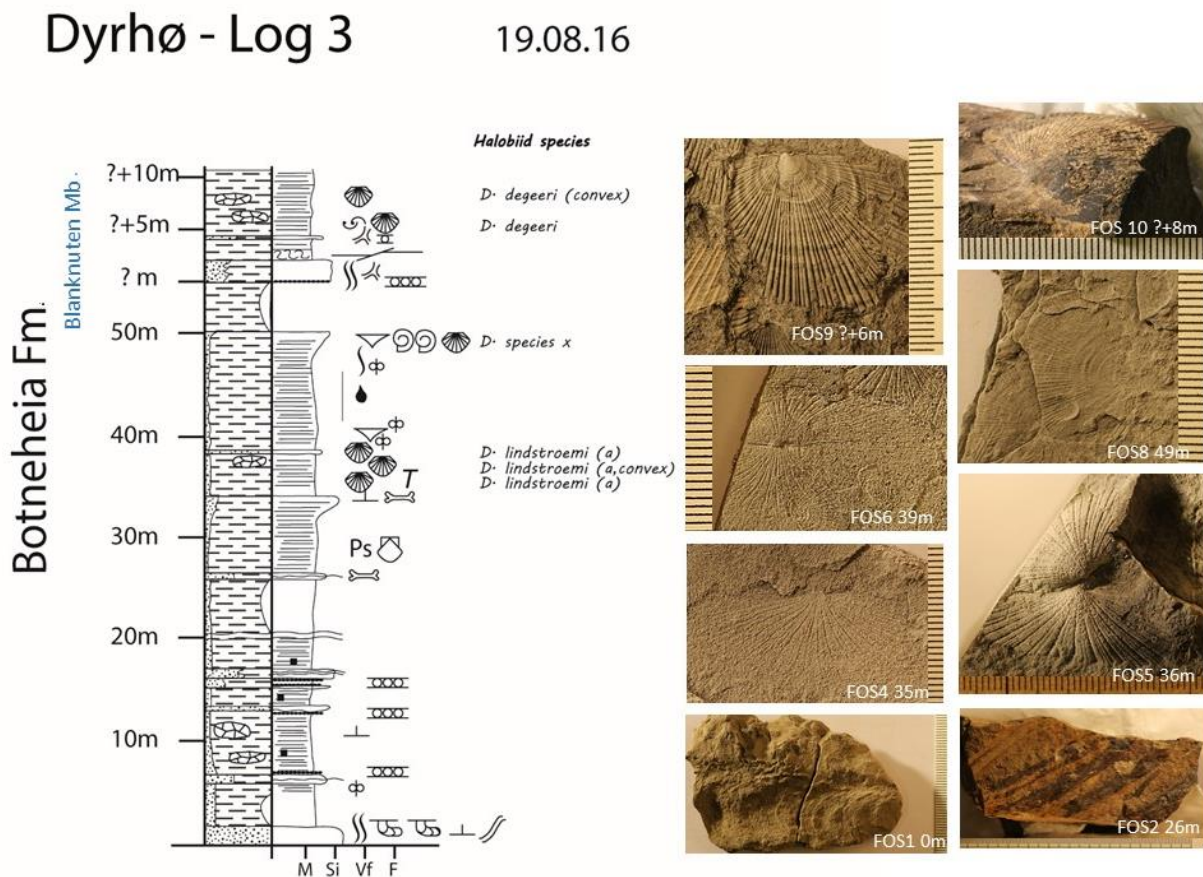
Figure 6.21: Log 3 from Dyrhø, which starts at the Rhizocorallium *marker bed, above which there are siltstones containing vertebrate rib bones. Three bedding planes are found to contain* Daonella lindstroemi *in both flattened and inflated form. A prominent bioturbated siltstone lies under the* Daonella degeeri *coquina layers at the top of the log. These layers contain both flattened specimens and several inflated specimens found around a large concretion above the coquina layer. Logged by NB, assisted by SB.*

The third section of approximately 65 m was measured at the south-eastern foot of Dyrhø, bordering Marmorbreen. At this location, the Botneheia Fm. gently dips into the valley floor forming an eroded plateau exposing the Blanknuten Mb. The exact elevation of the top 15 m of the log was impossible to measure precisely due to numerous gulleys which formed on top of the plateau. Large bedding planes of the middle part of the Botneheia Fm. are exposed at this location, allowing for good fossil collecting.

The log was started at the characteristic yellow siltstone, containing abundant *Rhizocorallium* and *Phycosiphon*. Above this, several horizons were found containing phosphate conglomerates and pellets. Two prominent yellow siltstone beds containing reworked phosphate nodules and oolitic grainstones were found 12 m above the *Rhizocorallium* siltstone. The first finds of halobiids, was made above a siltstone bench containing vertebrate rib fragments, interpreted to represent the base of the Blanknuten Mb.

Daonella lindstroemi was collected in three different bedding planes of varying lithologies. Specimens preserved in dark grey paper shale were articulated and flattened whilst those preserved in a cemented siltstone were either articulated or single-valved and retained a 3D convex form. The fragmented and disoriented single-valved specimens suggest that currents or mass flows may have had a role in forming those layers. *Daonella lindstroemi* was found together with large and small brachiopods below a section of unfossiliferous highly organic black paper shales. 10 m above the *Daonella lindstroemi* beds, a few fragmented specimens of an unidentified halobiid "species x" resembling *Daonella moussoni* were found in a dark grey shale. At the top of the log a coquina bed containing *Daonella degeeri* was found in close proximity to a large concretion where several inflated specimens were found (See Figure 6.21).

One can speculate that species of *Daonella* found in black shales are in fact not as flat as described by Schatz (2005) and others. Specimens of what appear to be the same species are found in a completely flat form in dark grey shales whilst inflated specimens are found in cemented siltstone beds and around large concretions (see photos of inflated *Daonella lindstroemi* and *Daonella degeeri* in Figure 6.21). According to Krajewski (2008), these "cement-stone beds", have a matrix composed of euhedral dolomitic microspar, suggesting that they are in fact of purely diagenetic origin, developing later during diagenesis, before ultimate compaction of the sediment. One can speculate that *Daonella* was not flat when living and that these bivalves are often preserved in this form due to compaction during burial, and those preserved in strata affected by diagenetic processes or coarser lithologies retain their original inflated shape.

72

The Botneheia succession at Dyrhø dips towards the southeast and is unusually thin, approximately 55-65 m thick as compared to 75 m at Milne Edwardsfjellet further north-west. A log was made of Roslagenfjellet lying approximately 10 km to the south-east of Dyrhø by Atle Mørk and Arne W. Forsberg in Vigran *et al.* (2014), where the entire Botneheia Fm. is measured to a mere 70 m compared to approximately 120 m at Hahnfjella measured in 2015, which lies on the eastern side of the LFZ. Thickness variations, specifically thinning of the Sassendalen Group west of the LFZ in the Billefjorden Trough are suggested in Mørk *et al.* (1982). One can speculate that the discordant erosional base of the Tschermakfjellet Fm. (Krajewski, 2008) could also accentuate thickness variations, which could explain the absence of the *Daonella degeeri* coquina layers at top of Dyrhø log 2.

6.2.3 Ryssen
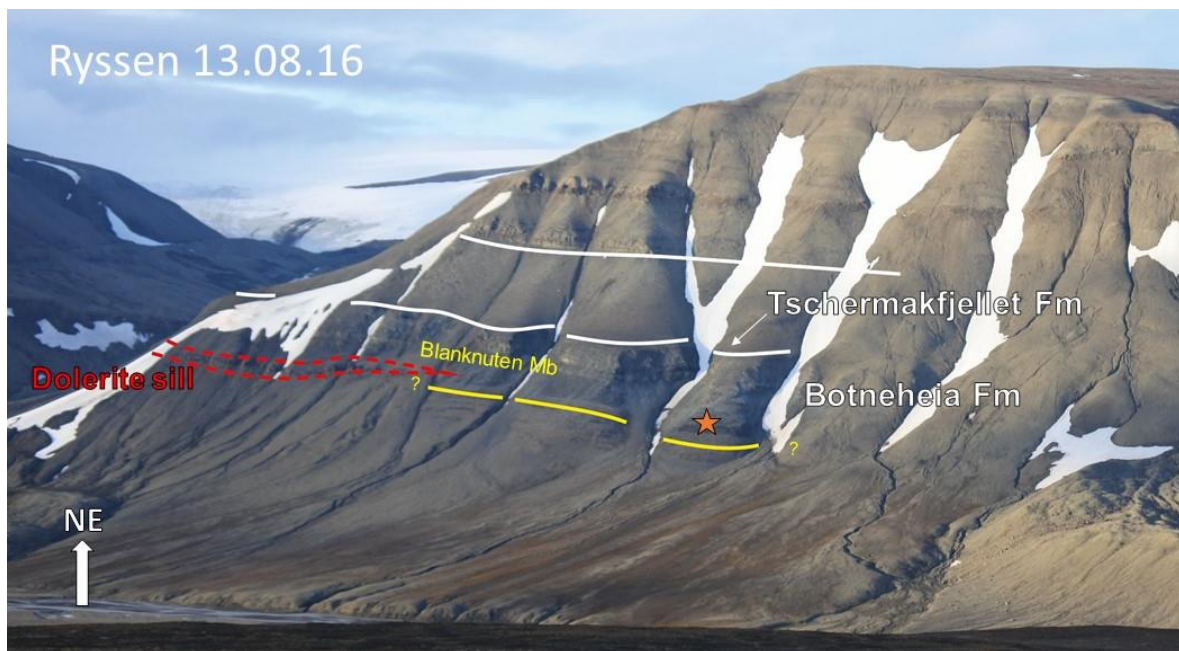
Figure 6.22: Overview of the south-eastern facing slope of Ryssen, Fulmardalen. Intense deformation is seen in the upper part of the Botneheia Fm, together with an intruding dolerite sill (red stippled line). Location of the fossiliferous concretion (orange star) and approximate formation (white) and member (yellow) boundaries.

*Figure 6.23: A, C-E) Fossil finds from a single concretion at the base of the Blanknuten Mb. at Ryssen. B) Highly deformed and metamorphosed calcitic remains of the upper Blanknuten Mb. containing Tasmanites, found in close proximity blocks of dolerite in scree. C) Single-*valve Daonella lindstroemi *with flared ribbing pattern found together with large rib bone fragments in E. D) ammonoid Frechites laqueatus, tentatively identified from Weitschat and Lehmann (1983), together with* Daonella lindstroemi, *places the fauna in the Late Anisian according to Wolfgang Weitschat in Hounslow et al. (2008). Fossil collectors: JR and SB (in photo) and NB.*

No log was made at Ryssen due to extensive scree coverage and to the highly deformed and metamorphosed rocks in the upper Botneheia Fm. However, a sizable amount of fossil material including halobiids, ichthyosaur remains and ammonoids, were collected from single fossil rich concretion near the base of the Blanknuten Mb, indicating the *Frechites laqueatus* Zone of the Late Anisian (Hounslow *et al.*, 2008; Mørk *et al.*, 1993; Weitschat & Lehmann, 1983), see Figure 6.23.

6.2.4 Milne Edwardsfjellet

A 103 m section of the upper part of Vikinghøgda Fm. and the entire Botneheia Fm. was logged along the south-eastern flank of the Milne Edwardsfjellet in Fulmardalen (Figure 6.24).

Figure 6.24: Overview of south-eastern flank of Milne Edwardsfjellet. Location of the logged section (orange stippled line) and approximate formation (white) and member (yellow) boundaries

Here, the base of the Botneheia Fm. occurs 7 m below a yellow *Rhizocorallium* bearing siltstone (Hounslow *et al.*, 2008). Phosphate nodules first start to appear above this bed. Two prominent yellow siltstones with reworked phosphate nodules are found 25 m above the base of the

Botneheia Fm. Articulated *Daonella arctica* was found in a siltstone bed at the base of the cliff-forming Blanknuten Mb., above an unidentified ammonoid, possibly *Frechites laqueatus* (tentatively identified using (Weitschat & Lehmann, 1983). At 90 m there is an intensively deformed 1 m thick section which is overlain by *Daonella degeeri* coquina beds. The coquina beds occur 8 m below the purple siderite nodules of the Tschermakfjellet Fm. at SE Milne Edwardsfjellet. Shell beds containing *Daonella frami* were found 2 m above the coquina beds. Above this, a deformation zone was found containing what appear to be deformed algae mats in thin section. A 2 m thick phosphate conglomerate horizon lies over this under a calcite cemented siltstone bed.
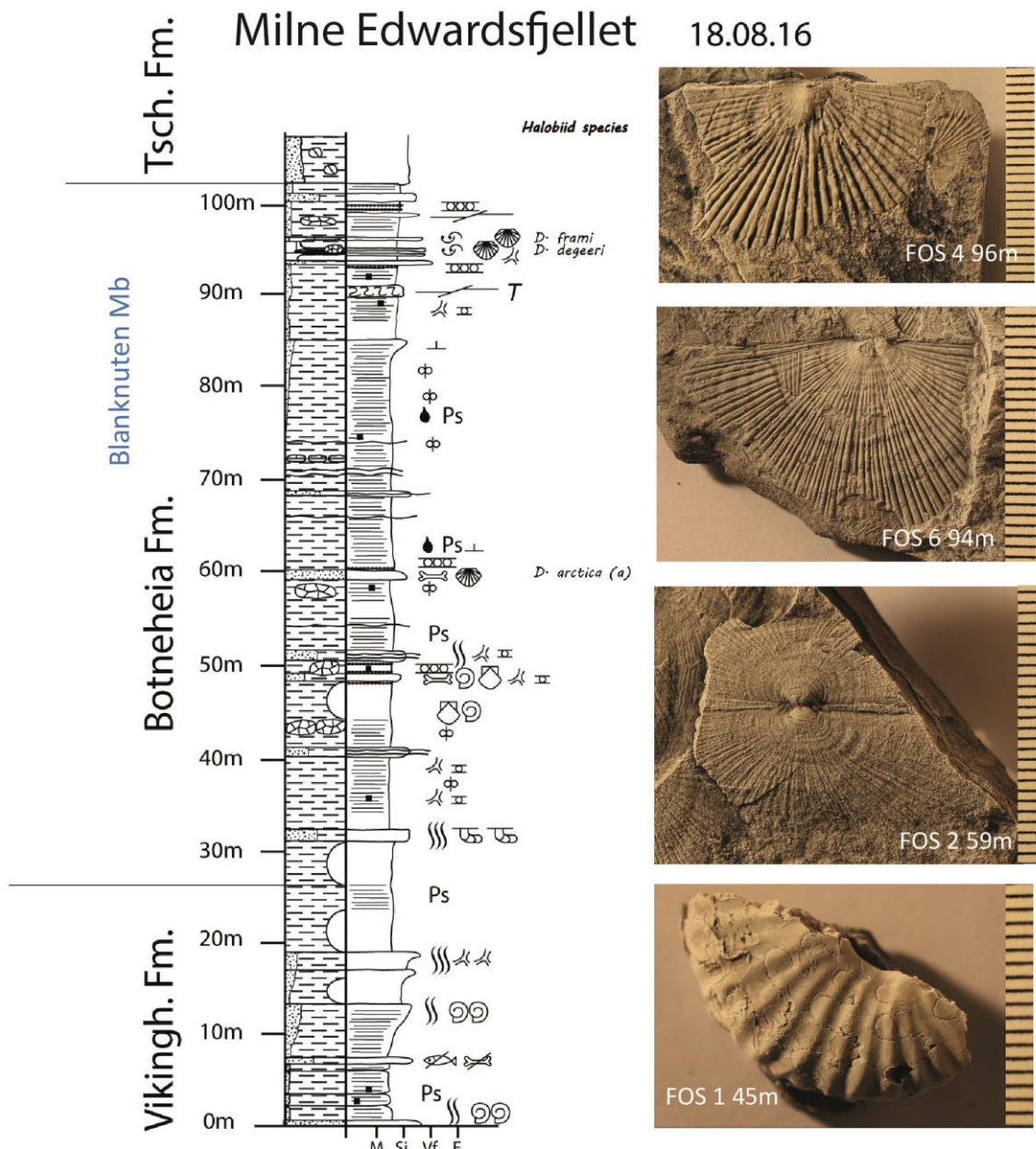
Figure 6.25: Log of SE Milne Edwardsfjellet, Fulmardalen. Ammonoid (unidentified) was found below a siltstone bed containing Daonella arctica *at the base of the Blanknuten Mb. Near the top of the log, a highly deformed and metamorphosed 1 m thick zone containing abundant Tasmanites underlies a coquina bed consisting of* Daonella degeeri. Daonella frami *was found 1 m above the coquina layers. Logged by NB, assisted by MV and JR.*

76
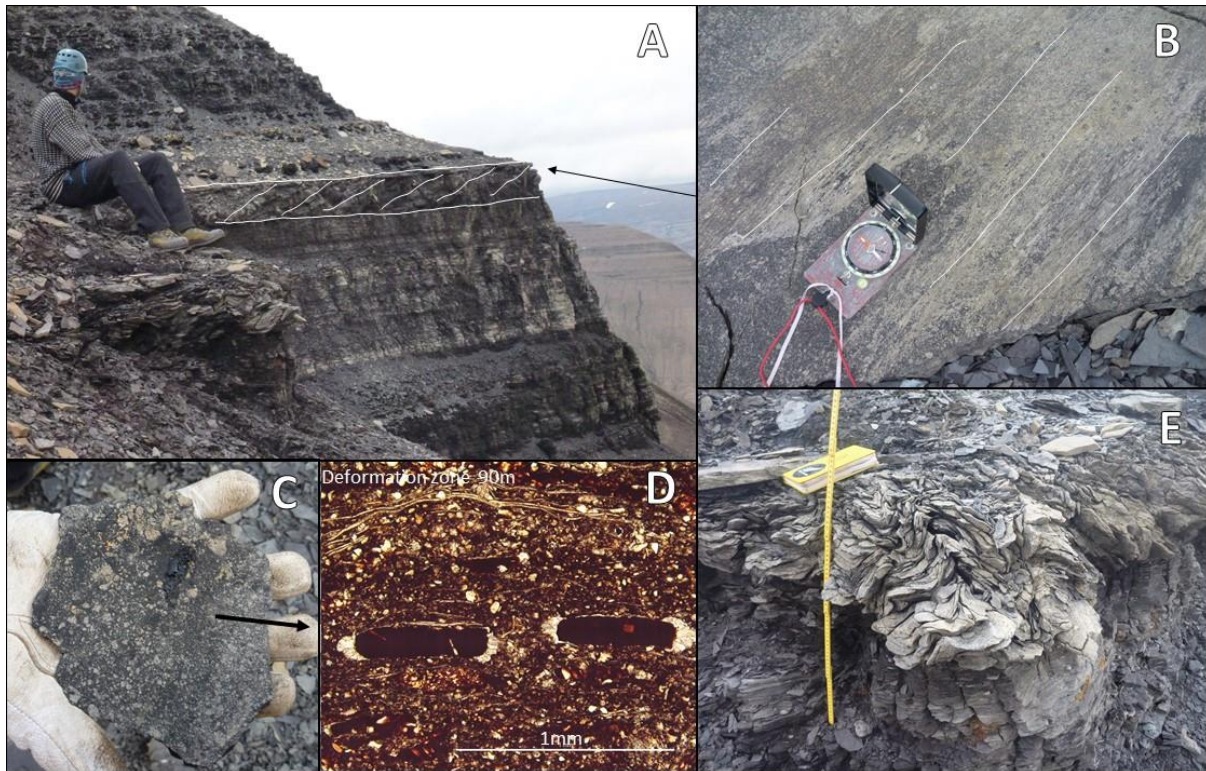
Figure 6.26: Deformation zone at SE Milne Edwardsfjellet. A) A 1 m thick deformation zone is completely confined within the mountain side. B) Slickenslides indicate a W-E trending movement. C) Light grey-black heterolithic metasediments from the highly folded deformation zone (E) where made into a thin section (D) revealing thin shelled bivalve microcoquina and flattened thermally decomposed Tasmanites, replaced by exudatinite (Brekke et al., 2014) and dolomite, in an organic rich matrix.

Two sections were logged of the Botneheia Fm. on the western side of Milne Edwardsfjellet in Sassendalen by Atle Mørk and dated using ammonoids and bivalves by Wolfgang Weitschat (Hounslow *et al.*, 2007b; Hounslow *et al.*, 2008; Vigran *et al.*, 2014). In addition to the *Daonella degeeri,* they found *Daonella lindstroemi* 11 m below and *Daonella subarctica* 3 m above the coquina beds. According to (Hounslow *et al.*, 2008), the succession on the eastern side of Milne Edwardsfjellet is a comparatively complete section exposing the latest Spathian to the middle Anisian, whereas the late Anisian to Ladinian is comparatively condensed into about 70 m, with the latest Ladinian being absent. There is a high sedimentation rate into the early Anisian at the lower part of the Botneheia Fm. (Hounslow *et al.*, 2008).

In addition to numerous fossil finds, south-eastern Milne Edwardsfjellet contains an interesting deformation zone, 12 m from the top of the Botneheia Fm. (Figure 6.26Figure 6.26A). The intense deformation appears to be completely isolated to a 1 m thick zone, bordered above and below by horizontally lying apparently unaffected dark grey shales and slickensides indicating

a W-E movement (Figure 6.26 B and E). Light grey metamorphosed sediments within the zone are full of *Tasmanites,* similar to what was found at Ryssen a few days earlier. A thin section was made of the material within the zone (Figure 6.26 C and D) which turned out to contain abundant *Tasmanites* algae and microcoquina (Figure 6.26 D).

Images of thin sections of flattened *Tasmanites* cysts from the Botneheia Fm. at Sticky Keep, further west in Sassendalen, presented by (Vigran *et al.*, 2008), have thick lipoid -rich walls which appear orange in the thin section with a void in the middle. *Tasmanites* cysts from the upper Blanknuten Mb. at Muen described by Brekke *et al.* (2014), are thermally decomposed, reaching advanced maturity due to nearby dolerite intrusions. In these thin sections, the decomposed *Tasmanites* cyst is partly replaced by quartz and partly by exudatinite, a product of the thermal decomposition of sedimentary marine organic matter (alginite, bitumite) into bitumen. Exudatinite is a secondary maceral forming solid residuum after generation, maturation and migration of bitumen in the source rock (Brekke *et al.*, 2014)

No dolerite sills were observed at any of the 4 localities visited on south-eastern slopes of the valley and are not visible in the geological map of the Fulmardalen area by the Norwegian Polar Institute (Dallmann, 2015b). According to (Brekke *et al.*, 2014), the thermal effects on organic matter reached out as far as 1.5 times the dolerite thickness. There is a possibility the dolerite sills could be located below the valley floor.

One can speculate that higher temperatures within the deformation zone resulted from a contained movement in an eastwards direction along soft incompetent organic rich layers, likely the Lower Decollement Zone of Andresen *et al.* (1992b) during the Tertiary deformation. This led to local maturing of the organic matter in the upper parts of the Blanknuten Mb., expelling hydrocarbons.

6.2.5 Botneheia

Two sections were measured on the northern facing slopes of Botneheia mountain along Sassenfjorden, the type section of the Tschermakfjellet Fm. (Mørk *et al.*, 1999b). These localities were visited in the second part of the 2016 field campaign, carried out from M/S *Stålbas* as a part of fieldwork with the Norwegian Petroleum Directorate.
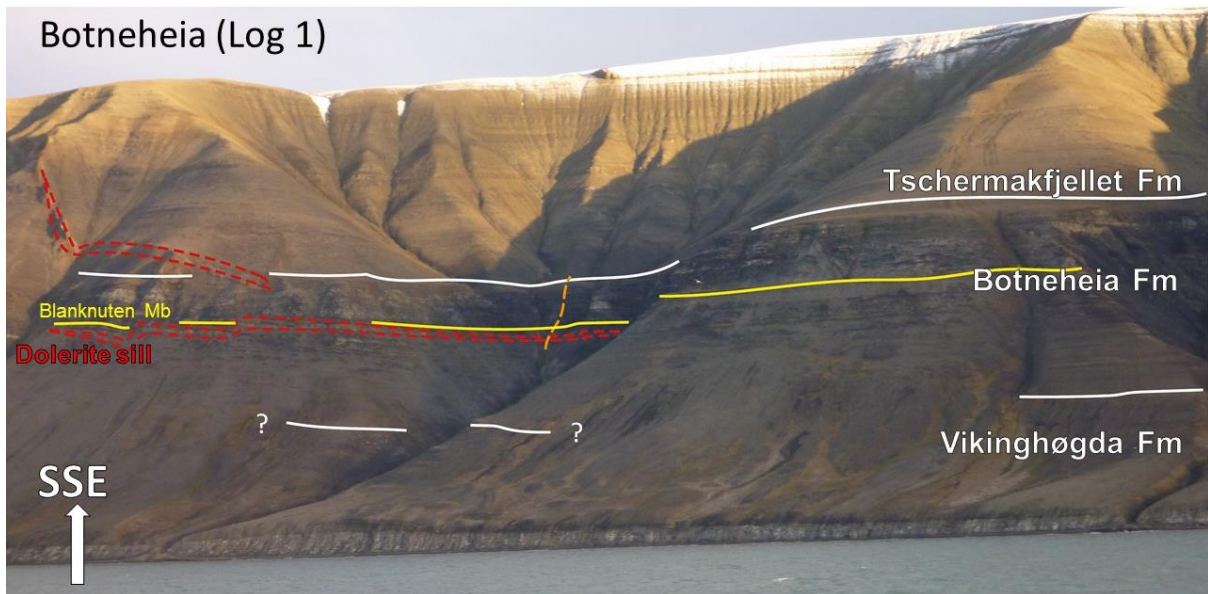
Figure 6.27: Overview of the first locality visited at Botneheia. Location of the logged section (orange stippled line) and approximate formation (white) and member (yellow) boundaries. Dolerite sill and dikes intrude the Botneheia and Tschermakfjellet formations.
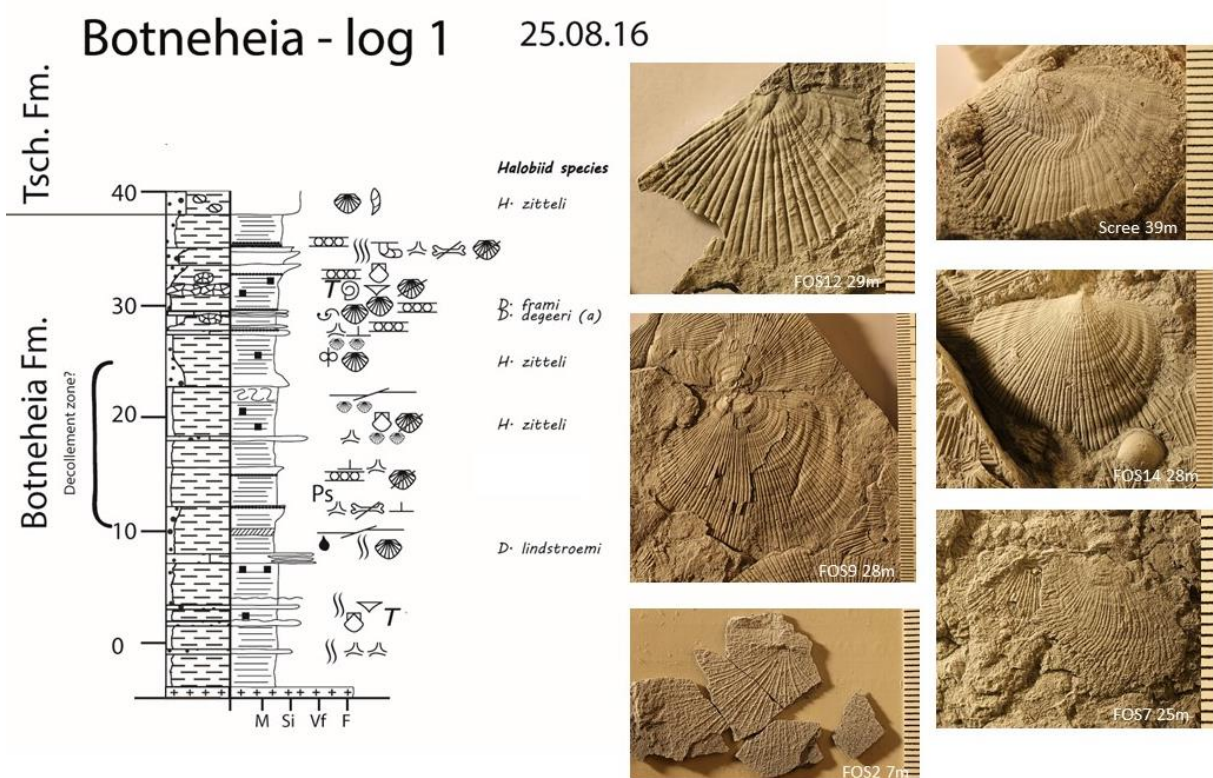
Figure 6.28: Log 1 of the northwards facing slope of Botneheia mountain. Logged by NB with assistance of TH.

The first locality visited in located in a steep valley between Elveneset and Vindodden. This section was measured by Atle Mørk, as presented in Vigran *et al.* (2014) and the ammonoid fauna below the Blanknuten Mb. was described by Wolfgang Weitschat in Xu *et al.* (2009). The base of the Botneheia Fm. can be approximately located by a siltstone bench on each side of the gully, but otherwise poorly exposed and covered in scree. Dolerite sills protrude from the mountain slope along the base of the Blanknuten Mb. and a smaller dyke cuts upward into the above lying Tschermakfjellet on the eastern side. The logged section starts just above the dolerite sill (Figure 6.27) in the lower Blanknuten cliff-forming unit. The top of the section forms a plateau and is well exposed, containing coquina beds and phosphate conglomerates.

The base of the cliff-forming unit appears a few metres above the dolerite sill. Here, occasional brachiopods and unidentified bivalves are found in dark grey shale with infrequent oolitic grainstone beds. The first halobiids, later identified as *Daonella lindstroemi*, appear above a heterolithic siltstone, bioturbated grainstone and shale bed. Above this is a black, unfossiliferous paper shale with a strong hydrocarbon smell and a narrow deformation zone contained within a few centimetres (Figure 6.29B). Above this is a calcite cemented zone consisting of black hydrocarbon rich paper shale and a calcite cemented siltstone bed containing vertebrate bones fragments and occasional phosphate nodules in horizons. At 20 m, seemingly undisturbed dark grey shales contain halobiids, later identified as *Halobia zitteli*. These lie below a small-scale calcite cemented z-fold and associated slickenslides found at 22 m (see Figure 6.29C). Above this second deformation zone, grey shales are found containing *Halobia zitteli* and phosphatised faecal pellets. This Carnian species is found 3 m below the characteristic Ladinian *Daonella degeeri* coquina beds. Within the coquina beds a rare flattened articulated specimen of *Daonella degeeri* was found. In a siltstone bed adjacent to the coquina beds several inflated specimens were found of the same species. In a shell bed just above this, *Daonella frami* was identified. At this location, the *Daonella degeeri* coquina beds are located 9 m below the purple siderite nodule marking the base of the Tschermakfjellet Fm. A above these coquina beds, a thick layer of phosphate conglomerate, an omission surface containing numerous brachiopods, two large septarian nodule horizons and several bioturbated calcite cemented siltstone beds, the uppermost containing *Rhizocorallium*. Within the non-calcitic grey shales of the Tschermakfjellet Fm., siderite nodules were found containing large specimens of *Halobia zitteli* and gastropods.

Figure 6.29: Structural features present at Botneheia, log 1. A) Large scale discordant bedding planes near the top of the Blanknuten Mb. B) Confined small-scale deformation zone within paper shale. C) small-scale Z-fold D) and associated slickenslides found in the middle of a section containing Halobia zitteli.

The finds of Carnian *Halobia zitteli* in the middle part of the Blanknuten Mb. suggests that there are repeated sections of the Middle-Late Triassic succession at this location. The combination of large-scale deformed discordant bedding planes in the mountain side Figure 6.29A, small scale fold structures at two locations half-way up the logged section (Figure 6.29B-D) and Carnian halobiids within the Botneheia Fm. (Figure 6.28, 25 m), can be interpreted to be a part duplex structures described by Andresen *et al.* (1992b). These structures, which are Tertiary in age, are formed as a result of reverse faulting and are known to be particularly well developed in the Botneheia Fm. This section serves as a prime example of the practical use of halobiid biostratigraphy in the Middle Triassic succession on Svalbard.

The second locality visited at Botneheia mountain lies approximately 1 km further west along the coast, towards Elveneset. A thick dolerite sill is emplaced in the lower parts of the Botneheia Fm, creating a formidable cliff-face which is possible to ascend through a narrow valley. A thin dolerite dyke climbs upwards through the Blanknuten Mb. on the eastern side of this valley, causing what is interpreted to be the uppermost Blanknuten to be uplifted, allowing for a detailed study of the boundary into the overlying Tschermakfjellet Fm. A 20 m section was measured of the sediments found in close contact with this boundary (Figure 6.30).
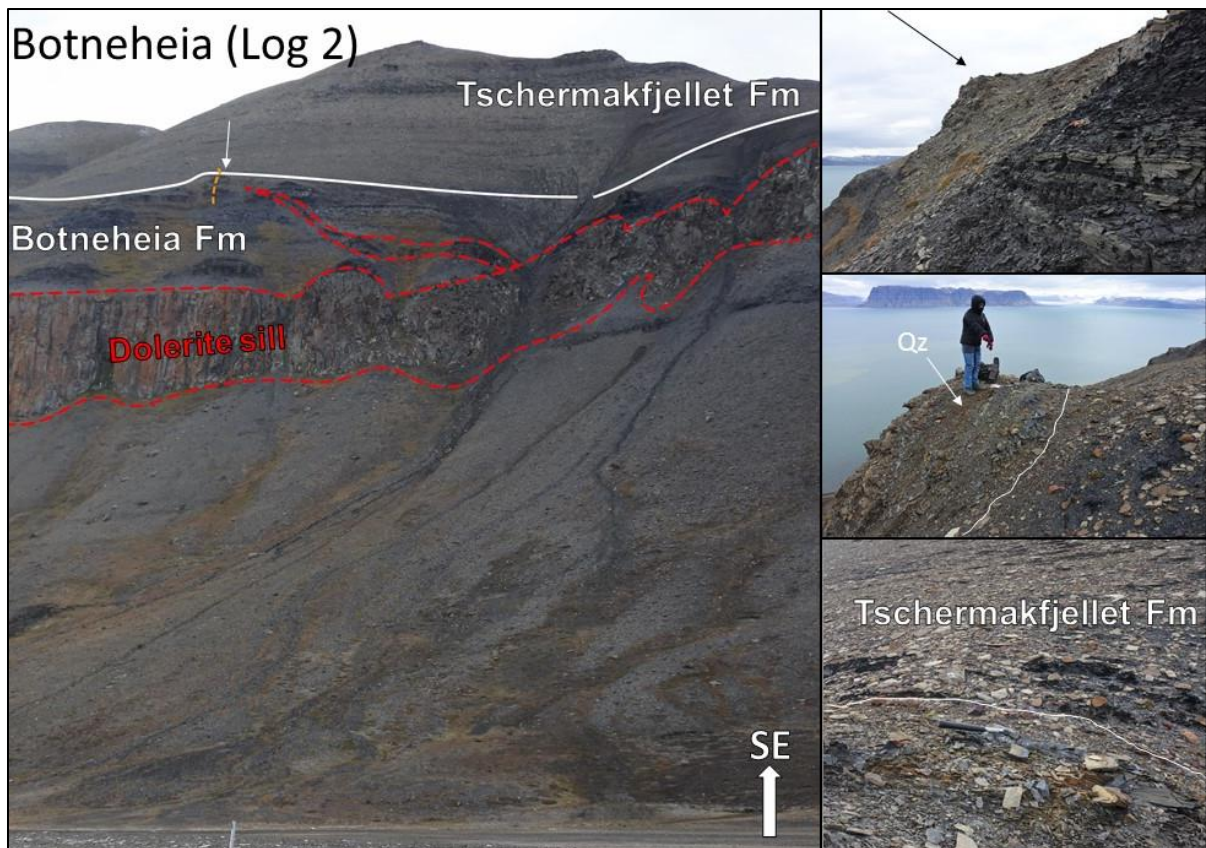
Figure 6.30: Overview of locality 2 on the northern slopes of Botneheia mountain. Location of the logged section (orange stippled line) above dolerite dykes and sills (red stippled line) and approximate formation boundaries (white).
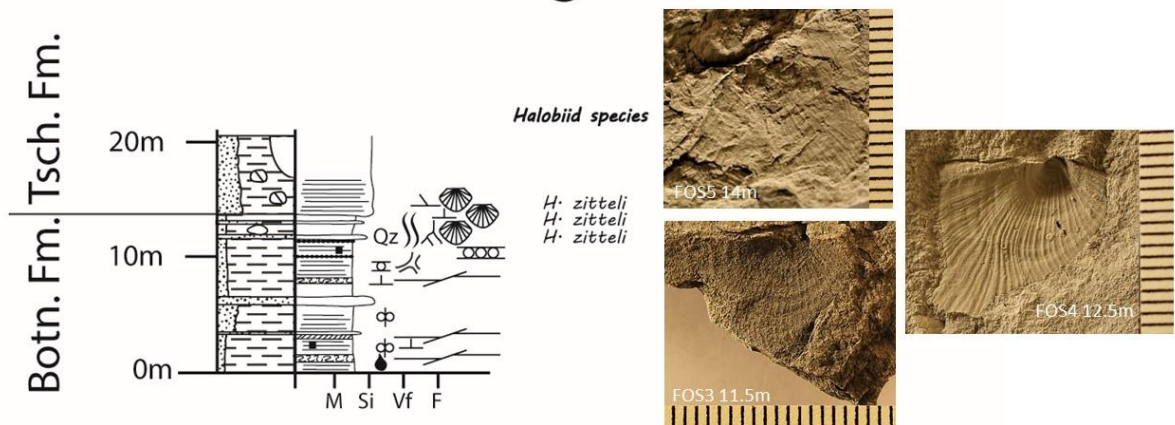
Figure 6.31: Log of locality 2 at Botneheia. A 7 m thick deformation zone is located at the lower part of the log consisting of calcitic and phosphatic metasediments. Above this, a red oxidised silica cemented bed (Qz) lies beneath bioturbated calcite cemented siltstones. Halobiid specimens collected at the boundary between the Botneheia Fm. and Tschermakfjellet Fm. are identified as Halobia zitteli. Logged by NB, with the assistance of TH.
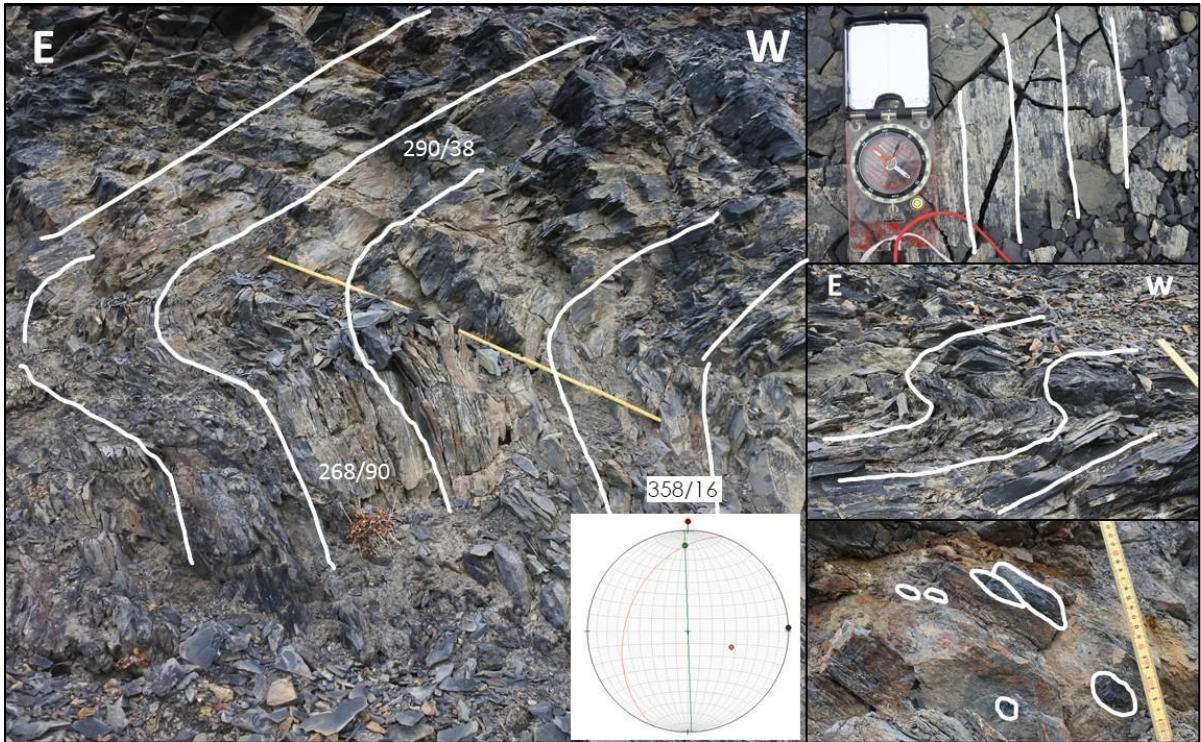
Figure 6.32: Structural features at locality 2, Botneheia. The large fold has a fold axis dipping slightly to the north. Slickenslides indicate movement in a SW-NE direction and small-scale z-folds indicate vergence from W to E. Metamorphosed sediments containing phosphate nodules are present at a highly deformed layer at the base of the deformation zone.

The log was started in a black, organic rich paper shale with a strong smell of hydrocarbons. Directly above this was a layer of highly folded light grey calcitic metamorphosed sediments with phosphate nodules at the lower boundary of a 7 m wide zone containing a series of several metamorphosed and folded phosphogenic shale beds (See Figure 6.32). A large fold in the dark shales indicate a fold axis slightly dipping to the north 358/16. Slicken slides indicated movement in a SW-NE direction. Small-scale z-folds indicated vergence in a west-east direction. These observations are in agreement with the Lower Decollement zone of Andresen *et al.* (1992b) which is Paleocene to Eocene in age and formed due to the formation of the West Spitsbergen Foldbelt to the west.

A red, oxidised and non-calcitic silica cemented bed, 0.5 m thick, was found (marked "Qz" in Figure 6.30 and Figure 6.31) 1.5 m below the interpreted boundary. This is the first locality in which this bed as found during the 2015/2016 field seasons, a similar bed at the uppermost boundary between the Botneheia Fm. and Tschermakfjellet Fm. was found at Tschermakfjellet.

Directly above this bed was a large concretion and calcite cemented siltstone beds containing Chondrites. At the interpreted boundary between the Botneheia Fm. and the overlying Tschermakfjellet Fm., a dark grey calcite cemented shale lies in direct contact with a non calcitic silty shale with purple siderite nodules (thin white line on

Figure 6.30). Numerous bivalve fossils were collected in a range from 1 m below and 1 m above the boundary between the calcitic and non-calcitic shales. Interestingly, after preparation and whitening, all the fossils samples had characteristics of *Halobia zitteli,* including a clear growth stop.

The finds of *Halobia zitteli* suggest that the calcite cemented siltstones and shales found directly below the characteristic grey non-calcitic siderite rich shales of the Tschermakfjellet Fm. are of Carnian age. One can suggest several explanations: i) the true lower boundary of the Carnian Tschermakfjellet Fm. lies at the red-oxidised silica cemented bed, where unfortunately no fossils were found, and that the lower most part of the Tschermakfjellet Fm. contains calcite cemented siltstones, ii) The lower boundary of the Tschermakfjellet Fm. is not calcite cemented and that Halobiids with growth stops existed in the uppermost portion of the Blanknuten Mb. i.e. the latest Ladinian on Svalbard (unlikely as this has not been reported), or iii) heat from the underlying dolerite dyke has caused calcite saturated fluids to migrate into the lower portion of the Tschermakfjellet Fm. shales and that this has overprinted the boundary, which occurs further down or is displaced due to thrust by the dolerite dyke. More fossil evidence is needed to make any conclusions.

6.2.6 Tschermakfjellet

The upper Vikinghøgda Fm., the entire Botneheia Fm. and the lower Tschermakfjellet Fm. are well exposed along a ridge to the south of Drachedalen at Tschermakfjellet mountain, Dickson Land (Figure 6.33).

A 90 m section was measured from a prominent siltstone near the base of the Botneheia Fm. to a fossiliferous siltstone bench 10 m above base of the purple siderite concretions of the Tschermakfjellet Fm.
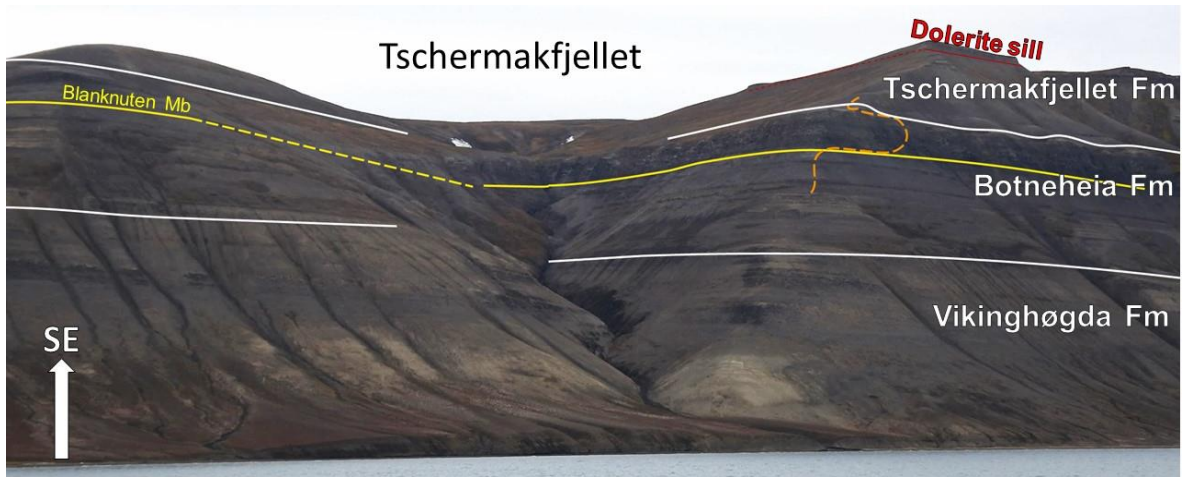
Figure 6.33: Overview of section logged along the ridge south of Drachedalen at Tschermakfjellet, Dickson Land. Location of the logged section (orange stippled line) below a dolerite sill (red stippled line) and approximate formation (white) and member boundaries (yellow).
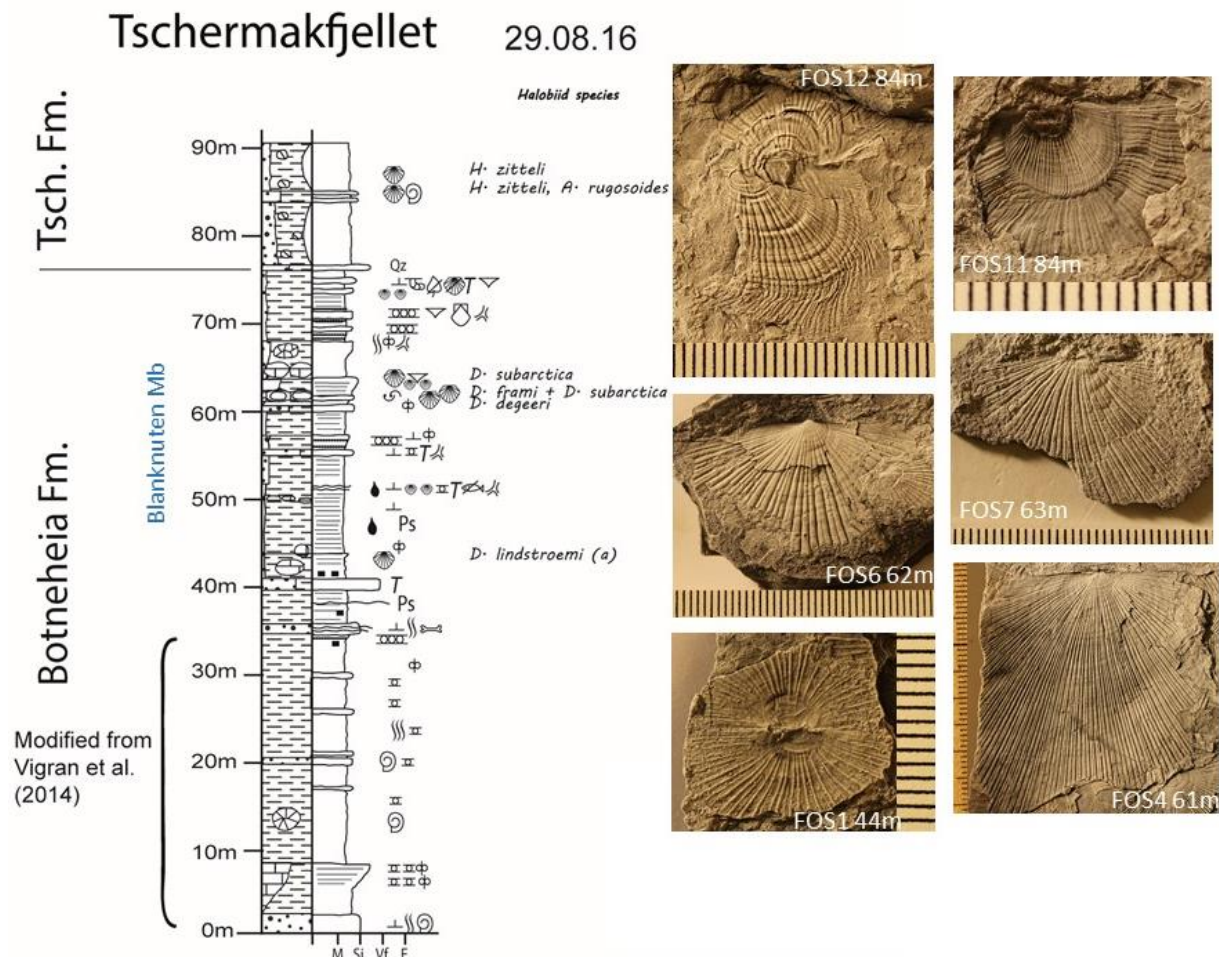
Figure 6.34: Log of Tschermakfjellet. Articulated Daonella lindstroemi *occurs near the base of the Blanknuten Mb. At this location* Daonella degeeri *coquina beds occur 15 m below the boundary to the Tschermakfjellet Fm, directly overlain by.* Daonella frami *is found directly above the coquina beds and siltstones dominated by* Daonella subarctica *above this. A red oxidized silica cemented sandstone occurs at the boundary to the Tschermakfjellet Fm. (marked as "Qz").* Halobia zitteli *is found together with rare* Aparimella rugosoides *in a siltstone horizon. Logged by NB with the assistance of TH.*

Tschermakfjellet represents the site located furthest to the west with the distal facies of the Botneheia Fm. in central and eastern Svalbard, equivalent to the more proximal lower prodeltaic Bravaisberget Fm. found along the west coast and to the south of Spitsbergen (Mørk *et al.*, 1982; Mørk *et al.*, 1999b; Vigran *et al.*, 2014). This locality, together with the successions logged at Botneheia, are located within the "Nordfjorden High" between the Pretender lineament to the west and the BFZ to the east. The Sassendalen Group is thin over the Nordfjorden Block, thickening and becoming especially organic rich eastwards of the Billefjorden lineament (Mørk *et al.*, 1982).

This section has proven to be the most successful site visited for collections of bivalves, however comparatively few ammonoids were found.

The lower half of the Botneheia Fm. is halobiid-poor and the log made by Atle Mørk presented in Vigran *et al.* (2014) was used as reference when measuring this section due to time constraints. Modifications have been made, such as the location of some of the siltstone beds and finds of phosphate nodules. The base of this log starts at two prominent massive siltstone beds located 45 m above the base of the Botneheia Fm. according to the published log.

Approximately 30 m above these beds, a prominent siltstone containing vertebrate bone fragments was found at the base of the cliff-forming Blanknuten Mb. The first finds of halobiids, later identified as articulated *Daonella lindstroemi* specimens were found 7 m above this bed in a concretion horizon. A thick calcite cemented highly organic black paper shale unit with sparse fossils and occasional phosphate conglomerate horizons, *Tasmanites* and bivalve microcoquina is found above this. The characteristic grey-beige *Daonella degeeri* coquina beds are found within a horizon containing large concretions 15 m below the purple siderite nodules of the Tschermakfjellet Fm. Approximately 0.5 m above these, a shell bed containing *Daonella frami* and one specimen of *Daonella subarctica* was found in dark grey shale, which was in turn overlain with 1 m by a grey siltstone dominated by *Daonella subarctica.* Between the *Daonella degeeri* coquina beds and the boundary to the Tschermakfjellet Fm., several yellow calcite cemented siltstones occur, the uppermost of which has abundant *Rhizocorallium* (similar to Botneheia Log 1). Thick phosphate conglomerates are found at several horizons.

Approximately 1.5 above the *Rhizocorallium* bearing siltstone, a 0.5 m thick bright red and purple silica cemented sandstone occurs (Figure 6.35). Dark grey non-calcitic shales with siderite nodules occur directly above this unit, and directly below it are calcite cemented shales. This unit is similar to the one found 1.5 m below the siderite nodule shales of the Tschermakfjellet Fm. at Botneheia (Log 2).

86
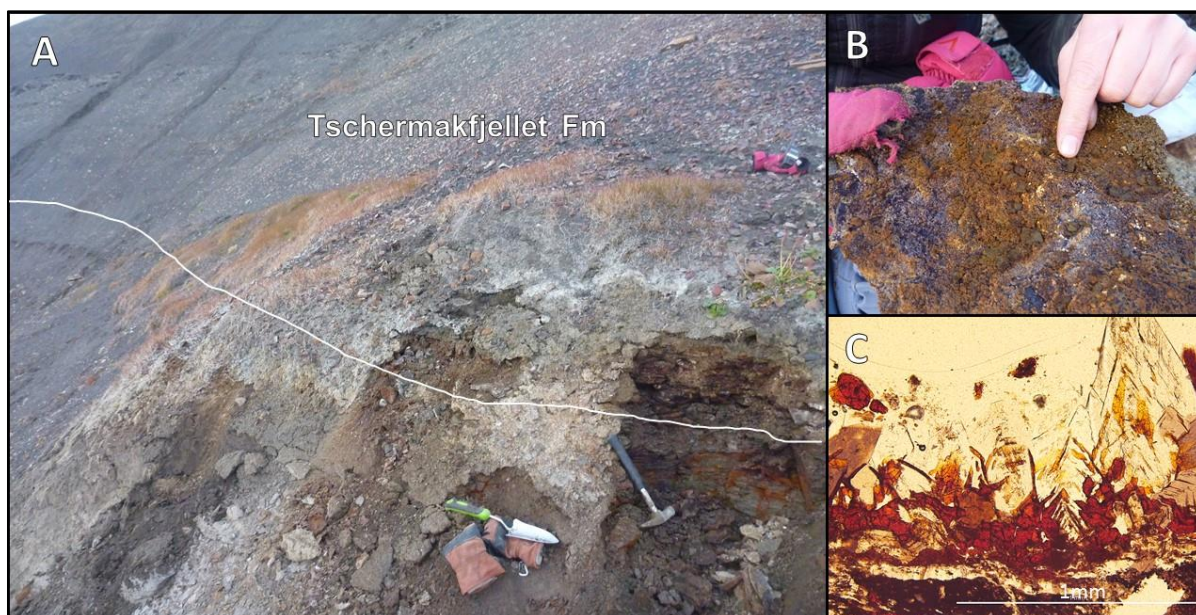
Figure 6.35: Lower boundary of the Tschermakfjellet Fm. at Tschermakfjellet. A) a bright red and purple layer (approx. 0.5 m) containing an oxidised silica cemented sandstone. B) Hand sample and corresponding thin section (C) consisting of algal remains in chert.

Algal remains in chert were identified in the thin section, with the help of Atle Mørk. Similar red algae fragments were described in thin sections from terrigenous-calcareous rocks in the Tschermakfjellet and De Geerdalen formations at several locations on eastern Svalbard by Tugarova and Fedyaevsky (2014), interpreted to represent discontinuity surfaces, developing during early diagenesis in shallow marine clastic facies. One can therefore speculate that this bed is a part of the Tschermakfjellet Fm. lower boundary.

However, according to Korčhinskaya (1982) there is a siliceous layer in the Ladinian known as the "Fosse sandstone" ((Hoel & Orvin, 1937; Mørk *et al.*, 1999b), referred to by previous workers as Upper Triassic. She reports finds of *Daonella subarctica* within this siliceous band in Sørkapp Land, indicating Late Ladinian age. According to Mørk *et al.* (1999b) the Van Keulenfjorden Member of the uppermost Bravaisberget Fm. of western Spitsbergen can be subdivided into two coarsening upwards units, the lower one is more massive and contains carbonate cemented siltstones, while the upper one is silica-cemented, fine-grained sandstone and containing spiculites. The member represents prodelta and delta top sediments and has a yellow-grey weathering colour (Mørk *et al.*, 1999b)

Krajewski *et al.* (2007) reports that lowermost unit of the Van Keulenfjorden Mb. lies above a thin grain supported lag horizon of reworked pyritized phosphate nodules, and consists of a dominant reddish weathering sandstone unit. Silicification is common in the Van Keulenfjorden

Mb and is manifested by silica overgrowths, resulting in a quartz-dominated dolomitic rock. According to Krajewski *et al.* (2007), the Van Keulenfjorden Mb. was deposited during the closing of the Middle Triassic shelf basin in Svalbard, and acted as a trap of pyrite due to sulphate reduction at methane oxidation font in shallow subsurface. The lack of early calcite cementation provided space for silicification and dolomitization processes during later stages of diagenesis. The member corresponds to a non-deposition (or emersion) period at the top of the Botneheia Fm. in central and eastern Svalbard.

Judging by the oxidized, silicified and reworked nature of the sediments within this layer, it probably represents a distal equivalent to the Van Keulenfjorden Mb. of the Bravaisberget Fm. in western Spitsbergen. It is found both at Tschermakfjellet and at Botneheia (log 1) and is interpreted to be the upper boundary of the Botneheia Fm. at these locations.

7. Systematics

An attempt has been made to summarize the diagnosis, age and correlations of each species of flat clam identified in literature from the Middle Triassic succession and its lower and upper boundaries on Svalbard. A detailed description of systematics is given of species identified from material collected during the field campaigns of 2015 and 2016. A brief account is given of species identified by other workers from Svalbard but which had not been identified in the material collected.

7.1   Family and generic designations

Following most recent publication, Alsen *et al.* (2017)

Class: BIVALVIA Linné (1758)

Order: PTERIOIDA Newell (1965)

Superfamily: POSIDONIOIDEA Frech (1909)

DIAGNOSIS: Thin-shelled, very low-convexity Pterioidina, having only very small auricles or none in maturity and lacking hinge teeth; ligament area duplivincular, alivincular (internal), or horizontally striated; musculature is anisomyarian or monomyarian (single posterior abductor muscle); in monomyarian forms, adductor scar oval or circular, not crescentic, and without an adjacent prominent posterior pedal retractor scar (Waller & Stanley, 2005).

REMARKS: The superfamily Posidonioidea is limited to two families, Posidoniidae and Halobiidae, which are worldwide in occurrence and have a stratigraphic range from Lower Carboniferous to Upper Jurassic. The Posidoniidae are considered to be the stem group for the Halobiidae ((Campbell, 1994; Chen & Stiller, 2010; Waller & Stanley, 2005).

On opposite sides of Panthalassa, in Eurasia and western Laurasia, there is a stratigraphic succession of first occurrences of the genera *Posidonia* (Lower Carboniferous), *Bositra* (Lower Triassic), *Enteropleura* (early Middle Triassic), *Daonella* (early Middle Triassic, but later than *Enteropleura*), transitional forms such as *Aparimella* (Campbell, 1994) or *Magnolobia* (Kurushin & Truschelev, 2001) (late Middle Triassic, near the Ladinian-Carnian boundary), and *Halobia* (Early-Late Triassic). Based on current knowledge of morphology, this succession of broadly interpreted genera represents a series of increasingly derived grades of evolution of ligament and shell morphology (Waller & Stanley, 2005).
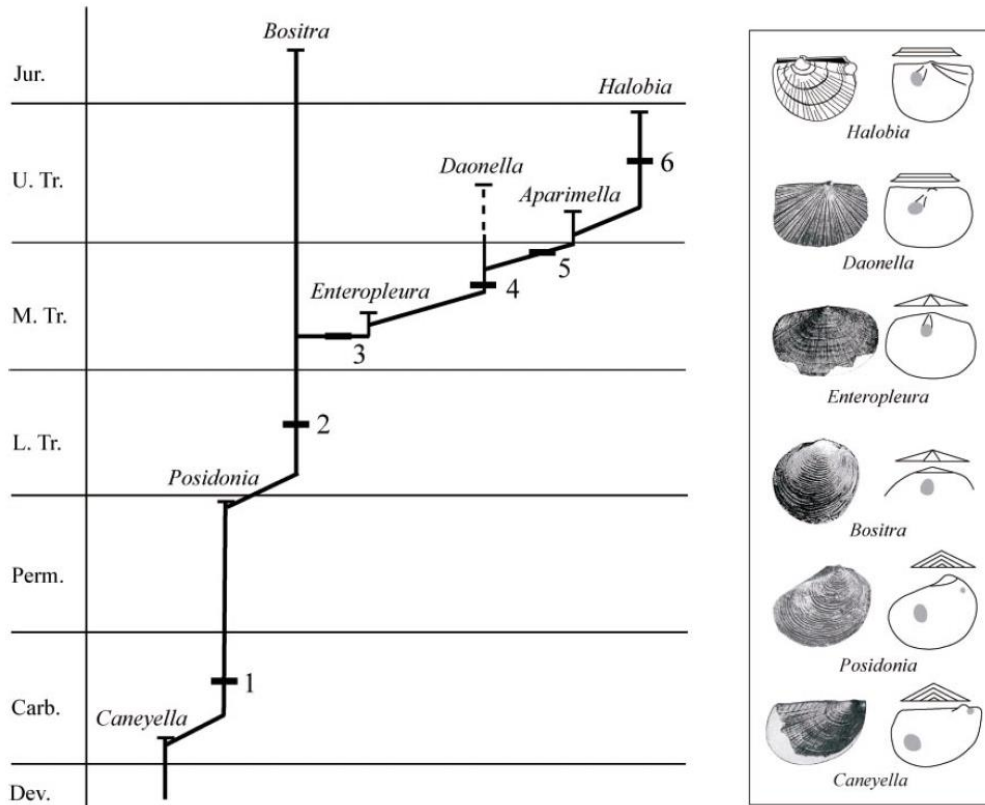
Figure 7.1: Systematic phylogeny and principle morphological changes and stratigraphic occurrences of flat clams and their likely Palaeozoic ancestors. From Waller and Stanley (2005).

Family: POSIDONIIDAE Bronn (1828)

Includes three genera, the first occurrences of which were: *Posidonia* (Late Palaeozoic), *Bositra* (Lower Triassic), and *Lentilla* Conti and Monari, 1992 (Jurassic) (Waller & Stanley, 2005).

Posidonia aranea Tozer (1961)

HOLOTYPE: GSC 14202, right valve in Tozer (1961). Figure in Tozer & Parker (1968, pl.25, fig. d) selected here in Figure 7.2.

TYPE LOCALITY: Otto Fiord, Ellesmere Island, Canada.

REMARKS: This is an important index fossil when locating the base of the Botneheia Fm. According to Hounslow *et al.* (2008), at Milne Edwardsfjellet *Posidonia aranea* occurs in a siltstone bed containing a rich fauna of ammonoids within the *Keyserlingites subrobustus* Zone at the top of the Vendomdalen Mb. of the Vikinghøgda Fm., approximately 15 m below the base of the Botneheia Fm.

Posidonia aranea
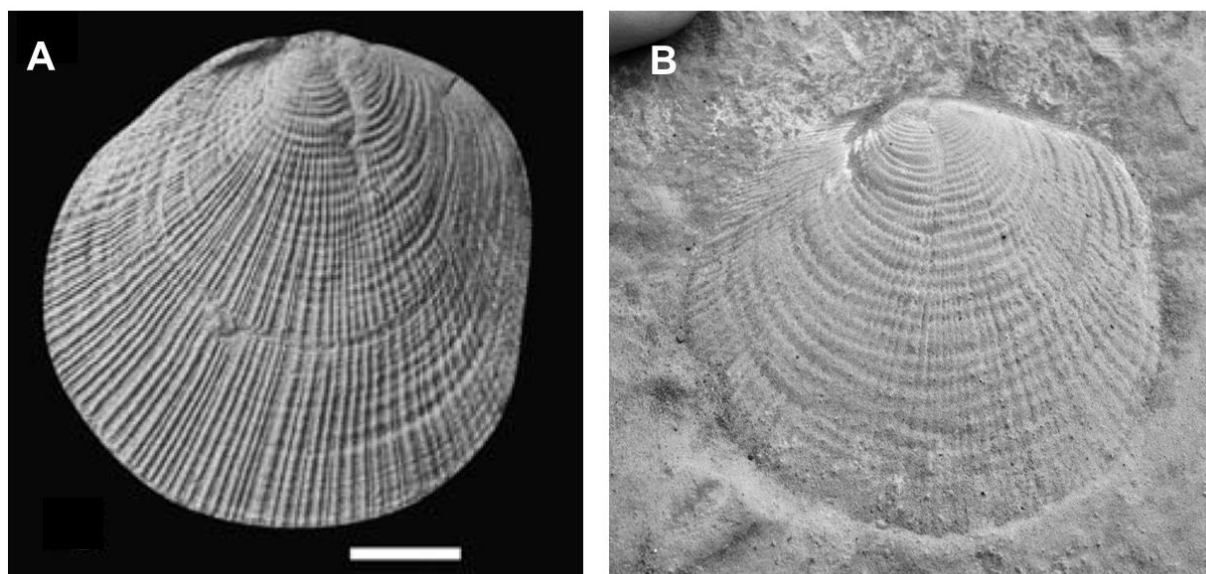
Figure 7.2: Posidonia aranea, collected at Edgeøya in Tozer & Parker (1968, pl. 25, fig. d), SM G1281. The same specimen is renamed Ellesmerella aranea in McRoberts (2010). B) Posidonia aranea, index fossil of upper Vikinghøgda formation, collected at Dyrhø in 2016, Log 2 0 m, Fulmardalen, NB field photo IMG DSC3178.

According to Waller and Stanley (2005) *Posidonia* is regarded as the stem group of the superfamily Posidonioidea. They generally lack a distinct byssal tube in maturity indicating a change from a byssate ancestor, such as *Caneyella* (see Figure 7.1), to a form with byssal attachment limited to early ontogeny. In later ontogeny *Posidonia* was more likely a recliner on soft substrates with only occasional opportunistic byssal attachment.

AGE: Late Olenekian

CORRELATIONS: Synonymous with *Claraia aranea* and *Ellesmerella aranea,* this species occurs in the *Keyserlingites subrobustus* Zone of high to mid-northerly latitudes. It was reported from Svalbard by Tozer and Parker (1968), and from Ellesmere Island in the Canadian Arctic by Tozer (1967) and is also reported as *Claraia aranea* in the northern Siberian and north-eastern Russian uppermost Olenekian bivalve zone of Konstantinov (2008).

Family: HALOBIIDAE Kittl 1912

According to Waller and Stanley (2005), this family includes three genera: *Enteropleura, Daonella* and *Halobia.* Two more transitional genera have been suggested: *Aparimella* (Campbell, 1994) and *Magnolobia* (Kurushin & Truschelev, 2001).

DIAGNOSIS: Posidonioidea with a single abductor muscle, with broadly expanded shells of low-convexity, hinge long, commonly nearly as long as shell length, ligament alivincular or horizontally striated, commarginal plicae limited to early ontogeny, radial costae, if present, stronger than commarginal ornament in late ontogeny (diagnosis emended in Waller and Stanley (2005)) .

Genus: *Enteropleura* Kittl, 1912

TYPE SPECIES: *Enteropleura bittneri*, described by Kittl, 1912 in Arthaber (1896, fig. 12).

DIAGNOSIS: Hopkin and McRoberts (2005) applied the name *Enteropleura* to Middle-Triassic thin-shelled bivalves having relatively short hinge margins, a clearly differentiated anterior auricle separated from the main disc by a radial groove and ornamented with faint radial ribs and commarginal growth lines. It differs from the genus *Daonella* in the absence of strong radial ornamentation and the clearly differentiated anterior sector with radial grooves (Hopkin & McRoberts, 2005).

REMARKS: According to Hopkin and McRoberts (2005), there are few published accounts of this genus, which is restricted to the Middle Anisian. *Enteropleura* is possibly the least understood of halobiid genera. *Enteropleura* has rarely been illustrated beyond the original sketch of *Enteropleura bittneri* Kittl, 1912 of Arthaber (1896, fig. 12). According to Waller and Stanley (2005) *Enteropleura* is regarded as a valid taxon at genus rank primarily because of the presence of an alivincular ligament. This genus has not yet been reported from Svalbard and has not been found in the material collected for this thesis.

Genus: *Daonella* Mojsisovics, 1874

TYPE SPECIES: *Halobia lommeli* Wissman, 1841.

DIAGNOSIS: Halobiidae lacking auricles and any obvious morphological shell structure related to emergence of a byssus. Ligament area alivincular but no secondary resilifers (Campbell, 1994) (see Figure 7.3).
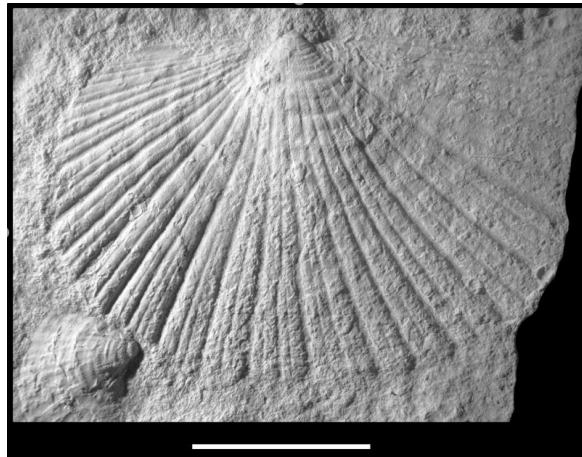
Figure 7.3: Type species of genus Daonella, Halobia lommeli *Wissmann (1841, pl. 16, fig.11), housed at the NHM in Vienna, BSPG AS-VII-1970 Münster. Photo courtesy of Simon Schneider, CASP.*

REMARKS: The genus *Daonella* was established by Mojsisovics (1874), with the type species *Halobia lommeli* recorded from the Ladinian in Austria. Mojsisovics (1874) described 26 species of halobiids, and established the genus *Daonella*, several of them from the Triassic of Spitsbergen. He indicated that the genus was evolved from *Posidonia.*

Genus: *Aparimella* Campbell, 1994

TYPE SPECIES: *Daonella apteryx* Marwick, 1953

DIAGNOSIS: Halobiidae with narrow but distinct anterior and posterior auricles (see Figure 7.4), which set the hinge off from the disc. No obvious morphological shell structure related to emergence of a byssus. Interpreted as an intermediate evolutionary step between *Daonella* and *Halobia* (Campbell, 1994).

REMARKS: Several of the specimens of *Daonella* collected in the study have auricles (see *Daonella frami, Daonella subarctica)*, as defined by Campbell (1994). A revision of the genus is needed; if one were to follow the definition of *Aparimella,* several late Ladinian species from Svalbard should be redefined. The only *Aparimella* reported from Svalbard is *Aparimella rugosoides,* identified from Tschermakfjellet by Campbell (1994), the original specimen of which is missing in the CASP collection. According to Waller and Stanley (2005), *Aparimella* occupies a stratigraphic position that lies between that of the last *Daonella* and the first abundant *Halobia*. There is some doubt, however, whether *Aparimella* is a true phylogenetic intermediary.
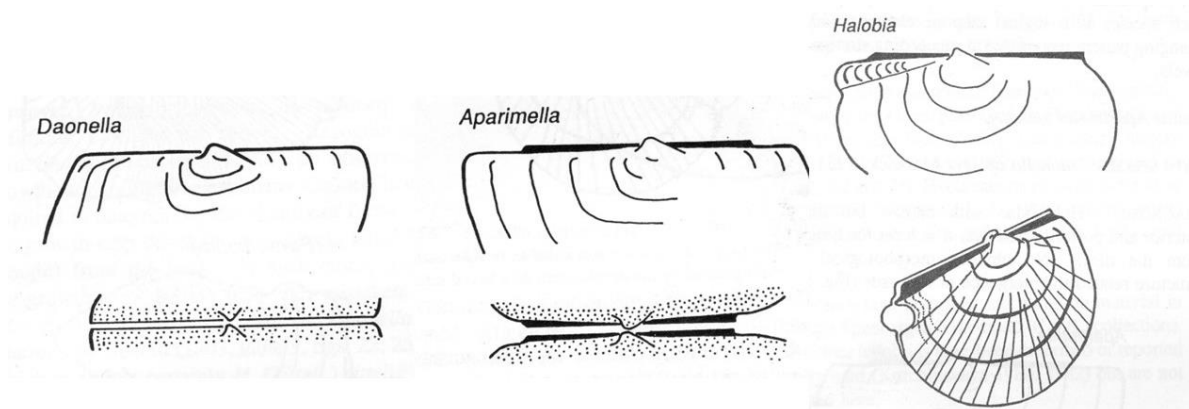
Figure 7.4: The hinge of Daonella; *an elongate simple structure involving the entire length of the dorsal shell margin. No auricles present. The hinge line of* Aparimella; *reduced length of the hinge and presence of auricles. The hinge line of* Halobia: *presence of auricles and byssal tube. From Campbell (1994).*

In Alsen *et al.* (2017), Christopher McRoberts argues that since the erection of *Aparimella,* it has now come to light that true auricles may be more pervasive in daonelliform species than previously thought and occur in several additional species across different species groups including *Daonella dubia* Gabb 1864, *Daonella elegans* McLearn 1937, *Daonella prima* Popov 1946, and *D. subarctica* Popov 1946. This distribution of true auricle across all daonelliform species needs to be further explored, so no attempt was made to transfer species possessing this trait from *Daonella* to *Aparimella* in the most recent literature.

Genus: *Magnolobia* Kurushin & Trushelev, 2001

TYPE SPECIES: *Daonella prima* Kiparisova, 1946

DIAGNOSIS: Kurushin and Truschelev (2001) established a new genus *Magnolobia* based on Ladinian Siberian type species *Daonella prima*, including other species known from Svalbard: *Daonella subarctica and Daonella densisulcata.* The genus is distinguished from *Daonella* by coarse radial ribs recurve either evenly along their entire length or more strongly at the umbo. The anterior is inflated and small triangular auricles are present.

In Alsen *et al.* (2017), Christopher McRoberts argued that the establishment of *Magnolobia* remains questionable as the genotype *Daonella lommeli* Wissmann (1841) was excluded as well as a number of other species including *Daonella lindstroemi* and *Daonella arctica* which possess, to some degree, curved radial ornament.

Genus: *Halobia* Bronn, 1830

TYPE SPECIES: *Halobia salinarum* Bronn, 1830

DIAGNOSIS: Halobiidae with narrow anterior and posterior auricles and an anterior "byssal tube" (Campbell, 1994) also described as a "shell tube" forming an inter-valve gap in Waller and Stanley (2005).

SUBGENERA: (1) *Halobia (Halobia)* with radial costation but no growth stops, (2) *Halobia (Zittelihalobia)* with radial costation and a growth-stop, (3) *Halobia (Parahalobia)* with no radial costation.

REMARKS: The function of the byssal tube in Campbell (1994) is to accommodate the byssus of a pendant bivalve attached to a benthic rooted organism such as an algae. Waller and Stanley (2005) argue that it represents a mantle gape related to feeding by means of an inhalant mantle tube, possibly to bring in hydrogen sulphide for chemosymbiotic bacteria. According to Waller and Stanley (2005), the evolutionary trajectory outlined in Figure 7.1. is one of decreasing dependence on a byssus, from byssal attachment in *Caneyella*, to byssal attachment in late ontogeny in *Posidonia*, to a benthic, possibly non-byssate reclining lifestyle in *Bositra*, *Aparimella*, and *Daonella*. It is unlikely that there would be a reversal in this trend in *Halobia.*

7.2   Identified Svalbard Halobiidae

Daonella arctica Mojsisovics (1874)

HOLOTYPE: Housed at Natural History Museum Vienna, originally figured in Mojsisovics (1874, pl.2, fig.4). Photo of holotype specimen in Figure 7.5(A).

TYPE LOCALITY: Norwegerdalen (Norskedalen), Dickson Land, Spitsbergen.

DIAGNOSIS: (summarized from Mojsisovics (1874) using google translate) Long and low, fairly strongly arched shape with very elongated posterior edge. The posterior is higher than the anterior. Numerous fine, and differently strong ribs, bunch at near the neck. The radial furrow towards the anterior are generally much wider, and towards the posterior become narrower. The ribs are very fine and weakly indicated towards the posterior. Occurs in the same rock as *Daonella lindstroemi* in Norskedalen on Spitsbergen.
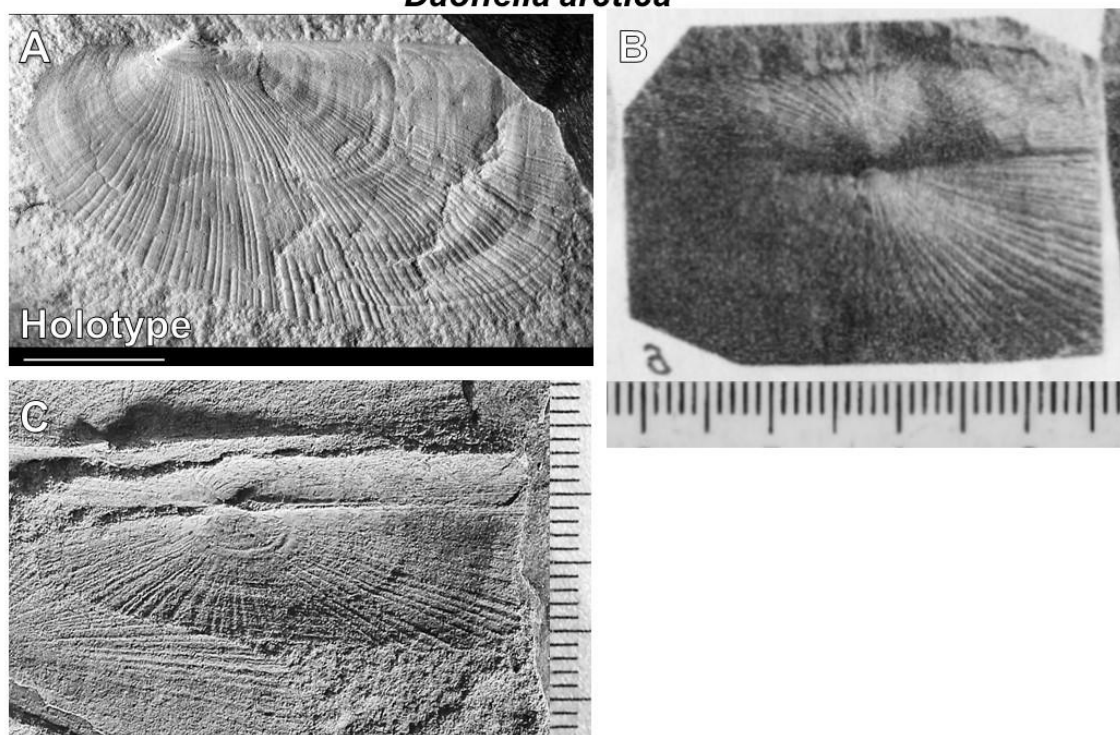
Figure 7.5: A) Holotype of Daonella arctica *Mojsisovics, photo courtesy of Simon Schneider, CASP. B)* Daonella arctica*, identified and imaged in publication by Korčhinskaya (1982) C)* Daonella arctica *commonly found in articulated form, Milne Edwardsfjellet 2016, FOS 5 59m, NB IMG0102.*

REMARKS: This species has been identified in Svalbard fossil collections in the following publications: Mojsisovics (1874) and Korčhinskaya (1982). The species is rare and was found at one locality, at eastern Milne Edwardsfjellet in Fulmardalen, approximately 35 m below the *Daonella degeeri* coquina beds. It was picked at the siltstone marker bed at the base of the cliff-forming Blanknuten Mb., and is thus the species of *Daonella* found lowest down in the stratigraphy.

AGE: (early) Late Anisian

The siltstone bed at the base of the Blanknuten Mb. is dated as basal late Anisian by Wolfgang Weitschat in Hounslow *et al.* (2008). According to Korčhinskaya (1982), *Daonella arctica* has been identified as from the upper substage of the Anisian, in the *Frechites laqueatum* Zone. This is the first appearance of *Daonella* on Svalbard, and correlates to the *Rotelliforme* Zone of British Columbia. Korčhinskaya (1982) reports this species together with *Daonella lindstroemi* at Wichebukta (Hahnfjella) in eastern Spitsbergen.

Daonella lindstroemi Mojsisovics (1874)

HOLOTYPE: L129, Natural History Museum, Vienna; original specimen of Mojsisovics (1874: pl.2, fig.16). Photo of holotype specimen in Figure 7.6 (A).

TYPE LOCALITY: Norwegerdalen (Norskedalen), Dickson Land, Spitsbergen.

Daonella lindstroemi
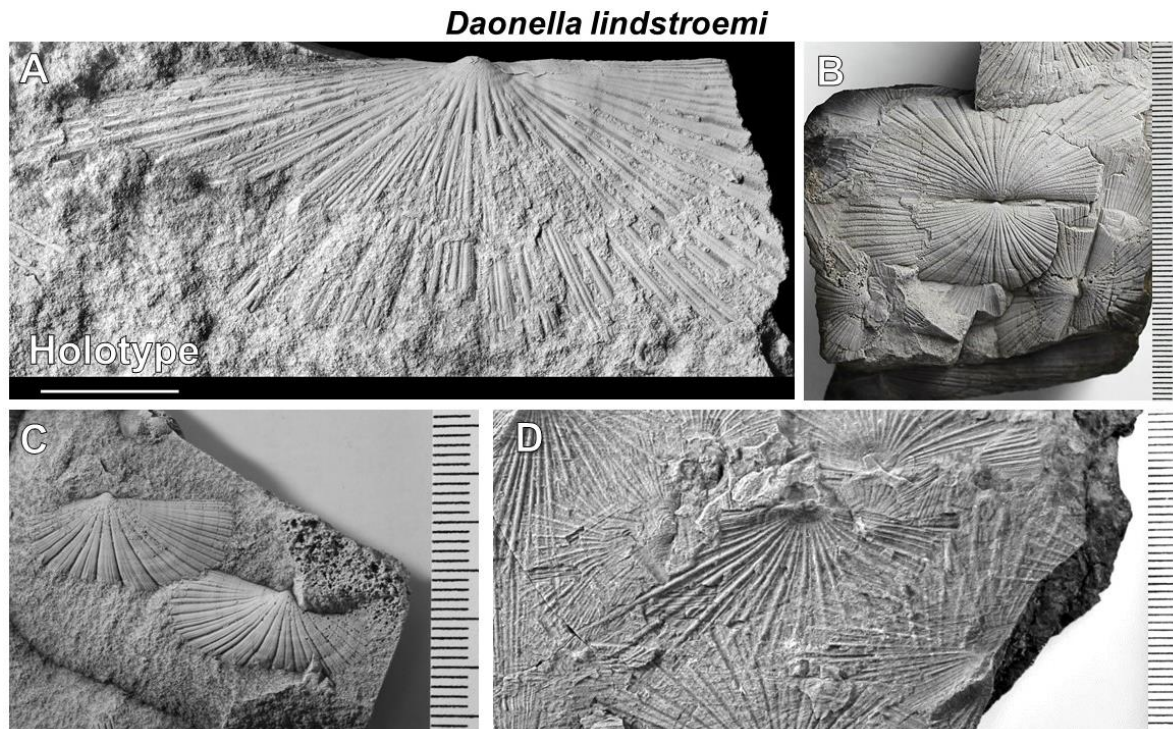
Figure 7.6: A) Holotype of Daonella lindstroemi *Mojsisovics, photo courtesy of Simon Schneider, CASP. B) Articulated specimen housed at CASP, C7547 NB IMG8665, courtesy of Simon Kelly. C) Inarticulated specimen with "flared" costae and 3D appearance, collected in a cemented siltstone bed at Dyrhø in 2016, Log 3 FOS5 172m NB IMG 0800. D) Specimen with "straight" costae and 2D appearance collected in dark grey shale at Tschermakfjellet in 2016, FOS1 7m NB IMG0395.*

DIAGNOSIS: (After Campbell (1994)) Small to moderately large, slightly inequilateral, moderately inflated, elongate, rounded rectangular shells with characteristics of the genus. Degree of posterior expansion variable. Hinge long. Costation strong over entire shell surface; a few regular, broad, flat costae in central disc with shallow secondary furrows; primary furrows narrow but open and deep; costation and furrow pattern in mid-disc appears fasciculate; costae are narrower and denser on anterior sector than on middle and still more so on posterior sector.

REMARKS: *Daonella lindstroemi* is far more common than *Daonella arctica* and appears to occur at quite a large range within the stratigraphy, at a slightly higher interval. According to Mojsisovics (1874), *Daonella lindstroemi* differs from *Daonella arctica* in that it is much longer and has different insertions of secondary ribbing. Like *Daonella arctica,* it is often found

articulated, sometimes in completely flattened form Figure 7.6(D) (often occurring in shale), or in inflated form Figure 7.6(C) with costae slightly bent outwards in both anterior and posterior directions, often in association with cemented siltstone beds. No preferred placement within the stratigraphy has been found and therefore they are considered the same species.

In Alsen *et al.* (2017), Christopher McRoberts describes *Daonella lindstroemi* as elongate, with dense radial ribbing and broader interplicae furrows, which flare strongly outwards across both anterior and posterior sectors, rather than just posteriorly like in *Daonella subarctica.*

AGE: Late Anisian to Early Ladinian

Collections of *Daonella lindstroemi* from western Milne Edwardsfjellet in central Spitsbergen were identified by Wolfgang Weitschat in Hounslow *et al.* (2008). The species is found in both the *Frechites laqueatus* Zone and the *Tsvetkovites varius* Zone (Weitschat & Lehmann, 1983). This is confirmed by two specimens of *Daonella lindstroemi* with ammonoids associated with these zones housed at CASP, courtesy of Simon Kelly. The species is identified as Late Anisian by Wolfgang Weitschat (Hounslow *et al.*, 2008), Korčhinskaya (1982), Tozer and Parker (1968) and Campbell (1994).

COMPARISONS: Mojsisovics (1874) suggested that *Daonella dubia* Gabb (1864) (Figure 7.7(A)), which he had studied in material from California, could be a link between *Daonella lindstroemi* and *Daonella lommeli*, but went away from the idea because of the wide lateral extent. Smith (1914) reported *Daonella lindstroemi* from Nevada, stating that it resembles *Daonella lommeli* Wissmann (1841) but differs in its coarser ribs with fewer bundles and in its greater elongation. He suggest that it is more related to *Daonella dubia* but differs from that species in its greater convexity and much coarser ribs with deeper furrows. Tozer and Parker (1968) also noted that *Daonella lindstroemi* closely resembles *Daonella dubia*, which is restricted to the upper part of the Upper Anisian of Nevada and to the high Anisian of Western Canada. He suggested that *Daonella dubia* may be present together with *Daonella lindstroemi* at Spitsbergen. According to Campbell (1994), *Daonella dubia, Daonella americana* and *Daonella jadii* Campbell (1994) (Figure 7.7(B)) (from the Anisian of New Zealand) are all related to *Daonella lindstroemi* but differ in shape and costation pattern.
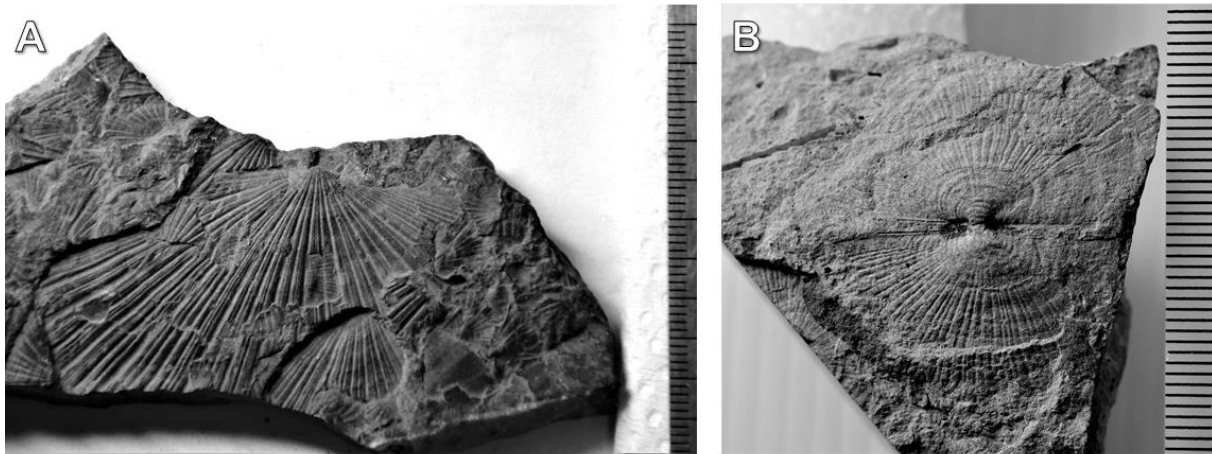
Figure 7.7: A) Daonella dubia *Gabb, housed at NHM London collection, specimen photographed in 2016, L82545 NB IMG0254, courtesy of Richard Twitchett., B) Holotype of* Daonella jadii *Campbell, housed at University of Otago, New Zealand, specimen photographed in 2016, OU16206 NB IMG DSC3978, courtesy of Ewan Fordyce.*

D*aonella degeeri* Böhm (1914)

LECTOTYPE: Housed at Natural History Museum in Stockholm. Original specimen of Böhm (1914, in text fig 3). Photo of Lectotype in Figure 7.8(A).

TYPE LOCALITY: Reindeer point (Reinodden), Bellsund, Spitsbergen.

DIAGNOSIS: (After Campbell (1994)) Moderate to large, inequilateral, moderately inflated, rounded to obliquely ovate sub-quadrilateral shells with characteristics of the genus. Hinge long. Costation over entire shell surface; costae numerous, narrow, round-topped and regular with narrow, shallow secondary furrows; primary furrows narrow, deep and rounded.

REMARKS: *Daonella degeeri* are often found in monospecific coquina beds, 5-15cm thick, which can be followed throughout study area. *Daonella degeeri* coquina beds were found approximately 18m above *Daonella lindstroemi* at Tschermakfjellet. Specimens are often very large (up to 12cm), but preserved in a highly varying degree of fragmentation, almost never articulated and without auricles. Beds of *Daonella frami* are found directly above *Daonella degeeri* coquina beds at several locations, and therefore are presumed younger.

Daonella degeeri
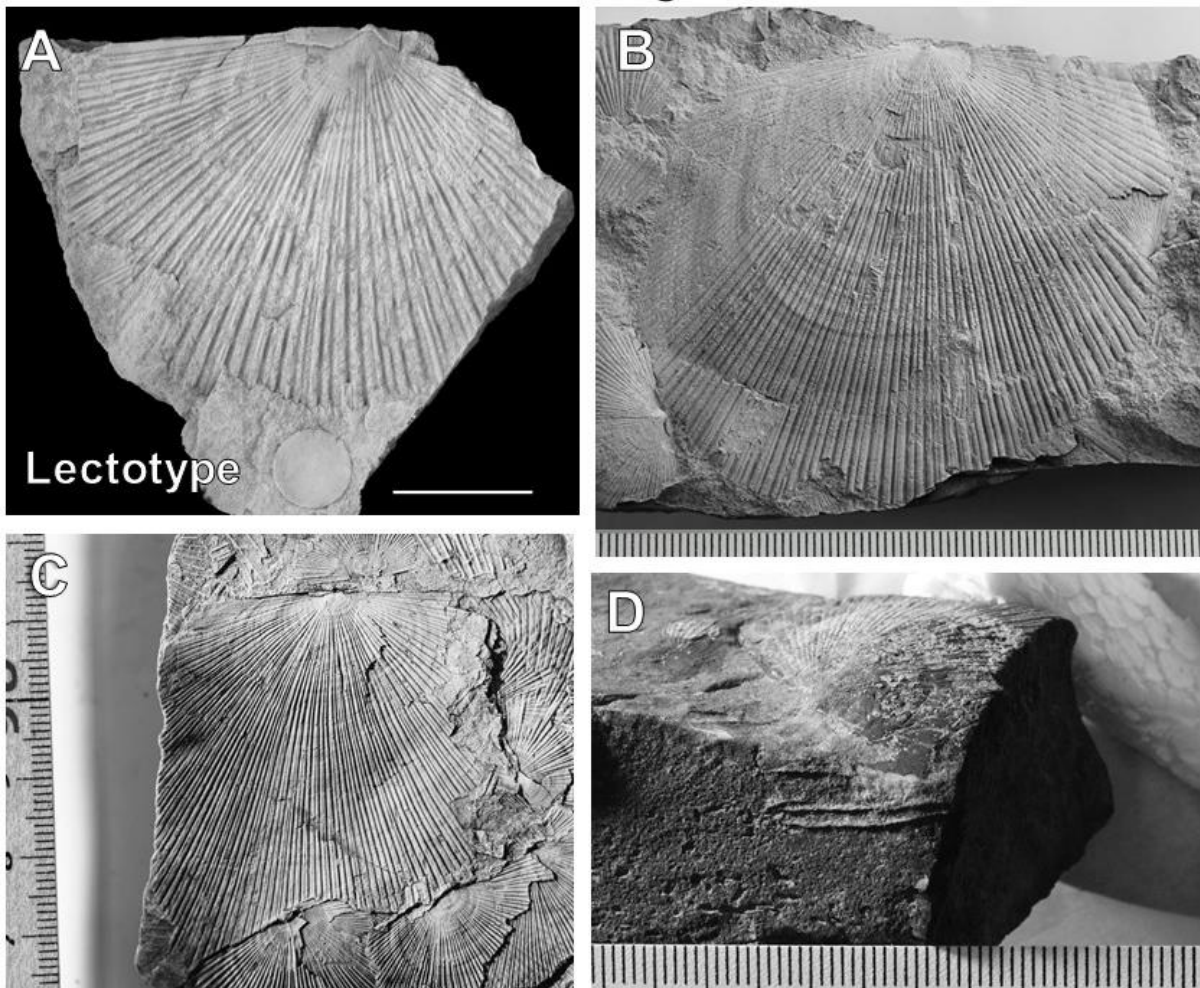
Figure 7.8: A) Lectotype of Daonella degeeri *Böhm, fig 3. p photo courtesy of Simon Schneider, CASP. B) Large flattened specimen housed at CASP, specimen photographed in 2016, C6989 NB IMG 8678, courtesy of Simon Kelly. C) Fragmented flattened specimen in coquina bed, collected at Tschermakfjellet in 2016, FOS 4 25.5m, NB IMG 0113. D) Inflated specimen in siltstone, collected at Dyrhø in 2016, Log 3 FOS 10 +8m, NB IMG 0713.*

AGE: Late Ladinian

Collections of *Daonella degeeri* from western Milne Edwardsfjellet in central Spitsbergen were identified by Wolfgang Weitschat in Hounslow *et al.* (2008). The species is found in the *Indigirites tozeri* Zone, confirming the stratigraphy of Weitschat and Lehmann (1983). This is contradicted in Korčhinskaya (1982), were the species was found in association with the *Ptychites nanuk* Zone, of the lower Ladinian. She found specimens of *Daonella degeeri* 10 m above beds containing *Daonella lindstroemi* at Wichebukta (eastern Spitsbergen), confirming the latter's wide age range. *Daonella degeeri* was found in the same sample as *Ussurites Spetsbergensis* and (possibly) *Aristoptychites kolymensis* in the CASP collection, confirming

the *Indigirites tozeri* Zone of Weitschat and Lehmann (1983) considered to be Late Ladinian by Wolfgang Weitschat (Hounslow *et al.*, 2008).

COMPARISONS: According to Tozer and Parker (1968), *Daonella degeeri* is found in association with *Nathorstites* and *Protrachyceras* leaving little doubt that *Daonella degeeri* beds are Ladinian, and could be correlated to the Lower Ladinian beds of *Daonella frami* in Arctic Canada, which was assigned to the *Poseidon* Zone.

Daonella frami Kittl (1907)

LECTOTYPE: Housed at the University of Oslo Natural History Museum. Original specimen of Kittl (1907, pl.1, fig 5). Photo of lectotype in

Figure 7.9(A).

TYPE LOCALITY: Blue Mountain, Ellesmere Island, Arctic Canada

DIAGNOSIS: (After Campbell (1994)) Moderate to large, equilateral, weakly inflated, rounded shells with characteristics of the genus. Negligible to slightly posterior expansion. Costation over entire shell surface; costae moderately broad, flat, with narrow shallow secondary furrow; primary furrows narrow, deep and rounded.

REMARKS: *Daonella frami* occurs slightly higher in the stratigraphy but within very close proximity to *Daonella degeeri*, and can therefore be easily confused. At Tschermakfjellet it is found 0.5m above *Daonella degeeri* coquina beds. The primary difference between the two is the number and width of ribs and shape of shell, where *Daonella degeeri* has a higher number of finer costae and *Daonella frami* has broader, fewer costae and a more equant shell shape. The first appearance of an auricle within the stratigraphy of the Botneheia Fm. occurs with this species. It is narrow and is located at the posterior of the shell (see Figure 7.9(C)). The size of the auricle varies between individuals.

Korčhinskaya (1982) also describes the presence of a posterior and possible anterior auricle: "Posteriorly, one or two non-branching ribs define a triangular "posterior" field, which either has no radial ribs or has an indistinct fine radial cross-hatching. A much narrower smooth field can be observed anteriorly (angle of posterior field 20°, angle of anterior field 10-12°), divided by a fine furrow into a wider upper part and a narrower lower part."
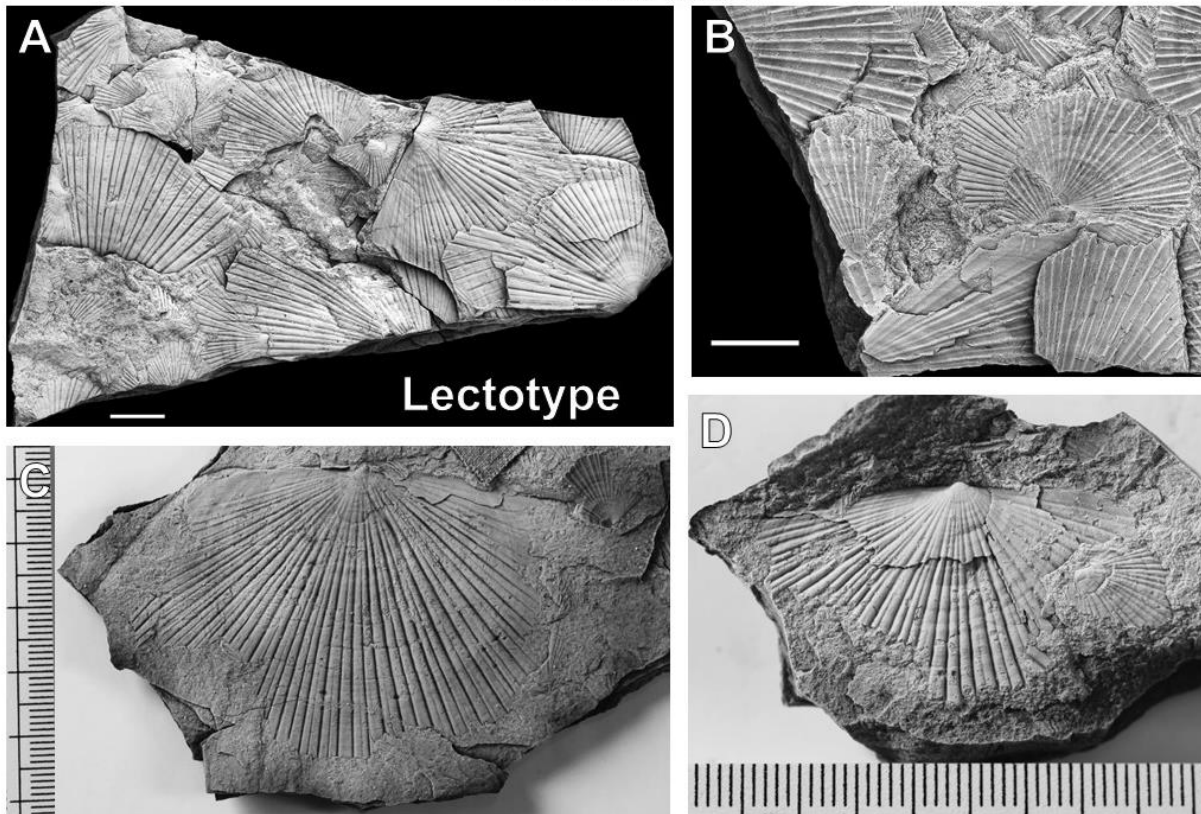
Figure 7.9: A) Lectotype of Daonella frami *Kittl, photo courtesy of Simon Schneider, CASP. B) Syntype material, NHM Oslo, S. Schneider, CASP. C) Large flattened specimen housed in CASP collection, photographed in 2016, J205 NB IMG 8708, courtesy of Simon Kelly. D) Specimen collected at Tschermakfjellet in 2016, FOS 6 26m NB IMG 0201.*

She goes on to remark: "In describing *Daonella frami*, Kittl called the areas with weak or no ornament anterior and posterior "ears", which casts some doubt on whether this species should be assigned to the Daonellids. However, in *Daonella* the "ears" that are typical of representatives of the genus *Halobia*, the posterior and anterior fields are smooth and are separated from the rest of the shell surface by a slightly weaker ornament" (Korčhinskaya, 1982).

The presence of an auricle suggests this *Daonella frami* could be the oldest described *Daonella* from Svalbard that could be considered a member of the genus *Aparimella*, as defined by Campbell (1994).

AGE: Late Ladinian

The species was first described by Kittl (1907) in material from the Blue mountains in Arctic Canada. The fossils were described as coming from a black bitumous calcareous slate of Ladinian age, below a grey shale containing *Halobia zitteli*.

Daonella frami was also identified by Tozer and Parker (1968) and was collected by the Cambridge Spitsbergen Expeditions at Kongressfjellet and according to Tozer could be variants of one species (conspecific) of *Daonella degeeri*. This view was supported by Weitschat and Lehmann (1983). Tozer suggested these beds where younger than basal Ladinian due to the association with *Nathorstites*.

According to Korčhinskaya (1982) *Daonella frami* occurs above sediments containing *Daonella degeeri* in the upper substage of the Ladinian, in the *Nathorstites mcconnelli* Zone in Russebukta on Edgeøya. In his monograph (Campbell, 1994), he states that *Daonella frami* occurs stratigraphically below *Daonella degeeri*. My investigations support Korčhinskaya's findings.

CORRELATIONS: According to Korčhinskaya (1982), *Daonella frami* is distributed in the Ladinian Stage of Svalbard, Canada, Alaska and New Siberian Islands. Konstantinov *et al.* (2013) confirms the presence of *Daonella frami* in the New Siberian Islands and assign the species to the Late Ladinian. It is described by Tozer (1967) from the lower Ladinian *Subasperum* Zone of Arctic Canada occurring with *Daonella degeeri*.

Daonella subarctica Popov (1946)

*defined as *Magnolobia subarctica* in Kurushin and Truschelev (2001)

HOLOTYPE: Housed at the Tchernyshew Central Geological Museum, St. Petersburg, no 16/6397. Photo of original specimen of Popov (1946), image of holotype in Kurushin and Truschelev (2001), Figure 7.10(A).

TYPE LOCALITY: Indigirka River, basin of the Sarba river, north-eastern Russia.

DIAGNOSIS: (After Alsen *et al.* (2017)) Moderate to large sized, equivalve, inequilateral, longer than high, small beak, positioned slightly posterior, with narrow anterior auricle which is acutely triangular, extending approx. one half the distance of the anterior length. Posterior auricle not preserved.

Daonella subarctica
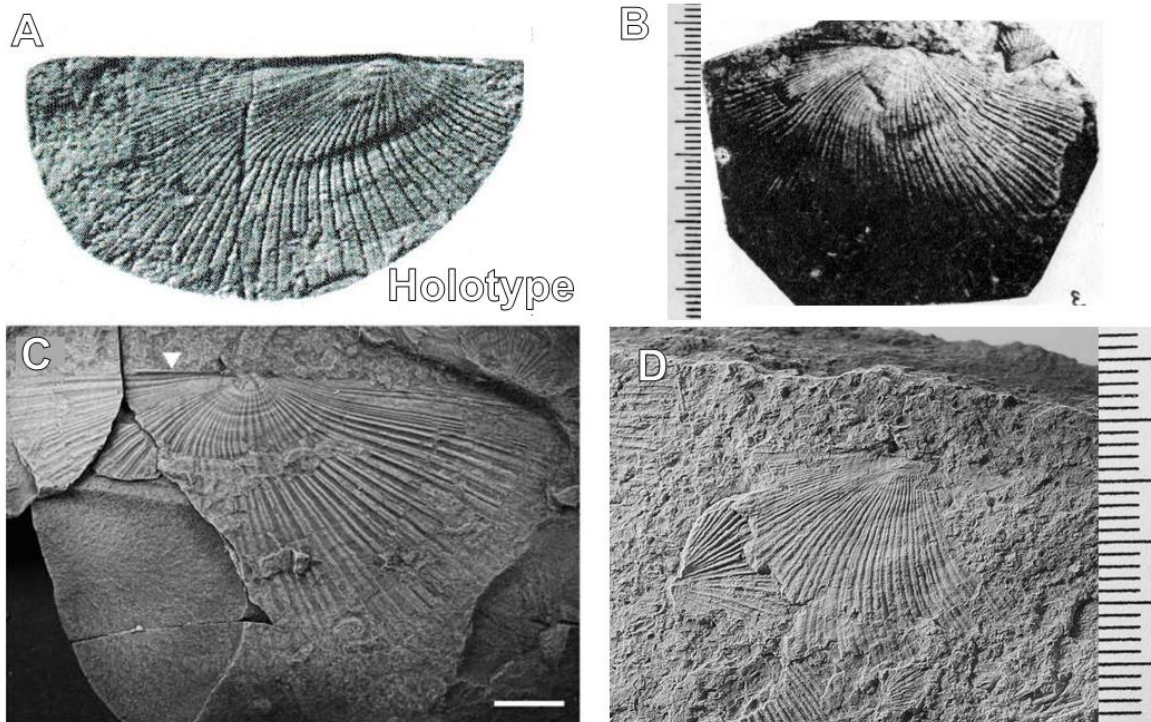
Figure 7.10: A) Most recently published image of the holotype of Daonella subarctica *Popov, from Kurushin and Truschelev (2001), no scale bar available. B) Specimen collected at the eastern shore of Wichebukta, Spitsbergen and identified by Korčhinskaya (1982, pl. XXIV, fig 3). C) Specimen collected in NE Greenland and housed at GEUS, Denmark, MGUH 31559. Identified by Christopher McRoberts, in Alsen et al. (2017). Triangle showing location of anterior (?) auricle. D) Specimen collected at Tschermakfjellet in 2016, FOS 7 28m, NB IMG 0323.*

Radial ornament consisting of broad and flat-topped plicae with and interplicae furrows of variable widths, more numerous and more narrowly-spaced and more subdued in the anterior and posterior sectors. Plicae run straight in early ontogeny and become weakly to moderately curved in the posterior direction across the central and posterior disk sectors with plicae relatively straight in the anterior sector throughout ontogeny, primary plicae may divide by means of insertion of narrow secondary furrow. Details of hinge and ligament system unknown.

REMARKS: *Daonella subarctica* is rare in material collected. It was found at Tschermakfjellet 3 m above *Daonella degeeri* coquina beds and was photographed is the vicinity of these coquina beds by Atle Mørk at Muen in 2007. Unlike *Halobia zitteli,* it does not have an obvious growth stop, nor does it have large auricles (only a small one) and associated "byssal tube". The curvature of the ribbing is gradual and over a large area.

In Alsen *et al.* (2017), Christopher McRoberts noted that within the material collected from Greenland, there was broad range of variation in the nature of the plicae, which can be attributed

104

to both natural variation within populations but also due to the nature of preservation. The strength and breadth of the plicae appeared to be dependant of the skeletal surface preserved as the plicae and often quite a bit sharper and narrower when observed on an outer surface.

Kurushin and Truschelev (2001) assigned *Daonella subarctica* to the genus *Magnolobia* which was established based on type species *Daonella prima* from north-eastern Asia. The genus consists of specimens whose coarse radial ribs recurve evenly along their entire length or more strongly at the umbo. Small auricles are present and there is anterior inflation.

Christopher McRoberts argues that *Daonella subarctica* is often found in beds with *Daonella prima* and *Daonella densisulcata,* and he believes the three species are morphological variants of the same species. They are all large, possess posteriorly curved plicae, that divide across the entire disc, *Daonella prima* radial plicae begin their curvature earlier in ontogeny, and *Daonella densisulcata* possess finer radial plicae (Alsen *et al.*, 2017).

The original specimen figured in Campbell (1994) and subsequently McRoberts (2010) is missing from the CASP collection.

AGE: Late – Latest Ladinian

According to (Korčhinskaya, 1982) in the first year of work of Soviet geologists in Svalbard, Petrenko found *Daonella subarctica* in the upper part of the horizon with daonellids on the NE slopes of Botneheia, which provided convincing evidence of the existence on Spitsbergen of Ladinian sediments. According to Dagys *et al.* (1993), Popov (1946) described *Daonella subarctica* at same stratigraphic level as representatives of the ammonoid genus *Nathorstites*, from Triassic beds of Yakutia in Siberia, assigning a Ladinian age. *Daonella subarctica* has been recorded in the upper part of Botneheia Fm. by Wolfgang Weitschat (Hounslow *et al.*, 2007a; Hounslow *et al.*, 2007b; Hounslow *et al.*, 2008; Weitschat & Dagys, 1989), in association with *Indigirophyllites spitsbergensis* (synonymous with *Ussurites spetsbergensis*) and *Protrachyceras sp.* at Milne Edwardsfjellet in Sassendalen, and with *and Nathorstites mcconnelli* which is characteristic of the uppermost Ladinian *Frankites sutherlandi* Zone in the Sverdrup Basin. In recent times, Christopher McRoberts in Alsen *et al.* (2017), established that Svalbardian *Daonella subarctica* lies stratigraphically above *Daonella degeeri* and is considered to be of Late Ladinian age.

CORRELATIONS: In Alsen *et al.* (2017), Christopher McRoberts describes *Daonella subarctica* as amongst the most widely distributed Ladinian *Daonella* species, occurring in high northern paleolatitudes with significant occurrences in NE Russia, Svalbard, Franz Joseph

Land and Arctic Canada. According to correlations of ammonoid zones, *Daonella subarctica* appeared in Northern Siberia, and subsequent migration to Svalbard and Greenland by latest Ladinian (Alsen *et al.*, 2017).

Konstantinov *et al.* (2013) confirms this, stating *Daonella subarctica* appears as middle-Upper Ladinian form in a recent stratigraphic overview of northern Siberia and north-eastern Russia.

Daonella subarctica is described from the Lower Ladinian Substage, *Poseidon* Zone, of Arctica Canada by Tozer (1967) and was found below *Daonella nitanae* McLearn, which is in turn replaced by *Daonella elegans* McLearn of the uppermost Ladinian *Sutherlandi Zone.*

Daonella elegans is also described from the New Pass Range, Nevada in Balini *et al.* (2007), occurring both with *Frankites sutherlandi* (uppermost Ladinian) and *Daxatina canadensis* (lowermost Carnian). Although a few individuals of the studied material possessed the "byssal tube" of *Halobia* the group was placed within the *Daonella* genus, and this is therefore the latest form of *Daonella* described. Neither of the North American youngest forms of *Daonella* have yet been described from Svalbard.

Halobia (Zittelihalobia) zitteli Lindstroem (1865)

HOLOTYPE: Housed at the NHM in Stockholm. Original specimen of Lindström (1865, pl.2, fig. 11) Photo of lectotype in Figure 7.11.

TYPE LOCALITY: "Skiferen ved Kapp Thordsen", Kapp Thordsen, Dicksonland, Spitsbergen.

DIAGNOSIS: (According to Campbell (1994)) Medium sized to very large, elongate, rounded, obliquely ovate, equilateral shells with characteristic growth stop of the subgenus *Zittelihalobia*. Strength and position of growth-stop variable, at between 7 and 16 mm in height. Costation developed over entire shell surface; primary costae numerous, regular, moderately broad, flat-topped, to gently rounded with shallow, narrow secondary furrow; primary furrows each less than half width of one costa, rounded and of variable strength but increasing progressively in depth from posterior to anterior sector.

Halobia zitteli
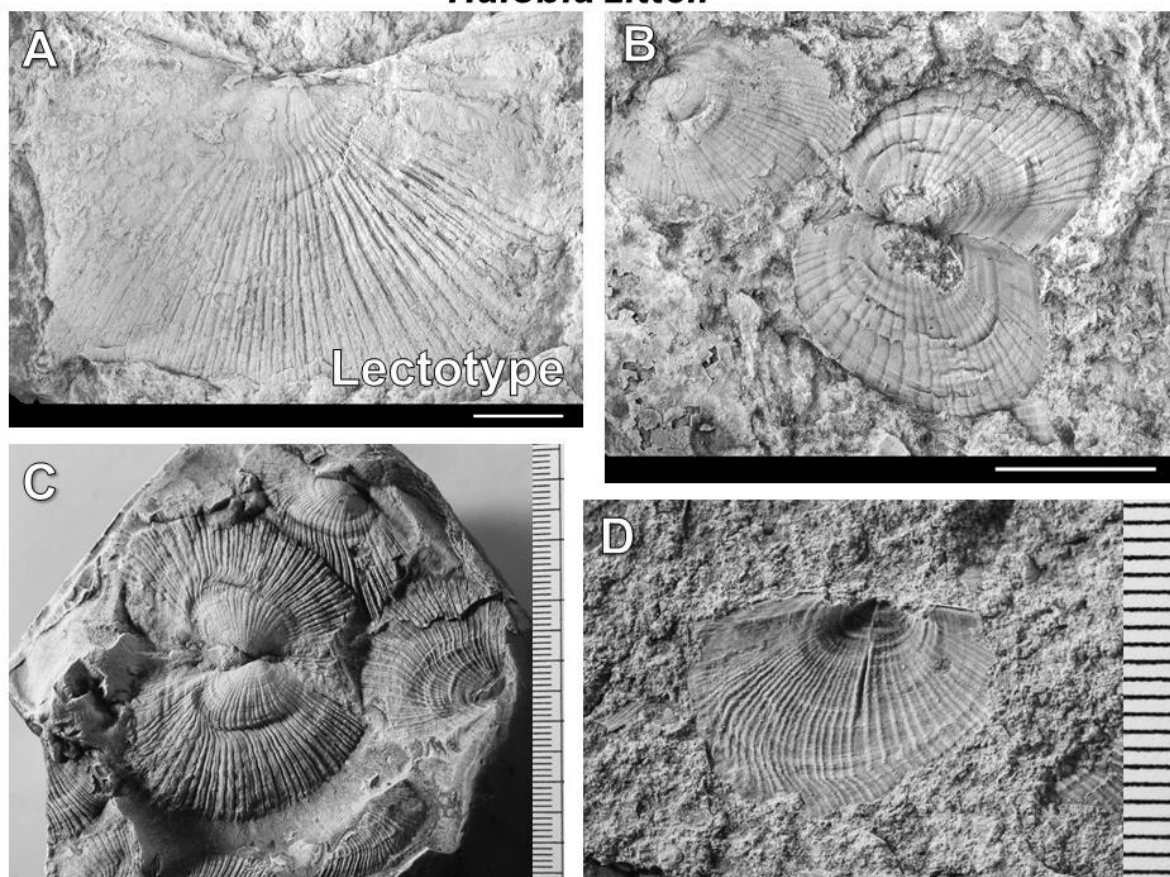
Figure 7.11: A) Lectotype of Halobia zitteli *Lindstroemi, housed at NHM in Stockholm, photo courtesy of Simon Schneider, CASP. B) Holotype material of juveniles, with growth stop slightly visible in one individual, NHM Stockholm, S. Schneider, CASP. C) A rare example of an articulated* Halobia zitteli *in a siderite concretion, collected at Dyrhø in 2016, log 1, NB IMG 1038. D) Juvenile specimen with starting stages of bending at growth stop, collected at Tschermakfjellet in 2016, FOS 12 NB IMG 0459.*

REMARKS: Most specimens in the material for this thesis have been collected in siderite concretions at the base of the Tschermakfjellet Fm. Measurements of height at beginning of the growth stop and statistics such as number of ribs at 1 cm from the umbo have confirmed that they are the same species. Auricles and "byssal tube" of Campbell (1994) are present in both juvenile specimens and large adult specimens.

AGE: Early Carnian

According to Campbell (1994), *Halobia zitteli* is restricted in occurrence to the Tschermakfjellet Fm., associated with *Nathorstites tenuis,* indicating Early Carnian age.

Korčhinskaya (1982) defined a *Halobia zitteli* Zone on Svalbard of Carnian age. Numerous ammonoids were described including *Nathorstites gibbosis,* as well as gastropods, brachiopods

and vertebrate bones. According to Tozer and Parker (1968) no ammonoids that unequivocally indicate a Carnian age have been described from Svalbard. However, the presence of *Halobia zitteli* indicates Carnian age.

CORRELATIONS: According to Korčhinskaya (1982), the *Halobia zitteli* Zone on Svalbard contains analogues of the earliest Carnian *tenuis* Zone of northern Siberia and north-eastern Russia, confirmed by Konstantinov *et al.* (2013). The species is also described from the lower Carnian Substage in Canada, in the *Obesum* and *Nanensi* Zones (Tozer, 1967).

McRoberts (2010) suggests a lowermost Carnian *Halobia zitteli* Zone in Boreal regions, correlating them to *Halobia rugosa* Zones of Lower Carnian age in Western Tethys and North America, within the *Daxatina canadensis* ammonoid zone (Mietto *et al.*, 2008).

Aparimella rugosoides Hsu 1944

HOLOTYPE: type specimen of *Halobia rugosoides* is figured in Chen (1976, pl. 35, fig.16). A sketch of original specimen of *Aparimella rugosoides* C7941, housed in the CASP collection defined by Campbell (1994) is selected here, in Figure 7.12(A).

TYPE LOCALITY: Yunnan, southern China.

DIAGNOSIS: (According to Campbell (1994)) Small to medium-sized, elongate and equilateral shells. Shell form prior to the growth-stop is small, circular, inflated and with relatively broad radial costae. Growth-stop at between 4 to 7 mm in height. Beyond growth-stop, shell becomes elongate, very weakly inflated, with sculpture of numerous fine, weak costae and shallow furrows over the entire disk. Ornamented cap-like early growth stage.

REMARKS: This species has only been described on Svalbard by H. J. Campbell (1994), at Tschermakfjellet. I also found it at this location, in the same siltstone beds as *Halobia zitteli*. All specimens were missing from the fossil collection at CASP and therefore identification has been based on the description and sketch in Campbell (1994).

AGE: Early Carnian

The species was reported to occur in the lower Tschermakfjellet Fm., in association with *Halobia zitteli* immediately above beds containing *Nathorstites tenuis* of Early Carnian age (Campbell, 1994).

Aparimella rugosoides
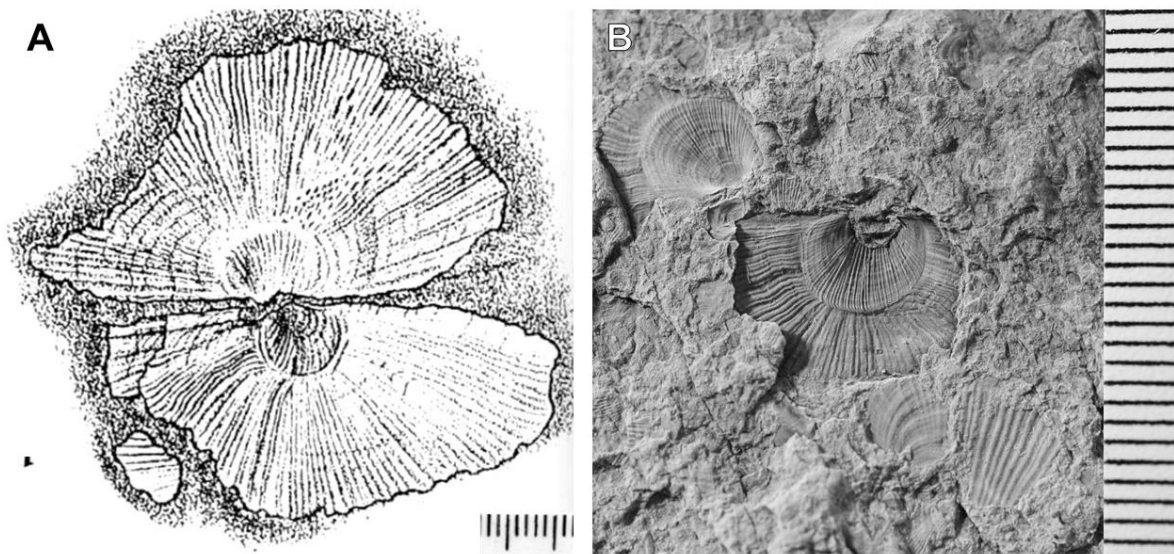
Figure 7.12: Sketch of Aparimella rugosoides, *identified from Tschermakfjellet by Campbell (1994).
B) Specimen collected from Tschermakfjellet in 2016, FOS 12 49m NB IMG 0447.*

CORRELATIONS: *Aparimella rugosoides* is described by Campbell (1994) as being ancestral to *Halobia rugosa* Gueumbel (1861). Interestingly, since *Halobia zitteli* is poorly represented in western North America, a *Halobia rugosa* Zone marks the Early Carnian in North America and the Western Tethys (see Chapter 4.3 Triassic flat clams of other regions). Campbell mentions that *Aparimella rugosoides* has not been recorded from Europe but is widespread in southern China and is restricted to Early Carnian age. *Halobia rugosoides* has been described by (Xiaofeng *et al.*, 2008) in the Laishke Fm., found together with *Trachyceras sp.* ammonoids and is thought to be of Early Carnian age, slightly younger than beds containing *Halobia lommeli* in the Western Tethys.

7.3   Species not identified in 2015/2016 fossil collection

Several species which have been reported from Svalbard have not been identified in the material collected for this thesis in 2015 and 2016. A brief description of each is given, which could be of importance for future fossil collecting activities on Svalbard.

***Daonella americana* Smith (1914)**

DIAGNOSIS: According to Smith (1914) *Daonella americana* is distinguished from *Daonella dubia* Gabb by its much finer and less bundled ribs, and from *Daonella moussoni* by its stronger radial ribs, weaker concentric wrinkles, and by the greater elongation of the shell (see Figure 7.13(A)).

AGE: Late Anisian (likely)

REMARKS: Resembles *Daonella arctica* and could be easily confused with it. This species was not found in material for this thesis but has been described from Svalbard by Pčelina (1965), at one locality in Wichebukta, eastern Spitsbergen, together with *Ussurites spetsbergensis, Frechites sp*. and *Parapopanoceras verneuili*. Described from the early Late-Anisian in north-eastern Russia in Konstantinov *et al.* (2013), in the Canadian Arctic by Tozer (1967) and boreal correlations by McRoberts (2010). According to Campbell (1994), *Daonella americana* is related to *Daonella lindstroemi* and *Daonella dubia,* the former reported from Svalbard. Smith (1914) reported that it commonly appears with *Daonella dubia* in Nevada.

Anisian forms

Daonella americana   *Daonella haraldi*
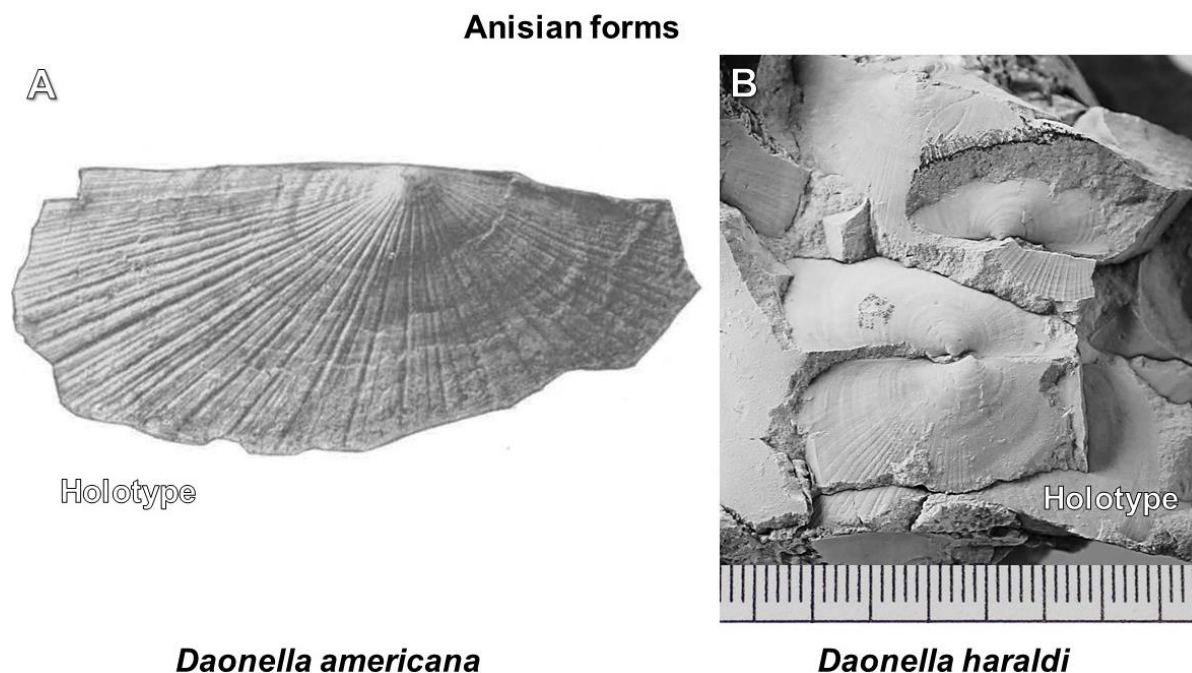
Figure 7.13: Anisian forms reported from Svalbard. A) Drawing of holotype of Daonella americana *Smith (1914, pl. XLIX, fig.4). B) Holotype of* Daonella haraldi, *housed in CASP collection, photographed in 2016, C7560 NB IMG 8694, courtesy of Simon Kelly.*

***Daonella haraldi* Campbell (1994)**

HOLOTYPE: C7560 in CASP collection, Cambridge. Photo in Figure 7.13(B)

TYPE LOCALITY: Vikinghøgda, Sassenfjorden, Spitsbergen.

DIAGNOSIS: Small to medium sized, inequilateral, rounded, obliquely ovate shells with characteristics of the genus *Daonella*. A prominent, inflated umbo. Weakly developed costation and notably absent in early growth stages. Regular, moderately broad, flat costae with numerous secondary furrows covering the rest of the disc; primary furrows shall, narrow. (Campbell, 1994)

AGE: Late Anisian

REMARKS: Campbell (1994) reported finding specimens of *Daonella haraldi* (see Figure 7.13 (B)), in a 1 m thick concretionary horizon, together with *Daonella lindstroemi*, 30 m below *Daonella degeeri* shellbeds at Vikinghøgda, Sassenfjorden. It is reported to closely resemble European form *Daonella boeckhi* Mojsisovics (1874) is size, costation strength and pattern. This species was not found in material for this thesis.

***Daonella moussoni* Merian (1853)**

DIAGNOSIS: (After Smith (1914)) Somewhat longer than high, the valves are rounded anteriorly and posteriorly. The umbo is low and projecting a little above the hinge line. The surface is covered with strong concentric wrinkles parallel to the striae of growth, much stronger on and near the umbo. The extremely fine radial ribs start out from the umbo and increase by intercalation. These are strongest in the middle of the shell, leaving the front and rear nearly smooth. There is no ear, as in *Halobia*, but the sculpture grows weaker toward the hinge line, giving a suggestion of an ear (see Figure 7.14(A)).

AGE: Early to Late Ladinian (boundary)

REMARKS: This species was reported from Edgeøya together with *Daonella frami* and *Daonella lommeli* by Lock *et al.* (1978). It is known from the boundary between the Early and Late Ladinian in Western Tethys (McRoberts, 2010).

Anisian-Ladinian boundary forms

Daonella moussoni

Daonella "species x"
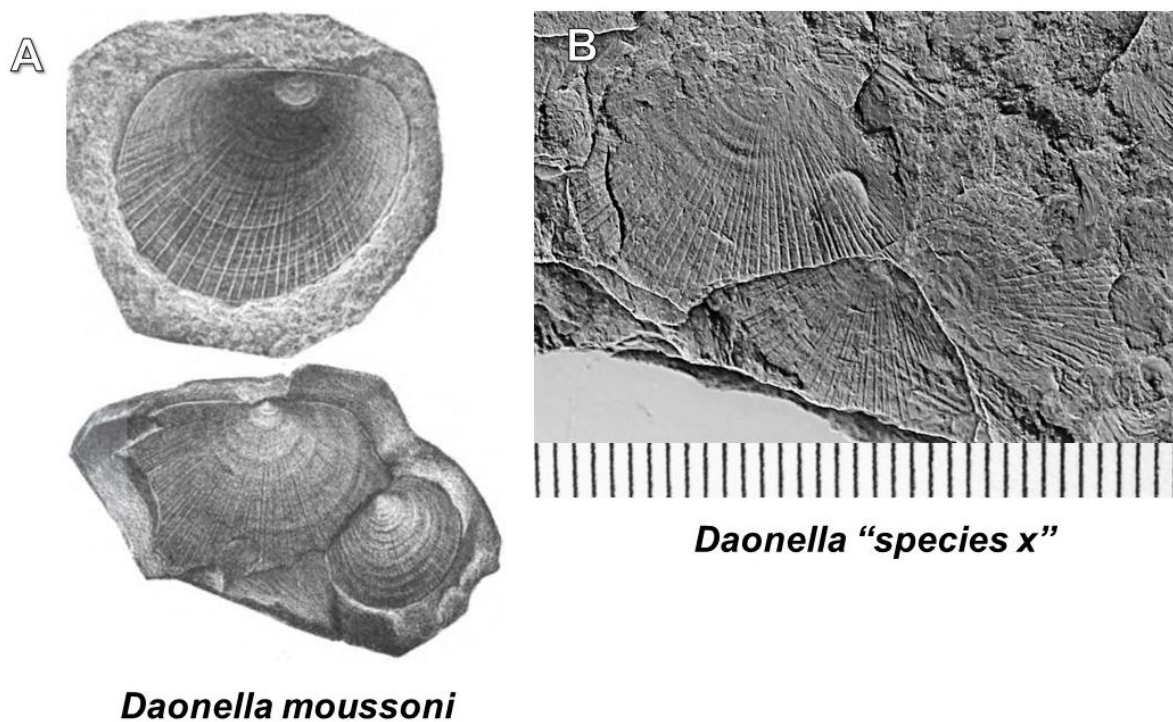
Figure 7.14: Anisian-Ladinian boundary form reported from Svalbard but not confirmed present in current collection. A) drawing of holotype of Daonella Moussoni *Merian, from Mojsisovics (1874, pl. III, fig. 18) B) A small group unidentified specimens, lying stratigraphically between beds containing* Daonella lindstroemi *(Late-Anisian) and* Daonella degeeri *(Late-Ladinian), collected from Dyrhø in 2016, Log 3 FOS 8 49m NB IMG 0747.*

A small number of relatively poorly preserved specimens were collected between bed containing *Daonella lindstroemi* and *Daonella degeeri* at Dyrhø in Fulmardalen in 2016. A tentative identification as *Daonella moussoni* can be made, but a larger number of specimens is needed, therefore these specimens are referred to as *Daonella* "species x".

Daonella lommeli Wissmann (1841)

DIAGNOSIS: (According to Mojsisovics (1874), using google translate) *Daonella lommeli* is significantly longer than high, ribs along the lower margin bend slightly backwards. The curvature is distributed evenly on both valves to the edge of the umbo (See Figure 7.15(B)).

Ladinian forms
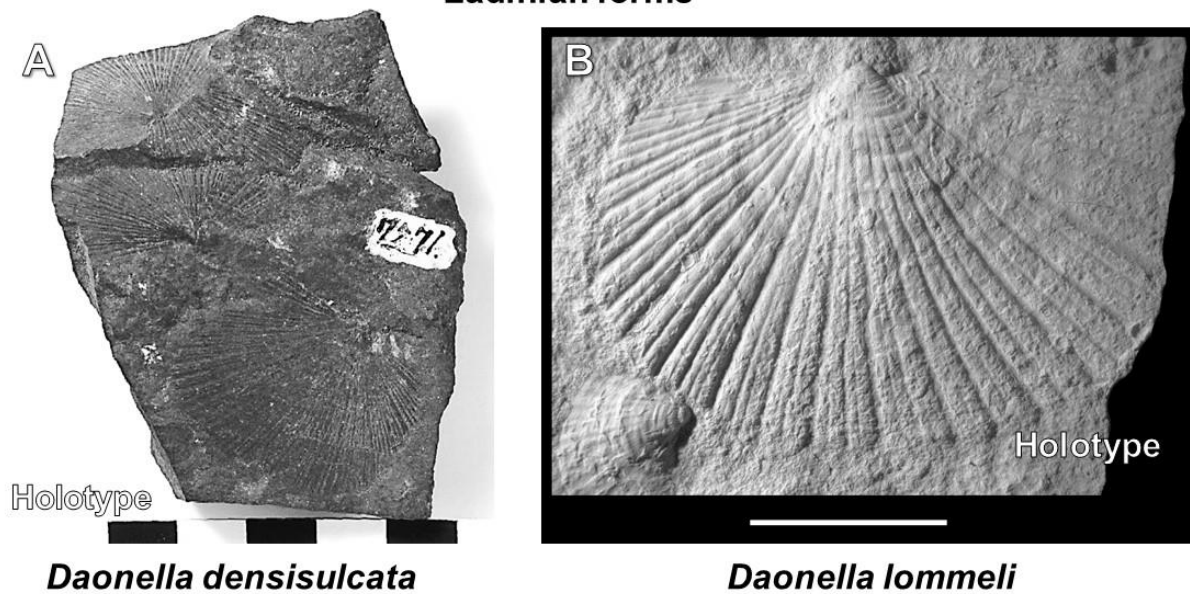
Figure 7.15: Ladinian Daonella *reported from Svalbard, but not identified in fossil material. A) Photograph of holotype of* Daonella densisulcata *Yabe & Shimizu (1927, pl. XII, fig. 9), photograph from Tokohu University Museum database. B) Type species of genus* Daonella, Halobia lommeli *Wissmann (1841, pl. 16, fig.11), housed at the NHM in Vienna, BSPG AS-VII-1970 Münster. Photo courtesy of Simon Schneider, CASP.*

AGE: Late Ladinian

REMARKS: This species was not found in material for this thesis but was described as a Late Ladinian species by Korčhinskaya (1982) at Roslagenfjellet, eastern Spitsbergen and Russebukta, Edgeøya. *Daonella lommeli* was reported to be found stratigraphically below *Daonella subarctica,* which in turn was directly below *Halobia zitteli.* This is the type specimen for the *Daonella* genus, as defined by Mojsisovics (1874), the holotype is in Figure 7.15(B). According to McRoberts (2010), *Daonella lommeli* Zone is found in the uppermost Ladinian of western Tethys.

Daonella densisulcata Yabe and Shimizu (1927)

HOLOTYPE: The holotype is defined by Yabe and Shimizu (1927, pl. XII, fig 9), housed at the Tokohu University Museum.

TYPE LOCALITY: Rifu Station, Rifu Province, Japan.

DIAGNOSIS: Furrows densely crowded over the entire surface. Many interstitial furrows of two or more cycles on the posterior part of the shell as on the anterior and middle parts. Less

crowed radial furrows on the anterior and posterior parts of the shell than *Daonella kotoi (Yabe & Shimizu, 1927)*.

AGE: Late Ladinian

REMARKS: This species, originally named *Daonella sakawana* by Mosisovics in 1888, is found in the Ladinian *Monophyllites* Zone in Japan (Yabe & Shimizu, 1927). It was described as Late Ladinian form in Svalbard by Korčhinskaya (1982), found at Dickson Land together with ammonoid *Indigirites neraensis* Popov in the *Nathorstites mcconnelli* Zone. It occurs above sediments containing *Daonella degeeri*. It was also reported together with *Daonella subarctica* from Barentsøya by Lock *et al.* (1978).

Halobia loveni Böhm (1904)

AGE: Early Carnian
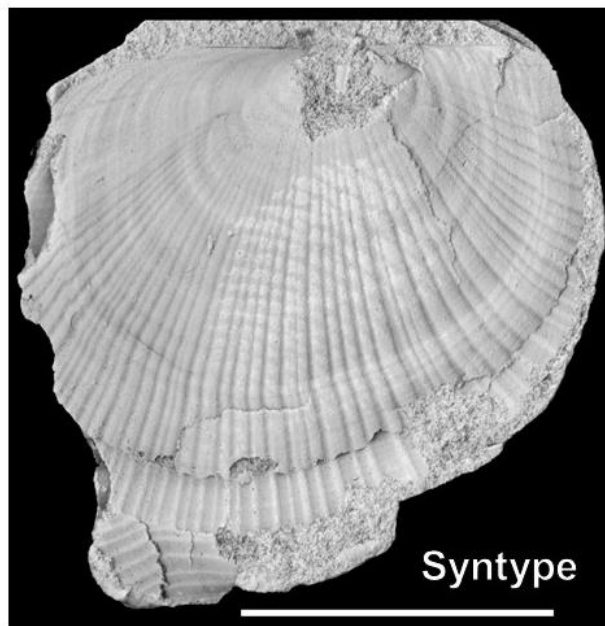
Figure 7.16: Early Carnian form reported from Svalbard but not identified in current fossil material. One of four syntypes of Halobia loveni *Böhm 1904, currently only reported from Bjørnøya, housed at the NHM in Stockholm, photo courtesy of Simon Schneider, CASP.*

REMARKS: According to the photo of the syntype in Figure 7.16, this species has clearly differentiated auricles and a "byssal tube", and is therefore considered a *Halobia* and is named

thereafter. According to (Korčhinskaya, 1982) *Daonella loveni* was a part of the hitherto richest and most varied fauna of the lower Carnian *Halobia zitteli* Zone collected on Bjørnøya by Böhm (1904), including ammonoids, gastropods, echinoderms and bivalves. This fauna is associated with the Carnian of NE USSR with no Ladinian specimens. *Halobia zitteli* was found together with *Daonella loveni,* suggesting they are of the same age. Campbell (1994) suggests that *Daonella loveni* is merely a pre-growth stop form of *Halobia zitteli.*

ANALYSIS: I was kindly given photos of four syntypes of *Halobia loveni* by Simon Schneider at CASP in December 2016. Using a measuring tool on tpsDig, I measured the size of the specimens on the images. None of the specimens had a growth stop, and had a maximum height of between 1.3-1.6 cm. Of the specimens of *Halobia zitteli* measured in this study the growth stop was located between 0.6-1.1 cm height, down from the umbo perpendicular to the hinge line. By this simple procedure one can tentatively suggest that *Halobia loveni* is not a pre-growth stop form of *Halobia zitteli*, and that they are in fact not the same species.

8. Data Analysis

8.1 Morphometrics

A morphometric analysis has been carried out on around 30-60 specimens of each species of *Daonella* and *Halobia.* An attempt has been made to objectively differentiate between species, and quantify changes in morphology upwards in the succession, relating physical differences between species to the paleoenvironment.

The term morphometrics refers to the measurement of the shapes and sizes of organisms, and the analysis of such measurements (Hammer & Harper, 2006). It is particularly crucial to palaeontology because genetic sequence data is missing. According to Stanley (1970), bivalves are ideal subjects for studying the relationship between morphology and ecology as shape and growth of most bivalve shells are directly controlled by habitat-specific factors, such as substrate, space, temperature, salinity, nutrition or competition. This is due to the more or less epi- or endobenthic life style of these animals. They therefore directly record paleoecological information and represent excellent tools for paleoenvironmental studies. Therefore, by distinguishing between species of *Daonella* and *Halobia* and studying the changes in their size, shape, and frequency within the Botneheia Fm., one can interpret changes in paleoenvironmental conditions on the Boreal shelf during the Middle-Late Triassic.

The largest problem when applying morphometrics to *Daonella* is preservation issues, as the vast majority of individuals are highly fragmented, making traditional methods such as measuring hinge length and shell height using a calliper difficult. Therefore, an alternative procedure is carried out, in accordance with suggestions made during personal communications with Øyvind Hammer at the NHM in Oslo. This entails a combination of methods described by Campbell (1994) and Schneider *et al.* (2010) and image analysis using various software programs.

Visualization of data is largely imitates a study of Jurassic bivalves from the Lusitanian Basin in central Portugal by Schneider *et al.* (2010). These bivalves where chosen for morphometric studies because of their abundance both in space and time and their variability in shell shape. They thrived in low-diversity/high-frequency associations, making them ideal objects for a comprehensive morphometric analysis. *Daonella* also occurs in such associations, and has a 2D shape and relatively simple geometry.

Campbell (1994) highlighted growth lines of *Daonella* specimens creating "commarginal plots, easily derived from flat-shell forms and which convey an accurate picture of shape without the

use of words". He suggested that using this graphic method precluded the need for tabulation of height and length measurements, hinge length, angle of byssal tube, and angle of obliquity, all of which he also found difficult to establish because of poor preservation of *Daonella*. Schneider *et al.* (2010) based their measurements on the length and height ratios of the *last traceable* growth line due to the fragmentation of most bivalve specimens in their material. They counted ribs along a clearly traceable growth line at the stage of maximum shell growth – in this way comparing specimens of a similar ontogenetic stage.

8.1.1 Measurement of morphological characteristics

Following lab procedures described in Chapter 5. Methods, lines were drawn along commarginal ridges onto high resolution images using Adobe Illustrator CC (2017) (Figure 8.1). The images with commarginal plots were then uploaded into the software package tpsDig 2.32, where a scale was set using the scalebar captured on the image.
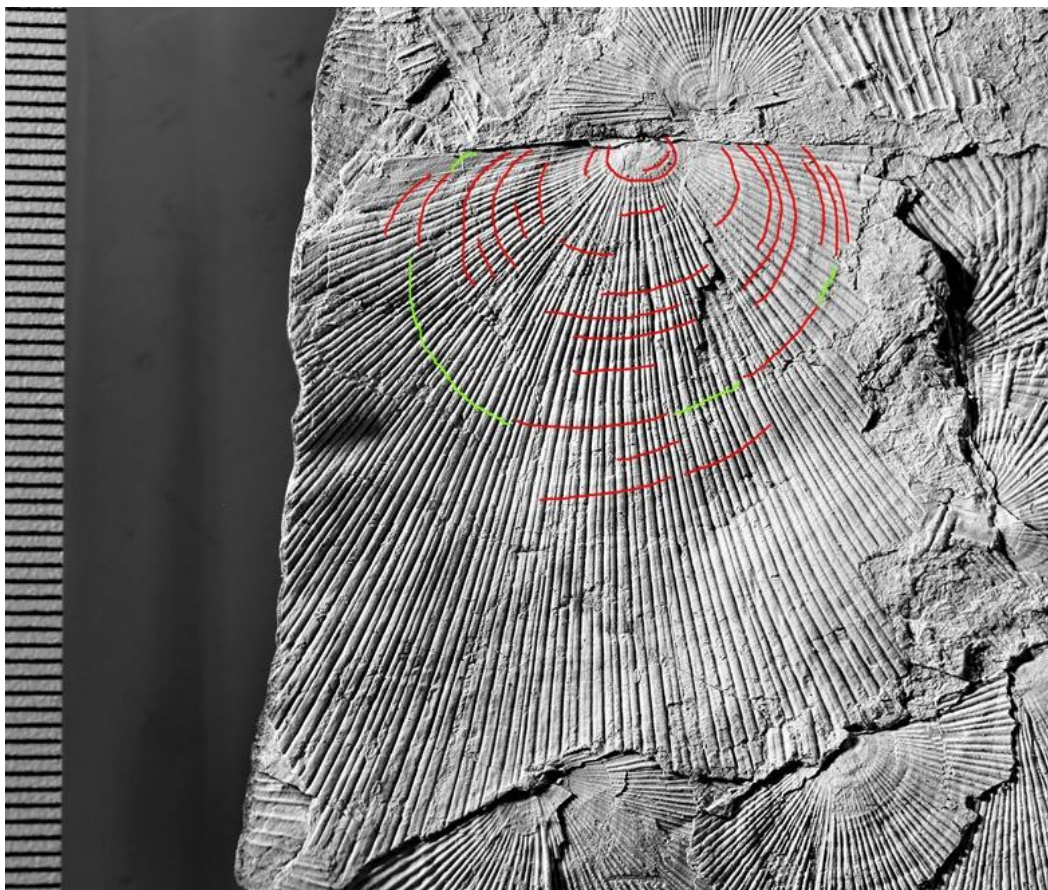
Figure 8.1: Commarginal plot of growth lines (red) on a fragmented specimen of Daonella degeeri. *Last traceable growth line with inferred extent (green). Created using Adobe illustrator CC 2017.*

After a traceable growth line was drawn on each individual, the height was measured directly below umbo, forming a right angle to the hinge line. The total length, and the length of the posterior and anterior sectors from the umbo were measured in order to determine the degree of shell asymmetry. Irrespective of the last traceable growth line, maximum preserved shell extent was measured in order to give an indication of individual size. Whether or not an individual was articulated (in butterfly position) or disarticulate was also noted. In the relevant species *Daonella frami, Daonella subarctica* and *Halobia zitteli*, width of auricles and maximum bending of the median (hinge perpendicular) rib was recorded along the last traceable growth line and at maximum extent (see Figure 8.2B).
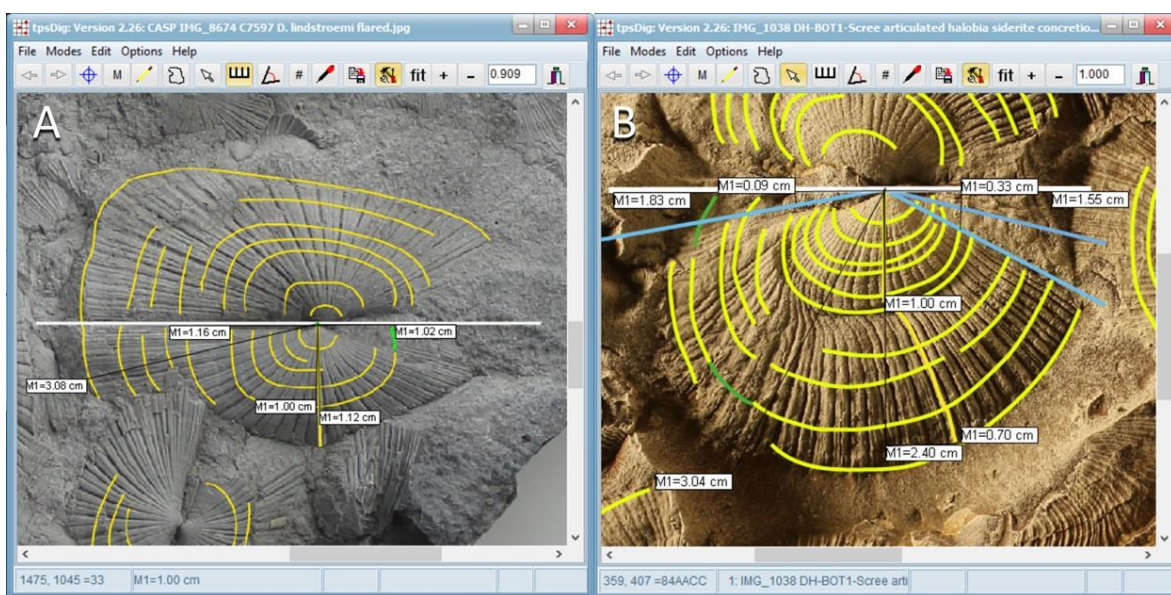
Figure 8.2: Screenshots of tpsDig 2.32 showing traced commarginal ridges and measured features of A) Daonella lindstroemi *(flared), and B)* Halobia zitteli. *Measured attributes include: Height and length of last traceable growth line, length of posterior and anterior and maximum shell extent. If present, width of auricles with byssal tube and deviation distance of median rib was also measured.*

Daonella lindstroemi has been divided into individuals with costae that flare outwards and individuals with completely straight costae. This has been done to objectively show variation within the species and determine if several species are present.

In order to reliably compare numbers of ribs between species, ribs were counted along a growth line at approximately 1 cm perpendicularly from umbo. If the height of the individual was < 1 cm, or highly fragmented, the minimum number of ribs visible was recorded.

Due to time limitations, 30-60 specimens of each species were measured. Most measured samples are from Tschermakfjellet, supplemented with well-preserved specimens from other

locations and the CASP collection in Cambridge. *D. arctica* and *D. subarctica* were only found at one location and in small numbers, and no specimens were housed in the CASP collection, so all 30-40 individuals of each species were measured. Only two valves were found of *Aparimella rugosoides* at Tschermakfjellet mountain, so this species has not been included in the statistical analysis. If no commarginal ridges are present, which was often the case with *D. subarctica*, then I inferred an outline of the whole shell.

8.1.2 Visualization of morphometric data

Height vs. length

The described measurements were tabulated in Microsoft Excel 2016 and data were visualized using box plots, histograms and scatterplots in Excel and PAST 3.14. Scatter plots of the height vs. length of each species were made with PAST and converted to a log scale (see Figure 8.3).
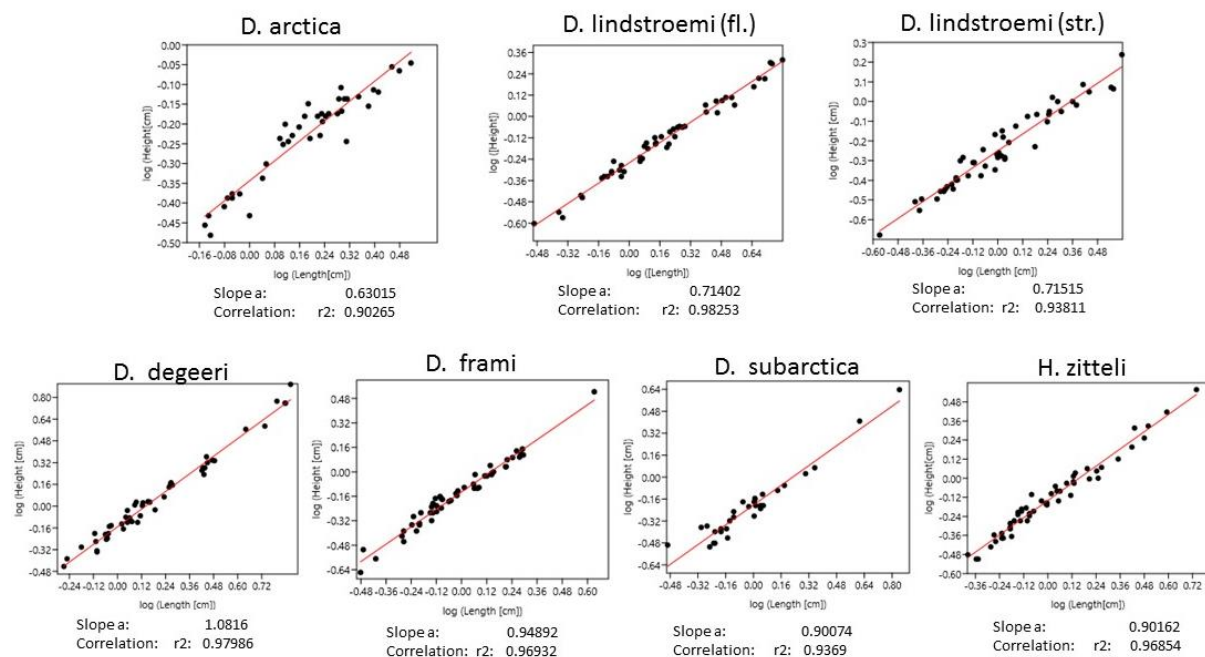
*Figure 8.3: Scatter plots of log transformed values of height vs. length for each species in order of position in stratigraphy (*Daonella arctica *is found lowest,* Halobia zitteli *is found stratigraphically highest). Slope of linear regression (a), where a = 1 indicates isometric growth and correlation coefficient (r^2) value, where r^2 = 1 indicates perfect correlation. There is a general trend of increasing isometry in growth as slope (a) approaches 1 upwards in the stratigraphy. Each sample shows good correlations, with r^2 values well above 0.9,* Daonella arctica *shows most variation with a correlation coefficient of 0.903. Graphs made using PAST 3.14 software.*

A statistical analysis was performed in PAST for the slope of the linear regression of the data and the correlation coefficient of determination value r^2. According to (Hammer & Harper,

2006), if there is no correlation then $r^2 = 0$ and if there complete correlation, $r^2 = 1$, indicating the proportion of variance that can be explained by linear association.

According to Hammer and Harper (2006), it is recommended to take logarithms of all measurements before further analysis. This is to take allometry into account - any change in proportions through ontogeny (for example the reduction of a human baby's head in proportion to body with age). By log transforming morphometric data, if the measurements adhere to the nonlinear allometric equation, the transformation will linearize the data, making it possible to use common analysis methods that assume linear relationships between variables. Such methods include linear regression, as presented in Figure 8.3.

While height and length are related through a power function, their logarithms are linearly related. On a log-transformed graph, if values fall along a straight line with a slope = 1, we have isometric growth, if the slope $\neq$ 1 we have allometric growth. If the points do not fall along a straight line at all, we also have allometry (Hammer & Harper, 2006) but not following the power function model. All the species display some form of allometric growth, however *Daonella degeeri* with slope = 1.08, displays a far more isometric growth pattern than *Daonella arctica* with slope = 0.63.

Without converting to a logarithmic scale, the length and height will be related through a power function with a constant *a* as the exponent (Hammer & Harper, 2006). This exponent is displayed in the equation of the power function trendlines of each species in Figure 8.4.

The exponent is the same value as the slope of the linear regression (a) in the logarithmic scale found in Figure 8.3. According to Hammer and Harper (2006), if $a = 1$, the ratio between length and width will be constant and we have isometric growth, if a > 1, we have positive allometry, if a < 1, we have negative allometry. Therefore, all the species display negative allometry to varying degrees, with *Daonella arctica* becoming the most elongate with age at a = 0.63. An exception is *Daonella degeeri,* which displays almost isometric growth but with slight positive allometry at a=1.08, i.e. the shell grows slightly higher in respect to length with time.
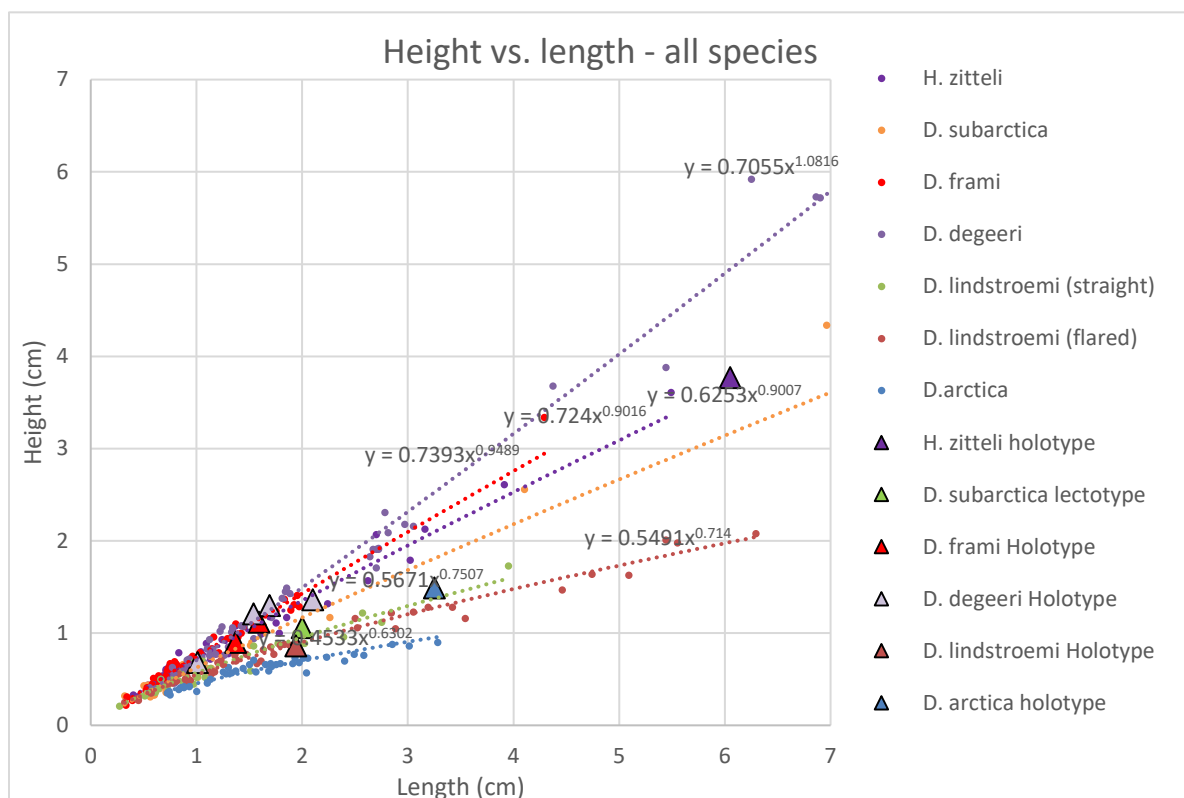
Figure 8.4: Scatter plot of non-log transformed height vs. length for all specimens measured, sorted into likely species and listed in relative position in stratigraphy. Power function trendlines of these groups show similar height vs. length in all specimens early in ontogeny. Larger specimens show a clear elongation in Daonella arctica *and* Daonella lindstroemi, *which are oldest taxa identified.* Daonella degeeri *and* Daonella frami *have a more equilateral growth patterns, shown by a steeper slope angle. Measurements of height vs. length of the holotypes have been included in triangles. Visualized in Microsoft Excel 2016.*

In the non-log transformed scatterplot of the heights and lengths of all measured specimens (Figure 8.4), there are clear differences between trends in growth. The oldest species collected, *Daonella arctica*, is generally small, and grows to be increasingly elongated, displaying allometry indicated by a bent point cloud. The variety of *Daonella lindstroemi* with a flared ribbing pattern*,* found stratigraphically just above *Daonella arctica* shows a similar development, however growing to be larger and slightly less elongated at maturity. The straight ribbed variety of *Daonella lindstroemi* is slightly less elongated. *Daonella degeeri* is found stratigraphically above *Daonella lindstroemi* and has a far more equilateral shape, clearly separated from *Daonella lindstroemi.* Interestingly, the valves of *Daonella frami* which lie just above *Daonella degeeri,* are generally smaller and slightly more elongated. This trend of elongation continues with *Daonella subarctica* and across the Carnian-Ladinian boundary to *Halobia zitteli.*

The data can be divided into three groups; the oldest taxa (group 1), *Daonella arctica* and *Daonella lindstroemi* (both straight and flared), which have low slope values indicating an elongated shape. Slope values of 0.60 and 0.71 respectively and bent point clouds (Figure 8.3) indicate allometric growth in these species. The second group (group 2) includes the younger *Daonella degeeri, Daonella frami, Daonella subarctica* with less anisometric growth than group 1 and slope angles of 1.08, 0.95 and 0.90, respectively. Group 3 is not as easily differentiated on the basis of height vs. length but contains *Halobia zitteli,* a genus defined on the presence of an anterior tube and large auricles (Campbell, 1994). Interestingly anisotropy seems to increase upwards in group 2.

Holotype data

I was kindly provided photos of the holotypes and lectotypes of most species of *Daonella* reported from Svalbard by Simon Schneider during my visit to CASP in December 2016. According Boris Shurygin, a museum curator at the Central Siberian Geological museum of Institute Petroleum Geology and Geophysics SB RAS, the holotype of *Daonella subarctica* is not available due to renovations (personal communication 26 Jan. 2017). The most recently taken photo of the holotype appears in Kurushin and Truschelev (2001). This image is unfortunately not provided with a scalebar so measurements have been based on an image of a specimen of *Daonella subarctica* identified from northeast Greenland by Christopher McRoberts in (Alsen *et al.*, 2017). These "model" specimens provide the best blueprint of the species for morphometric analysis and are herein referred to as holotype specimens.

Measurements were taken of morphological features of holotype specimens on images as described previously. These holotype measurements are plotted together with all the height vs. length data of each species in Figure 8.4. Visually, the holotype data fit well with the power function trendlines of each corresponding measured species from the 2015/2016 material. The holotype of *Daonella arctica* seems to deviate the most from the species trendline.

In order to test this hypothesis, a Student's *t*-test was run on the data. As outlined in Hammer and Harper (2006), a one-sample Student's *t*-test can be used to test the mean of one univariate sample (the H/L ratios of each species group) against a single value (the H/R ratio of the holotype of that species). In PAST, a value for *t* and p (two-tailed) is given. Providing the sample size is large enough, a low probability ($p < 0.05$) indicates statistically significant result, meaning that

Table 3: T-test of whether there is a significant difference between single-case holotype H/L ratio and the H/L ratios of the species sample set. Unlike Figure 8.4, only the lectotypes are displayed here

.

Holotype	Hol. H/R	Sample set size	Sample mean H/R	T-test (t)	T-test p(two-tailed)
H. zitteli	0.62	59	0.73	-1.31	0.20
D. subarctica	0.53	33	0.64	-0.97	0.34
D. frami	0.66	52	0.74	-1.27	0.20
D. degeeri	0.65	52	0.74	-1.00	0.32
D. lindstroemi (str.)	0.44	51	0.57	-1.10	0.28
D. lindstroemi (fl.)	0.44	49	0.50	-0.51	0.61
D. arctica	0.46	41	0.40	0.96	0.34

the H/R ratio of the holotype differs significantly to the average of the entire sample. The results are presented in Table 3. Holotypes of *Daonella arctica* and *Daonella frami* display the lowest *p*-values, indicating that they fit the sample data the least, confirming the visual impression in Figure 8.4.
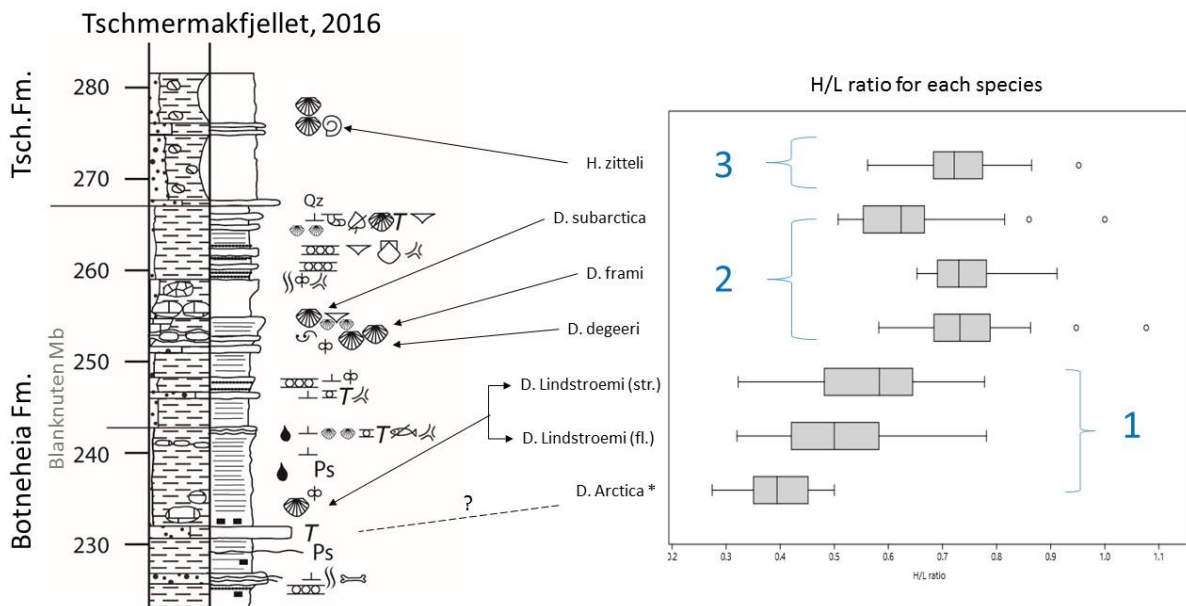
Figure 8.5: H/L ratios for each species, in order of relative position in stratigraphy. There seems to be a continuous gradation of anatomical change over space and time toward more equant shapes, with the exception of Daonella subarctica. **note* Daonella arctica *is not found at Tschermakfjellet, but relative position has been construed from a log from Milne Edwardsfjellet.*

The holotypes of other species were run against each species sample in order to test similarities between groups. The holotypes of *Daonella arctica* and *Daonella lindstroemi* were significantly different from all the species of group 2. The holotypes of *Daonella degeeri* and *Daonella frami* in group 2 were significantly different to the *Daonella arctica* sample but more similar to *Daonella lindstroemi* as well as group 2 species. Interestingly, *Daonella subarctica* was more similar to the *Daonella lindstroemi* sample than the rest of group 2 or *Daonella arctica*. Finally, the *Halobia zitteli* showed most similarity to *Daonella lindstroemi* and to *Daonella subarctica*.

In order to highlight variations between the species, the H/L ratios have been visualized with a box plot according to relative position in the stratigraphy at Tschermakfjellet, Figure 8.5.

Discussion on height vs. length data

The log transform data in Figure 8.3 shows that there is limited variation within the sample and that the height vs. length data of specimens assigned to a species group correlate well, as would be expected. However, differences in the slopes of the linear regressions suggest that there are changes in growth patterns between the species groups.

These differences in growth are better visualized in Figure 8.4, where the data suggests that the species are very similar in height vs length early in ontogeny. Campbell (1994) notes the striking resemblance between the larval shells of different Halobiidae and suggested similar mode of life in these early stages.

The slope of the power function trendlines suggest that the oldest taxa *Daonella arctica* grew allometrically, becoming the most elongate form with age, closely followed by *Daonella lindstroemi* (both forms). The species found stratigraphically above them, *Daonella degeeri,* grew isometrically, becoming approximately equally high and long with age, and reached very large sizes (seen by the length of the trendline). Above this, *Daonella frami* grew in a similar fashion but only medium sized individuals were measured. *Daonella subarctica* and *Halobia zitteli* grew to medium to large sizes, displaying moderate allometry with growth, becoming slightly elongated.

In Figure 8.4, the holotype data correlates well visually with corresponding sample group trendline, as would be expected. However, the height vs length of the holotype of *Daonella arctica* appears to deviate the most from its corresponding species group.

How much the H/L ratios of holotypes deviate from the species groups was tested using a t-test in Table 1. None of the holotypes were significantly different from their corresponding sample

group, however *Daonella arctica* in addition to *Daonella frami* displayed the lowest *p*-values, suggesting that they were slightly more different to their corresponding samples than the other holotypes.

In Figure 8.5, H/L ratios visualized in box plots give an impression of gradual trend of a less elongated form upwards in the stratigraphy (except for *Daonella subarctica*). Visually, one notices two groups, clearly separated both in the H/L ratio distribution and within the stratigraphy.

A second t-test was carried out with the holotype data, where it was found that the H/L ratios of the holotypes of the group lowest down in the stratigraphy (group 1) were statistically significantly different to the samples of all the species higher up in the stratigraphy (group 2 and group 3).

Although the height vs. length cannot necessarily prove that the species groups have been correctly identified or that they are different species, it does indicate trends of less elongated growth with time and that there seems to be two groups, separated not only in their shape but also within the stratigraphy.

Due to the incoherent systematics of *Daonella,* Schatz (2001; 2004) attempted to revise the Tethyan *Daonella* genera *Arzelella* and *Moussonella*, using unambiguous taxonomically significant biometric characters and Principle Component Analysis (PCA). He found that most daonellids are not determinable by univariate or bivariate methods and that PCA is needed to detect groups of similar holomorphs in multivariate space. He suggested that data from PCA should subsequently be applied to canonical discriminant function analysis in order to decide whether two groups are different enough to be separated into two species.

This highlights the limitations of using height vs. length measurements to distinguish species and therefore the morphometric data collected here has only been used to show general trends in shape and growth.

8.1.3 Other attributes

Boxplots are useful tools to visualize the distribution of one or several univariate data sets. The range of values is immediately apparent, as is the position of the median. It is easy to spot if a distribution is asymmetric, or strongly peaked (Hammer & Harper, 2006). Box plots have been made of the number of ribs at similar ontogenetic stage and width of auricles of measured specimens, sorted in order of relative position in the stratigraphy (Figure 8.6).
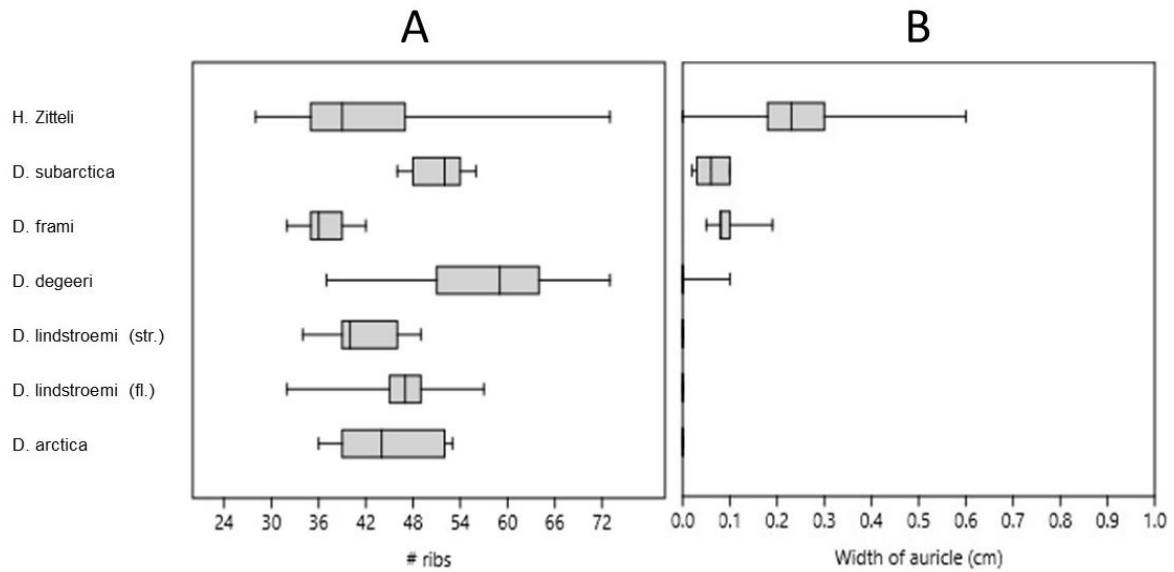
Figure 8.6: Box plots of species in other of relative position in the stratigraphy: A) minimum number of visible ribs at the 1 cm commarginal ridge and B) width of the largest auricle at 1 cm height. Visualized in PAST 3.14.

Number of ribs

The number of ribs at 1 cm height varies widely between the species. The distributions displayed in Figure 8.6A are strongly dependant on preservational issues as ribs were often not easy to see or part of the specimen was missing. Therefore, only the information of the maximum number of ribs is considered relevant here. *Daonella degeeri* and *Halobia zitteli* show the finest costation whilst *Daonella frami* consistently has the fewest ribs at this size. The dramatic reduction in the number of ribs between the species is suggested to be the most recognizable way to separate these two species in the field, which were considered to be conspecific by Tozer and Parker (1968) and Weitschat and Lehmann (1983).

Width of auricles

The evolution of the auricle and anterior tube or "byssal tube" of Campbell (1994) is apparent in Figure 8.6B, with an increase in the width of the auricles upwards in the stratigraphy. The widest auricles were seen in *Halobia zitteli*, as expected, as the area measured includes the anterior tube. Although there is a change towards wider auricles with time, the evolution does not seem to be gradual. *Daonella frami,* which is found slightly lower down in the stratigraphy, has wider auricles than *Daonella subarctica*. In a sample containing numerous *Daonella frami*, one specimen of *Daonella subarctica* was found. The possibility of this being in support of the

theory of punctuated equilibrium of Gould and Eldredge (1977) is discussed in Chapter 9.4 The evolutionary trends of *Daonella.*

Size-frequency distributions

The maximum shell extent was measured in order to get an impression of the size of the individuals. Due to the fragmented and incomplete nature of most of the specimens, this was measured from the umbo to the point furthest from it, regardless of direction. The resulting size distribution represents the specimens which were complete enough to make the aforementioned measurements around the umbo, but were usually otherwise fragmented. In most cases the specimen would have been significantly larger, had it been complete. This is a major uncertainty in the data.
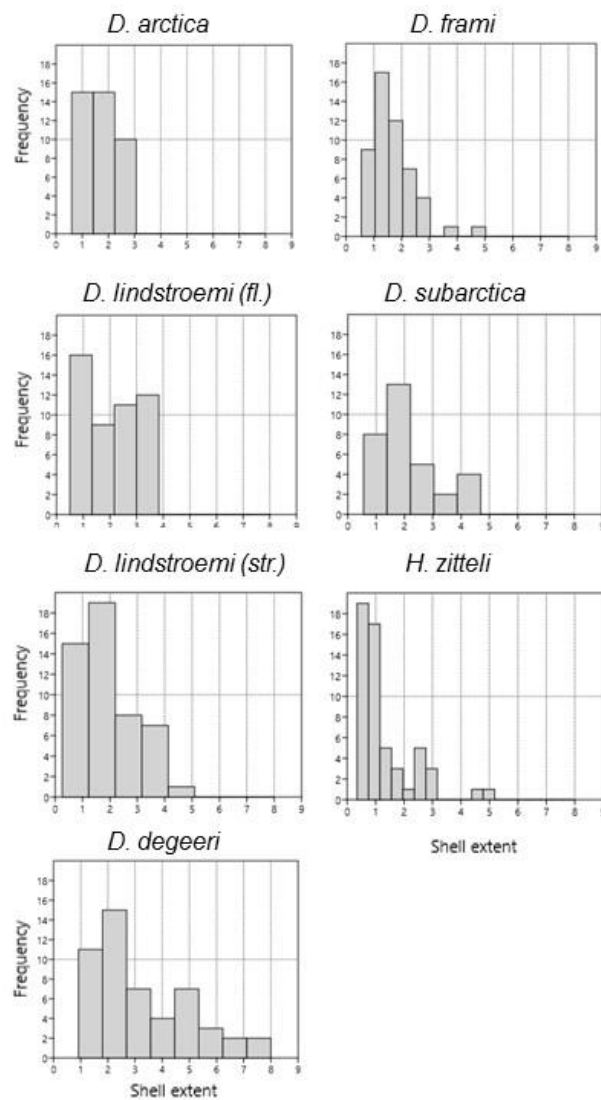
Figure 8.7: Histograms of maximum shell extents in the various species. Visualized in PAST 3.14.

In his study of transported bivalve death assemblages, Hallam (1967), found that positively skewed death assemblages primarily reflects normal growth and mortality rates, somewhat modified by the selective destruction of small shells. He suggested that sorting appeared not to play a major role, as symmetrical bell shaped distributions were exceptional. He found that strong positive skewness and symmetrical distribution are less common than moderate positive skewness and that bimodal distributions reflect a sudden death of a large number of individuals in an event.

A strong to moderate positive skewness is seen in all of the species, with an exception of *Halobia zitteli* which shows very strong positive skewness. Unlike his data, my samples are not collected from a single bedding plane so bimodal peaks in size distribution due to sudden deaths events would not be revealed. The size distribution of the species rather reflects their environment.

From modern analogues, Hallam (1967) found that the first year natural mortality is usually higher than in subsequent years. This is due to that young bivalves are more prone to removal form the sediment by strong water movements.

The size fraction 0-0.5 cm seems to be missing in most samples. In *Daonella degeeri,* the 0-1 cm fraction is completely missing. Suggesting that these sizes could have been swept away with currents. The largest amount of very small sizes is found in *Halobia zitteli*, suggesting different environmental controls to *Daonella degeeri.*

After experiments simulating reworking, Hallam (1967) found that strong positive skewness shifted appreciably to the right. This is because shells of different size and thicknesses have different hydrodynamic properties. Juveniles and small shells are much more prone to breakage presumably due to their thinner shell.

Hallam found that fossil assemblages often concentrated due to slow sedimentation rates. According to Hounslow *et al.* (2008), the Blanknuten Mb. of the Botneheia Fm. is highly condensed. At Milne Edwardsfjellet, they found that the entire late Anisian to early Ladinian is condensed into 20 m. The first occurrences of *Daonella* occur in the late Anisian on Svalbard (Korčhinskaya, 1982). Hallam (1967) suggested that in condensed beds, there would most likely be a wider scattering in size frequency distribution because of the mixing of forms which grew at varying speeds at differing times. Also, diagenetic solution of small thin shell was more likely to occur.

The widest size distribution is found in the *Daonella degeeri* coquina beds. The coquina beds which contain *Daonella degeeri* are often highly fragmented, suggesting that reworking is an important factor. The degree of fragmentation varies within cm's, where large, whole individuals are found on top of a matrix of highly crushed shell. This species shows a size distribution with the highest number large to very large shells. As mentioned, the 0 – 1 cm fraction is completely missing suggesting that the smallest individuals could have been removed with currents, that reworking lead to the destruction of smaller shells or that the condensed nature of the sediments and diagenetic solution removed them. The very nature of the *Daonella degeeri* coquina beds, which contains countless millions of individuals within a 0.1 – 0.5 cm interval, suggests that this could be a condensed bed. The interval has a very wide lateral extent and has been traced from western to eastern Svalbard. One can suggest that this cannot be explained by a single event of mass death of very large planktonic or benthic organisms (see chapter on mode of life), rather that large numbers of dead adult individuals were concentrated on the sea floor during a time of very low clastic sedimentation. Regionally low sedimentation rates would explain the wide extent of this deposit. According to Hallam (1965), if short-lived catastrophic benthic events leave any record at all, they usually leave a thin band of fossils that contain all sizes.

According to Hallam (1967), if reworking leading to the destruction of small shells is a factor, then argillaceous deposits should contain a higher proportion of juveniles than arenaceous deposits. There is a possibility that this is the case with samples containing *Daonella frami*. This species is found directly above the coquina beds containing *Daonella degeeri* but is usually in dark grey shale. Following Hallam's reasoning, the smaller sizes would have been more easily preserved here. However, the lack of very large individuals suggests that other environmental controls, perhaps sources of food, could have been a contributing factor too. The smallest size fraction is reduced in comparison to individuals above 1 cm size, suggesting the smallest individuals have been removed, possibly due to currents. Individuals were usually fragmented to an extent, suggesting that reworking has been an important factor here too, though not to the same degree as *Daonella degeeri*.

The flared individuals of *Daonella lindstroemi* were primary measured form cemented siltstone beds whilst those with a straighter rib patterns were often found in grey to dark-grey shale samples. There appeared to be no preferred position of these groups within in the stratigraphy. In light of this, no attempt is made here to separate the groups into two species. One can speculate that differences that do emerge between the two groups is partly due to the substrate

130

they were found in, altering their final preserved shape. The size distribution of the straight ribbed *Daonella lindstroemi* is more positively skewed. This seems to support the possibility that small sizes are more readily preserved in shale.

Hallam (1965) suggested that black shales usually signify deposition in stagnant water in which disturbance was at a minimum. Black shales where water is severely restricted and hydrogen sulphide is generated by sulphate-reducing bacteria typically contain minute shells thought to be stunted adults. A condition of declining mortality rate with age, combined with lack of selective destruction may give rise to strong juvenile peak and a very small number of much larger adults.

This might be the case with *Halobia zitteli.* The size distribution of this species is strongly positive, consisting of very large numbers of individuals in the size range of 0.5 – 1 cm. Whether these represent juveniles or adults cannot be proven here. A few large adults displaying growth stops were occasional observed amongst a high number of small individuals of about 1 cm size.

Schatz (2001; 2005) carried out a similar study of size distribution on Tethyan *Daonella moussoni*. This species was most commonly found forming thick allochthonous lumachellas of fragmented and specimens preserved in butterfly position. Rare, autochthonous assemblages of articulated specimens with closed valves showed population structures dominated by sub-adults and adults. He interpreted horizontally oriented closed articulated individuals to be autochthonous. In such assemblages, juvenile specimens of *Daonella* were very rare but larval shells and juvenile specimens were found in great numbers in some layers. These were interpreted as mass mortality events triggered by seasonal oxygen fluctuations.

Daonella arctica show a strong positive distribution composed of small to medium sized daonellids, with no large specimens and no juveniles. There was minimal fragmentation in these samples and the individuals were almost exclusively preserved in butterfly position (Figure 8.10 in following subchapter of orientation statistics). The narrow distribution of the individuals seems to agree with Schatz's findings of autochthonous assemblages of *Daonella,* however age of the individuals is beyond the scope of this work, and whether they represent adults or sub-adults is unknown. Schatz (2001) noted that butterfly preservation is normally rare for daonellids and is only known from small-sized species, suggesting that they may in fact represent adult forms.

Butterflied vs. disarticulated preservation

Observations were made of whether the individuals measured above were found in articulated butterfly position or as disarticulated single-valves. This data is presented in Figure 8.8.
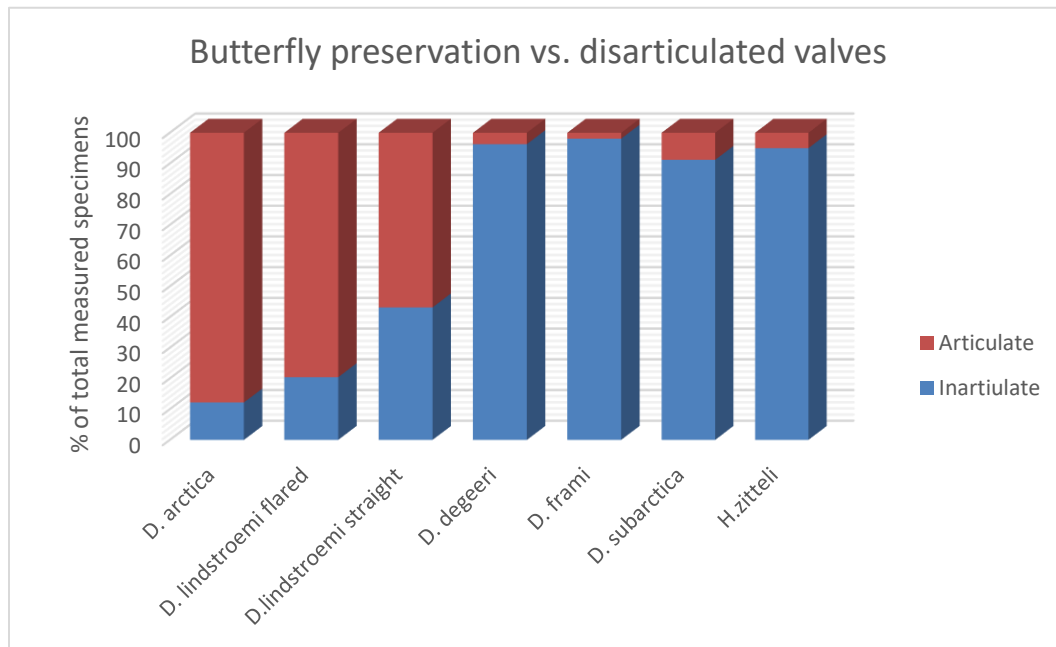
Figure 8.8: Overview of percentage of articulated vs. disarticulated valves of measured specimens of each species

There seems to be a steady decrease in the number of individuals preserved in butterfly position upwards in the stratigraphy. A simplistic explanation for this is that is a general increase in energy, as would be expected by a regressive cycle towards the top of the Botneheia Fm. (Mørk *et al.*, 1982), leading to more reworking and subsequent disarticulation of the valves.

According to Schatz (2005) the preservational-styles of daonellids (disarticulated, butterfly preservation, cone-in-cone preservation and articulated with closed valves) are a products of different taphonomic processes. Daonellids from coquina beds are always disarticulated and often broken, indicating shell-shell interaction though post-mortem transport, either by bottom currents or turbidites. This suggests that especially *Daonella degeeri* coquina beds, could be interpreted as allochthonous taphocoenoses.

He suggests that individuals that were found in butterfly position (relevant here for *Daonella arctica* and *Daonella lindstroemi*), did not necessarily represent autochthonous assemblages, as examples had been found in low-density, low velocity turbidites.

8.2 Orientation statistics

A relatively simple method for testing for currents on the sea floor or post mortem transportation of shells is to measure their orientation within a bedding plane. Directional statistics is an important application in palaeontology and can be used to investigate whether or not directions of body or trace fossils are randomly distributed (Hammer & Harper, 2006). Samples containing at least 10 specimens were chosen in order to get a statistically reliable result. The samples were not oriented in the field so interpretations of paleocurrent directions are not possible. However, an indication of the presence of currents can be inferred, and whether these are unidirectional or bidirectional. Orientations of the hinge line from "north" were measured using the angle tool in tpsDig 2.32 and then plotted on rose diagrams in PAST 2.14.

Orientation was measured in two ways: perpendicular to the hinge line in single valve specimens and along the hinge line towards the posterior in articulated individuals. This is to make up for the fact that the articulated and disarticulated valves will orientate themselves differently in a unidirectional current (Øyvind Hammer, personal communication 2017).

Population statistics, specifically Rayleigh's test, were used to determine the presence of preferential orientation. According to (Hammer & Harper, 2006), a small p-value ($p < 0.05$) shows statistically significant preference for one direction in the Rayleigh's test, however this method is not appropriate for samples with bimodal distributions. For two or more preferred directions, a small p-value ($p < 0.05$) in the chi-test will indicate non-uniformly distributed directions, and that some directions are more common than others.

Samples with statistically significant orientations are interpreted to be deposited in an environment effected by either bidirectional wave or unidirectional currents on the sea floor.

Nagle (1967) conducted laboratory experiments on wave and current orientations of shells using flume and wave tank experiments, applying these concepts to paleocurrent reconstructions of marine Middle and Upper Devonian strata in north-eastern Pennsylvania. He proposed that shells attain a more uniform and more readily measurable configuration than mineral particles, and therefore a study of shell configuration should reflect some sedimentary processes more clearly than the study of other clastic particles.
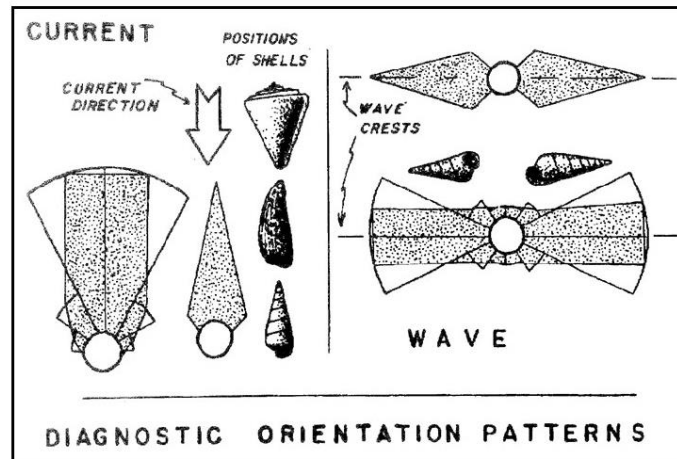
Figure 8.9: Diagnostic orientation in rose diagrams of wave and current oriented shells (Nagle, 1967).

According to Nagle (1967), rose diagrams of **current** oriented shells show one strong maximum, where elongate or plate-form shells point into or away from the current, depending on the geometry and mass distribution of the shell (see Figure 8.9). In ideal current conditions, all elongate shells will point the same way with the long axes parallel to and the apex pointing into the current direction, however realistically as little as two thirds of the shells may have the same orientation.

Waves, shoaling but offshore from the swash zone, were observed to move elongate shells back and forth, while aligning the long axes parallel to the wave crests. Approximately half the shells point in one direction. Rose diagrams of wave oriented shells therefore have two sub-equal and opposite maxima, parallel to the wave crests. In a low angle swash zone, orientations show the two maxima of wave patterns, but the shells are aligned perpendicular to ripple marks by incoming and outgoing swash (Nagle, 1967).

8.2.1 Rose diagrams of fossil material

The orientations of the largest sample of each species is given in order of position in the stratigraphy in the following figures Figure 8.10 to Figure 8.17. Examples of *Daonella lindstroemi* in various lithologies, not necessarily in stratigraphical order are given.

Note: the geographical convention option for visualization was used when converting the orientation data from tpsDig 2.32 to PAST. This caused the orientations to be offset in the rose plot by approximately 90 degrees.
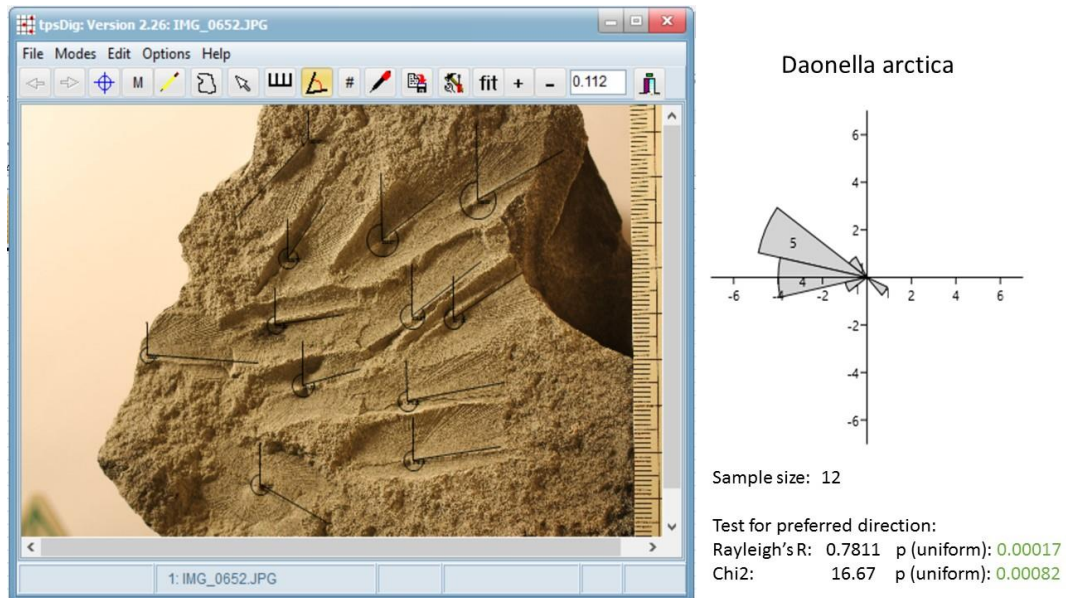
Figure 8.10: Orientation measurements of Daonella arctica, *found in a siltstone at the base of the Blanknuten Mb. at eastern Milne Edwardsfjellet, FOS 5 59m NB IMG0652. The individuals are preserved in butterfly position and therefore measurements were taken along the hinge axis towards posterior. The orientation distribution suggests a unidirectional current, supported by a low Rayleigh's p-value.*
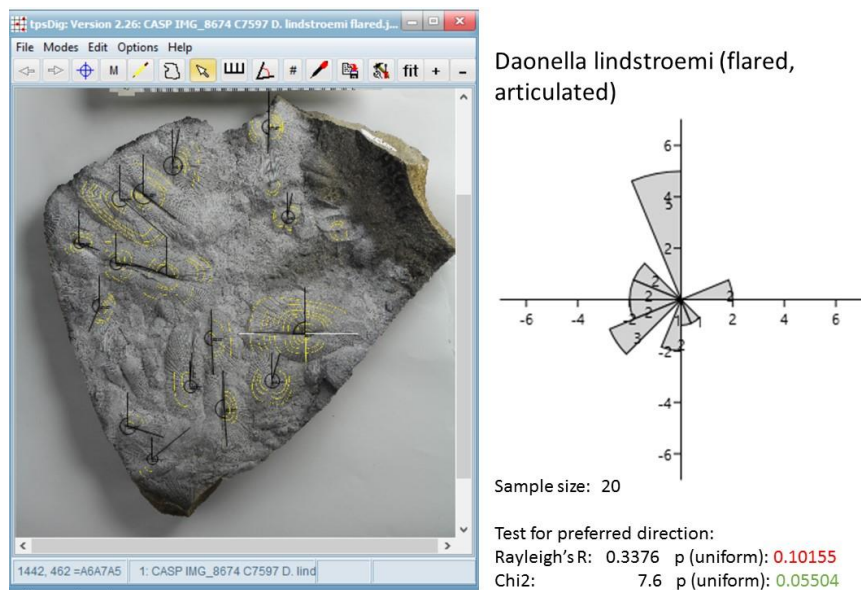
Figure 8.11: Orientation measurements of a siltstone slab of articulated Daonella lindstroemi *(variety with flared rib pattern), from CASP, C7597 NB IMG8674, courtesy of Simon Kelly. Individuals are preserved in butterfly position. Measurements taken along the hinge axis towards anterior. The orientation distribution suggests a bimodal distribution, where two directions are dominant, roughly perpendicular to one another. One can suggest that this sample represents a population which lived in the presence of unidirectional currents, where individuals actively orientated themselves into the current when all alive, and became passively oriented post mortem. The low p-value for the Chi^2 test indicates non-uniformly distributed directions, where some directions are more common than others.*
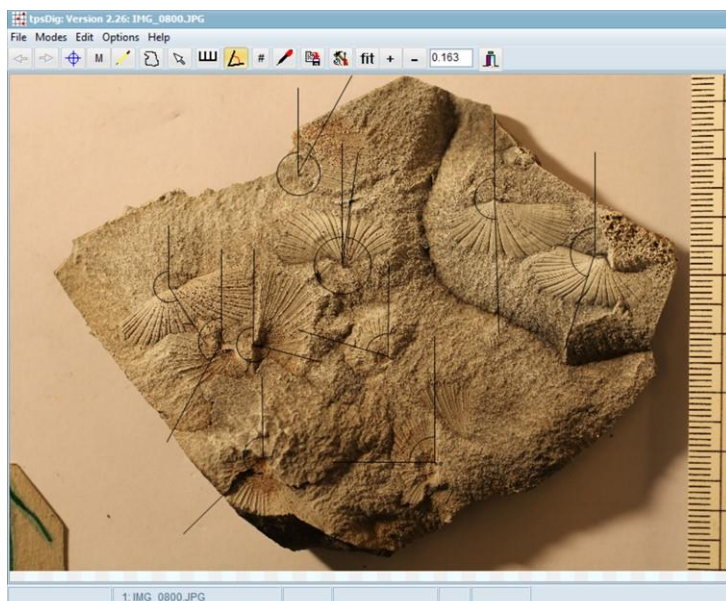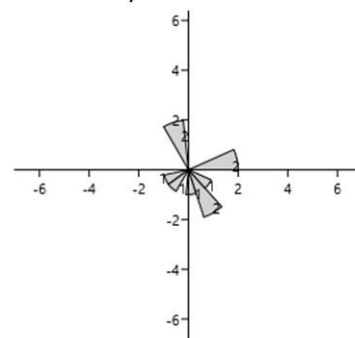
Figure 8.12: Orientation measurements of a siltstone slab of single valves of Daonella lindstroemi *(flared variety), found at Dyrhø in Fulmardalen, Log 3 FOS5 36m NB IMG0800. Individuals are not found in butterfly position and therefore all measurements were taken from the dorsal to ventral part of the shell, perpendicular to the hinge line. Orientation cannot be confirmed by the p-value for either the Rayleigh's R or the Chi² test. One could suggest that these single valve specimens have been transported, but a larger sample size is needed for significance.*
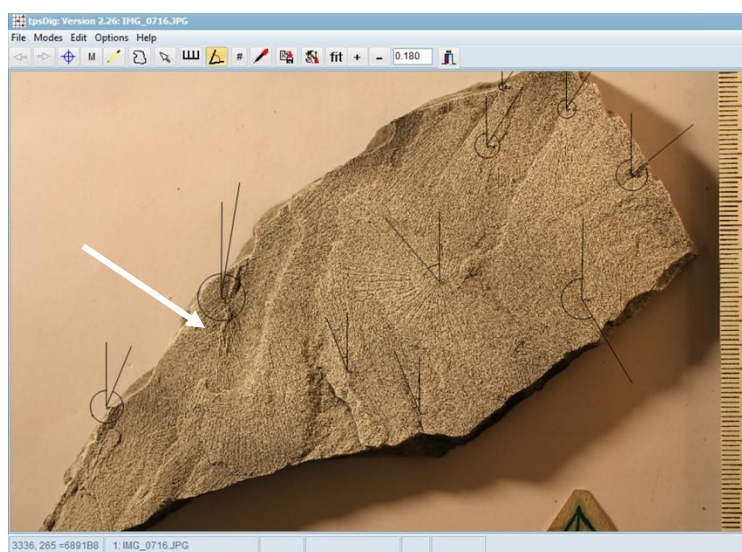
Figure 8.13: Orientation measurements of a highly organic, black shale slab of flattened Daonella lindstroemi *(straight ribbed variety), found at Dyrhø in Fulmardalen, Log 3 FOS4 35m NB IMG0716. The individuals are preserved in butterfly position and therefore measurements were taken along the hinge axis towards posterior. The orientation distribution suggests a unidirectional current, supported by a low Rayleigh's p-value < 0.05. One individual appears to be closed and articulated (indicated with the white arrow) suggesting that this sample might represent an autochthonous assemblage of oriented individuals.*
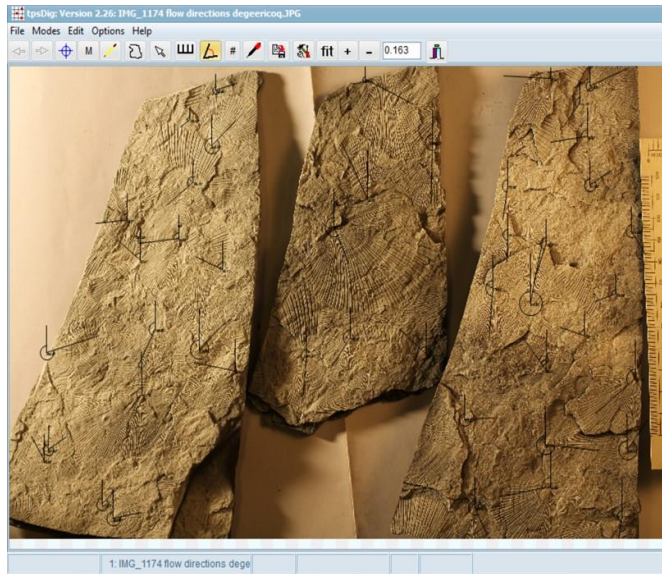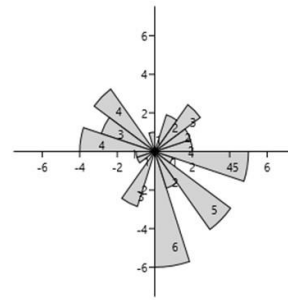
Figure 8.14: Orientation measurements of a large sample of flattened Daonella degeeri *found in a slab of coquina, pulled apart into three pieces with the same orientation. Collected at Dyrhø in Fulmardalen, Log 1 Scree NB IMG1174. Individuals are large and medium sized, and are somewhat fragmented. Measurements were taken from the dorsal to ventral part of the shell, perpendicular to the hinge line. Orientation distribution suggests a bimodal distribution, which could be an indicator orientation by wave action. This interpretation is supported by a low Chi^2 test p-value < 0.05, which indicates non-uniformly distributed directions, where some directions are more common than others.*
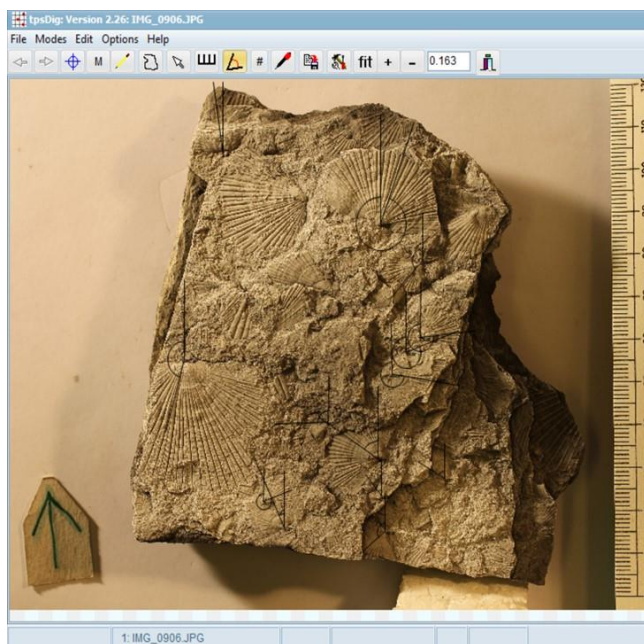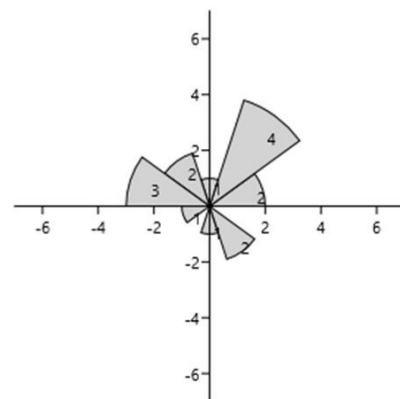
Figure 8.15: Orientation measurements of Daonella frami *found in dark grey shales 1 m above* Daonella degeeri *coquina beds at Botneheia, Log 1 FOS12 29m NB IMG0906. Individuals are small to medium sized, and are somewhat fragmented. Measurements were taken from the dorsal to ventral part of the shell, perpendicular to the hinge line. Visually, the orientation distribution suggests random to slightly bimodal distribution, however this is not backed up by the statistical tests, a larger sample is needed.*
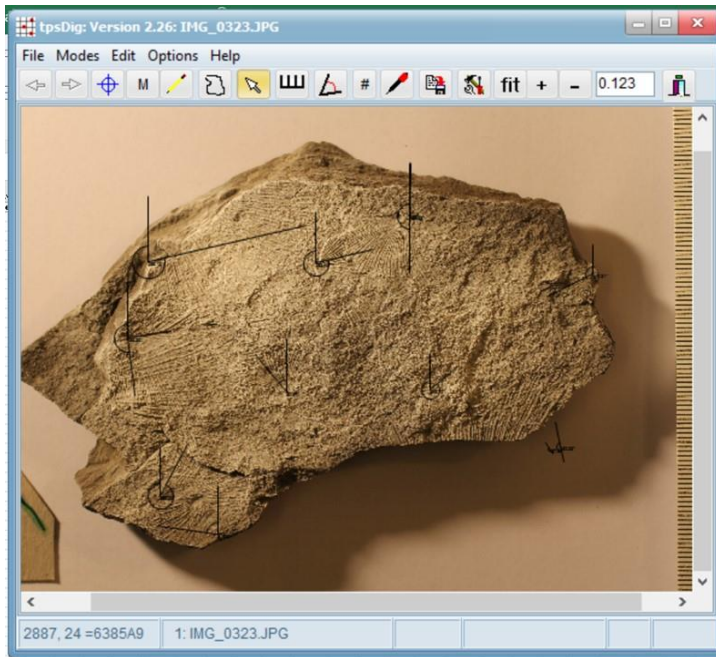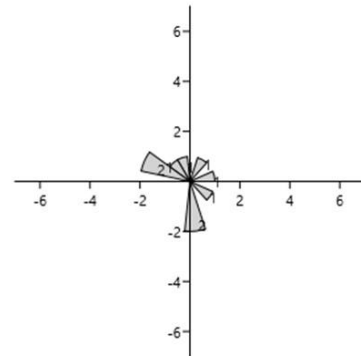
137

Figure 8.16: Orientation measurements of the largest sample of Daonella subarctica *found in silty dark grey shales 2 m above* Daonella degeeri *coquina beds at Tschermakfjellet, FOS7 28m NB IMG0906. Individuals are medium to large sized, and are all somewhat fragmented. Measurements were taken from the dorsal to ventral part of the shell, perpendicular to the hinge line. There seems to be a bimodal distribution however this is not backed up by t- tests, a larger sample is needed.*
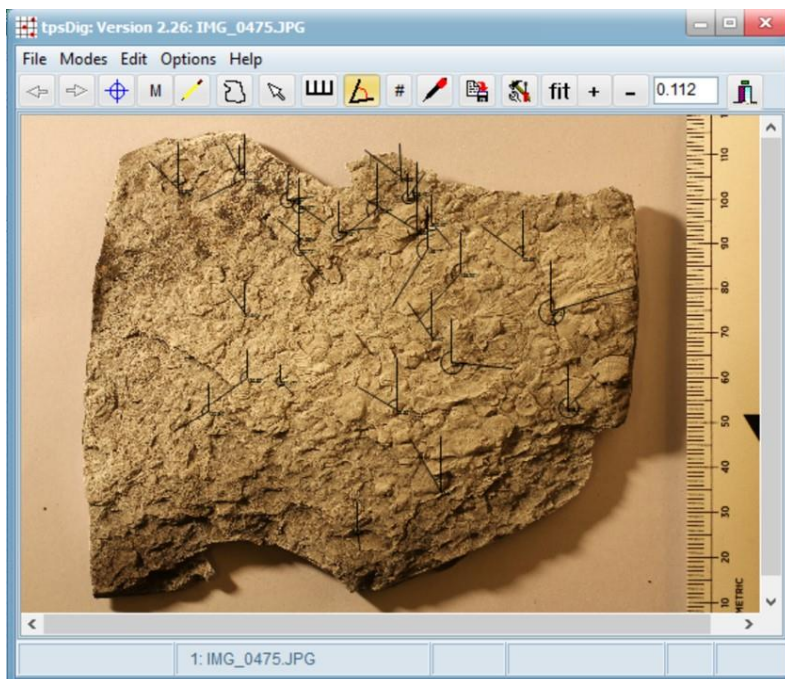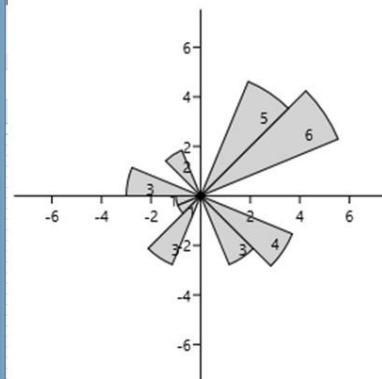
Figure 8.17: Orientation measurements of a siltstone containing Halobia zitteli *found in Tschermakfjellet Fm. at Tschermakfjellet, FOS11 48.5m NB IMG0475. The sample consist of large number small individuals and one larger adult specimen, randomly oriented on the bedding plane. This might represent a sample with stunted adults, see discussion.*

Discussion on orientation patterns

Samples showing a statistically significant *p*-values (<0.05) in the Rayleigh's test are interpreted to have been deposited in an environment dominated by a unidirectional current. This type of orientation was found in a siltstone sample of the resumed oldest taxon *Daonella arctica,* preserved in articulated position (Figure 8.10). Unidirectional orientation was also found in a dark grey to black shale sample containing *Daonella lindstroemi* in butterfly position and one specimen with closed valves (Figure 8.13). The statistically significant unidirectional orientations of these samples suggest the presence of a unidirectional current on the sea floor during deposition of these individuals. Schatz (2005) found that occurrences on undisturbed laminated bedding planes showing preferred hinge orientation indicated most port-mortem transportation, and that butterfly position does not necessary indicate autochthony.

A second sample of articulated *Daonella lindstroemi* preserved in a siltstone (Figure 8.11) did not have a unidirectional distribution, but rather a perpendicular bimodal distribution. Though bimodal, the perpendicular nature of the distribution does not support the influence of wave action as this shows two preferred orientations at roughly 180 degrees to each other (Figure 8.9). One possibility is that the filter feeding individuals actively oriented themselves into or away from the current in life, and became passively oriented after death. A third sample of *Daonella lindstroemi* containing only single valves (Figure 8.12), some of which were fragmented, did not show a bimodal distribution, and is interpreted to have been deposited by reworking, for example by a storm event or in a mass flow. Varying depositional regimes seem to have been dominant during the time period represented by *Daonella lindstroemi,* however unidirectional currents seem to have had an influence rather than wave induced currents.

Samples showing two directional peaks are interpreted to indicate an environment dominated by bidirectional currents, in other words, wave action or tidal action. This was found in a large sample of *Daonella degeeri*, where individuals were large sized and often fragmented. The Botneheia Fm. records a second-order transgressive-regressive cycle along an open shelf in the Svalbard basin (Mørk *et al.*, 1982), culminating in an erosional unconformity at the Ladinian-Carnian boundary due to a global sea level drop (Biddle, 1984). In view of this, one would expect progressively more wave action further up in the stratigraphy as the shelf became shallower.

The samples containing *Daonella frami, Daonella subarctica* and *Halobia zitteli* show no statistically sound preferential direction. One can speculate that *Daonella frami* and *Daonella subarctica*, the individuals of which were all fragmented to some degree, were reworked for

example during a storm event or deposited by mass flow in a higher energy environment. The pristine nature of the individuals in the sample of *Halobia zitteli* suggests they have not been deposited in a mass flow but rather that the shells settled in an environment without strong currents, allowing them to orient themselves randomly.

Limitations

A major limitation for the reliability of the orientation measurements is the number of individuals found in a single sample of material. This is especially true of the samples containing *Daonella frami* and *Daonella subarctica*. More statistically reliable results could be achieved by doing orientation measurements on large exposed bedding planes in the field, for example, the large siltstone platform at Muen on Edgeøya. Lighting standardised in the top left of each photo may also create a bias towards certain orientations as costae oriented into the light source are more difficult to see on the final photo. This problem may also be mitigated by taking measurements in the field.

One should not forget that elongated flattened objects such as the shells of *Daonella arctica* and *Daonella lindstroemi* will behave very differently in currents than the more equant plate-formed rounded shells of *Daonella degeeri, Daonella frami and Daonella subarctica.* An elongated flat object is far more likely to become uniformly oriented into the current than a round flat object, and this could be a partial explanation for the more random orientations found in the round-form shells presented above.

This was discussed by Nagle (1967), where in flume and wave-tank experiments, he found that equant plate shell forms rarely attained a diagnostic current orientation, while elongated asymmetrical plate forms (such as *Daonella arctica*), always attained diagnostic current orientations. The rounded forms oriented themselves away from the current more often, and tended to develop indistinct current orientation patterns, probably because there is no long axis for the current to act upon. Symmetrical elongated plates (more like *Daonella lindstroemi*) commonly become oriented cross-wise to the current with the beak pointing into the current. The orientation of elongate asymmetrical plates and cones seem to be dependent only on current direction and Nagle considered them to be the best to use in paleocurrent interpretations.

Another important aspect discussed by Nagle (1967) was basing the orientation measurements on shells that were not in contact with other shells as this affects their orientation and could yield a non-diagnostic pattern. The nature of the shell beds of *Daonella* makes this distinction impossible, and therefore this will remain a limitation of this kind of data.

8.3 Summary

Although bivariate measurements are not sufficient to objectively prove the existence of the difference species or that they have been correctly identified from the holotype, they have still been useful. These measurements have revealed trends in morphology that suggest separation of the measured specimens into three groups: 2 groups of daonellids and 1 group consisting of *Halobia* (Figure 8.18). The groups are separated by both their physical characteristics, by their position within the stratigraphy and by their reported age.
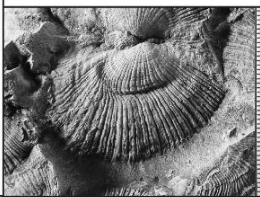
		Species charcteristics based measured attributes in 2015/2016 fossil material
GROUP 3		**Halobia zitteli** Slightly anisometric growth and elongation with age. Sample studied contained whole, randomly oriented individuals suggesting little reworking by currents or mass flow. Strongly positive skewed size distribution for all measure specimens, could suggest the presence of stunting. Attributes include a characteristic growth stop, an anterior tube and large auricles.
GROUP 2		**Daonella subarctica** Species showed moderately allometric growth, with a trend towards more elongation with age. Random orientation and fragmentation within a sample, in addition to very few small individuals suggests reworking. Reduction in the auricle size as compared to *Daonella frami*.
		Daonella frami Similar isometic growth pattern and equant shell form as *Daonella degeeri* but with much coarser costation and smaller individuals. Possibly due to preferential preservation of small adult size in dark shale lithology. Random orientation and fragmentation within a sample and absence of smallest sizes suggest reworking. Lack of large adult sizes could also indicate less food. Sizable auricles and straight ribs.
		Daonella degeeri Isometric growth pattern and equant shape with numerous, straight ribs. Occurs in a coquina bed traceable from west to eastern Spitsbergen, possibly a condensed section. Episodically highly reworked with orientations in one sample suggesting the strong influence of currents, possibly wave action. Most widely spread size distribution of all measured species. Smallest individuals are likely removed and large specimens preferentially preserved during reworking due to their robust shells, but exceptionally large sizes may also indicate a time of good conditions and increased food supply .
GROUP 1		**Daonella lindstroemi** Allometric growth pattern, becoming increasingly elongated. Intraspecies variation in rib pattern, flared or straight, possibly due to differences in preservation potential of surrounding lithology. Often found articulated in butterfly postion. Samples representing allochthonous assemblages are not oriented and probably reworked. A sample containing a closed articulated specimen is interpreted as autochthonous and indicates unidirectional currents on the sea floor.
		Daonella arctica Strongly allometric growth, becoming increasingly elongated. Species dominated by small specimens, but smallest fractions are missing. A measured sample shows unidirectional orientation and indiviuals preserved almost exclusively in butterfly position. Whether this is an allochthonous or autochthonous assemblage , both indicate unidicrectional currents on the sea floor.

Figure 8.18: Summary of attributes of the measured species in 2015/2016 material.

Group 1 is composed of *Daonella arctica* and *Daonella lindstroemi,* which are often found in butterfly position and the samples of which, unless reworked, were found to be unidirectionally

oriented. These specimens are found in the lower part of the Blanknuten Mb. and according to Weitschat and Lehmann (1983) and Korčhinskaya (1982), are of late Anisian to lower Ladinian age.

Group 2 consists of daonellids which are situated in the upper part of the Blanknuten Mb., which have a more equant form and are usually found disarticulated and fragmented. The measured samples were generally disoriented, with the exception of possible wave orientation in the *Daonella degeeri* coquina bed. All group 2 species indicate a late Ladinian age.

Group 3 consists of *Halobia zitteli* which is of Carnian age and which differentiates itself by the presence of an anterior tube and a size distribution which is strongly skewed towards smaller individuals with the presence a few very large specimens.

9. Discussion

9.1 Correlations and ages of halobiid zones across Svalbard

All fossil halobiid material collected during the 2015/2016 field seasons, of which species could be identified with relative certainty, has been placed within corresponding logs for each locality. The species have been correlated between localities visited furthest west at Tschermakfjellet and to Muen furthest east. This data has been synthesized in a similar style to palynological data presented in (Vigran et al., 2014) (Figure 9.1).
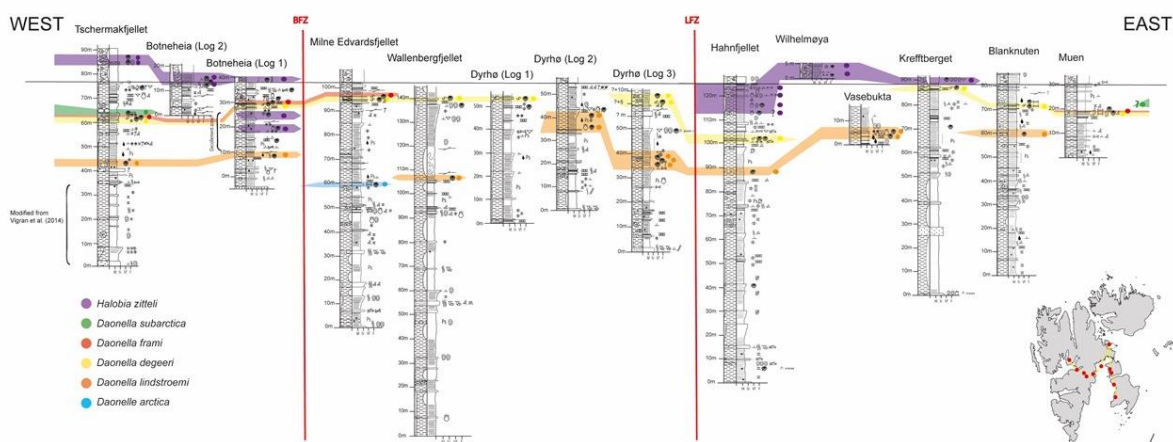
Figure 9.1: Biostratigraphic correlations of Middle to early Late Triassic halobiid material from 2015/2016 field seasons across Spitsbergen and eastern Svalbard, using the base of the purple siderite shales of the Tschermakfjellet as a datum for correlation. Relevant major fault zones are indicated: Billefjorden Fault Zone (BFZ) and Lomfjorden Fault Zone (LFZ) with red, solid lines. Halobiid species: Daonella arctica *(light blue),* Daonella lindstroemi *(orange),* Daonella degeeri *(yellow),* Daonella frami *(red),* Daonella subarctica *(green) and* Halobia zitteli *(purple). A scaled-up version is presented in Appendix 3.*

A pattern emerges of the relative positions of the species in the stratigraphy. The taxa interpreted to be the oldest, *Daonella arctica,* was found in a siltstone bed at the base of the cliff-forming Blanknuten Mb. at Milne Edvardsfjellet. All the identified occurrences of *Daonella lindstroemi,* are generally found above this prominent siltstone. *Daonella lindstroemi* seems to occupy a relatively large biostratigraphic range, within the lower half of the Blanknuten Mb. The overlying *Daonella degeeri* coquina beds are easily recognisable, and is found to be present at all localities where the upper part of the Blanknuten Mb. was exposed. An exception to this was at Dyrhø (Log 2) on central Spitsbergen where shales containing *Daonella lindstroemi* were directly overlain by the purple siderite shales of the Tschermakfjellet Fm.

Daonella frami was found at four localities within 0.5 - 1.5 m of the *Daonella degeeri* coquina beds. *Daonella subarctica* was only precisely placed within the stratigraphy at the westernmost locality, Tschermakfjellet, occurring 1-2 m above the *Daonella frami* beds. Photos taken by Atle Mørk on Muen furthest east in the study area, indicate the presence of *Daonella* subarctica there too, although the precise position within the stratigraphy is unknown. Observations at Tschermakfjellet suggest that is most likely occurs just above the *Daonella frami* beds there, and one can infer that the species should be found in these relative positions across Svalbard, unless the beds have been removed by subsequent erosion. Useful samples of these species from eastern and central localities were unfortunately not collected during the first field season in 2015.

Above the beds containing *Daonella subarctica*, reworked cemented siltstones and phosphate conglomerates generally do not allow for the preservation of adult halobiid material. A few poorly preserved small specimens were found of a halobiid with characteristics of juvenile *Halobia* at the top of the section at Hahnfjella, well below the purple siderite nodules of the Tschermakfjellet Fm.

Halobia zitteli was found at base of the Tschermakfjellet Fm. at many localities, and represents the youngest halobiid, indicating Carnian age. At Botneheia (Log 1), folding and thrusting has forced *Halobia zitteli* between the beds containing *Daonella lindstroemi* and the overlying *Daonella degeeri* coquina beds.

The relative positions of the identified halobiids within the stratigraphy fits especially well with reported species and age estimates presented by Wolfgang Weitschat (Hounslow *et al.*, 2007a; Hounslow *et al.*, 2008; Weitschat & Lehmann, 1983), summarized in Table 1 in Chapter 4.2. Age estimates differ between Weitschat and Korčhinskaya (1982), and the recommended ages of the former has been adopted in this project. *Daonella frami* and *Daonella arctica* have not been described by Weitschat, but are identified and described by Korčhinskaya on Svalbard and at Franz Josef Land (Korčhinskaya, 1982; 1985).

An ideal method for establishing the age ranges of these halobiids is to study ammonoid specimens that occur in the same bedding planes. Unfortunately, relatively few ammonoids were collected in the 2015/2016 field seasons so only a few comparisons could be made. However, whitened images of samples containing both *Daonella* and ammonoids in the fossil material at CASP in Cambridge were taken in December 2016, with the help of Simon Kelly. Tentative identifications of the ammonoids were made using images of specimens from the Botneheia Fm. by Weitschat and Lehmann (1983), shown in Figure 9.2.
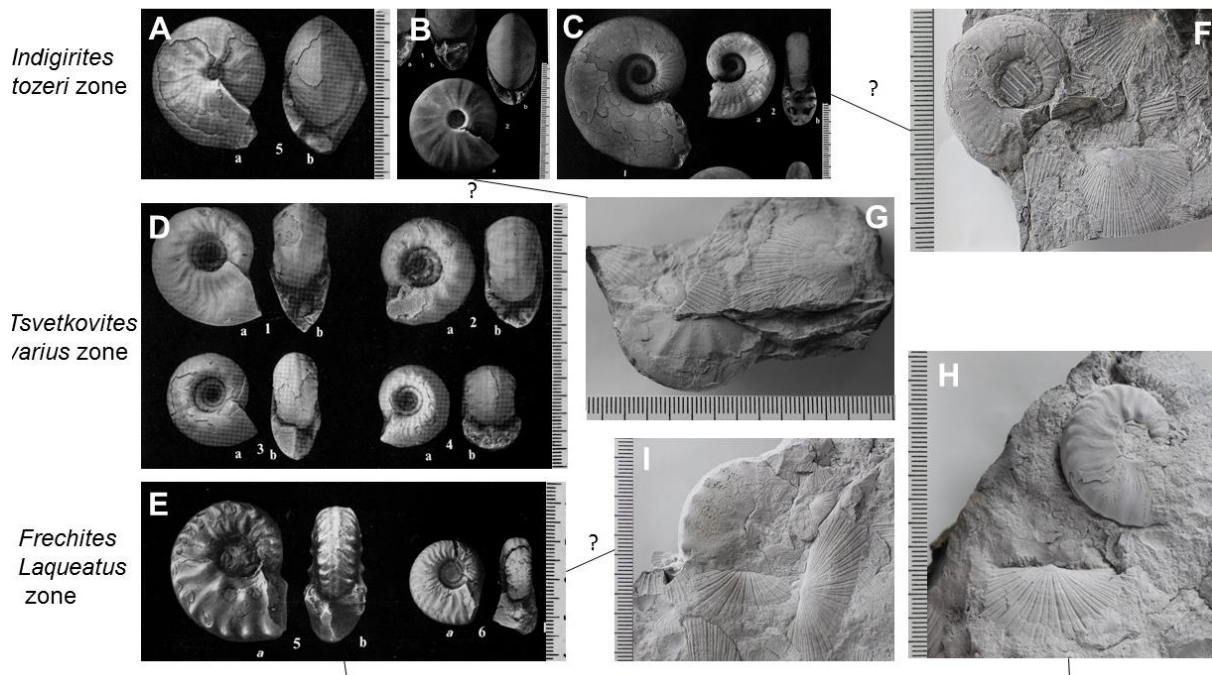
Figure 9.2: Photos were taken of samples containing both ammonoids and Daonella *in the CASP collection, with the kind help of Simon Kelly. All identifications agree with the biostratigraphic scheme of Wolfgang Weitschat in Mørk et al. (1993). Ammonoids in A-E are presented in Weitschat and Lehmann (1983) and F-I are images of bivalves and ammonoids housed in the CASP collections. From the late Ladinian* Indigirites tozeri *Zone: A)* Indigirites tozeri, *B)* Aristoptychites kolymensis, *C)* Ussurites Spetsbergensis *F)* Daonella degeeri *and* Ussurites Spetsbergensis *G)* Daonella degeeri *and* Aristoptychites kolymensis. *From the Late Anisian* Frechites laqueatus *Zone: E)* Frechites laqueatus *F)* Daonella lindstroemi. *E) ammonoid* Tsvetkovites varius *Zone of early Ladinian age. No halobiids were identified from this zone in the material examined.*

The samples at CASP were found containing both *Daonella lindstroemi* and *Frechites laqueatus,* confirming that these species occur at the same time, reported by Weitschat and Lehmann (1983) as the late Anisian. In Hounslow *et al.* (2008), Wolfgang Weitschat also describes *Daonella lindstroemi* co-occurring with *Tsvetkovites varius* at Milne Edwardsfjellet, indicating early Ladinian age.

In the CASP collections, two samples of *Daonella degeeri* were found together with *Aristoptychites kolymensis* and *Ussurites Spetsbergensis,* placing *Daonella degeeri* within the *Indigirites tozeri* Zone, of the early Anisian (Weitschat & Lehmann, 1983). In Hounslow *et al.* (2008), Wolfgang Weitschat adjusted the *Indigirites tozeri* Zone to the late Ladinian.

9.2 Paleoenvironmental interpretation

The paleoenvironment during the deposition of the Botneheia Fm. is discussed in light of previous interpretations while also considering fossil material collected in the 2015/2016 field seasons.

The informal units of the Botneheia Formation

The most recent and detailed bed-by-bed study made of the Botneheia Fm. is that of Krajewski (2008; 2013), who used petrographic methods, such as Rock-Eval pyrolysis and P-Fe-S geochemistry in order to characterise the relative roles of redox conditions and oceanic productivity in the deposition of the organic carbon rich facies of the Botneheia Fm. at localities on Barentsøya and Edgeøya. Nine informal units were assigned to the Botneheia Fm., each containing shales with different properties presented by Krajewski (2013).

In the non-phosphogenic shales of the Muen Mb. (units 1-4), amounts of terrestrial and autochthonous marine organic matter (kerogen type II and III) was found to increase upwards in the succession, interpreted to represent an oxic environment related to an early transgressive phase and back-stepping of the prodelta system (Krajewski, 2013).

The phosphogenic shales of units (5-9), were interpreted to have been deposited in oxygen minimum zone (OMZ) of the open shelf environment during the late transgressive to regressive phases under conditions of high biological productivity. This can considered to indicate surpressed sedimentation rates and fluctuating bottom redox conditions. All the phosphogenic units, with the exception of unit 7, were interpreted to have been deposited in shallower conditions, during high input of autochthonous organic matter (kerogen type II), creating oxic to dysoxic conditions on the sea floor, episodes of reworking and intense precipitation of phosphorous. Unit 7, in the middle part of the Blanknuten Mb., was suggested by Krajewski (2013) to represent the development of euxinia in the deeper parts of the OMZ during a high-stand and contains kerogen type I and II. The base of the Tschermakfjellet was found to be dominated by kerogen type III.

_____

Figure 9.3 Interpreted depositional phases and corresponding conditions at the water-sediment interface of the Botneheia Fm. at Edgeøya, from Krajewski (2013), correlated to the measured succession at Tschermakfjellet, with relative positions of species of Daonella *within the stratigraphy*
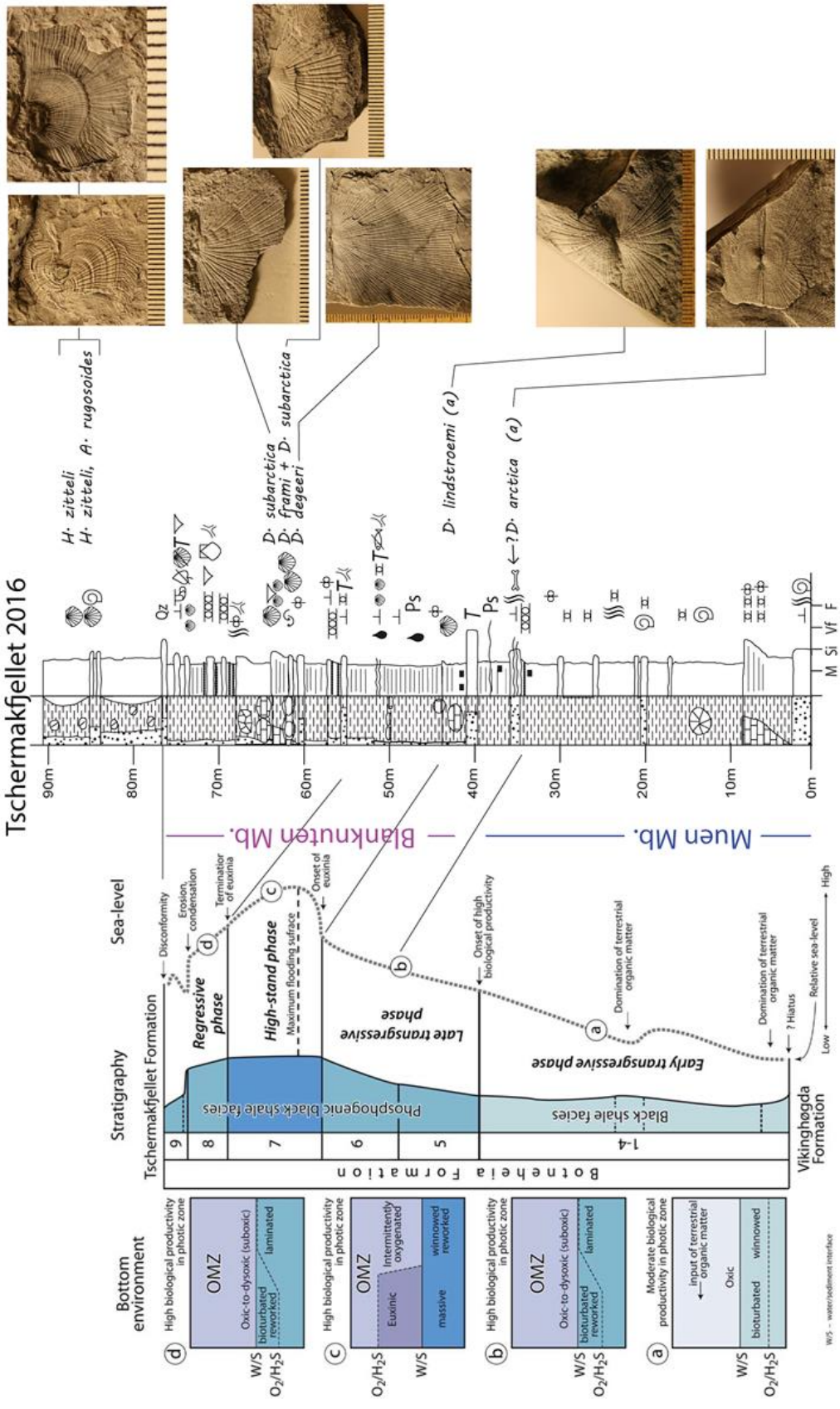
Krajewski (2013) created a detailed reconstruction of the water-sediment interface at different intervals during the deposition of the Botneheia Fm. A comparison has been made between the paleoenvironmental interpretation presented by Krajewski (2013), based on the geochemical constraints, and the characteristics of the identified species of *Daonella* in relative position in the stratigraphy at Tschermakfjellet (Figure 9.3). Though situated far from Muen, the section logged at Tschermakfjellet had the most complete record of fossils and in addition, no major deformation structures were observed.

Units 1-4

The non-phosphogenic interval, consisting of units 1-4 at Edgeøya, was found to contain a mixture of continental-derived and autochthonous marine organic matter, and was interpreted to represent a fully oxygenated prodelta environment.

At Tschermakfjellet, the interpreted correlating unit, below the Blanknuten Mb., was found to contain numerous phosphate nodules and bioturbated siltstone beds. No benthic invertebrates were found in this interval, which is unusual if this sequence does indeed indicate oxygenated bottom conditions.

Krajewski (2008) reported that the lowermost part of the Botneheia Fm. in Edgeøya and Barentsøya are phosphate-free whilst a basal phosphorite bearing horizon is usually found elsewhere on Svalbard (Mørk *et al.*, 1982). He suggested that the lowermost phosphate free part is missing in the remainder of Svalbard or that shifts in biological productivity centres in the shelf basin may have led to later migration of zones of bottom phosphogenesis. The lack of *Daonella* in this zone could be explained by that the earliest *Daonella* are on a global scale are of late Anisian age (McRoberts, 2010).

Unit 5

The uppermost part of the Muen Mb. is assigned to the phosphogenic unit 5 of Krajewski (2013). The base of this unit occurs at the transition between non-phosphogenic and phosphogenic shales on Edgeøya and Barentsøya. The boundary is marked by an increase in the content of alginite particles and phosphate nodules interpreted to be the result of an increase of planktonic productivity. Krajewski (2013) interpreted this layer to be deposited during oxic-dysoxic conditions on the sea floor, resulting in alternating layers of bioturbated and laminated beds.
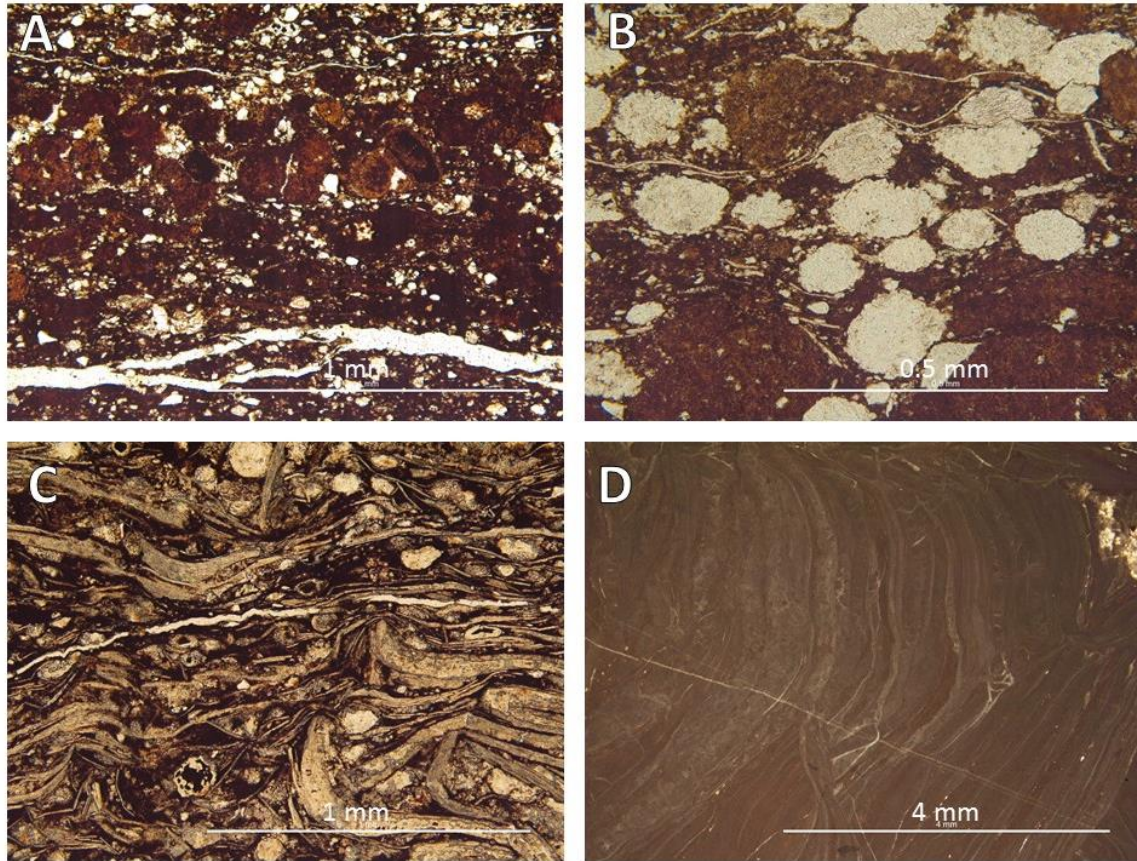
Figure 9.4: A) Unit 5: Allochthonous phosphatic grainstone composed of reworked pellets, 15 m below Daonella lindstroemi*, DH-16-BOT3 151m, B) Unit 6: Black shale from phosphogenic* Daonella lindstroemi *beds. Radiolarians and microcoquina are common, DH-16-BOT3 FOS 4, C) Unit 8:* Daonella degeeri *coquina layer containing reworked shells. Fragmented thin shells bent around more robust larger shells, matrix consisting of pyrite crystals and radiolarians, DH-16-BOT 3 FOS 9, D) Unit 8: Algal mat found in a deformation zone in the uppermost part this unit and of the Botneheia Fm. at Milne Edwardsfjellet MILF-16-BOT1.*

All the material collected containing *Daonella* was above this zone, starting at the base Blanknuten Mb. A thin section was made of the equivalent to unit 5, a dark grey shale with thin phosphatic oolitic grainstone beds composed of reworked faecal pellets at Dyrhø Log 3 20m, in Fulmardalen, located 15 m below *Daonella lindstroemi* beds, see Figure 9.4A.

Unit 6

Unit 6, the base of the Blanknuten Mb., is described as a cliff-forming unit of maximum lithological diversity, with beds of black shales and bioturbated siltstone beds containing a spectrum of phosphate accumulations (Krajewski, 2013). Similar to unit 5, unit 6 is interpreted to have been deposited during times of oxic-dysoxic conditions on the sea floor, resulting in alternating layers of bioturbated and laminated beds.

The base of the Blanknuten Mb. corresponds to base of the late Anisian (Hounslow *et al.*, 2008). This stratigraphic position is reported to be location of the first occurrences of *Daonella* on Svalbard according to Korčhinskaya (1982).

The first adult forms of *Daonella* were observed at this level in the field. Group 1 species *Daonella arctica* and *Daonella lindstroemi* typically have elongated shapes and are mostly found in articulated butterfly position. The non-reworked samples of these species indicated a preferred orientation, suggesting the presence of unidirectional currents on the sea floor at this time.

A thin section was made of a black shale containing articulated *Daonella lindstroemi,* Figure 9.4*B*. Radiolarians and phosphatised faecal pellets are abundant, as well as microcoquina, which are hardly large enough to see in the hand sample.

Unit 7

A thick black unfossiliferous calcite cemented paper shale with a strong smell of hydrocarbons was often observed in measured sections above *Daonella lindstroemi*. This is interpreted to represent period of sea level high-stand phase in the Barents Sea, corresponding to unit 7 of Krajewski (2013). It has been suggested euxinic conditions at the water-sediment interface below continued high biological production in the form of algae and radiolarian in the water masses above (Krajewski, 2013). This interval was dated to be early Ladinian in Spitsbergen (Weitschat & Lehmann, 1983; Weitschat & Dagys, 1989).

No adult *Daonella* were found in this unit and no thin section was made. Krajewski (2013) presents a thin section containing moulds of radiolarian and *Tasmanites* and common juvenile bivalves. According to Schatz (2005), microcoquina beds could indicate juvenile mass mortality events, leading to monospecific deposits of opportunistic species, like those described by Noe-Nygaard (1987). This could also represent layers of larval stage bivalves which died upon settling in an anoxic shale, where no adult forms could establish themselves, an interpretation supported by Mørk and Bromley (2008) and Krajewski (2013).

The microcoquina are just visible in Figure 9.4B, in an image that has been strongly magnified, and which was not possible to see in the hand sample. This calls into question that the microcoquina one sees in the field, often observed in this unit, are in fact young adult populations which have managed established themselves on the sediment surface and experience a sudden local onset of anoxia leading to a thin, concentrated death bed of halobiids roughly the same age.

Unit 8

Unit 8 is described to have similar lithology to unit 6, with recurrent bivalve coquinoidal shale beds. The unit is interpreted by Krajewski (2013) to represent the start of the regressive phase which continues to the top of the Botneheia Fm. during continued high biological productivity and recurrent non-deposition events, which aid the formation of bone and coquinoidal beds. This unit is regarded to have been deposited during times of oxic-dysoxic conditions on the sea floor, resulting in alternating layers of bioturbated and laminated beds (Krajewski, 2013).

Beds containing the group 2 adult daonellids *Daonella degeeri, Daonella frami* and *Daonella subarctica* occur in close proximity to one another within this unit. All specimens (except for one solitary individual of *Daonella degeeri)* were found disarticulated within these sediments. The largest specimens and widest size distribution was found amongst the highly reworked *Daonella degeeri* coquina beds.

 A thin section was made of the coquina beds, see Figure 9.4C, which appear to contain crushed juveniles around large, fragmented adults in a matrix of radiolarians and pyrite crystals. According to Krajewski (2008), authigenic pyrite crystals indicate the formation of an anoxic acidic environment below the water-sediment interface.

Another thin section was made of material collected 2 m below the basal phosphate conglomerate of Unit 9, within a deformation zone containing what appears to be algal material. According to (Korčhinskaya, 1982), the Ladinian sediments typically contain phosphorites and thin intercalations of organic limestones and algal limestones.

Unit 9

The youngest described unit from the Botneheia Fm. in Krajewski (2013), consists of a basal conglomerate overlain by a black phosphatic shale that is discordantly overlain by sideritic shales of the Tschermakfjellet Fm. This unit possibly lies above a condensed or erosional boundary. At the termination of the regressive phase, *Tasmanites* algae blooms contributed to local enrichment of organic carbon in the topmost black shales of unit 9.

Fragments of small halobiid individuals have been found in the calcite cemented siltstones above the phosphate conglomerate sequence near the top of the Botneheia Fm. but they are usually poorly preserved and too small for identification.

Above the informal units assigned to the Botneheia Fm. are the purple siderite shales of the Tschermakfjellet Fm. Here, large specimens of *Halobia zitteli* where found within siderite concretions and within siltstone beds. The siltstone beds were found to contain abundant small adults, a few large specimens of *Halobia zitteli* and rare small specimens of *Aparimella rugosoides*.

A stratified water column

The Botneheia Fm. records a second-order transgressive-regressive cycle in the Svalbard basin, that was developed in an open shelf environment in a large embayment that had a northern connection with deep basins of the Panthalassa ocean (Mørk *et al.*, 1989). Deposition followed a major transgression in the early Anisian (Mørk *et al.*, 1982; Worsley, 1986) and the rise in sea level and local paleogeography led to the development of sluggish circulation close to the sea bottom (Krajewski, 2000; Mørk *et al.*, 1982; Smelror *et al.*, 2009; Worsley, 1986; 2008). This transgressive episode established a deep shelf with anoxic conditions can be, especially in the Billefjorden trough area, and anoxic conditions were interpreted due to the high organic content and by the lack of bioturbation of the preserved black shales (Mørk & Bjorøy, 1984).

It was suggested that periodic storm ventilation of this quiet bottom led to the development of trace fossils and phosphatic burrow infills which are often associated with silty horizons. The phosphate nodules were redeposited in basal lags during extreme storm situations (Mørk *et al.*, 1982). Local coarse-grained units were suggested by Lock *et al.* (1978) to indicate the development of local shoals contrasting with the surrounding euxinic basin.

Mørk and Bromley (2008), conducted detailed observations of trace-fossil assemblages within the Botneheia Fm. at several localities across Svalbard. They observed co-occurrences of mass-mortality shells, high organic content of the sediment and local thorough bioturbation resulting from fluctuating oxic conditions. Possible causes for this can be (Mørk & Bromley, 2008): i) systematic seasonal changes, ii) long oxic periods interrupted by brief anoxic events due to algal blooms, or iii) anoxic conditions briefly interrupted by brief oxic ventilation periods. Phosphate nodules were interpreted to be synthesized by extensive *Thalassinoides* traces, indicating long periods of exposure in a fully oxygenated environment. The depositional environment was interpreted to be dominantly anoxic, although interrupted by pronounced oxic and energetic incursions.

152

Vigran *et al.* (2008) suggested that free-swimming larvae or bivalves living on the sea floor would have experienced oxygen deficiency due to algal blooms in the upper parts of the stratified water column cutting off oxygen supply. She suggested that *Tasmanites* algae and microcoquina recovered from siltstones represented storm-agitated, recycled material that settled out of suspension with the silt fraction, and were preserved by being covered by organic-rich fine mud, thereby preventing oxygen supply.

Littke *et al.* (1991) described the calcareous highly organic sediments of the Jurassic Posidonia Shale from western Germany. During the Jurassic, present-day Europe was located on the broad and extensive Laurussian continental shelf that opened to the deep Tethyan Ocean towards the southeast. The high maceral content was interpreted to be a result of high amounts of phytoplankton controlled by land-derived nutrients. The absence of burrowing, the abundance of organic matter and pervasive diagenetic pyrite, demonstrated anoxia below the sediment-water interface, and euxinia just above the depositional surface. Abundant *Posidonia bronni* occur in the middle section of this shale, indicating that tolerable conditions sometimes occurred. Anoxia was interpreted to be due to an impingement of a Tethyan oxygen minimum zone on the adjacent epeiric area following a general transgression, i.e. water column stratification. Interestingly, the Posidonia Shales contain only minor phosphate in the coquina beds, and all shale samples presented in this paper had a phosphorus content of less than 0.3%.

A Triassic upwelling zone

In later publications by Krajewski (2008; 2013), it was suggested that the succession records a transgressive-regressive interplay between the prodelta depositional system sourced in the southern Barents Sea (the Muen Mb.), and the open shelf phosphogenic system related to upwelling and nutrient supply from the Panthalassa Ocean to the north (the upper-part of the Muen Mb. and the Blanknuten Mb.).

Parrish *et al.* (2001) described the paleoenvironment of the Anisian to Norian Shublik Fm., an organic-, phosphate-, and glauconite-rich shale from the Triassic of Arctic Alaska. The facies geochemistry, ichnofabrics and taphonomy were interpreted to be related to onshore-offshore gradients in biologic productivity and redox conditions, similar to that of modern upwelling zones, such as off the coast of south-west Africa. Low oxygen conditions within the basin were interpreted to be caused by high biological productivity and normal oceanic circulation.

According to Parrish *et al.* (2001), anoxia is known to be generated in modern upwelling zones, from the
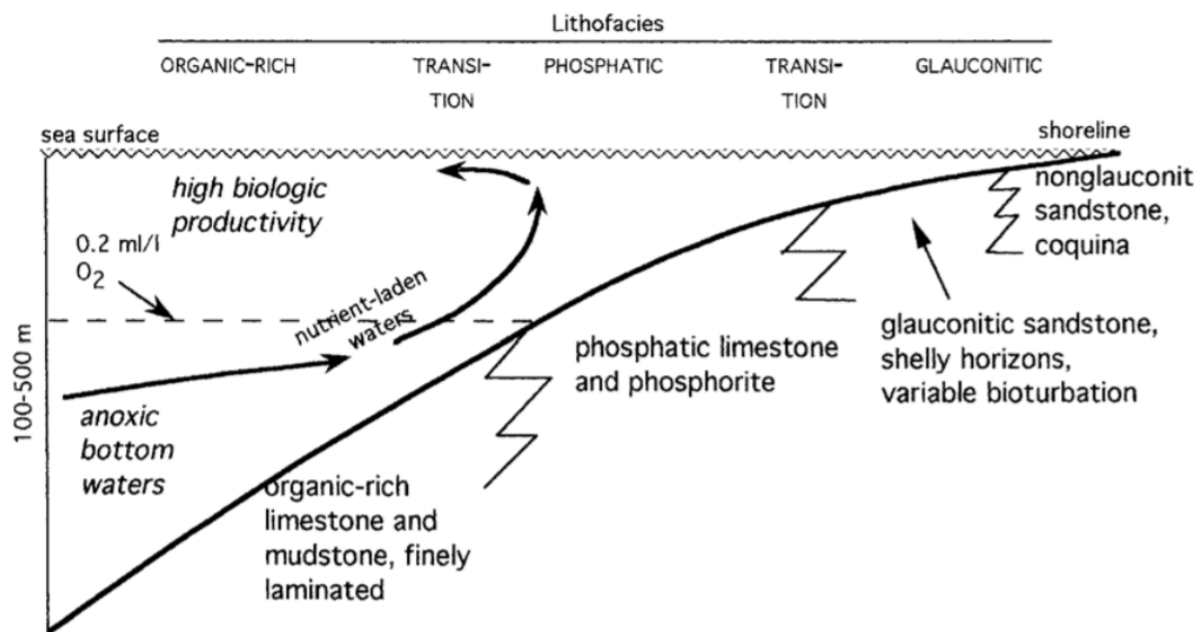
Figure 9.5: Schematic reconstruction of the continental shelf and vertical shelf circulation perpendicular to the paleo-shoreline during deposition of the Shublik Fm., showing the distribution of lithofacies typical of modern upwelling zones. From Parrish et al. (2001).

overwhelming supply or organic detritus which consumes all available oxygen, followed by phosphate formation due to the high rate of supply of organic matter at the sediment-water interface. The vertically alternating layers of phosphatic limestone and finely laminated shale were interpreted to cause lateral migrations of the lithofacies due to smaller fluctuations in sea level.

Parrish *et al.* (2001) reported huge numbers of *Halobia* and *Monotis* in the phosphatic black shales and interpreted them to have been pelagic bivalves. This could due to anoxic conditions not being able to sustain benthic communities over longer periods of time. In addition, all specimens were found as disarticulated single valves. Parrish *et al.* (2001) suggested that the large numbers of *Halobia* were due to: i) an abundant food supply, sourced from the upwelling zone, ii) mass death events due to occasional upwelling of anoxic waters, or iii) due to slow sedimentation. Mass death events were considered to be the more likely cause, as only complete specimens were found, which would be unlikely if the assemblage was exposed to currents over time. The occurrence of large marine reptile could be linked to the presence of abundant food in the at the upwelling system. Observations of interbedded flat-laminated fossiliferous layers,

154

wavy laminated layers and homogenous calcarenite layers on scales of a few millimetres to a few centimetres, was interpreted to be due to micro-turbidites (Parrish *et al.*, 2001).

The possibility of coastal upwelling zone along the Alaskan Triassic continental margin or in the Svalbard and Sverdrup basins during the Anisian to Norian was rejected by Embry *et al.* (2002). This rejection was on the grounds of the similarity in lithologies between these regions, specifically the high concentrations of phosphate. It was also considered impossible for an open access to upwelling currents along the northern shelf margin due to the location of a land mass to the north of the Svalbard and Sverdrup basins, known as Crocker Land. High productivity leading to phosphogenesis was attributed instead to continental runoff and rapid transgression of low-relief areas. In the discussion (Embry *et al.*, 2002), Parrish *et al.* replied that upwelling zones have been formed in shallow basins of less than 100 m depth in extensional basin settings, and that upwelling can be driven either by deep ocean currents or by wind.

In Lundschien *et al.* (2014) it is suggested that the large scale north-westerly prograding Late Triassic paralic deposits are considered to be the source of the supply of sediments to the Sverdrup Basin, explaining the missing Crockerland and perhaps also the fluvial Triassic sediments of Franz Joseph Land. This theory is supported by zircon dating in Anfinson *et al.* (2016), suggesting a source area for these sediments in the Urals.

Krajewski (2013) suggested that two mechanisms could lead to the expansion of the oxygen minimum zone (OMZ) on the Svalbard shelf: i) limited water renewal in stratified basins, or ii) the enhanced oxygen demand resulting from excess decomposition of organic matter within the OMZ. The organic rich facies of a stratified basin should theoretically concentrate organic matter derived from various sources, including an important land-derived fraction, whilst organic matter deposited from under productivity zones will concentrate indigenous organic matter. A regional association of marine organic matter, pyrite and authigenic apatite, such as that found in the Botneheia Fm., is considered typical of an upwelling-related zone of high biological productivity and oxygen depletion. He suggested that a zone of productivity and oxygen depletion straddled the shelf margin and expanded southwards to the north-western Barents Sea shelf following the Anisian transgression, allowing the inflow of nutrient-rich seawater over the submarine swell in northern Svalbard. In his model of sedimentation of the Botneheia Fm., Krajewski (2013) suggests that the euxinic organic rich facies, developed during the highstand in unit 7, extended from Edgeøya and Barentsøya, southward into the Svalbard Platform and westward to central and western Spitsbergen and towards the north.

The *Daonella* specimens interpreted to be the oldest were found at a siltstone in unit 6 at the base of the black, cliff-forming unit at Milne Edwardsfjellet. The base of the Blanknuten Mb. is interpreted to be of late Anisian age, when the first reports of *Daonella* are described from both Svalbard (Korčhinskaya, 1982) and worldwide (McRoberts, 2010). Unit 6 overlies a unit with a marked increase in alginite and phosphate pellets within the rock according to Krajewski (2013), which is confirmed in thin section from Dyrhø.

The best exposures of the lower part of the Blanknuten Mb. was at Kapp Payer, where rocks containing *Zoophycos,* were often found in close proximity to *Daonella lindstroemi* in articulated butterfly position and large ammonoids. This suggests that oxygenated bottoms did exist at this time and that there were favourable conditions in the water masses. The bedding planes, containing abundant *Zoophycos,* found at Kapp Payer occurred in beds underlying phosphate nodules that are a product of bioturbation of *Thalassinoides*, especially abundant in eastern areas of Svalbard (Mørk & Bromley, 2008).

Well preserved, articulated specimens of *Daonella arctica* in butterfly position displayed statistically significant orientations that suggested a unidirectional current. A sample containing possibly autochthonous *Daonella lindstroemi* was found in a black shale, which also appear to be oriented in a unidirectional manner. Microcoquina is also found in a thin section of this sample. The elongated, flat shape of the group 1 *Daonella* must have been favourable for these conditions of soft, soupy sediments which were dominated by a unidirectional current.

These observations suggests that weak unidirectional currents were present on the sea floor in the lower part of the Blanknuten Mb., and that adult *Daonella*, if transported, were not transported far, and managed to survive in these conditions in monospecific opportunistic communities. The sedimentation rate was probably high enough in the lower parts of the Blanknuten Mb. to allow for relative rapid burial of the articulated and orientated shells. Storms or mass flows reworked some shell beds, leading to disarticulation of these valves and the deposition of phosphate lag deposits (Mørk & Bromley, 2008).

According to Krajewski (2013), geochemical indicators suggest the presence of alternating oxic to dysoxic conditions on the sea floor throughout this unit. The onset of dysoxic conditions during this time were probably the result of high productivity in the water masses above the unidirectional currents that swept along the sea floor, bringing with it nutrients. The organic

matter which settled out of the water masses above would have consumed oxygen as it decomposed on the sea floor, creating an oxygen minimum zone.

Temporarily oxygenated conditions on the sea floor would have allowed for bioturbation and the planktonic larvae which settled out of the water masses above to establish themselves on the sea floor (Mørk & Bromley, 2008) and grow to adulthood before a local flush of anoxic water killed off the community. One can also suggest that anoxic pillow on the sea floor grew when the unidirectional current fluctuated or was temporarily halted. The interplay between an oxygen and nutrient rich bearing bottom current and the consummation of oxygen due to large amounts of organic decay could have led to switching conditions on the sea floor.

Above beds containing group 1 *Daonella,* a thick unfossiliferous succession of highly organic black shale was often observed. This interpreted to be unit 7, which contains geochemical indicators of euxinia and represents maximum transgression according to Krajewski (2013). No finds of adult *Daonella* were made in this zone and only minor bioturbation suggests that these benthic communities were unable to survive is these hostile conditions. Microcoquina beds resulted from the death of the larval specimens as they settled out of the water masses and on to the sea floor.

Above the scattered beds containing group 1 *Daonella* and unit 7, the more equant shells of the group 2 species are almost exclusively found disarticulated and fragmented. A sample containing fragmented *Daonella degeeri* indicated slight bimodal distribution of the shell in this coquina bed, suggesting the presence of wave influenced orientation during deposition. This bed can be interpreted to represent a condensed section, where bidirectional storm wave currents could have episodically reached the sea floor. Extreme storms could have led to mass fragmentation of the valves which were exposed at the sediment surface due to low sedimentation. The lowering of the sea level post high stand phase could have lowered storm wave base to the water depths containing benthic communities of *Daonella* which otherwise thrived and grew to be large individuals due to abundant food source along the continuous upwelling system.

Inconsistencies

Although several aspects characteristics of 2015/2016 *Daonella* fossil material fits well with the upwelling system and model presented by Parrish *et al.* (2001) and Krajewski (2013), it remains puzzling that the distribution of glauconite which was interpreted to be consistent with

dysoxic conditions in (Parrish *et al.*, 2001) is not present in the more proximal parts of the basin, for example to the west within the Bravaisberget Fm. or to the south of Svalbard. One reason could be due to high sedimentation rates inhibiting the formation of glauconite in these areas (personal communications, Atle Mørk, 2017).

The interpretation of the pelagic mode of life for *Halobia* in the upwelling zone of the Shublik Fm. by Parrish *et al.* (2001), based on the absence of articulated bivalves, does not agree with the fossil material collected or the associations of bioturbation, *Daonella* and pelagic ammonoids observed in the field on Svalbard during this project.

An in-depth summary of the proposed life habits of the halobiids has been given in Chapter 3.2.3 Mode of Life. The most recently advocated mode of life, supported by Christopher McRoberts (McRoberts, 2011; McRoberts, 2010), Wolfgang Schatz (Schatz, 2004; 2005) and Thomas Waller (Waller & Stanley, 2005) support an epibenthic mode of life. *Daonella* is here interpreted to have been an epi benthic bivalve with planktonic larval stages, explaining its wide dispersal.

As previously mentioned, Parrish *et al.* (2001) linked the occurrence of large marine reptiles to the presence of abundant food in the at the upwelling system, and argued that *Halobia* were pelagic bivalves because of the lack of evidence for predation and that either the bivalves were inedible or that the assemblages represent mass kills by suffocation that would have also effected the predators.

A specimen found in the *Daonella degeeri* coquina beds at Dyrhø Log 3 seems to have sustained an injury which has been healed (Figure 9.6). The valve seems so have continued normal growth after this event and the individual grew to be quite large. Although one cannot prove that such a deformation was due to an injury invoked from a predator, one is tempted to suggest that this non-rounded gash has been made by a creature with teeth. Suspects are quite limited: According to McRoberts (2001), molluscan predation during the middle-Triassic was dominated by shell-breaking fish, shell-crushing cephalopods and marine reptiles Figure 9.7.

Figure 9.6: Possible sign of predation and subsequent shell repair, DH-BOT3-FOS9
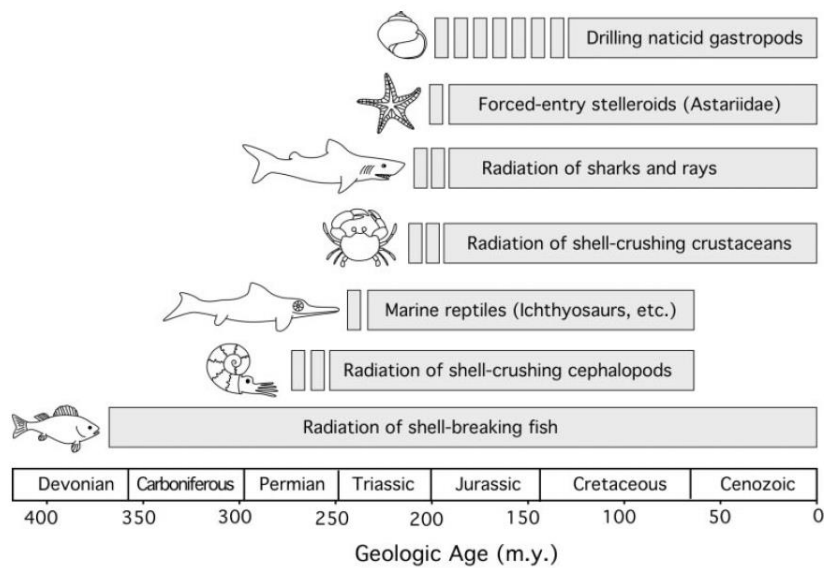
Figure 9.7: Representation of the first appearances and diversification of major marine molluscivores, from (McRoberts, 2001)

One can imagine that the proliferation of plankton in the water masses due to the upwelling of nutrient rich water would have provided an abundant food source for benthic filter feeding *Daonella*, which in turn may have been part of the abundant food source of animals higher up in the food chain: the fish, ichthyosaurs and cephalopods.

9.3 The evolutionary trends of *Daonella*

The two groups established in the Chapter 8. Data Analysis are separated by a maximum transgression which occurs in unit 7. Though the amount of time represented in unit 7 is beyond the scope of this work, but it is clear that the two groups are separated by both time and depositional environment. Late Anisian to early Ladinian group 1 was deposited in a more quiescent environment dominated by a unidirectional current where an elongated form was more advantageous. Whilst group 2 formed in an environment dominated by lower sedimentation rates and more reworking. The condensed nature of the sedimentary succession of the Blanknuten Mb. interpreted in Hounslow *et al.* (2008), could be interpreted to explain close proximity of the species in group 2.

In the 2015/2016 fossil material, a single specimen of *Daonella subarctica* was found in a sample otherwise dominated by *Daonella frami* at Tschermakfjellet, see Figure 9.8.

Figure 9.8: Sample containing Daonella frami *(below) and* Daonella subarctica *(above), from Tschermakfjellet, FOS 6 62m.*

This sample could represent: i) allochthonous reworked sediment bed, by mass flow or otherwise, ii) a condensed bed representing a large time span, or iii) punctuated evolution of *Daonella* as described by Gould and Eldredge (1977). The theory of punctuated equilibrium suggest that evolution is concentrated in very rapid events of speciation, as too little time is available for change by standard gradualistic rates. They suggested that evolutionary trends are not the product of slow, directional transformation within lineages; they represent the

differential success of certain species within a clade (Gould and Eldredge, 1977). The regressive phase in unit 8 (in which these species were found) could have resulted in a changing environment where perhaps the characteristics of *Daonella subarctica*, a more elongated form with finer costae which are bent, would have been more advantageous. A closer look at the boundary between these species could reveal more.

9.4 Applications of halobiid biostratigraphy on Svalbard

9.4.1 Thickness variations in the Botneheia Formation

In Figure 9.1, biostratigraphical correlations are superimposed on sedimentological boundaries. Using the purple siderite shales of the base of the Tschermakfjellet Fm. as a datum, one notices significant thickness variations of the Botneheia Fm. This becomes even more apparent when one uses the *Daonella degeeri* coquina beds as a datum, in **Error! Reference source not found.**. Correlations have been inferred between the purple siderite nodules of the base of the Tschermakfjellet Fm., the prominent siltstone at the base of the black cliff forming unit of the Blanknuten Mb. and the yellow *Rhizocorallium* bearing marker beds occurring 7 m above the base of the Botneheia Fm. (Hounslow *et al.*, 2008)

The monospecific *Daonella degeeri* coquina beds serve as an appropriate datum for correlation as they are easily recognized and traceable in the field. These coquinas are filled with individuals occurring in the millions in a 0.1-0.5 m thick grey-beige calcitic bed. The coquina bed was found at all localities visited in 2015 and 2016, except for exposures with extensive scree coverage or the presence of an unconformity, for example at Dyrhø (Log 2). *Daonella degeeri* has only been found in this limited zone which is directly overlain by beds containing *Daonella* frami, suggesting that *Daonella degeeri* occurred during a relatively limited time span across Spitsbergen.

Thickness variations of the Botneheia Fm. in **Error! Reference source not found.**, occur both above and below the *Daonella degeeri* coquina bed. A significant increase in sediment thickness occurs between the *Daonella degeeri* datum and the base of the cliff-forming units eastwards across the BFZ, where it continues eastwards at similar thicknesses.

Figure 9.9: W-E correlations of measured sections, with Daonella degeeri coquina beds as a datum. Relative location of major fault zones indicated. Correlated beds: Base of Tschermakfjellet Fm. (purple), the base of the black cliff-forming unit (likely base of Blanknuten Mb.) (blue), Rhizocorallium bearing siltstone marker bed of Hounslow et al. (2008) (yellow).
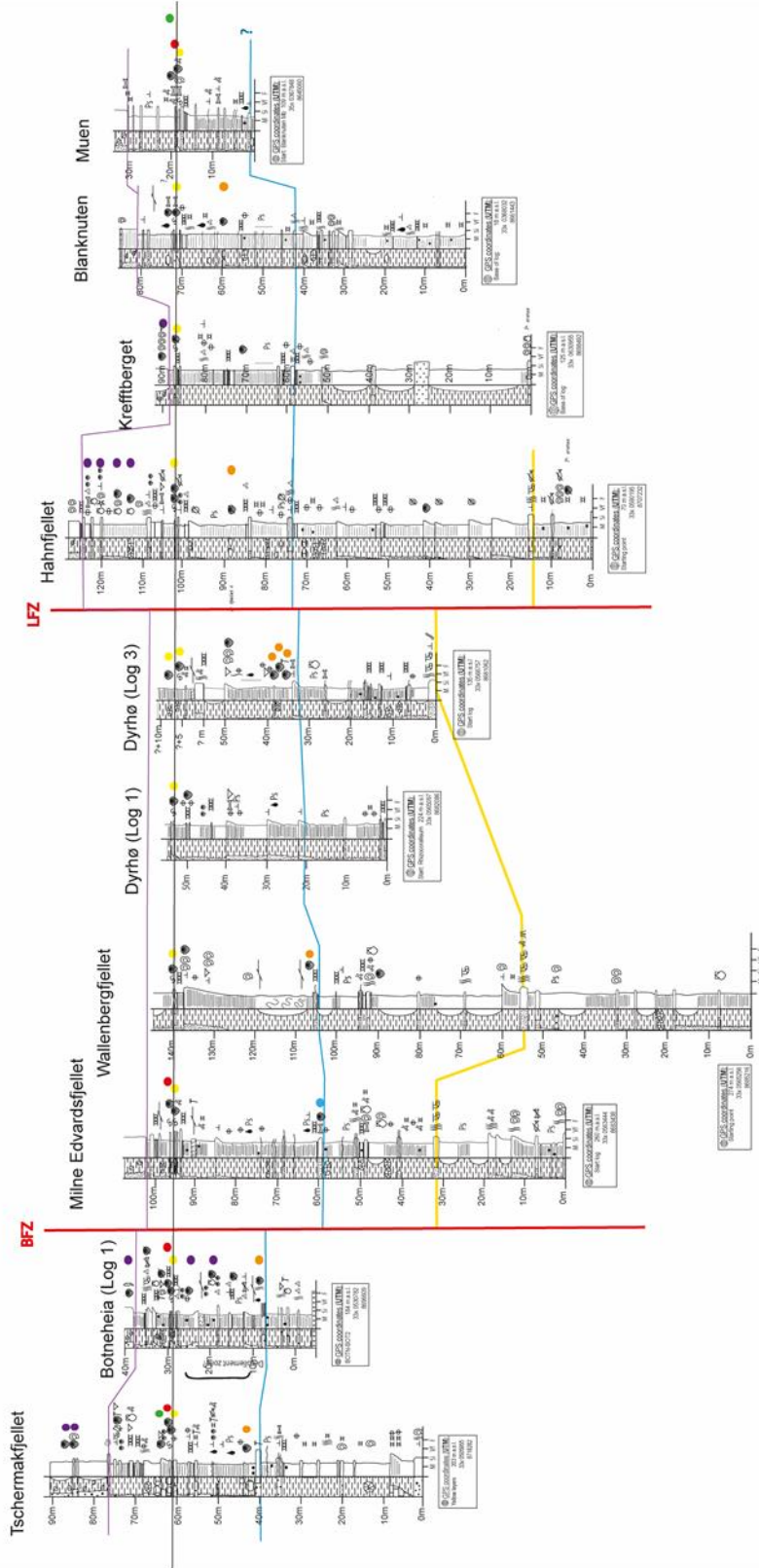
Another increase in sediment thickness occurs at Hahnfjella where the thickest succession logged in the study area is found. A significant increase in sediment thickness in upper part of the Botneheia Fm. is observed eastwards across the LFZ.

Stratigraphic thickness variations within the Mesozoic sequence on Svalbard have been addressed by several workers and are suggested by some to be solely due to the Tertiary compressional tectonic event (Andresen *et al.*, 1992b; Haremo *et al.*, 1990), whilst other explanations include periodic subsidence along the major lineaments, through Early and Middle Triassic time (Mørk *et al.*, 1982).

According to Andresen *et al.* (1992b), thin skinned deformation on Svalbard is characterized by thickening units in the Mesozoic succession due to extensive reverse faulting. This movement occurs within one or possibly two decollement zones positioned in the Triassic Sassendalen Group (Lower Decollement Zone) and the Upper Jurassic/Lower Cretaceous Janusfjellet Subgroup (Upper Decollement zones) (Andresen *et al.*, 1992a; Haremo *et al.*, 1990)(see Figure 9.10). The reverse faulting, often resulting in duplex structures, is particularly well developed in the Triassic Botneheia Fm., and can be traced from outer Isfjorden region in the west, across Spitsbergen to Storfjorden in the east (Andresen *et al.*, 1992b).

Figure 9.10: A diagrammatic west-east cross-section across Spitsbergen showing main structural features. The location of the Billefjorden Fault Zone (BFZ), the Lomfjorden Fault Zone (LFZ) and corresponding Nordfjorden and Ny Friesland structural blocks. Ts, TJk and JKa representing the Sassendalen, Kapp Toscana and Adventdalen groups, respectively (separated by stippled lines). From Andresen et al. (1992a)
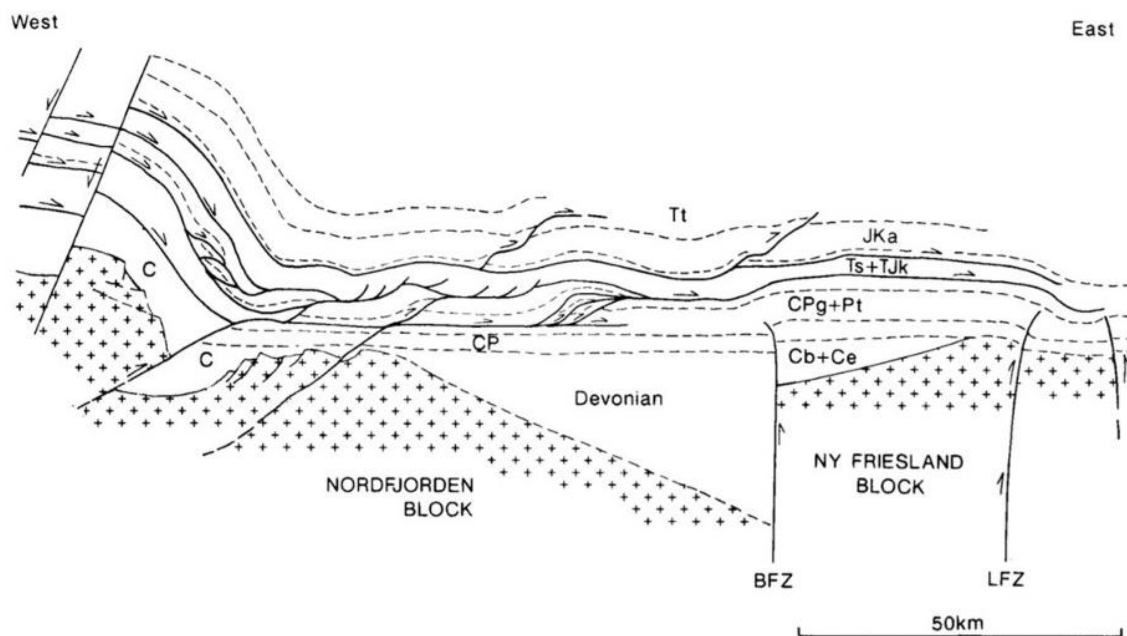
Andresen *et al.* 1992b they suggested that most of the thickness variations within the Botneheia Fm. were attributable to post depositional Tertiary tectonic processes. However, around the LFZ, at Agardhdalen they observed some possible syn- to post-depositional Triassic extensional faults (Andresen *et al.*, 1992b).

According to Mørk *et al.* (1982) the Botneheia Fm. is thin over the Nordfjorden block (Figure 9.10), thickening eastwards across the BFZ. Periodic subsidence along this lineament was thought to have resulted in the development of local depressions with anoxic bottom conditions to the east of the trough. Other lineaments were interpreted to have been largely inactive during deposition of the Botneheia Fm. They suggested a diachronous age for basal deposits of the formation in eastern islands.

The thickness variations observed using the *Daonella degeeri* coquina datum in **Error! Reference source not found.** agree with thickening of the lower part of the Botneheia Fm. across the BFZ reported by Mørk *et al.* (1982). However, several narrow deformation zones documented in the Blanknuten Mb. at the localities visited in western and central Spitsbergen (Botneheia, Milne Edwardsfjellet, Wallenbergfjellet and Dyrhø) suggest thickening due to eastward verging Tertiary compressional tectonics, in agreement with (Andresen *et al.*, 1992b).

The thickness increases seen in the Botneheia Fm. further east, across the LFZ, occurs above the *Daonella degeeri* coquina bed where no deformation was observed. At Hahnfjella several transitional halobiid specimens were found with characteristics of juvenile *Halobia.* These specimens were found in the *Indigirites Zone* of the latest Ladinian. One could image that these have been at this location due to a structural regime with ties to the possible syn- to post-depositional Triassic extensional faults reported from the Agardhdalen area suggested by Andresen *et al.* (1992b). Hahnfjella lies on Olav V fault block which is displaced down-to-the-east of the Lomfjorden Fault Zone (LFZ) (Andresen *et al.*, 1992b). However, the characteristics of such a fault zone or when it was formed is beyond the scope of this work.

Krajewski (2013) suggested the possibility that the upper part of the Blanknuten Mb. is incompletely preserved due to intraformational erosion and condensation. The phosphorite conglomerate at the base of unit 9 is recognized in most sections in east Svalbard but overlies erosional surface that cuts in to the massive phosphate mudstone of unit 7 at southern Barentsøya. Such an unconformity might explain the contact between *Daonella lindstroemi* bed and the overlying purple siderite shales of the Tschermakfjellet Fm. at Dyrhø log 2. Further and more detailed observations are necessary in order to make any reasonable interpretations on this.

164

9.4.2 Regional and global correlations

Findings of halobiids from north-eastern Greenland, in an area with a sedimentary succession recently uncovered from under a retreating ice sheet, aptly named Isranden Fm. has been reported by Alsen *et al.* (2017). The dark shales had previously been assigned to the Jurassic and thermal events had left polymorphs rarely preserved so microfossil dating was not possible. Christopher McRoberts in Alsen *et al.*(2017), identified *Daonella subarctica* from fossil material collected at this site, assigning a Ladinian age of the sediments, based on correlations to Svalbard, north-eastern Russia, Franz Josef Land and Arctic Canada. Sediments with similar age and lithology to the Botneheia Fm. on Svalbard, have also been previously only identified from eastern Peary Land, to the north-east along the coast of Greenland. More fossil material has since been collected and awaits identification in order to assign an age estimate for the entire succession exposed at Kilen, in north-eastern Greenland (Personal communications, Peter Alsen, 2017).

Global correlations of the halobiids has been carried out by McRoberts (2010), and halobiid occurrences have proven to be an effective tool for dating across the continents. Further refining of this biostratigraphic scheme could provide tools systematically analysing the mechanisms for the distribution of these bivalves around the Panthalassic and Tethyan oceans.

One of the greatest challenges of making a global scheme based on these bivalves is the multitude of species names assigned to the halobiids and the incoherent systematic classification (Schatz, 2001; 2004). Schatz attempted to objectively simplify many of the assigned species names of the Tethyan *Daonella* subgenera *Arzelella* and *Moussonella* based on an analysis of biometric characteristics and Principle Component Analysis.

Another method which could prove to be effective is an object analysis of the shape of these bivalves based on images. The relative flat shape and size of halobiids allows for differentiation between and determination of species based on images (confirmed by images of Svalbard 2015/2016 material).

Machine learning is playing an increasingly large role in automatization of our daily lives. Image recognition technology has become widespread, is used in everything from tagging photos of friends on Facebook to self-driving cars. In its most basic form, the technology translates images from the real world to numerical or symbolic information which can interface with other thought processes and elicit appropriate action. This image understanding can be

seen as the disentangling of symbolic information from image data using models constructed with the aid of geometry, physics, statistics, and learning theory (Ponce *et al.*, 2011).

Creating a database of images of species of *Daonella* and *Halobia* from different parts of the world and categorizing them based on a training set of systematically identified specimens with assigned species names or groups may one day prove to be an effective way to objectively systemize the halobiids. A long list of significant challenges would include the number of images needed of each species in order to create a reliable training set.

Software developer and application architect Johan Reitan discusses these challenges from a technical point of view in Appendix 1.

Approximately 800 images were taken of whitened samples from the 2015/2016 Svalbard fossil material containing *Daonella* and *Halobia* specimens. These images contained both complete and highly fragmented specimens. These photos, in addition to photos taken in the field, were categorized into the species present and made into a database.

These images have subsequently been processed by Johan Reitan to create a preliminary version of a *Daonella* image recognizing application, as presented in Appendix 1.

10. Conclusions

- A relatively simple biostratigraphical scheme is presented for the Middle to early Late Triassic bivalves *Daonella* and *Halobia* Svalbard. This has been based on an established ammonoid scheme, previous reports of halobiids from different workers and fossil material collected in 2015/2016. Identification has been based on holotype material as misidentifications are common in established collections.

- The resulting scheme covers a wide lateral extent on Svalbard indicating that the genus *Daonella* occurs between the base of the Blanknuten Mb. and the top of Botneheia Fm., and is replaced by *Halobia* at the base of the Tschermakfjellet Fm.

- Three species groups are identified based on morphology, preservation and position within the stratigraphy: group 1 includes the late Anisian to early Ladinian forms *Daonella arctica* and *Daonella lindstroemi*, group 2 includes early to late Ladinian forms *Daonella degeeri, Daonella frami* and *Daonella subarctica,* and group 3 consists of the coexisting Carnian forms *Aparimella rugosoides* and *Halobia zitteli.*

- The nature of monospecific associations and preservational style suggests *Daonella* were facies dependant, reclining epibenthic opportunists in a fluctuating dysoxic-oxic milieu, with a planktonic larval phase allowing for the widespread distribution of species.

- Shell orientations within small samples suggest the presence of a unidirectional current on the sea floor in the lower part of the Blanknuten Mb., overlain by partly wave influenced, reworked and condensed shell deposits in the upper part.

- Previously published interpretations of redox conditions at sediment-water interface and a transgressive phase followed by high stand and stepwise regression is supported by the collected fossil evidence.

- A combination of reported geochemical indicators, the orientation of shells, and the characteristics of the fossil assemblage supports the interpretation of a Triassic upwelling zone along the northern shelf of Pangea.

- Applications of the Svalbard halobiid biostratigraphical scheme includes: identification of erosion truncation or repeated sections relating to thrusting within Triassic black shales in the field on Svalbard, further refinement of dating and correlations in the Boreal region, and the creation of a dataset on which to develop fossil image recognition technology.

11. Future work

- A detailed study of the shell orientations on larger bedding planes, such as the one exposed at Muen on Edgeøya may provide an insight into where the unidirectional currents originated from in the lower part of the Blanknuten Mb. Population statistics from a single bedding plane with a large sample may reveal peaks in size distributions linked to specific mass death events.

- Principle Component Analysis (PCA) has been proven to be a useful tool in the differentiation of Tethyan *Daonella* species within a subgenus (Schatz, 2001; 2004). A similar study of Boreal species may help to simplify systematics in this region and aid in correlations.

- Further refinement of halobiid biostratigraphic scheme may be achieved by a more detailed study of the simultaneously occurring ammonoids and *Daonella* using material collected in the field and samples housed in collections.

- The further development of species recognition based on images using image recognition technology may aid in the simplification and correlations of *Daonella* at a global scale.

References

Abay, T. B., Karlsen, D. A., Lerch, B., Olaussen, S., Pedersen, J. H., & Backer-Owe, K. (2017). Migrated petroleum in outcropping mesozoic sedimentary rocks in Spitsbergen: organic geochemical characterization and implications for regional exploration. *Journal of Petroleum Geology, 40*(1), 5-36.

Alsen, P., McRoberts, C., Svennevig, K., Bojesen-Koefoed, J. r., Hovikoski, J., & Piasecki, S. (2017). The Isrand Formation: a Middle Triassic Daonella-bearing, black shale unit in Kilen, North Greenland (with a note on the Triassic in Amdrup Land). *Newsletters on Stratigraphy, 50*(1), 31-46. doi:10.1127/nos/2016/0341

Andresen, A., Bergh, S. G., & Haremo, P. (1992a). Basin inversion and thin-skinned deformation association with the Tertiary transpressional West Spitsbergen Orogen. *ICAM Proceedings*, 161-166.

Andresen, A., Haremo, P., Swensson, E., & Bergh, S. G. (1992b). Structural geology around the southern termination of the Lomfjorden Fault Complex, Agardhdalen, east Spitsbergen. *Norsk Geologisk Tidsskrift, 72*, 83-91.

Anfinson, O. A., Embry, A. F., & Stockli, D. F. (2016). Geochronologic Constraints on the Permian–Triassic Northern Source Region of the Sverdrup Basin, Canadian Arctic Islands. *Tectonophysics, 691*, 206-219. doi:http://dx.doi.org/10.1016/j.tecto.2016.02.041

Balini, M., Jenks, J. F., McRoberts, C., & Orchard, M. J. (2007). The Ladinian-Carnian boundary succession at South Canyon (New Pass Rang, Central Nevada). *New Mexico Museum of Natural History and Science Bulletin, 40*, 127-138.

Balini, M., Lucas, S. G., Jenks, J. F., & Spielmann, J. A. (2010). Triassic ammonoid biostratigraphy: an overview. *Geological Society, London, Special Publications, 334*, 221-262.

Biddle, K. T. (1984). Triassic sea-level changes across the Ladinian-Carnian stage boundary. *Nature, 308*, 631-633.

Black, R. M. (1970). Mollusca *The elements of palaeontology* (pp. 34-103). Cambridge: Cambridge University Press.

Blomeier, D. (2015). Historical geology: Carboniferous. In W. K. Dallmann (Ed.), *Geoscience atlas of Svalbard* (pp. 106-109). Tromsø: Norwegian Polar Institute.

Böhm, J. (1904). Ueber de Obertriasische fauna der Baereninsel. *Kungliga Svenska Vetenskaps-Akademiens Handlingar, 37*(3), 1-76.

Böhm, J. (1914). Uber Triasversteinerungen vom Bellsunde auf Spitzbergen. *Arkiv fur Zoologi, 8*, 1-15.

Brack, P., & Rieber, H. (1993). Towards a better definition of the Anisian/Ladinian boudary: New biostratigraphic data and correlations of boundary sections from the Southern Alps. *Eclogae geol., 86*(2), 415-527.

Brekke, T., Krajewski, K. P., & Hubred, J. H. (2014). Organic geochemistry and petrography of thermally altered sections of the Middle Triassic Botneheia Formation on south-western Edgeøya, Svalbard. *Norwegian Petroleum Directorate Bulletin, 11*, 111-128.

Buchan, S. H., Challinor, A., Harland, W. B., & Parker, J. R. (1965). The Triassic Stratigraphy of Svalbard. *Norsk Polarinstitutt Skrifter, 135*, 92 pgs.

Campbell, H. J. (1994). The Triassic bivalves *Daonella* and *Halobia* in New Zealand, New Caledonia and Svalbard. *Institute of Geological and Nuclear Sciences Monograph, 4*, 166 pgs.

Chen, J.-h., & Stiller, F. (2010). An early Daonella from the Middle Anisian of Guangxi, southwestern China, and its phylogenetical significance. *Swiss Journal of Geosciences, 103*(3), 523-533. doi:10.1007/s00015-010-0035-z

Cox, L. R. (1969). General features of Bivalvia. In R. C. Moore (Ed.), *Treatise on Invertebrate Paleontology, Part N, Volume 1, Molluscca 6, Bivalvia* (pp. N2-N129): Geological Society of America Incorporated and Univeristy of Kansas. .

Daderot. (2015, 23.12.2012). Placuna placenta - Osaka Museum of Natural History. Retrieved from https://commons.wikimedia.org/wiki/File:Placuna_placenta_-_Osaka_Museum_of_Natural_History_-_DSC07845.JPG#metadata

Dagys, A. S., & Weitschat, W. (1993). Correlation of the Boreal Triassic. *Mitt. Geol.-Palaont. Inst. Univ. Hamburg, 75*, 249-256.

Dagys, A. S., Weitschat, W., Konstantinov, A., & Sobolev, E. (1993). Evolution of the boreal marine biota and biostratigraphy at the Middle/Upper Triassic boundary. *Mitt. Geol.-Palaont. Inst. Univ. Hamburg, 75*, 193-209.

Dallmann, W. K. (1999). Outline of the geological history of Svalbard. In W. K. Dallmann (Ed.), *Lithostratigraphic Lexicon of Svalbard* (pp. 17-20). Tromsø: Norwegian Polar Institute.

Dallmann, W. K. (2015a). Tectonics and tectonothermal events. In W. K. Dallmann (Ed.), *Geoscience atlas of Svalbard*. Tromsø: Norsk Polarinstitutt.

Dallmann, W. K., Midbøe, P. S., Nøttvedt, A., & Steel, R. J. (1999). Tertiary lithostratigraphy. In W. K. Dallmann (Ed.), *Lithostratigraphic lexicon of Svalbard* (pp. 215-262). Tromsø: Norwegian Polar Institute.

Dallmann, W. K. (Ed.) (2015b). *Geoscience Atlas of Svalbard*. Tromsø: Norsk Polarinstitutt.

Davidson, A., & Brown, G. W. (2012). Paraloid B-72: Practical tips for the vertebrate fossil preparator. *Collection Forum, 26*(1), 99-119.

Donahue, J., Jia, Y., Vinyals, O., Hoffman, O., Zhang, J., Tzeng, E., & Darrell, T. (2014). DeCAF: A Deep Convolutional Activation Feature for Generic Visual Recognition. *Icml, 32*, 647-655.

Doyle, P. (1996). Molluscs: Bivalve and Gastropods *Understanding fossils, an introduction to invertebrate palaeontology* (Vol. 1, pp. 136-158). Chichester, England.: John Wiley & Sons.

Dypvik, H., Mørk, A., Smelror, M., Sandbakken, P. T., Tsikalas, F., Vigran, J. O., . . . Faleide, J. I. (2004). Impact breccia and ejecta from the Mjølnir crater in the Barents Sea—the Ragnarok Formation and Sindre Bed. *Norwegian Journal of Geology, 84*, 143-167.

Eiken, O. (1985). Seismic mapping of the post-Caledonian Svalbard. *Polar Research, 3*(2), 167-176. doi:10.3402/polar.v3i2.6950

Elvevold, S., Dallmann, W., & Blomeier, D. (2007). *Geology of Svalbard*.

Embry, A. F. (1991). Mesozoic history of the Arctic Islands. In H. P. Trettin (Ed.), *Geology of the Innuitian Orogen and Arctic Platform of Canada and Greenland* (Vol. 2): Geological Survey of Canada.

Embry, A. F., Krajewski, K. P., & Mørk, A. (2002). A Triassic upwelling zone: the Shublik Formation, artic Alaska, U.S.A. - discussion and reply. *Journal of Sedimentary Research, 72*(5), 740-743.

Enga, J. (2015). *Paleosols in the Triassic De Geerdalen and Snadd Formations.* (Master's degree), Norwegian University of Science and Technology, Trondheim.

Forsberg, C. S. (2017). *A sedimentological study of the deltaic De Geerdalen Formation in Fulmardalen and of fluvial deposists in the Snadd Formation on the Finnmark Platform.* (M.Sc.), Norwegian University of Science and Technology, Trondheim.

Gould, S. J., & Eldredge, N. (1977). Punctuated equilibria: the tempo and mode of evolution reconsidered. *Paleobiology, 3*, 115-151.

Hallam, A. (1965). Environmental causes of stunting in living and fossil marine benthonic invertebrates. *Palaeontology, 8*(1), 132-155.

Hallam, A. (1967). The interpretation of size-frequency distribution in molluscan death assemblages. *Palaeontology, 10*(1), 25-42.

Hammer, Ø., & Harper, D. (2006). *Paleontological Data Analysis*: Blackwell Publishing.

Haremo, P., Andresen, A., Dypvik, H., Nagy, J., Elverhøi, A., Eikeland, T. A., & Johansen, H. (1990). Structural development along the Billefjorden Fault Zone in the areas

between Kjellstømdalen and Adventdalen/Sassendalen, central Spitsbergen. *Polar Research, 8*, 195-216.

Harland, W. B. (1997). *The geology of Svalbard* (Vol. 17). London: The Geological Society Memoir.

Haugen, T. (2016). *A sedimentological study of the De Geerdalen Formation with focus on the Isfjorden Member and palaeosols.* (Master's Degree), Norwegian University of Science and Technology, Trondheim.

Hayami, I. (1969). Notes of Mesozoic "planktonic" bivalves. *The Journal of the Geological Society of Japan, 75*(7), 375-385.

Heggem, B. (2017). *An analysis of facies in the De Geerdalen Formation and provenance across the Middle to Late Triassic boundary on Spitsbergen, Svalbard.* (M.Sc.), Norwegian University of Science and Technology, Trondheim.

Hoel, A., & Orvin, A. K. (1937). Das Festungsprofil auf Spitzbergen. Karbon-Kreide. I: Vermessungsresultate. *Skrifter om Svalbard og Ishavet, 18*, 1-59.

Hopkin, E. K., & McRoberts, C. A. (2005). A New Middle Triassic Flat Clam (Pterioida: Halobiidae) from the Middle Anisian of North-Central Nevada, USA. *Journal of Paleontology, 79*(4), 796-800. doi:10.1666/0022-3360(2005)079[0796:anmtfc]2.0.co;2

Hounslow, M. W., Hu, M., Mørk, A., Vigran, J. O., Weitschat, W., & Orchard, M. J. (2007a). Magneto-biostratigraphy of the Middle Upper Triassic transition, central Spitsbergen, arctic Norway. *Journal of the Geological Society, London, 164*, 581-597.

Hounslow, M. W., Hu, M., Mørk, A., Weitschat, W., Vigran, J. O., Karloukovski, V., & Orchard, M. J. (2007b). Intercalibration of Boreal and Tethyan timescales. The magneto-biostratigraphy fo the Botneheia Formation (Middle Triassic), and the Late Early Traissic, Svalbard (Arctic Norway). *New Mexico Museum of Natural History and Science Bulletin, 41*, 68-70.

Hounslow, M. W., Hu, M., Mørk, A., Weitschat, W., Vigran, J. O., Karloukovski, V., & Orchard, M. J. (2008). Intercalibration of Boreal and Tethyan time scales: the magnetobiostratigraphy of the Middle Triassic and the latest Early Triassic from Spitsbergen, Arctic Norway. *Polar Research, 27*(3), 469-490. doi:10.1111/j.1751-8369.2008.00074.x

Hurum, J., Roberts, A. J., Nakrem, H. A., Stenløkk, J. A., & Mørk, A. (2014). The first recovered ichthyosaur form the Middle Triassic of Edgeøya, Svalbard. *Norwegian Petroleum Directorate Bulletin, 11*, 97-110.

Hurum, J. H., Druckenmiller, P. S., Hammer, Ø., Nakrem, H. A., & Olaussen, S. (2016). The theropod that wasn't: an ornithopod tracksite from the Helvetiafjellet Formation (Lower Cretaceous) of Boltodden, Svalbard. *Geological Society, London, Special Publications, 434*(1), 189-206. doi:10.1144/sp434.10

Jenks, J. F., Monnet, C., Balini, M., Brayard, A., & Meier, M. (2015). Biostratigraphy of Triassic ammonoids. In C. Klug, D. Korn, K. De Baets, I. Kruta, & R. H. Mapes (Eds.), *Ammonoid paleobiology: from macroevolution to paleogeography* (Vol. 44). Dordrecht, Heidelberg, New York, London: Springer.

Johansen, S. K. (2016). *Sedimentologi and facies distribution of the Upper Triassic De Geerdalen Formation in the Storfjorden area and Wilhelmøya.* (Master's degree), Norwegian University of Science and Technology, Trondheim.

Kelly, S. R. A. (1980). The use of silicone rubbers in the preparation of casts from natural fossil moulds. *Geol. Mag., 117*(5), 447-454.

Kittl, E. (1907). Die Triasfossilen vom Heureka Sund *Report of the Second Norwegian Arctic Expedition in the Fram 1892-1902, 7*.

Klubov, B. A. (1965). On the occurence of Permian rocks on Barentsøya (Spitsbergen achipelago). *Dokl. Akad. Nauk SSSR, 162*, 629-631.

Konstantinov, A. G. (2008). Debatable questions of Boreal Triassic stratigraphy: boundary between middle and upper series. *Russian Geology and Geophysics, 49*(1), 64-71. doi:10.1016/j.rgg.2007.05.004

Konstantinov, A. G., Sobolev, E., & Yadrenkin, A. V. (2013). Triassic stratigraphy of the Eastern Laptev Sea cost and New Siberian Islands. *Russian Geology and Geophysics, 54*, 792-807.

Korčhinskaya, M. V. (1982). An explanatory note to the stratigraphic scheme of the Mesozoic (Trias) of Svalbard. *Ministry of Geology USSR, NPO, "Sevmorgeo"*, 99 pgs.

Korčhinskaya, M. V. (1985). A faunal characterization of the Triassic deposits of Franz Josef Land. *Stratigraphy and palaeontology of Mesozoic basins of the North of USSR*, 16-27.

Krajewski, K. P. (2000). Phosphogenic facies and processes in the Triassic of Svalbard. *Studia Geologica Polonica, 116*, 7-84.

Krajewski, K. P. (2008). The Botneheia Formation (Middle Triassic) in Edgeøya and Barentsøya, Svalbard: lithostratigraphy, facies, phosphogenesis, paleonenvironment. *Polish Polar Research, 29*(4), 319-364.

Krajewski, K. P. (2013). Organic matter–apatite–pyrite relationships in the Botneheia Formation (Middle Triassic) of eastern Svalbard: Relevance to the formation of petroleum source rocks in the NW Barents Sea shelf. *Marine and Petroleum Geology, 45*, 69-105. doi:10.1016/j.marpetgeo.2013.04.016

Krajewski, K. P., Karcz, P., Wozny, E., & Mørk, A. (2007). Type section of the Bravaisberget Formation (Middle Triassic) at Bravaisberget, western Nathorst Land, Spitsbergen, Svalbard. . *Polish Polar Research, 28*(2), 79-122.

Kurushin, N. I., & Truschelev, A. M. (2001). Magnolobia: a new bivalve genus from the boreal Ladinian. *Paleontological Journal, 35*, 243-248.

Leith, T. L., Weiss, H. M., Mørk, A., Århus, N., Elvebakk, G., Embry, A. F., . . . Borisov, A. V. (1993). Mesozoic hydrocarbon source-rocks of the Arctic region. *Arctic Geology and Petroleum Potential, 2*, 1-25.

Lindstroem, G. (1865). Om Trias- och Juraforsteningat fran Spetsbergen. *Kungliga Svenska Vitenskaps-Akademiens Handlingar, 6*, 1-20.

Littke, R., Baker, D. R., Leythaeuser, D., & Rullkotter, J. (1991). Keys to the depositional history of the Posidonia shale (Toarcian) in the Hils Syncline, nothern Germany. *Geological Society Special Publication, 58*, 311-333.

Lock, B. E., Pickton, C. A. G., Smith, D. G., Batten, D. J., & Harland, W. B. (1978). The geology of Edgøya and Barentsøya, Svalbard. *Norsk Polarinstitutt Skrifter, 168*, 7-64.

Lord, G. S. (2017). *Sequence stratigraphy and facies development of the Triassic succession of Svalbard and the northern Barents Sea.* (Doctoral thesis), Norwegian University of Science and Technology, Trondheim.

Lord, G. S., Johasen, S. K., Støen, S. J., & Mørk, A. (2017). Facies development of the Upper Triassic succession on Barentsøya, Wilhemøya and NE Spitsbergen, Svalbard. *Norwegian Journal of Geology, 97*(1), 33-62.

Lord, G. S., Mørk, A., Støen, S. J., Johansen, S. K., & Haugen, T. (2016). *Late Triassic: geology and facies development of nothern Storfjorden and Wilhelmøya.* Retrieved from

Lord, G. S., Solvi, K. H., Ask, M., Mørk, A., Hounslow, M. W., & Paterson, N. W. (2014). The Hopen Member: A new member of the Triassic De Geerdaln Formation, Svalbard. *Norwegian Petroleum Directorate Bulletin, 11*, 88-96.

Lundschien, B. A., Høy, T., & Mørk, A. (2014). Triassic hydrocarbon potential in the Northern Barents Sea: integrating Svalbard and stratigraphic core data *Norwegian Petroleum Directorate Bulletin, 11*, 3-20.

McRoberts, C. (2001). Triassic bivalves and the initial marine Mesozoic revolution: A role for predators? *Geology, 29*(4), 359-362.

McRoberts, C. (2011). Late Triassic bivalvia (chiefly halobiidae and monotidae) from the Pardonet Formation, Williston Lake area, northeastern British Columbia, Canada. *Journal of Paleontology, 85*(4), 613-664.

McRoberts, C. A. (2000). A Primitivehalobia(Bivalvia:Halobioidea) from the Triassic of Northeast British Columbia. *Journal of Paleontology, 74*(4), 599-603. doi:10.1666/0022-3360(2000)074<0599:aphbhf>2.0.co;2

174

McRoberts, C. A. (2010). Biochronology of Triassic bivalves. *Geological Society, London, Special Publications, 334*(1), 201-219. doi:10.1144/sp334.9

Mietto, P., Manfrin, S., Preto, N., & Gianolla, P. (2008). Selected ammonoid fauna from Prati di Stuores/Stuores Wiesen and related sections across the Ladinian-Carnian boundary (southern Alps, Italy). *Rivista Italiana di Paleontologia e Stratigrafia, 114*(3), 377-429.

Mojsisovics, E. (1874). Uber Die Triadischen Pelecypoden–Gattungen *Daonella* und *Halobia*. *Abhandlungen der k. k. Geologischen Reichsanstalt, 7*, 1-35.

Mørk, A. (1994). Triassic transgressive-regressive cycles of Svalbard and other Arctic areas: a mirror of stage subdivision. *Memoires de Geologie, 22*, 69-82.

Mørk, A. (2015). Historical geology: Triassic. In W. K. Dallmann (Ed.), *Geoscience Atlas of Svalbard* (pp. 114-117). Tromsø: Norwegian Polar Institute.

Mørk, A., & Bjorøy, M. (1984). Mesozoic source rocks on Svalbard. *Petroleum Geology of the North European Margin*, 371-382.

Mørk, A., & Smelror, M. (2001). Correlation and non-correlation of high order circum-Arctic Mesozoic sequences *Polarforschung* (69), 65-72.

Mørk, A., & Bromley, R. G. (2008). Ichnology of marine regressive system tract: the Middle Triassic of Svalbard. *Polar Research, 27*, 339-359.

Mørk, A., Knarud, R., & Worsley, D. (1982). Depositional and diagenetic environments of the Triassic and Lower Jurassic succession of Svalbard. *Canadian Society of Petroluem Geologists Memoir, 8*, 371-398.

Mørk, A., Embry, A. F., & Weitschat, W. (1989). Triassic transgressive-regressive cycles in the Sverdrup Basin, Svalbard and the Barents Shelf. *Correlation in Hydrocarbon Exploration*, 113-130.

Mørk, A., Vigran, J. O., & Hochuli, P. A. (1990). Geology and palynology of the Triassic succession of Bjørnøya. *Polar Research, 8*(2), 141-163. doi:10.1111/j.1751-8369.1990.tb00382.x

Mørk, A., Vigran, J. O., Korchinskaya, M. V., Pčelina, T. M., Fefilova, L. A., Vavilov, M. N., & Weitschat, W. (1993). Triassic rocks in Svalbard, the Arctic Soviet islands and the Barents Shelf: bearing on their correlations. *Arctic Geology and Petroleum Potential, 2*, 457-479.

Mørk, A., Elvebakk, G., Forsberg, A. W., Hounslow, M. W., Nakrem, H. A., Vigran, J. O., & Weitschat, W. (1999a). The type section of the Vikinghøgda Formation: a new Lower Triassic unit in central and eastern Svalbard. *Polar Research, 18*, 51-82.

Mørk, A., Dallmann, W. K., Dypvik, H., Johannessen, E. P., Larssen, G. B., Nagy, J., . . . Worsley, D. (1999b). Mesozoic lithostratigraphy. In W. K. Dallmann (Ed.), *Lithostratigraphic Lexicon of Svalbard. Upper Paleozoic to Quarternary bedrock. Review and recommendation for nomenclature used.* (pp. 127-214). Tromsø: Norwegian Polar Institute.

Mørk, M. B. E. (2013). Diagenesis and quartz cement distribution of low-permeability Upper Triassic–Middle Jurassic reservoir sandstones, Longyearbyen CO2 lab well site in Svalbard, Norway. *American Association of Petroleum Geologists Bulletin, 97*, 577-596.

Nagle, J. S. (1967). Wave and current orientation of shells. *Journal of sedimentary petrology, 37*, 1124-1138.

Noe-Nygaard, N. (1987). Bivalve mass mortality caused by toxic dinoflagellate blooms in a Berriasian-Valanginian Lagoon, Bornholm, Denmark. *PALAIOS, 2*, 263-273.

Oeberg, P. (1877). Trias-Forsteningar från Spetsbergen. *Kungliga Svenska Vetenskaps-Akademiens Handlingar, 14*(14), 4-24.

Olaussen, S. (2015). 6-8: Historical geology: Jurassic. In W. K. Dallmann (Ed.), *Geoscience Atlas of Svalbard* (pp. 118-121). Tromsø: Norwegian Polar Institute.

Parrish, J. T., Droser, M. L., & Bottjer, D. J. (2001). A Triassic upwelling zone: the Shublik Formation, Arctic Alaska, U.S.A. *Journal of Sedimentary Research, 71*(2), 272-285.

Pčelina, T. M. (1965). Stratigraphy and some characteristics of the composition of the Mesozoic sediments in the southern and eastern regions of Vestspitsbergen. In V. N. Sokolov (Ed.), *Stratigraphy of Spitsbergen* (pp. 164-204): The British Library.

Pčelina, T. M. (1985). History of Triassic sedimentation in Spitsbergen and on the adjacent shelf of the Barents Sea. *Stratigraphy and palaeontology of Mesozoic basins of the North of USSR*, 135-155.

Ponce, J., Forsyth, D., Willow, E.-p., Antipolis-Méditerranée, S., d'activité RAweb, R., Inria, L., & Alumni, I. (2011). Computer vision: a modern approach. *Computer, 16*(11).

Popov, Y. N. (1946). Fauna of the Ladinian (Trias) from the vicinity of Oymyakova. *Materials on the geology of geology and useful minerals of the NE USSR*(2), 48-61.

Riis, F., Lundschien, B. A., Høy, T., Mørk, A., & Mørk, M. B. E. (2008). Evolution of the Triassic shelf in the norther Barents Sea region. *Polar Research, 27*, 318-338.

Russakovsky, O., Deng, J., Su, H., Krause, J., Satheesh, S., Ma, S., & Berg, A. C. (2015). Imagenet large scale visual recognition challenge. *International Journal of Computer Vision, 115*(3), 211-252.

Samuel, A. (1959). Some Studies in Machine Learning Using the Game of Checkers. *IBM Journal, 3*(3), 535-554.

Savrda, C. E., & Bottjer, D. J. (1991). Oxygen-related biofacies in marine strata: an overview and update. *Modern and Ancient Contintental Shelf Anoxia, 58*, 201-219.

Schatz, W. (2001). Taxonomic significance of biométric characters and the consequences for classification and biostratigraphy, exemplified through moussoneliform daonellas (Daonella, Bivalvia; Triassic). *PalZ, 75*(1), 51-70. doi:10.1007/bf03022598

Schatz, W. (2004). Revision of the subgenus *Daonella* (*Arzelella*) (Halobiidae; Middle Triassic). *J. Paleont., 78*(2), 300-316.

Schatz, W. (2005). Palaeoecology of the Triassic black shale bivalve Daonella—new insights into an old controversy. *Palaeogeography, Palaeoclimatology, Palaeoecology, 216*(3-4), 189-201. doi:10.1016/j.palaeo.2004.11.002

Schneider, S., Fürsich, F. T., Schulz-Mirbach, T., & Werner, W. (2010). Ecophenotypic plasticity versus evolutionary trends—Morphological variability in Upper Jurassic bivalve shells from Portugal. *Acta Palaeontologica Polonica, 55*(4), 701-732.

Seilacher, A. (1990). Aberrations in bivalve evolution related to photo- and chemosymbiosis. *Historical Biology, 3*(4), 289-311. doi:10.1080/08912969009386528

Smelror, M., Petrov, O. V., Larssen, G. B., & Werner, S. C. (2009). *Geological history of the Barents Sea.* Trondheim: Geological Survey of Norway.

Smith, D. G. (1975). The stratigraphy of Wilhelmøya and Hellwaldfjellet, Svalbard. *Geol. Mag., 112*(5), 481-491.

Smith, J. P. (1914). The Middle Triassic marine invertebrate faunas of North America. *U.S. Geological Survey Professional Paper, 83*, 1-248.

Stanley, S. M. (1970). Relation of shell form to life habits of the Bivalvia (Mollusca). *Geological Society of America, Memoir, 125*(1-296).

Steel, R. J., Gjelberg, J., Helland-Hansen, W., Kleinspehn, K., & Nøttvedt, A. (1985). The Tertiary strike-slip basin and orogenic belt of Spitsbergen. *SEPM Special Publication, 37*, 339-360.

Stemmerik, L., & Worsley, D. (2005). 30 year on - Arctic Upper Palaeozoic stratigraphy, depositional evolution and hydrocarbon prospectivity. *Norwegian Journal of Geology, 85*, 151-168

Støen, S. J. (2016). *Late Triassic sedimentology and diagenesis of Barentsøya, Wilhelmøya and eastern Spitsbergen.* (Master's degree), Norwegian University of Science and Technology, Trondheim.

Szegedy, C., Vanhoucke, V., Ioffe, S., Shlens, J., & Wojna, Z. (2016). Rethinking the inception architecture for computer vision. . *Proceedings of the IEEE Conference on Computer Vision and Pattern Recognition*, 2818-2826.

Tozer, E. T. (1967). A standard for Triassic time. *Geological Survey of Canada, Bulletin, 156*, 1-103.

Tozer, E. T., & Parker, J. R. (1968). Notes on the Triassic biostratigraphy of Svalbard. *Geol. Mag., 105*(6), 526-542.

Tugarova, M. A., & Fedyaevsky, A. G. (2014). Caclareous microbialites in the Upper Triassic succession of Eastern Svalbard. *Norwegian Petroleum Directorate Bulletin, 11*, 137-152.

Vermeij, G. J. (1977). The Mesozoic Marine Revolution: Evidence from Snails, Predators and Grazers. *Paleobiology, 3*(3), 245-258.

Vigran, J. O., Mangerud, G., Mørk, A., Bugge, T., & Weitschat, W. (1998). Biostratigraphy and sequence stratigraphy of the lower and middle Triassic deposits from the Svalis Dome, Central Barents Sea, Norway. *Palynology, 22*(1), 89-141. doi:10.1080/01916122.1998.9989505

Vigran, J. O., Mørk, A., Forsberg, A. W., Weiss, H. M., & Weitschat, W. (2008). Tasmanites algae—contributors to the Middle Triassic hydrocarbon source rocks of Svalbard and the Barents Shelf. *Polar Research, 27*(3), 360-371. doi:10.1111/j.1751-8369.2008.00084.x

Vigran, J. O., Mangerud, G., Mørk, A., Worsley, D., & Hochuli, P. A. (2014). Palynology and geology of the Triassic succession of Svalbard and the Barents Sea. *Geological Survey of Norway, Special Publication, 14*, 269.

Waller, T. R., & Stanley, G. D. (2005). Middle Triassic pteriomorphian bivalvia (mollusca) from the New Pass Range, west-central Nevada: systematics, biostratigraphy, paleoecology, and paleobiogeography. *Journal of Paleontology, 79*, 1-58.

Weitschat, W., & Lehmann, U. (1983). Stratigraphy and ammnoids from the Middle Triassic Botneheia Formation (*Daonella* Shales) of Spitsbergen. *Mitt. Geol.-Palaont. Inst. Univ. Hamburg, 54*, 27-54.

Weitschat, W., & Dagys, A. S. (1989). Triassic biostratigraphy of Svalbard and a comparison with NE-Siberia. *Mitt. Geol.-Palaont. Inst. Univ. Hamburg, 68*, 179-213.

Wignall, P. B. (1994). Black shales. *Oxford Monographs on Geology and Geophysics, 30*, 1-127

Wissmann, H. L. (1841). Taxonomic names, in Beiträge zur Geognosie und Petrefacten-Kunde des südöstlichen Tirols vorzüglich der Schichten von St. Cassian. *Beiträge zur Petrefacten-Kunde, 4*, 1-152.

Worsley, D. (1986). *The geological history of Svalbard* (O. J. Aga Ed.). Stavanger: Den norske stats oljeselskap a.s.

Worsley, D. (2008). The post-Caledonian development of Svalbar and the western Barents Sea. *Polar Research, 27*, 298-317.

Xiaofeng, W., Bachmann, G. H., Hagdorn, H., SANDER, P., Cuny, G., Xiaohong, C., . . . Fansong, M. (2008). THE LATE TRIASSIC BLACK SHALES OF THE GUANLING AREA, GUIZHOU PROVINCE, SOUTH-WEST CHINA: A UNIQUE MARINE REPTILE AND PELAGIC CRINOID FOSSIL LAGERSTÄTTE. *Palaeontology, 51*(1), 27-61.

Xu, G., Hannah, J. L., Stein, H. J., Bingen, B., Yang, G., Zimmerman, A., . . . Weiss, H. M. (2009). Re-Os geochronology of the Arctic black shales to evaluate the Anisian-Ladinian boundary and global faunal correlations. *Earth and Planetary Science Letters, 288*, 581-587.

Yabe, H., & Shimizu, S. (1927). The Triassic fauna of Rifu, near Sendai. *Science Report Tohoku University, 11*(2), 101-136.

Yonge, C. M. (1977). Form and Evolution in the Anomiacea (Mollusca: Bivalvia)--Pododesmus, Anomia, Patro, Enigmonia (Anomiidae): Placunanomia, Placuna (Placunidae Fam. Nov.). *Philosophical Transactions of the Royal Society of London. B, Biological Sciences, 276*(950), 453-523. doi:10.1098/rstb.1977.0005

Appendix 1

Image recognition technology and the classification of Halobiidae

Author: Johan Reitan* and Nina Bakke.

*software consultant and application developer at Knowit AS

Machine learning is a subfield within computer science and statistics, with strong ties to artificial intelligence, that gives "computers the ability to learn without being explicitly programmed" (Samuel, 1959). Computer vision is one area where machine learning is essential, as it is far too complex to program the domain by hand.

In order to learn how to classify different images of objects into a predefined set of classes, supervised learning is a good approach. This requires a training data set where example images are grouped by their respective classes. A machine learning algorithm uses this mapping of examples to train a model, where descriptive patterns are identified and aggregated. The trained model can then be used to efficiently classify new, unseen images, based on the experience learned from the training data set.

The quality of the training data set used is imperative to the performance of the resulting model, and there are some considerations to keep in mind when compiling the data set. If any of the examples are wrongly mapped in the training data set, the noise will confuse the algorithm, introducing error. The environment in which the photos have been taken is important as well. If the application is meant to classify fossils outside in the field, the training data set should contain mostly photos from the field. That being said, using photos taken in several different environments helps the learning algorithm to identify the patterns that actually describes the object in question, so that features like background colour or differences in lighting are identified as irrelevant. The pattern detection of the learning algorithm also requires a lot of training data: if training from scratch, an image recognition model could require thousands of images of each class in order to perform well.

In this project, the data set consists of 8 classes: different species of the genome Halobiidae. The number of images in each class ranges from 22 to 212. A big problem with the data set is the small number of images in each class, but the imbalance between the number of images in each class is also an issue. A solution for this, which also makes it easier to set up a proof of concept, is re-training an existing model for image recognition (Donahue *et al.*, 2014). Inception v3 (Szegedy *et al.*, 2016) is an open source computer vision model developed by Google researchers, which is trained on the ImageNet data set (Russakovsky *et al.*, 2015), consisting of 1000 categories and 1.2 million images. This model performs very well on general image classification, and by redefining its output to the different species of Halobiidae, and further training the model on images of these species, it is possible to develop a model of modest performance from the few images available. If more images were available, building a new model from scratch would likely lead to better results.

When training the model, the data is split into three sets with random selection: 80 % for training, 10 % for validation, and 10 % for testing. The training algorithm can only see the training set, but the validation set is used continuously throughout the training to make sure that the model is actually learning the concept, not just memorizing data. Finally, when the model is trained, the last set, that has been held out from the training completely, is used to give an estimate on how the model will perform on unseen data.

The model for the Halobiidae data set was trained for 8000 iterations. For each iteration, the performance was measured on the training and validation sets and reported as accuracy, which is how often the predictions match the correct labels. The results are shown in Figure A1.1. As the model learns the training set better, the training accuracy approaches 1. The evaluation accuracy, however, increases in the beginning, but has little growth in later iterations. This means that the model is not able to learn the concept better with the current data. The first step to solve this problem is to gather more data, and ensure the data is correct.

After the training was completed, the resulting model was tested on the held-out testing set, and achieved an accuracy of 58.6%. While this may not be accurate enough for practical use, it shows that the model was able to learn from the images available. With more images more

evenly distributed among the different species, and further tweaking of the learning algorithm, the model should improve considerably.
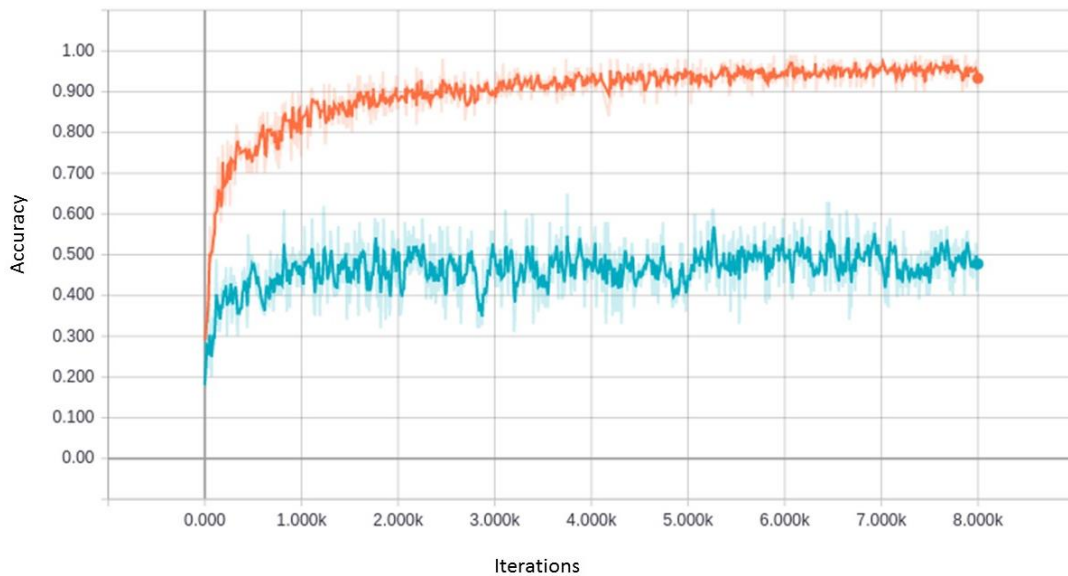

Figure A1.1: Graph of training accuracy (orange) and evaluation accuracy (blue) of model vs. number of iterations.

In order to get a sense of the performance of the model, a mobile application was built. It classifies images from the camera, and displays up to three most likely classifications of the image, and their probability of being correct. Screenshots are shown in Figure A1.2.
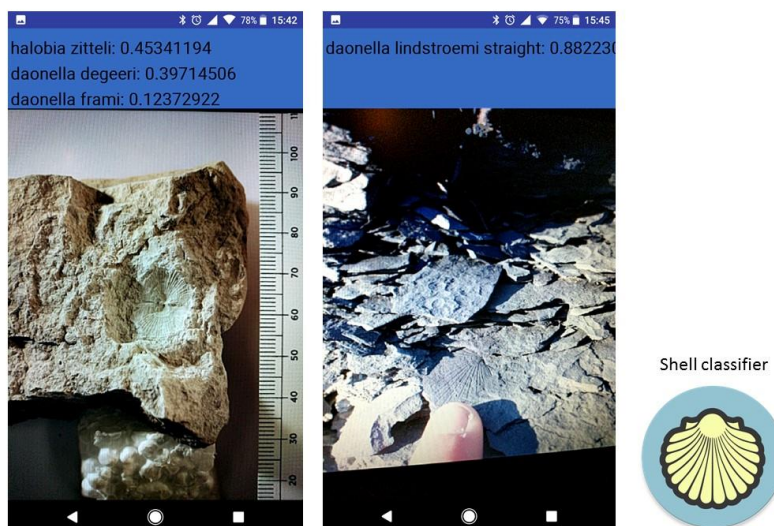

Figure A1.2: Screenshots of mobile application "Shell classifier", classifying images from the camera.

Appendix 2

UTM coordinates of logged sections in field seasons 2015/2016

Field season 2015

Name of mountain	Name of log	UTM Start (Zone, East, North, Elevation)	UTM End (Zone, East, North, Elevation)
Muen	MUEN-15-BOT1	35X, 0367848, 8645060, 109m	35X, 0367481, 8644678, 139m
Blanknuten	BLK-15-BOT1	35X, 0368032, 8661443, 0m	35X, 0367940, 8661516, 112m
Wilhelmøya	W-15-BOT1	33X, 0622408, 8783496, 0m	33X, 0622420, 8783428, 5m
Hahnfjella (day 1)	HAF-15-BOT1	33X, 0590195, 8707232, 70m	33X, 0589893, 8707360, 198m
Vossebukta	VBK-15-BOT1	33X, 0627058, 8707854, 0m	33X, 0627034, 8707780, 4m
Krefftberget	KFT-15-BOT1	33X, 0630955, 8698492, 125m	33X, 0631050, 8698552, 225m

Field season 2016

Name of mountain	Name of log	UTM Start (Zone, East, North, Elevation)	UTM End (Zone, East, North, Elevation)
Wallenbergfjellet	WBF-16-BOT1	33X, 0565256, 8685216, 274m	33X, 0565492, 8685404, 434m
Dyrhø, log 1	DH-16-BOT1	33X, 0564927, 8682174, 274m	33X, 0564883, 8682124, 309m
Dyrhø, log 2	DH-16-BOT2	33X, 0565532, 8681742, 237m	33X, 0565424, 8681704, 277m
Dyrhø, log 3	DH-16-BOT3	33X, 0566757, 8681063, 135m	33X, 0566396, 8680923, 217m
Milne Edwardsfjellet	MILF-16-BOT1	33X, 0563444, 8683438, 260m	33X, 0563104, 8683725, 351m
Botneheia, log 1	BOTN-16-BOT1	33X, 0532115, 8695908, 163m	(no data)
Botneheia, log 2	BOTN-16-BOT2	33X, 0530782, 8696609, 184m	(no data)
Tschermakfjellet	TSCH-16-BOT1	33X, 0505996, 8718231, 242m	33X0506059, 8718119, 267m

Appendix 3

Biostratigraphic correlations of Halobiid material from 2015/2016 field seasons